UNIVERSITY OF ALBERTA

ROLE OF CYTOCHROME P450 ENZYMES IN THE PATHOGENESIS OF CARDIAC HYPERTROPHY AND DOXORUBICIN-INDUCED CARDIOTOXICITY

By

BESHAY NAZMY MOUNIR ZORDOKY

A thesis submitted to the Faculty of Graduate Studies and Research in partial fulfillment of the requirements for the degree of

DOCTOR OF PHILOSOPHY

IN

PHARMACEUTICAL SCIENCES

FACULTY OF PHARMACY AND PHARMACEUTICAL SCIENCES

© Beshay Nazmy Mounir Zordoky

SPRING 2012

EDMONTON, ALBERTA

Permission is hereby granted to the University of Alberta Libraries to reproduce single copies of this thesis and to lend or sell such copies for private, scholarly or scientific research purposes only. Where the thesis is converted to, or otherwise made available in digital form, the University of Alberta will advise potential users of the thesis of these terms.

The author reserves all other publication and other rights in association with the copyright in the thesis and, except as herein before provided, neither the thesis nor any substantial portion thereof may be printed or otherwise reproduced in any material form whatsoever without the author's prior written permission.

Library and Archives Canada

Published Heritage Branch

395 Wellington Street
Ottawa ON K1A 0N4
Canada

Bibliothèque et Archives Canada

Direction du Patrimoine de l'édition

395, rue Wellington
Ottawa ON K1A 0N4
Canada

Your file Votre référence
ISBN: 978-0-494-87889-7

Our file Notre référence
ISBN: 978-0-494-87889-7

NOTICE:

The author has granted a non-exclusive license allowing Library and Archives Canada to reproduce, publish, archive, preserve, conserve, communicate to the public by telecommunication or on the Internet, loan, distrbute and sell theses worldwide, for commercial or non-commercial purposes, in microform, paper, electronic and/or any other formats.

The author retains copyright ownership and moral rights in this thesis. Neither the thesis nor substantial extracts from it may be printed or otherwise reproduced without the author's permission.

AVIS:

L'auteur a accordé une licence non exclusive permettant à la Bibliothèque et Archives Canada de reproduire, publier, archiver, sauvegarder, conserver, transmettre au public par télécommunication ou par l'Internet, prêter, distribuer et vendre des thèses partout dans le monde, à des fins commerciales ou autres, sur support microforme, papier, électronique et/ou autres formats.

L'auteur conserve la propriété du droit d'auteur et des droits moraux qui protege cette thèse. Ni la thèse ni des extraits substantiels de celle-ci ne doivent être imprimés ou autrement reproduits sans son autorisation.

In compliance with the Canadian Privacy Act some supporting forms may have been removed from this thesis.

While these forms may be included in the document page count, their removal does not represent any loss of content from the thesis.

Conformément à la loi canadienne sur la protection de la vie privée, quelques formulaires secondaires ont été enlevés de cette thèse.

Bien que ces formulaires aient inclus dans la pagination, il n'y aura aucun contenu manquant.

Canada

This work is dedicated to my family,

Mariam

Mary & Irene

Thank you

ABSTRACT

Heart failure (HF) affects more than 5 million patients in North America with about half a million new cases every year. Cardiac hypertrophy and drug-induced cardiotoxicity are two important predisposing factors to HF. Several cytochrome P450 (CYP) enzymes have been identified in the heart and their levels have been reported to be altered during cardiac hypertrophy and HF. Moreover, CYP enzymes have been shown to metabolize arachidonic acid to the cardioprotective epoxyeicosatrienoic acids (EETs) and the cardiotoxic 20-hydroxyeicosatetraenoic acid (20-HETE). Therefore, the objective of the present work was to investigate the role of CYP enzymes and CYP-mediated arachidonic acid metabolism in the pathogenesis of cardiac hypertrophy and doxorubicin (DOX)-induced cardiotoxicity. Our results showed that isoproterenol-induced cardiac hypertrophy caused a significant induction of *CYP1A1*, *CYP1B1*, and *CYP4A3* and a significant inhibition of *CYP2C11* and *CYP2E1* gene expression in the rat heart. In addition, there was a significant induction of the soluble epoxide hydrolase (sEH) which metabolizes the EETs to the less biologically active dihydroxyeicosatrienoic acids. These changes in CYP and sEH expression altered CYP-mediated arachidonic acid metabolism with a decrease in the EETs and an increase in the 20-HETE formation rates. Interestingly, we have also shown that induction of CYP1A1 and CYP1B1 by aryl hydrocarbon receptor ligands caused hypertrophy of the cardiac derived H9c2 cells. With regard to DOX-induced cardiotoxicity, we demonstrated that DOX induces several CYP and sEH enzymes in both the rat heart and the H9c2 cells. The overall alteration of CYP and sEH expression resulted in altered CYP-mediated arachidonic acid metabolism with a

significant increase in the 20-HETE and a significant decrease of the EETs formation. Interestingly, we have demonstrated that acute DOX toxicity alters the expression of CYP and sEH in an organ-specific manner. Most notably, sEH induction and the subsequent decrease in formation of EETs were observed only in the heart of DOX-treated rats but not in the kidney or the liver. In conclusion, induction of cardiac CYP and sEH enzymes and the subsequent derailed CYP-mediated arachidonic acid metabolism may be involved in the pathogenesis of cardiac hypertrophy and DOX-induced cardiotoxicity and their progression to HF.

ACKNOWLEDGEMNENTS

I would like to express my deepest gratitude and my sincere appreciation to my supervisor, Dr Ayman El-Kadi, for his continuous guidance, unconditional support, and invaluable mentorship through working on these research projects.

I wish also to thank my supervisory committee members, Dr Dion Brocks and Dr Jason Dyck, for their valuable suggestions and endless advice.

I would like to thank my senior lab members, Drs Gharavi, Korashy, and Elbekai, who taught me several techniques and offered me valuable advice. My special appreciation is extended to my colleagues, Mona and Anwar, who helped me in several experiments. Likewise, I sincerely appreciate Dr Somayaji for his excellent technical assistance with the LC-ESI-MS. I would also like to thank Dr John Seubert and Mr Haitham El-Sikhry for their help with the phase contrast microscopy.

I am grateful to Dr Bruce Hammock for providing us with the sEH inhibitor, tAUCB, as well as the sEH primary antibody. I am also grateful to Dr Darryl Zeldin for providing us with the CYP2J primary antibody.

I am grateful to the reviewers who reviewed the publications resulting from this work. Their valuable comments helped me to improve the quality of the work.

I am grateful to the Egyptian Government, Alberta Innovates – Health Solutions, University of Alberta, and the Faculty of Pharmacy and Pharmaceutical Sciences for their financial support.

I wish to thank the Heart and Stroke Foundation of Canada (HSFC) and the Canadian Institutes of Health Research (CIHR) for the financial support of this research.

Last but not least, I wish to thank all the administrative and support staff in the Faculty of Pharmacy and Pharmaceutical Sciences for their kindness, with special thanks to Mrs Joyce Johnson and Mr Jeff Turchinsky.

TABLE OF CONTENTS

LIST OF TABLES

LIST OF FIGURES

LIST OF ABBREVIATIONS

3-MC	3-Methyl cholanthrene
AhR	Aryl hydrocarbon Receptor
ANOVA	Analysis of Variance
ANP	Atrial Natriuretic Peptide
ARNT	AhR Nuclear Translocator
BaP	Benzo(a)pyrene
BNF	β-Naphthoflavone
BNP	B-type Natriuretic Peptide
CAR	Constitutive Androstane Receptor
COX	Cyclooxygenase
CVD	Cardiovascular Disease
CYP	Cytochrome P450
DAN	2,3-Diaminonaphthalene
DCF	Dichlorofluorescin
DCF-DA	Dichlorofluorescin diacetate
DEPC	Diethyl pyrocarbonate
DHET	Dihydroxyeicosatrienoic acid
DME	Drug Metabolizing Enzymes
DMEM	Dulbecco's Modified Eagle's Medium
DOX	Doxorubicin
EDHF	Endothelium-derived Hyperpolarizing Factor
EET	Epoxyeicosatrienoic acid
ERK	Extracellular signal Regulated Kinase
FXR	Farnesoid X Receptor
GAPDH	Glyceraldehyde-3-phosphate dehydrogenase
GPCR	G Protein Coupled Receptor
GR	Glucocorticoid Receptor
GSK-3	Glycogen Synthase Kinase-3
HETE	Hydroxyeicosatetraenoic acid
HF	Heart Failure

IGF	Insulin-like Growth Factor
IL-6	Interleukin-6
iNOS	Inducible Nitric Oxide Synthase
JNK	c-Jun N-terminal Kinase
K_{ca}	Calcium-activated Potassium Channel
LC-ESI-MS	Liquid Chromatography – Electrospray Ionization – Mass Spectrometry
LOX	Lipoxygenase
LPS	Lipopolysaccharide
LXR	Liver X Receptor
MAPK	Mitogen-Activated Protein Kinase
MEF2	Myocyte Enhancer Factor-2
mTOR	Mammalian Target of Rapamycin
MTT	3-(4,5-Dimethylthiazole-2-yl)-2,5-diphenyltetrazolium bromide
NFAT	Nuclear Factor of Activated T cells
NF-κB	Nuclear Factor-κB
PCR	Polymerase Chain Reaction
PG	Prostaglandin
PI3K	Phosphoinositide 3-kinase
PKA	Protein Kinase A
PKB	Protein Kinase B
PKC	Protein Kinase C
PPAR	Peroxisome Proliferator Activated Receptor
PXR	Pregnane X Receptor
ROS	Reactive Oxygen Species
RXR	Retinoid X Receptor
SD	Sprague Dawley
SDS-PAGE	Sodium Dodecyl Sulfate – Polyacrylamide Gel Electrophoresis
sEH	Soluble Epoxide Hydrolase

SHHF	Spontaneously Hypertensive Heart Failure
SHR	Spontaneously Hypertensive Rats
STAT	Signal Transducer and Activator of Transcription
SXR	Steroid X Receptor
tAUCB	trans-4-[4-(3-Adamantan-1-yl-ureido)-cyclohexyloxy]-benzoic acid
TCDD	2,3,7,8-Tetrachlorodibenzo-p-dioxin
TNF-α	Tumor Necrosis Factor-α
TxA_2	Thromboxane A_2
VSMC	Vascular Smooth Muscle Cell
β-MHC	β-Myosin Heavy Chain

CHAPTER 1 – INTRODUCTION

1.1. Heart Failure (HF)

HF is defined by the American Heart association/American College of Cardiology guidelines as "a complex clinical syndrome that can result from any structural or functional cardiac disorder that impairs the ability of the ventricle to fill or eject blood" (Hunt, Abraham et al. 2005). HF is becoming a major health concern and it has been singled out as an emerging epidemic (Braunwald 1997). HF affects more than 5 million people in North America with about half a million of new cases every year (Kim and Hunt 2003). In Canada, HF affects more than 400,000 people and costs more than one billion dollars annually for inpatient care alone (O'Connell 2000). The increasing prevalence of HF may be attributed to increased incidence and/or increased survival of HF patients (Roger 2010). Despite the advent of several new medications to manage HF, the prognosis of HF is still poor, with an estimated survival rate of 50% and 10% after 5 and 10 years, respectively (Roger 2010).

The etiology of HF is a complex issue as HF may result as an end point for several cardiovascular diseases (CVDs). Nevertheless, the most common causes of HF are: coronary artery diseases, hypertension, vulvular heart diseases, and several cardiomyopathies including familial cardiomyopathy, diabetic cardiomyopathy, and drug-induced cardiomyopathy (Aaronaes, Atar et al. 2007). Epidemiological studies have reported that coronary artery diseases are the cause of HF in 36 – 52% in new HF cases (Cowie, Wood et al. 1999; Fox, Cowie et al. 2001), whereas hypertension and vulvular heart diseases represent 14% and 7%, respectively (Cowie, Wood et al. 1999). Another important contributing factor to

the etiology of HF is drug-induced cardiotoxicity. Several medications have been reported to cause cardiotoxicity and/or to worsen a pre-existing HF. Drug-induced HF can be attributed to the use of thiazolidinedione anti-diabetic drugs, several anti-arrhythmic medications with negative inotropic effect, non-steroidal anti-inflammatory drugs especially those with selective cyclooxygenase-2 (COX-2) inhibition, medications that cause volume overload (e.g. glucocorticoids), and several anti-neoplastic agents (e.g. doxorubicin, DOX) (Maxwell and Jenkins 2011).

Similar to its etiology, the pathophysiology of HF is also complex. Several neurohormonal pathways are activated in patients with HF (Dube and Weber 2011). Circulating levels of cortisol, angiotensin II, aldosterone, norepinephrine, epinephrine, and parathyroid hormone are elevated in HF patients (Anker, Chua et al. 1997). In addition to the neurohormonal activation, HF pathophysiology includes: an increased oxidative stress in several organs, an immunostimulatory state, and an inflammatory phenotype (Dube and Weber 2011). The rennin-angiotensin-aldosterone system (RAAS) seems to be the most important player in these pathophysiologic processes (Mansur, Hage et al. 2010). Rennin is synthesized in the juxtaglomerular cells of the kidney and cleaves its substrate, angiotensinogen, to angiotensin I which is then converted to the active angiotensin II by the angiotensin converting enzyme (ACE) (Mansur, Hage et al. 2010). Angiotensin II is a very potent vasoconstrictor, a pro-hypertrophic, a pro-oxidant, and a pro-inflammatory mediator (Montecucco, Pende et al. 2009). Another key effector in the RAAS is aldosterone which is a major regulator of

sodium and potassium balance and thus the extracellular volume (Mansur, Hage et al. 2010). In addition, clinical and scientific evidence suggest that aldosterone is associated with greater incidence of left ventricular hypertrophy, cardiac fibrosis, and remodeling which are independent of its effect on blood vessels (Young and Funder 2002; Fiebeler and Haller 2003; White 2003; Shieh, Kotlyar et al. 2004; Vasan, Evans et al. 2004; Yoshimura 2005; Funder 2006).

Cardiac hypertrophy is an independent risk factor for HF and the most potent predictor of adverse cardiovascular events in hypertensive patients (Gradman and Alfayoumi 2006). In addition, cardiomyocyte hypertrophy and fibrosis are prerequisites for the development of HF; therefore, research into the molecular basis of hypertrophy can be considered as research into the initial steps of HF (Ritter and Neyses 2003).

1.2 Cardiac hypertrophy

Cardiac hypertrophy is often associated with other CVDs such as hypertension, ischemic heart diseases, and HF (Ho, Wu et al. 1998). It is characterized by an increase in the cardiomyocyte size, increased protein synthesis, as well as altered sarcomeric organization (Rohini, Agrawal et al. 2010). Macroscopically, cardiac hypertrophy can be defined as a thickening of the ventricular wall and/or septum (Liang and Gardner 1999) leading to alterations in chamber size and geometry, and collectively called remodeling (Braunwald and Bristow 2000). Hypertrophy can be considered as a compensatory mechanism that transiently balances biochemical stress and optimizes cardiac pump function;

however, prolonged hypertrophy is a significant risk factor for HF, dilated cardiomyopathy, arrhythmia, and even sudden death (Carreno, Apablaza et al. 2006; Rohini, Agrawal et al. 2010).

1.2.1 Classifications of cardiac hypertrophy

Cardiac hypertrophy may be a physiological or a pathological condition. Physiological hypertrophy occurs during normal postnatal growth, pregnancy, or chronic exercise (Bernardo, Weeks et al. 2010). It is characterized by normal or improved cardiac function, no changes in the cardiac gene expression pattern, and proportional enlargement of the cardiac chambers (Fagard 1997). With regard to cardiac energy metabolism, physiological hypertrophy is characterized by enhanced fatty acid oxidation as well as enhanced glucose utilization (Dyck and Lopaschuk 2006; Bernardo, Weeks et al. 2010). On the other hand, pathological hypertrophy occurs due to chronic pressure or volume overload in a disease setting such as hypertension or valvular heart disease (Bernardo, Weeks et al. 2010). It is characterized by cardiac dysfunction, fibrosis, cardiomyocyte apoptosis or necrosis, and changes of chamber size and geometry (Levy, Labib et al. 1990; Weber and Brilla 1993). At the molecular level, pathological hypertrophy is characterized by re-activation of the cardiac fetal gene expression pattern i.e. upregulation of atrial natriuretic peptide (ANP), B-type natriuretic peptide (BNP), β-myosin heavy chain (β-MHC), and α-skeletal actin (Nadal-Ginard, Kajstura et al. 2003). Regarding cardiac energy metabolism, fatty acid oxidation is decreased, whereas glucose utilization is increased in pathological hypertrophy (Dyck and Lopaschuk 2006; Bernardo, Weeks et al. 2010).

Cardiac hypertrophy can also be classified morphologically to concentric and eccentric hypertrophy (Bernardo, Weeks et al. 2010). Concentric hypertrophy is characterized by an increase in the wall thickness and cardiac mass with a small reduction in the chamber volume (Bernardo, Weeks et al. 2010). Microscopically, it is characterized by parallel additions of the sarcomeres leading to an increase in the cardiomyocyte width more than its length (Gerdes 2002). Concentric hypertrophy usually occurs in response to chronic pressure overload which may be pathological (e.g. hypertension) or physiological (e.g. strength training) (Bernardo, Weeks et al. 2010; Rohini, Agrawal et al. 2010). On the other hand, eccentric hypertrophy is characterized by an increase in the cardiac mass with an increase in the chamber volume leading to cardiac dilatation (Bernardo, Weeks et al. 2010). Microscopically, the sarcomeres are added in series leading to an increase in cardiomyocyte length more than width (Gerdes 2002). Eccentric hypertrophy usually occurs in response to chronic volume overload which may be pathological (e.g. valvular heart disease) or physiological (e.g. endurance training) (Bernardo, Weeks et al. 2010; Rohini, Agrawal et al. 2010).

1.2.2 Signaling pathways in cardiac hypertrophy

1.2.2.1 Calcineurin/nuclear factor of activated T-cells (NFAT)

Calcineurin is a calmodulin-dependent calcium-activated phosphatase that activates transcription factors of the NFAT family by dephosphorylation (Li, Rao et al. 2011). Several mechanical and neurohormonal factors stimulate Ca^{++}-calmodulin binding, which activates the calcineurin/NFAT pathway which in turn

activates other transcription factors such as GATA-4, leading to cardiac hypertrophy (Diedrichs, Hagemeister et al. 2007). In several rodent models of cardiac hypertrophy, pharmacological inhibition of calcineurin attenuated agonist- and pressure overload-induced cardiac hypertrophy (Sussman, Lim et al. 1998; Meguro, Hong et al. 1999). On the other hand, activation of the calcineurin/NFAT pathway in transgenic mice is sufficient to induce cardiac enlargement and HF (Molkentin, Lu et al. 1998). Finally, mice deficient in calcineurin Aβ are generally resistant to several hypertrophic stimuli such as pressure overload or angiotensin II or isoproterenol infusion (Bueno, Wilkins et al. 2002). Of interest, when mice carrying NFAT-luciferase reporter gene were subjected to both physiological and pathological hypertrophic stimuli, NFAT luciferase reporter activity was upregulated only in the pathological models (Wilkins, Dai et al. 2004). Therefore, the calcineurin/NFAT pathway is considered to regulate pathological rather than physiological hypertrophy (Bernardo, Weeks et al. 2010).

1.2.2.2 PI3K/Akt/GSK-3 dependent signaling

Phosphoinositide 3-kinase (PI3K) activation is a downstream target to the stimulation of tyrosine kinase receptors such as insulin-like growth factor (IGF), fibroblast growth factor, transforming growth factor, and G protein coupled receptors (GPCRs). The serine/threonine kinase Akt, also known as protein kinase B (PKB), is one of the principal targets of PI3K activation (Rohini, Agrawal et al. 2010). Cardiac PI3K has been shown to be activated in a model of pressure overload cardiac hypertrophy (Naga Prasad, Esposito et al. 2000). In addition, overexpression of a constitutively active PI3K mutant induced cardiac

hypertrophy in transgenic mice (Shioi, Kang et al. 2000). Similarly, transgenic overexpression of Akt/PKB has been shown to induce cardiac hypertrophy (Shioi, McMullen et al. 2002). Of interest, cardiac systolic function was not affected in all the previous models, suggesting a direct effect of PI3K/Akt activation on the cardiomyocyte size rather than an adaptation to impaired contractility (Frey and Olson 2003). PI3K/Akt activation is thought to induce cardiac hypertrophy through two well-defined downstream targets of Akt, glycogen synthase kinase-3 (GSK-3) and mammalian target of rapamycin (mTOR) (Frey and Olson 2003). mTOR regulates protein synthesis via p70S6 kinase and 4EBP1/eIF4E (Fingar, Salama et al. 2002), whereas GSK-3 activation can induce cardiac hypertrophy through phosphorylation of numerous transcription factors including NFAT, c-Jun, c-myc, signal transducer and activator of transcription (STAT), and nuclear factor κB (NF-κB) (Frey and Olson 2003). It is worth mentioning that the PI3K/Akt signaling pathway is critical for physiological exercise-induced cardiac hypertrophy but not pathological hypertrophy (Bernardo, Weeks et al. 2010).

1.2.2.3 GPCRs

The most important cardiac GPCRs are the adrenergic (several subtypes of α- and β-receptors) and the muscarinic receptors which play an essential role in regulating cardiac function and its adaptation to changes in hemodynamic burden (Rockman, Koch et al. 2002). These receptors are coupled with three main classes of GTP-binding proteins, G_s, G_q/G_{11}, and G_i, which transduce agonist or antagonist-induced signals to the intracellular effectors (Frey and Olson 2003). Angiotensin II, endothelin 1, and α-adrenergic receptors are coupled to $G_{q/11}$, and

all are known to induce cardiomyocyte hypertrophy upon agonist stimulation (Nicol, Frey et al. 2000). The downstream targets of $G_{q/11}$ activation include phospholipase C, mitogen-activated protein kinases (MAPKs), protein kinase C (PKC), and protein kinase A (PKA) which are implicated directly or indirectly in the development of pathological cardiac hypertrophy (Bernardo, Weeks et al. 2010). On the other hand, the β1-receptor which is the most abundant adrenergic receptor in the cardiac tissues is coupled to G_s which in turn activates adenylate cyclase (Frey and Olson 2003). In transgenic mice, overexpression of β1-receptor resulted in an initial increase of the contractile function with a later deterioration of cardiac performance, cardiomyocyte hypertrophy, and fibrosis (Bisognano, Weinberger et al. 2000). Moreover, mice deficient in β1 and β2 adrenergic receptors demonstrated an attenuated hypertrophic response to pressure overload with reduced fibrosis (Kiriazis, Wang et al. 2008). Interestingly, resting catecholamine plasma levels were significantly higher in a mouse model of pathological hypertrophy compared to a mouse model of physiological hypertrophy (Perrino, Naga Prasad et al. 2006). In contrast to the β1-receptor, β2-receptors that couple G_i proteins mediate cardioprotection due to activation of the PI3K/Akt pathway (Chesley, Lundberg et al. 2000).

1.2.2.4 MAPK pathways

MAPK pathways can be classified into three main subfamilies: extracellularly responsive kinases (ERKs), c-Jun N-terminal Kinases (JNKs), and p38 MAPKs (Frey and Olson 2003). Interestingly, overexpression of MAPK phosphatase 1, which inhibits all the three main MAPK pathways, prevented both

agonist-induced hypertrophy *in vitro* and pressure overload-induced hypertrophy *in vivo* (Bueno, De Windt et al. 2001). In addition, transgeneic overexpression of MEK1, a MAPK kinase that activates ERK1/2, induced cardiac hypertrophy characterized by supernormal systolic function and diastolic dysfunction (Bueno, De Windt et al. 2000). In another MAPK module, activation of MEK5 resulted in serial addition of sarcomeres *in vitro* and a severe form of dilated cardiomyopathy *in vivo* (Nicol, Frey et al. 2001). MEKK1/JNK has also been shown to be involved in the hypertrophic response of cardiomyocytes secondary to G_q-coupled receptor stimulation (Bogoyevitch, Andersson et al. 1996). Similarly, p38 activity is increased in pressure overload as well as in phenylephrine- and endothelin-1-induced cardiac hypertrophy models (Ueyama, Kawashima et al. 1999; Takeishi, Huang et al. 2001). Of interest, p38 activates several transcription factors implicated in the hypertrophic response such as myocyte enhancer factor-2 (MEF2) and NFAT (Frey and Olson 2003).

1.2.2.5 Gp130/STAT3 signaling

GP130 activation causes STAT3 translocation to the nucleus with the subsequent induction of several genes involved in hypertrophy and survival pathways (Yamauchi-Takihara and Kishimoto 2000). In transgenic mice, overexpression of STAT3 induced cardiomyocyte hypertrophy both *in vitro* and *in vivo* (Kunisada, Tone et al. 1998; Kunisada, Negoro et al. 2000). On the other hand, gp-130 deficient mice developed dilated cardiomyopathy with massive cardiomyocyte apoptosis when challenged with pressure overload due to aortic band ligation (Hirota, Chen et al. 1999). Therefore, this signaling pathway is

required for the heart's adequate adaptation to biomechanical stresses by promoting cardiomyocyte survival (Frey and Olson 2003).

1.2.2.6 Small G proteins

Small G proteins are also implicated in the development of cardiac hypertrophy. There are five families of these small G proteins: Rho, Ras, ARFs, Rab, Ran (Frey and Olson 2003). Overexpression of a constitutively activated mutant of Ras induced cardiac hypertrophy in transgenic mice (Clerk and Sugden 2000). Ras signaling is coupled to several downstream effectors including PI3K, Raf, MAPK, and NFAT which are implicated in the hypertrophic response (Frey and Olson 2003). Similarly, constitutive activation of Rac in cardiomyocytes induced hypertrophy both *in vitro* and *in vivo* (Pracyk, Tanaka et al. 1998; Sussman, Welch et al. 2000). Finally, overexpression of Rab1a induced cardiac hypertrophy in transgenic mice with subsequent cardiac dilatation and HF (Wu, Yussman et al. 2001).

1.2.2.7 NF-κB

NF-κB is a transcription factor regulating over 200 genes involved in a variety of cellular processes (Ghosh, May et al. 1998; Pahl 1999; Kumar, Takada et al. 2004; Pereira and Oakley 2008). The NF-κB family is comprised of hetero- or homo-dimers of five members, p50, p52, p65 (RelA), RelB, and c-Rel (Kumar, Takada et al. 2004; Pereira and Oakley 2008). Each subunit has its own biological activity; therefore, different dimeric combinations of these subunits have different effects on cell function (Pereira and Oakley 2008). NF-κB can be activated by

many stimuli including cytokines, viruses, oxidative stress, and chemical agents (Guijarro and Egido 2001). Several studies have identified a strong link between NF-κB and cardiac hypertrophy as well as HF (Van der Heiden, Cuhlmann et al. 2010). Activated forms of NF-κB have been found in failing human hearts but not in normal hearts (Saito and Giaid 1999; Frantz, Fraccarollo et al. 2003). Interestingly, activation of NF-κB has been shown to be involved in the hypertrophic response induced by myotrophin in rat neonatal cardiomyocytes (Gupta, Purcell et al. 2002). Similarly, both pharmacological and genetic inhibition of NF-κB attenuated the development of cardiac hypertrophy in aortic-banded rats (Li, Ha et al. 2004). In addition, it has been shown that reactive oxygen species (ROS)-mediated activation of NF-κB is involved in tumor nectrosis factor –α (TNF-α)-induced cardiomyocyte hypertrophy (Higuchi, Otsu et al. 2002). More recently, it has been shown that NF-κB inhibition attenuates cardiac hypertrophy but does not alter the course of stress-induced left ventricular remodeling, suggesting that NF-κB is required for adaptive cardiac hypertrophy (Zelarayan, Renger et al. 2009).

1.2.2.8 Other signaling pathways

There are several other pathways that have also been implicated in cardiac hypertrophy including: MEF2, Na^+/H^+ exchanger, peroxisome proliferator activated receptor (PPAR), and NADPH oxidase (Frey and Olson 2003; Rohini, Agrawal et al. 2010). Overexpression of calcium/calmodulin-dependent protein kinase induced cardiac hypertrophy which was associated with stimulation of MEF2 activity (Zhang, Johnson et al. 2002). Enhanced Na^+/H^+ exchanger activity

increases intracellular Ca^{++} levels which trigger cardiomyocyte hypertrophy via several pathways including Ca^{++}/calmodulin, calcineurin, and MAPK (Luedde, Katus et al. 2006). It has been demonstrated that PPARα expression is significantly reduced during pressure overload-induced cardiac hypertrophy (Rohini, Agrawal et al. 2010). However, it has been demonstrated that PPARα activation causes contractile dysfunction in rat hearts subjected to pressure overload (Young, Laws et al. 2001). With regard to NADPH oxidase, it has been shown that induction of cardiac hypertrophy by angiotensin-II is dependent on NADPH oxidase activation (Hingtgen, Tian et al. 2006).

1.3 DOX-induced cardiotoxicity

Doxorubicin (DOX, adriamycin) is a potent anthracycline chemotherapeutic agent used to treat a wide variety of human malignancies. However, the clinical use of this highly effective drug is limited by a significant DOX-induced cardiotoxicity which can progress to end-stage HF (Christiansen and Autschbach 2006; Outomuro, Grana et al. 2007). DOX has both acute and chronic toxic effects on the cardiovascular system. The acute effects occur in approximately 11% of patients during or soon after DOX administration and include various arrhythmias, hypotension, and acute HF (Takemura and Fujiwara 2007; Zhang, Shi et al. 2009). On the other hand, chronic DOX toxic effects are dose-dependent, irreversible cardiomyopathic changes that affect 1.7% of patients treated with DOX (Von Hoff, Layard et al. 1979). Hearts affected by DOX cardiotoxicity are enlarged with dilatation of all chambers with mural thrombi detected in both ventricles (Takemura and Fujiwara 2007). Myofibrillar loss and vacuolar degeneration are also two features of DOX cardiotoxicity when cardiomyocytes are examined by electron microscopy (Buja, Ferrans et al. 1973).

1.3.1. DOX metabolism and pharmacokinetics

After intravenous (IV) administration of DOX, its plasma concentrations fall dramatically because of its rapid distribution into the tissues with a distribution half-life of 0.036 h (Gustafson, Rastatter et al. 2002). This fast distribution phase is followed by a slow elimination phase due to biliary and renal excretion and metabolism with an elimination half-life of 10.3 h in mice receiving

6 mg/kg of DOX by IV injection (Gustafson, Rastatter et al. 2002). Similar data were reported in humans as DOX distribution and elimination half-lives have been shown to be 0.07 h and 9.87 h, respectively (Bronchud, Margison et al. 1990). The same study has shown that the maximum concentration (C_{max}) of DOX in patients plasma was 2.3 μg/ml (3.9 μM) after a 60 mg/m^2 IV dose (Bronchud, Margison et al. 1990). DOX is mainly metabolized by reductase enzymes to the active metabolite doxorubicinol, and by reductive cleavage of the sugar moiety to the inactive aglycone (Pan and Bachur 1980; Ahmed, Felsted et al. 1981). DOX volume of distribution at steady state (V_{ss}) was estimated to be 15.4 l/kg (Mross, Mayer et al. 1990). It has been shown that DOX distribution from plasma to tissues is correlated with the tissue DNA concentration. In addition, DOX favourably binds to anionic lipids, especially cardiolipin (Terasaki, Iga et al. 1982; Nicolay, Timmers et al. 1984).

1.3.2. Mechanisms of DOX-induced cardiotoxicity

The exact mechanism of DOX-induced cardiotoxicity and its progression to HF has not been fully elucidated yet; however, several mechanisms have been proposed. These mechanisms include increased oxidative stress, apoptotic cell death, altered molecular signaling, and alteration of myocardial energy metabolism (Nakamura, Ueda et al. 2000; Ueno, Kakinuma et al. 2006; Takemura and Fujiwara 2007).

1.3.2.1 Oxidative stress

DOX tends to generate ROS during its metabolism (Wallace 2003). It has been shown that DOX is converted to an unstable semiquinone intermediate that favours ROS generation (Neilan, Blake et al. 2007). In addition, mitochondrial DNA damage induced directly by DOX or indirectly by DOX-generated ROS further lead to respiratory chain failure and generation of more ROS (Lebrecht and Walker 2007). DOX-induced oxidative stress is evident through increased levels of ROS, lipid peroxidation, and reductions in the antioxidants and sulfhydryl group levels (Doroshow, Locker et al. 1979; Doroshow 1983; Singal, Segstro et al. 1985). Of importance, cardiomyocytes express only low levels of the antioxidant enzyme catalase. In addition, selenium-dependent glutathione peroxidase as well as CuZn superoxide dismutase activities are readily reduced by DOX, indicating that reduction in the level of diverse antioxidant enzymes represents a common response to DOX (Li, Danelisen et al. 2002). In addition, cardiomyocytes are very rich in mitochondria which represent about 50% of the cardiomyocyte mass; these mitochondria can serve as a source of as well as a target for ROS (Berthiaume and Wallace 2007). Interestingly, overexpression of physiological antioxidant enzymes such as catalase, superoxide dismutase, thioredoxin-1, or metallothionein in transgenic mice has shown beneficial effects on DOX cardiotoxicity (Simunek, Sterba et al. 2009). Unfortunately, several antioxidant agents like vitamin E or N-acetylcysteine failed to delay or prevent cardiomyopathy in patients treated with DOX (Ladas, Jacobson et al. 2004). Nevertheless, dexrazoxane, the only clinically used agent to prevent DOX

cardiotoxicity, is an iron chelating agent that exerts its protective effect by inhibiting iron-mediated ROS generation (Seifert, Nesser et al. 1994).

1.3.2.2 DOX-induced cell death

Several *in vitro* and *in vivo* studies have suggested that DOX-induced cardiotoxicity is associated with cardiomyocyte apoptosis; however, other forms of cell death can also be implicated in DOX cardiotoxicity (Zhang, Shi et al. 2009). DOX-generated ROS promotes the release of calcium from the sarcoplasmic reticulum by opening the ryanodine receptor, leading to an increase in intracellular calcium levels (Kim, Kim et al. 2006). Mitochondria can capture a large quantity of the released calcium, leading to an increase in mitochondrial calcium levels above a threshold. This high mitochondrial calcium overload triggers mitochondrial permeability transition which eventually results in the release of cytochrome c and apoptosis inducing factor (Childs, Phaneuf et al. 2002; Deniaud, Sharaf el dein et al. 2008). In addition, DNA lesions induced directly by DOX or indirectly by DOX-generated ROS result in increased expression and activation of p53 which up-regulates p53 downstream genes such as the pro-apoptotic Bax (Liu, Mao et al. 2008).

Necrotic cell death is also implicated in DOX cardiotoxicity. Several studies have demonstrated that cardiac expression of pro-inflammatory cytokines, inflammatory cell infiltration, and necrotic cells are increased in the hearts of DOX-treated animals (Riad, Bien et al. 2009; Zhang, Shi et al. 2009). Mechanistically, DOX-generated ROS can lead to mitochondrial calcium

overloading and opening of mitochondrial permeability transition pores which results in mitochondrial swelling, ATP depletion, and eventually necrotic cell death (Gustafsson and Gottlieb 2008). Recently, it has been shown that autophagy also contributes to DOX-induced cell death that was attenuated by GATA-4 preservation (Kobayashi, Volden et al. 2010). Finally, cardiomyocyte senescence may also play a role in DOX cardiotoxicity as it has been shown that cultured neonatal rat cardiomyocytes treated with DOX exhibited characteristic changes similar to cardiomyocytes of aged rats (Maejima, Adachi et al. 2008).

1.3.2.3 Suppression of gene expression

DOX inhibits the expression of several cardiac muscle-specific proteins (Takemura and Fujiwara 2007). It has been shown that DOX causes a dose-dependent inhibition of the expression of α-actin, troponin I, myosin light chain 2, and M isoform of creatine kinase in cardiac muscles which explains the myofibrillar loss that characterizes DOX cardiotoxicity (Ito, Miller et al. 1990). In addition, DOX treatment depletes GATA-4 which regulates myocardial expression of sarcomeric proteins such as myosin heavy chain and troponin I (Kim, Ma et al. 2003; Aries, Paradis et al. 2004). Mechanistically, DOX-induced GATA-4 depletion can be attributed to the inactivation of ERK in hearts affected by DOX cardiotoxicity (Lou, Danelisen et al. 2005).

1.3.2.4 Myocardial energy metabolism

Numerous studies have shown that DOX reduces cardiac energy reserves, particularly ATP and phosphocreatine (PCr), in different animal models of

cardiotoxicity as well as in patients receiving DOX treatment (Tokarska-Schlattner, Wallimann et al. 2006; Tokarska-Schlattner, Zaugg et al. 2006; Maslov, Chacko et al. 2010). This energetic deficit caused by DOX has been firstly attributed to the compromised mitochondrial function (Wallace 2003). More recently, DOX-induced cardiotoxicity has been shown to affect the phosphotransfer network of creatine kinase and the AMP-activated protein kinase signaling pathway (Tokarska-Schlattner, Zaugg et al. 2005).

1.4 Cytochrome P450 (CYP)

Drug Metabolizing Enzymes (DMEs) play a pivotal role in the metabolism, biotransformation, and detoxification of xenobiotics (exogenous compounds) as well as endobiotics (endogenous compounds). DMEs include phase I and phase II metabolizing enzymes in addition to phase III transporters (Meyer 1996; Rushmore and Kong 2002). Phase I DMEs consist mainly of the CYP superfamily of heme-containing enzymes which are expressed abundantly in the liver and at varying degrees in other tissues including the kidney, lung, and heart (Imaoka, Hashizume et al. 2005).

Of interest, several studies examined the expression of CYP enzymes in the heart (Geetha, Marar et al. 1991; Yamada, Kaneko et al. 1992; McCallum, Horton et al. 1993; Fulton, Mahboubi et al. 1995). At the *in vitro* level, gene expression and protein activity of many CYP isozymes have been reported in cultured cardiomyocytes (Thum and Borlak 2000). *In vivo*, CYP enzymes have been reported in explanted human hearts (Thum and Borlak 2000; Delozier, Kissling et al. 2007; Michaud, Frappier et al. 2010) and in the left ventricle of Sprague Dawley (SD) and Spontaneously Hypertensive rats (SHR) (Thum and Borlak 2002).

1.4.1 CYP Classification

CYP consists of families and subfamilies that are classified according to their amino acid sequence similarities (Gonzalez and Nebert 1990; Guengerich 2003). In humans, CYP1, CYP2, and CYP3 families are believed to play the

major role in hepatic and extra-hepatic drug metabolism (Lewis 2003). Other CYP families are more involved in the biosynthesis and/or metabolism of endogenous substances such as arachidonic acid, steroids, vitamin D, and retinoic acid (Danielson 2002).

1.4.1.1 CYP1 family

The CYP1 family includes three members: CYP1A1, CYP1A2, and CYP1B1. CYP1A1 and CYP1B1 are primarily expressed in extra-hepatic tissues, whereas CYP1A2 is mainly expressed in the liver (Danielson 2002). CYP1A1 is responsible for the metabolism of numerous xenobiotics including polycyclic aromatic hydrocarbons (PAHs); therefore, it is associated with the etiology of several cancers (Schrenk 1998). CYP1A2 is involved in the metabolism of many drugs such as amitriptyline, theophylline, warfarin, and zolmitriptan (Danielson 2002).

CYP1A1 and CYP1B1 mRNAs have been detected in rat left ventricular tissue (Thum and Borlak 2002). In humans, the expression of CYP1A1 mRNA has been reported in the right ventricle and the left atrium of patients with dilated cardiomyopathy and in the left ventricle of healthy subjects, whereas CYP1A2 was not detected (Thum and Borlak 2000; Thum and Borlak 2002). In another study, CYP1A1 mRNA was detected in the left ventricular tissue of explanted human hearts (Michaud, Frappier et al. 2010). It is important to mention that the human data were usually extracted from explanted human hearts from patients with end-stage HF who were treated for long periods with several medications

that may have affected CYP expression. The inducibility of CYP1A1 in the heart by treatment with β-naphthoflavone (BNF) *in vivo* and Aroclor 1254 *in vitro* has been reported previously (Granberg, Brunstrom et al. 2000; Thum and Borlak 2000; Brauze, Widerak et al. 2006). A few studies have reported the expression of CYP1A2 in heart tissues. For instance, CYP1A2 mRNA has been detected in the pig heart (Messina, Chirulli et al. 2008). In explanted human hearts, *CYP1B1* has been shown to be the second most abundantly expressed *CYP* gene (Bieche, Narjoz et al. 2007). It was also found to be expressed at a higher basal level than CYP1A1 in human cardiac fibroblasts (Dubey, Jackson et al. 2005). In another study, it has been shown that concentrated ambient particles induce CYP1B1 mRNA in rat hearts (Ito, Suzuki et al. 2008). Similarly, benzo(a)pyrene (BaP), a component of cigarette smoke, has been shown to induce both CYP1A1 and CYP1B1 in the rat heart (Aboutabl, Zordoky et al. 2009). In addition, the aryl hydrocarbon receptor (AhR), which is a transcriptional factor that regulates CYP1A1 and CYP1B1, is highly expressed in the heart (Korashy and El-Kadi 2006). Interestingly, CYP1B1 has been shown to be constitutively expressed in the hearts of both control and AhR deficient mice, which implies the involvement of other pathways that regulate cardiac CYP1B1 (Shimada, Sugie et al. 2003).

1. 4.1.2 CYP2 family

The CYP2 family is considered to be the largest family of CYP in humans (Lewis 2004). CYP2A6 is primarily expressed in the liver where it oxidizes numerous compounds of clinical and toxicological importance (Koskela, Hakkola et al. 1999). However, little information is known about CYP2A7 and CYP2A13

(Danielson 2002). In rodents, CYP2B subfamily enzymes are abundant in hepatic tissues and strongly inducible by bartbiturates; nevertheless, the CYP2B subfamily in humans consists only of CYP2B6 which accounts for less than 1% of hepatic CYP content (Danielson 2002). However, CYP2B6 is involved in the metabolism of some therapeutically important drugs such as selegiline (Hidestrand, Oscarson et al. 2001). CYP2C subfamily proteins represent about 20% of the total hepatic CYP content in humans (Imaoka, Yamada et al. 1996) and are responsible for the metabolism of approximately 20% of all clinically administered drugs (Guengerich 2006).

Although CYP2D6 constitutes only 2% of the total hepatic CYP content in humans, it supports the oxidative metabolism of more than 70 different drugs (Danielson 2002). CYP2E1, the only member of the CYP2E subfamily in humans, catalyzes the metabolism of more than 70 substrates, the majority of which are small hydrophobic compounds that have toxicological importance (Hakkak, Korourian et al. 1996). Moreover, CYP2E1 produces free radicals which cause tissue injury independently of substrate metabolism (Lieber 1997). CYP2J2 is expressed primarily in extrahepatic tissues where it is involved in the metabolism of arachidonic acid into epoxyeicosatrienoic acids (EETs) with significant biological activity (Wu, Moomaw et al. 1996; Zeldin, Foley et al. 1996).

CYP2A6/7, CYP2B6/7, CYP2C8/9/19, CYP2D6, CYP2E1, and CYP2J2 have been detected in human heart tissues (Thum and Borlak 2000; Delozier, Kissling et al. 2007). CYP2E1 mRNA was detected in various parts of the human

heart including the right and left atria, right and left ventricle, and the ventricular septum, whereas *CYP2B6/7, CYP2D6*, and *CYP2C8-19* gene expression were found predominantly in the right ventricle (Thum and Borlak 2000). CYP2J2 has been shown to be the main CYP isoform expressed in human hearts (Bieche, Narjoz et al. 2007; Delozier, Kissling et al. 2007; Michaud, Frappier et al. 2010). In a recent study, the mRNAs of CYP2B6 and CYP2C9 were detected at low levels in only some of the examined human hearts (Michaud, Frappier et al. 2010). In rat, CYP2A1/2, CYP2B1/2, CYP2C23, CYP2E1, and CYP2J3 mRNA were detected in ventricular tissue (Thum and Borlak 2002; Imaoka, Hashizume et al. 2005). Similarly, CYP2D1/5 mRNA was detected at low levels in rat heart (Hiroi, Imaoka et al. 1998). On the contrary, CYP2C11 mRNA was detected only in isolated rat cardiomyocytes (Thum and Borlak 2000) but not in heart tissue (Thum and Borlak 2002). There is not sufficient data about the expression of CYP2B2 in the heart; however, one study detected CYP2B2 in fetal rat heart at the protein level (Czekaj, Wiaderkiewicz et al. 2000). CYP2S1 mRNA was detected at very low levels in fetal and adult human heart as well as in mouse heart (Choudhary, Jansson et al. 2003; Choudhary, Jansson et al. 2005).

1.4.1.3 CYP3 family

In humans, the CYP3A subfamily comprises 4 genes, *CYP3A4*, *CYP3A5*, *CYP3A7*, and *CYP3A43* (Gellner, Eiselt et al. 2001). The most important DME is CYP3A4 which is primarily expressed in the liver and comprises up to 60% of the total hepatic CYP content and is responsible for the metabolism of more than 30% of clinically used drugs (Anzenbacher and Anzenbacherova 2001). CYP3A4 is

involved in the metabolism of a wide variety of drugs including benzodiazepines, macrolide antibiotics, statins, dihydropyridine calcium channel blockers, and others (Martinez-Jimenez, Jover et al. 2007).

CYP3A4/5/7 and CYP3A1/2 have not been detected in human and rat heart tissues, respectively (Thum and Borlak 2002). *In vitro,* CYP3A1 mRNA was detected in isolated cardiomyocytes after 24 hours in culture or after aroclor treatment (Thum and Borlak 2000). In addition, one study detected CYP3A protein in the heart tissue of the pilot whale (Celander, Moore et al. 2000).

1.4.1.4 Other CYP families

Other CYP families are more involved in the biosynthesis and/or metabolism of endogenous compounds. CYP4 family is expressed abundantly in the kidney and to a lesser extent in the liver (Anwar-mohamed, Zordoky et al. 2010; Theken, Deng et al. 2011). The CYP4A isoforms metabolize medium and long chain fatty acids at their ω-carbon (Okita and Okita 2001; Danielson 2002). CYP5A1 (thromboxane A_2 (TxA2) synthase) is the only isoform in the CYP5 subfamily. TxA_2 is derived from arachidonic acid to stimulate platelet aggregation (Nusing, Lesch et al. 1990; Ullrich and Nusing 1990). On the other hand, CYP8A1 is a prostacyclin synthase that converts prostaglandin H_2 (PGH_2) to prostaglandin I_2 (PGI_2, prostacyclin) which counteracts platelet aggregation stimulated by TxA_2 (Ishida, Kuruta et al. 1999). CYP7, CYP11, CYP19, and CYP21 are involved in steroid biosynthesis (Danielson 2002). CYP27B1

catalyzes the conversion of 25-hydroxyvitamin D3 to 1α,25-dihydroxyvitamin D3 which is the active form of vitamin D3 (Inouye and Sakaki 2001).

With regard to the expression of CYP4 enzymes in the heart, CYP4A1 was detected in dog heart tissues and freshly isolated rat cardiomyocytes (Thum and Borlak 2000; Nithipatikom, Gross et al. 2004). Cyp4a12 mRNA was detected in mice hearts (Theken, Deng et al. 2011). CYP4F was also found in the human and dog heart (Cui, Nelson et al. 2000; Bylund, Bylund et al. 2001; Nithipatikom, Gross et al. 2004). CYP11A mRNA was detected in normal and failing human hearts (Young, Clyne et al. 2001), whereas CYP11B1 and CYP11B2 were not detected in normal human heart (Young, Clyne et al. 2001), but CYP11B2 mRNA was detected in rat heart (Silvestre, Robert et al. 1998).

1.4.2 Transcriptional regulation of CYP enzymes

1.4.2.1 AhR

AhR is a member of the basic-helix-loop-helix per-Arnt-Sim gene superfamily of transcription factors (Hahn 2002). The unliganded AhR is found almost exclusively in the cytoplasm complexed with a dimmer of Heat shock protein 90 (Hsp90) and treatment with a ligand causes translocation of the AhR into the nucleus where it heterodimerizes with the AhR nuclear translocator (Arnt) (Xu, Li et al. 2005). Thereafter, the AhR-Arnt heterodimer recognizes a xenobiotic responsive element (XRE) enhancer sequence resulting in the activation of target genes (Xu, Li et al. 2005). AhR regulates the expression of many *CYP* genes including members of the CYP1 family (CYP1A1, CYP1A2,

and CYP1B1) in addition to CYP2S1 (Saarikoski, Rivera et al. 2005). Of interest, it has been shown that the AhR is highly expressed in the heart tissues (Korashy and El-Kadi 2006). In addition, it has been shown that AhR expression is increased in hearts of patients with ischemic and dilative cardiomyopathies as compared to healthy controls (Mehrabi, Steiner et al. 2002). Recently, it has been demonstrated that DOX activates the AhR in the hearts of SD rats as well as in cardiac derived H9c2 cells (Volkova, Palmeri et al. 2011).

1.4.2.2 Constitutive Androstane Receptor (CAR)

CAR is a nuclear receptor which plays an important role in regulating the expression of a battery of genes involved in drug metabolism (Roy-Chowdhury, Locker et al. 2003). Most notably, CAR has been shown to be involved in the regulation of CYP2B6, CYP2C8/9, and CYP3A4 (Sueyoshi, Kawamoto et al. 1999; Goodwin, Hodgson et al. 2002; Xiong, Yoshinari et al. 2002; Pascussi, Gerbal-Chaloin et al. 2003). CAR heterodimerizes with the retinoid X receptor (RXR) which can bind to an array of nuclear receptor binding sites (Baes, Gulick et al. 1994; Pascussi, Dvorak et al. 2003). These binding sites have been identified in several major *CYP* genes: *CYP2B6* (Sueyoshi, Kawamoto et al. 1999), *CYP2C9* (Gerbal-Chaloin, Daujat et al. 2002), and *CYP3A4* (Goodwin, Hodgson et al. 2002). Moreover, CAR has been shown to regulate the expression of CYP reductase (Ueda, Hamadeh et al. 2002), which represents a critical component of CYP-dependent metabolism. Regarding its expression in the heart, one study has shown that the human heart does not express the wild type CAR mRNA; however, it only expresses CAR splice variants which demonstrated compromised

transcriptional activation of a CYP2B6 luciferase reporter (Lamba, Lamba et al. 2004).

1.4.2.3 Pregnane X Receptor (PXR)

PXR or its human ortholog steroid X receptor (SXR) is the predominant regulator of the expression of *CYP3A* genes (Anakk, Kalsotra et al. 2004). Interestingly, the tissue specific distribution of PXR expression resembles that of CYP3A (Beigneux, Moser et al. 2002; Coumoul, Diry et al. 2002). In addition to *CYP3A* genes, PXR can recognize and bind to the responsive elements in CYP2B and CYP2C genes (Ferguson, LeCluyse et al. 2002; Wang, Faucette et al. 2003; Nannelli, Chirulli et al. 2008).

1.4.2.4 Glucocorticoid Receptor (GR)

The role of GR in the regulation of CYP has been a matter of debate (Wang and LeCluyse 2003). Although glucocorticoids such as dexamethasone were identified as CYP3A inducers at the transcriptional level more than 25 years ago (Schuetz, Wrighton et al. 1984), the cloned sequence from the CYP3A promoter failed to bind to GR (Schuetz and Guzelian 1984; Huss, Wang et al. 1996). Moreover, it has been shown that the basal expression of CYP3A was not affected in GR-null mice (Schuetz, Schmid et al. 2000). Pascussi et al showed that treatment with dexamethasone results in a GR-mediated increase in the expression of PXR and/or CAR that leads to the transactivation of CYP3A4 (Pascussi, Drocourt et al. 2001) and the GR can bind to the promoter region of CAR in the presence of dexamethasone (Pascussi, Busson-Le Coniat et al. 2003). However,

the role of the PXR is debated because glucocorticoid-mediated induction of CYP3A4 is decreased by a single base-pair mutation that had no effect on the PXR-mediated induction of CYP3A4 (El-Sankary, Bombail et al. 2002). Recently, it has been demonstrated that GR activation is essential for CYP3A4 induction by glucocorticoids and PXR agonists (Cooper, Cho et al. 2008).

Similar to CYP3A4, dexamethasone potentiated the expression of CYP2B6 induced by several PXR ligands; however, it did not increase CYP2B6 expression when given alone (Wang, Faucette et al. 2003). In addition, glucocorticoid responsive element was identified in the regulatory region of the CYP2C9 promoter (Gerbal-Chaloin, Daujat et al. 2002). In conclusion, GR is an important player in the regulation of many CYP isoforms despite the debate about the exact mechanism by which GR regulates the CYP2 and CYP3 families.

1.4.2.5 PPAR

PPARs are believed to play a crucial role in the regulation of lipoprotein and fatty acid metabolism (Yu, Rao et al. 2003). Activated PPAR binds to a specific upstream region of its target genes known as peroxisome proliferator response elements (Lambe and Tugwood 1996; Tugwood, Aldridge et al. 1996). CYP4A genes are regulated by PPAR and could be induced by a number of peroxisome proliferators such as clofibrate (Xu, Li et al. 2005).

1.4.2.6 RXR

RXR is a common partner which forms heterodimers with other nuclear receptors. The formation of a heterodimer with RXR is an essential step for facilitating the binding and activation of PXR, CAR, and PPAR (Mangelsdorf and Evans 1995; Wang and LeCluyse 2003). Therefore, RXR plays an important role in the CYP transcriptional regulation.

1.4.2.7 Liver X Receptor (LXR) and Farnesoid X Receptor (FXR)

LXRs are transcription factors known as cholesterol sensors as they regulate the transport and metabolism of sterols and fatty acids (Xu, Li et al. 2005). They are primarily located in the nucleus and must form heterodimers with RXR for activation (Khan and Vanden Heuvel 2003). CYP7A (cholesterol 7α-hydroxylase) was identified as the first target gene of LXR (Lehmann, Kliewer et al. 1997). The endogenous oxysterols, such as cholesterol metabolites, are LXR ligands; therefore, a cholesterol rich diet can upregulate CYP7A (Menke, Macnaul et al. 2002). Unlike the LXR, FXR can negatively regulate CYP7A expression (Xu, Li et al. 2005).

1.4.3 CYP expression during HF and cardiac hypertrophy

In human, it has been demonstrated that there is an increase in gene expression of *CYP2A6/7* and *CYP4A11* of two to three fold in hypertrophic left ventricles in comparison to controls (Thum and Borlak 2002). CYP2E1 expression in the microsomal fraction of the myocardium was found to be much

higher in dilated cardiomyopathy than that in healthy human hearts (Sidorik, Kyyamova et al. 2005). In addition, an up-regulation of CYP2J2, CYP1B1, CYP4A10, and CYP2F2 has been reported in the failing human heart (Tan, Moravec et al. 2002; Elbekai and El-Kadi 2006). In rats, expression of CYP1B1, CYP2A1/2, CYP2B1/2, CYP2E1, and CYP2J3 were significantly increased by 8-, 50-, 6-, 6-, and 4-fold respectively in left ventricular tissues of SHRs as compared to normotensive rats (Thum and Borlak 2002). CYP11B1 and CYP11B2 mRNA were found in some chambers of the failing heart, but not in normal heart (Young, Clyne et al. 2001). The changes in CYP expression during cardiac hypertrophy and HF are summarized in table (1.1).

Table (1.1): Changes in *CYP* gene expression during cardiac hypertrophy and HF

Gene	Species	Change	Reference
CYP1B1	Rat	Increased	(Thum and Borlak 2002)
CYP2A1/2	Rat	Increased	(Thum and Borlak 2002)
CYP2A6/7	Human	Increased	(Thum and Borlak 2002)
CYP2B1/2	Rat	Increased	(Thum and Borlak 2002)
CYP2E1	Rat	Increased	(Thum and Borlak 2002)
CYP2E1	Human	Increased	(Sidorik, Kyyamova et al. 2005)
CYP2J3	Rat	Increased	(Thum and Borlak 2002)
CYP4A11	Human	Increased	(Thum and Borlak 2002)
CYP11B1, CYP11B2	Human	Increased	(Young, Clyne et al. 2001)

1.5 CYP-mediated Arachidonic Acid Metabolism

There are several pathways for arachidonic acid metabolism and most of the generated metabolites have distinct biological activity. First, the release of arachidonic acid from its phospholipid storage is catalyzed by activation of intracellular phospholipases (Jenkins, Cedars et al. 2009). Thereafter, free arachidonic acid can be metabolized by cyclooxygenases (COXs), lipoxygenases (LOXs), and CYP enzymes (Roman 2002). The metabolism of arachidonic acid to prostaglandins and leukotrienes by COXs and LOXs, respectively, was recognized many years ago (Roman 2002). LOXs metabolize arachidonic acid to hydroperoxyeicosatetraenoic acids and dihydroxyeicosatetraenoic acids which are subsequently converted to hydroxyeicosatetraenoic acids (HETEs), leukotrienes, or lipoxins (Elbekai and El-Kadi 2006). The role of CYP enzymes in the LOX pathway is limited. In the second pathway, COXs metabolize arachidonic acid to prostaglandins G_2 (PGG_2) and PGH_2. Although this reaction is not catalyzed by CYP enzymes, CYP plays an important role in the subsequent metabolism of PGH_2 to biologically active compounds such as PGI_2 by CYP8A1 (prostacyclin synthase) and TxA_2 by CYP5A1 (thromboxane synthase). However, the role of CYP pathway in arachidonic acid metabolism has recently drawn scientific attention. CYP enzymes involved in arachidonic acid metabolism can be generally classified into CYP epoxygenases and CYP hydroxylases which metabolize arachidonic acid to EETs and HETEs, respectively (Fig. 1.1-2) (Roman 2002).

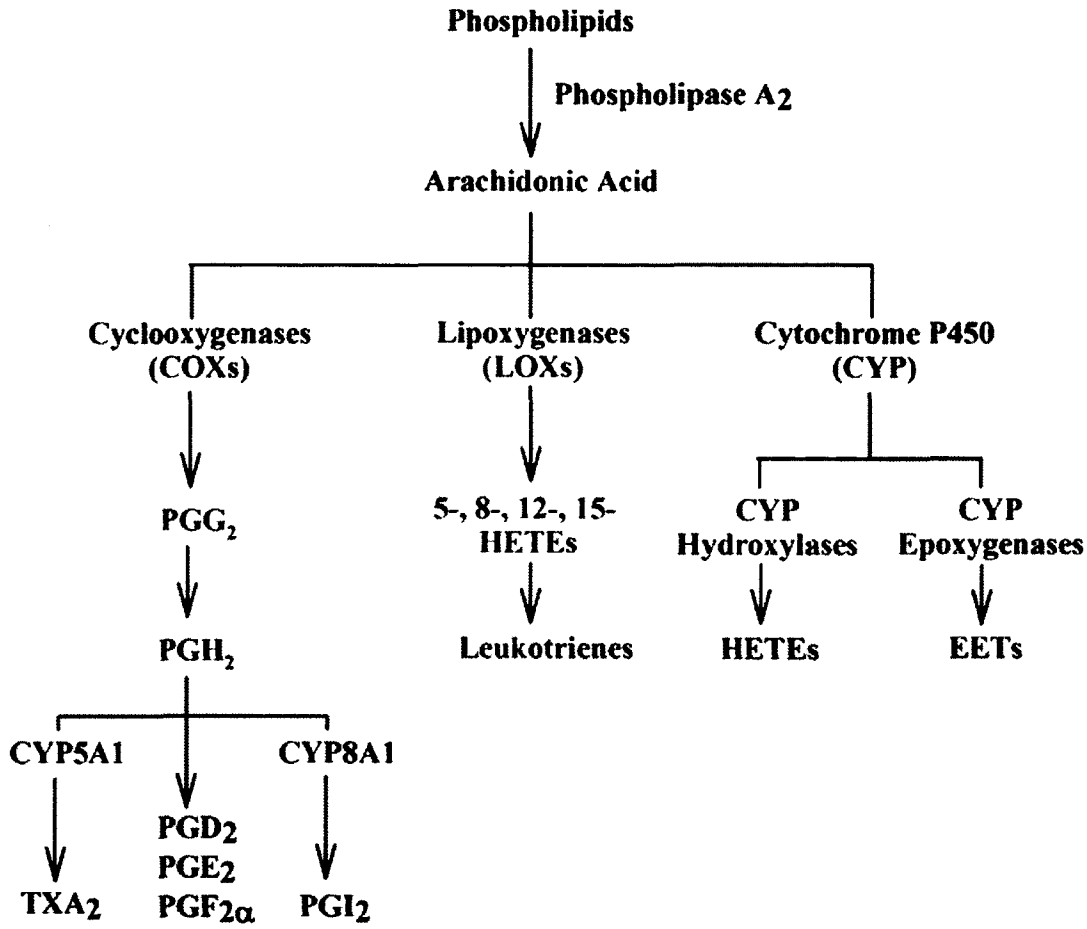

Fig. 1.1 Pathways of arachidonic acid metabolism. Arachidonic acid is metabolized by cyclooxygenases (COXs), lipoxygenases (LOXs), and cytochrome P450 (CYP). COXs metabolize arachidonic acid to PGH_2 which is further metabolized by CYP5A1 and CYP8A1 to TxA_2 and PGI_2, respectively. Leukotrienes are the final arachidonic acid metabolites in the LOXs-mediated pathway. The third pathway is mediated by CYP enzymes that metabolize arachidonic acid to EETs and HETEs.

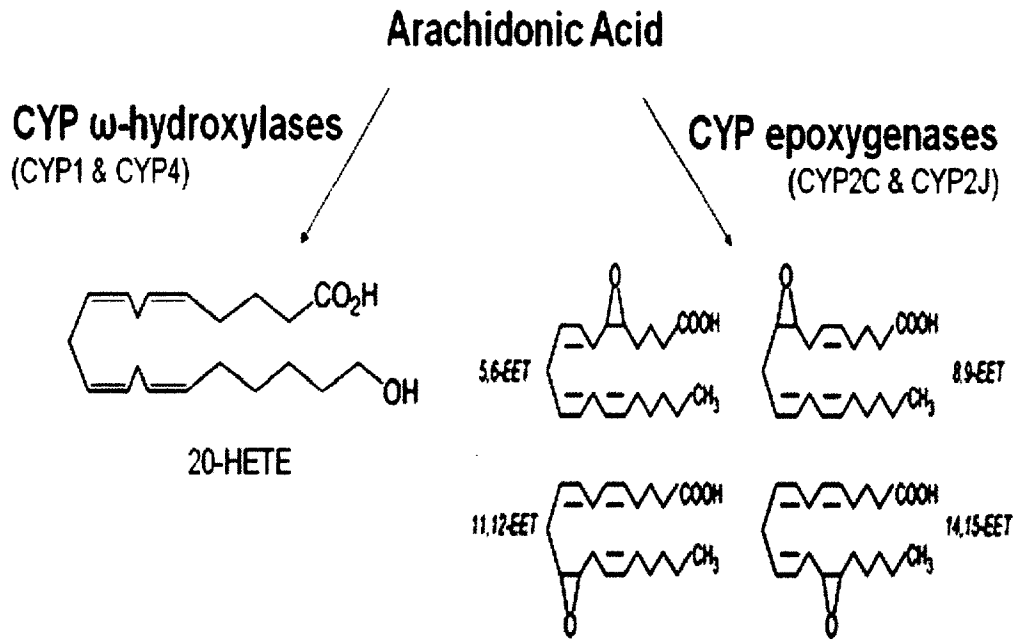

Fig. 1.2 CYP-mediated arachidonic acid metabolism. Arachidonic acid is metabolized by cytochrome P450 (CYP) ω-hydroxylases to 20-hydroxyeicosatetraenoic acid (20-HETE) and by CYP epoxygenases to 5,6-, 8,9-, 11,12-, and 14,15-epoxyeicosatrienoic acids (EETs).

Several CYP enzymes can be considered as CYP epoxygenases and metabolize arachidonic acid to EETs. These mainly include the CYP1A, CYP2B, CYP2C, CYP2E, and CYP2J subfamilies (Imig 2000; Zeldin 2001). Nevertheless, it is generally believed that the CYP2C and CYP2J subfamilies are the major enzymes involved in EET synthesis, especially in cardiovascular tissues (Kroetz and Zeldin 2002; Elbekai and El-Kadi 2006; Jenkins, Cedars et al. 2009). The role of EETs in cardiovascular physiology has been the focus of several excellent reviews (Imig 2000; Zeldin 2001; Kroetz and Zeldin 2002; Roman 2002; Elbekai and El-Kadi 2006; Jenkins, Cedars et al. 2009). Briefly, EETs have been reported to possess vasodilating (Pomposiello, Carroll et al. 2001; Pratt, Li et al. 2001; Zhang, Oltman et al. 2001), anti-inflammatory (Node, Huo et al. 1999; Campbell 2000), fibrinolytic (Node, Ruan et al. 2001), anti-apoptotic (Chen, Capdevila et al. 2001), and potential anti-fibrotic effects (Levick, Loch et al. 2007).

Mechanistically, EETs trigger the opening of calcium-activated potassium channels (K_{Ca}) which may be mediated through activation of PKA (Gebremedhin, Ma et al. 1992). Many reports have proposed that EETs function as the endothelium-derived hyperpolarizing factor (EDHF) because they possess potent vasodilating effects and hyperpolarize vascular smooth muscle cells (VSMCs) by activating K_{Ca} (Hecker, Bara et al. 1994; Gebremedhin, Harder et al. 1998; Medhora, Narayanan et al. 2001). It is important to mention that the vasodilating effect of EETs is regioisomer-selective and organ-specific. Generally, EETs are vasodilators; however, 5,6- and 8,9-EETs can be metabolized by COXs to vasoconstrictor metabolites (Imig, Navar et al. 1996; Zhu, Bousamra et al. 2000;

Roman 2002). Similarly, EETs were found to constrict pulmonary arteries of rabbits *in vitro* and to augment acute hypoxic vasoconstriction in isolated mouse lung (Zhu, Bousamra et al. 2000; Keseru, Barbosa-Sicard et al. 2008). However, the impact of these observations *in vivo* is questionable because a recent report has demonstrated that soluble epoxide hydrolase (sEH) inhibitors which increase the biological level of EETs prevent monocrotaline-induced pulmonary hypertension in rats (Revermann, Barbosa-Sicard et al. 2009).

In addition to their vasodilating effect, EETs have potent anti-inflammatory properties (Node, Huo et al. 1999). They have been reported to decrease the cytokine-induced endothelial expression of vascular cell adhesion molecule-1 and to decrease leukocyte adhesion to the vascular wall by inhibiting NF-κB and IκB kinase (Node, Huo et al. 1999). In addition, activation of the tyrosine kinase and the MAPK signaling pathway may also be involved in mediating the anti-inflammatory effect of EETs (Roman 2002).

In the vascular bed, EETs have been reported to increase endothelial cell growth and angiogenesis (Munzenmaier and Harder 2000; Potente, Fisslthaler et al. 2003; Wang, Wei et al. 2005; Michaelis and Fleming 2006). On the other hand, they inhibit the proliferation of human VSMCs (Davis, Thompson et al. 2002). Therefore, EETs have been proposed to have dual protective effects by promoting neovascularisation in ischemic tissues and inhibiting atherosclerosis (Larsen, Campbell et al. 2007). In addition, EETs have antithrombotic effects by inhibiting platelet adhesion to endothelial cells, inhibiting platelet aggregation, and

enhancing the expression and activity of tissue plasminogen activator (Node, Ruan et al. 2001; Jiang, McGiff et al. 2004; Krotz, Riexinger et al. 2004).

EETs have been reported to be cardioprotective against ischemia-reperfusion injury (Seubert, Yang et al. 2004), DOX-induced cardiotoxicity (Zhang, El-Sikhry et al. 2009), and phenylephrine- or angiotensin II-induced cardiac hypertrophy (Xu, Li et al. 2006). These cardioprotective effect of EETs have been attributed to activation of ATP-sensitive potassium channels, p42/p44 MAPK pathway, and PKA-dependent signaling pathways (Seubert, Yang et al. 2004; Lu, Ye et al. 2006; Batchu, Law et al. 2009) as well as inhibition of NF-κB (Xu, Li et al. 2006). In addition, EETs modulate the activation of several cardiac ion channels. Briefly, EETs have been reported to inhibit cardiac sodium channels (Lee, Lu et al. 1999), modulate cardiac calcium currents (Lu, Lee et al. 1999; Xiao, Ke et al. 2004), and enhance Kv4.2 channels (Ke, Xiao et al. 2007).

In the kidney, EETs are important regulators of glomerular filtration by activating the Na^+/H^+ exchanger (Harris, Munger et al. 1990). In addition, EETs mediate pressure natriuresis and long-term control of blood pressure (Dos Santos, Dahly-Vernon et al. 2004). Furthermore, the role of EETs in cerebral circulation cannot be ignored as they are important regulators of cerebral blood flow (Alkayed, Birks et al. 1996). Astrocytes have been reported to produce EETs upon stimulation by excitatory neurotransmitters (Alkayed, Birks et al. 1997). Therefore, it has been proposed that upon astrocytes stimulation by excitatory neurotransmitters, EETs are synthesized and released to act on cerebral VSMCs to dilate cerebral arteries recruiting more blood flow to the more active regions of

the brain (Harder, Alkayed et al. 1998). EETs are metabolized by sEH to dihyroxyeicosatrienoic acids (DHETs); therefore, sEH inhibitors are used to enhance the biological activity of EETs (Yu, Xu et al. 2000). Several studies have reported that DHETs relax coronary arteries and are equipotent to the EETs (Oltman, Weintraub et al. 1998). However, other studies show that DHETs are not active or less active than EETs (Carroll, Schwartzman et al. 1987; Campbell, Deeter et al. 2002).

With regard to CYP ω-hydroxylases, CYP4A and CYP4F enzymes mainly catalyze the ω-hydroxylation of arachidonic acid to 20-HETE (Powell, Wolf et al. 1998). In addition, CYP1A1, CYP1B1, and CYP2E1 were reported to produce different regioisomers of HETEs (Elbekai and El-Kadi 2006). The role of HETEs in the control of cardiovascular functions has been reviewed previously (Roman 2002; Elbekai and El-Kadi 2006). Most notably, 20-HETE is a potent constrictor of renal, cerebral, mesenteric, and skeletal muscle arterioles (Alonso-Galicia, Falck et al. 1999; Gebremedhin, Lange et al. 2000; Kunert, Roman et al. 2001; Wang, Zhang et al. 2001). The vasoconstrictor effect of 20-HETE can be explained mechanistically through blocking of K_{Ca} in the VSMCs, leading to the increase in intracellular potassium levels with subsequent activation of voltage-gated calcium channels (Harder, Gebremedhin et al. 1994; Imig, Zou et al. 1996; Zou, Fleming et al. 1996; Roman 2002). In addition, 20-HETE mediates growth response in VSMCs in response to norepinephrine and angiotensin II through the MAPK signaling pathway (Muthalif, Benter et al. 1998; Uddin, Muthalif et al. 1998; Muthalif, Parmentier et al. 2000). Similarly, it contributes to the

vasoconstrictor and natriuretic actions of endothelin-1 in the kidney (Oyekan and McGiff 1998). Regarding the cerebral circulation, cerebral microvessels produce 20-HETE when incubated with arachidonic acid (Harder, Gebremedhin et al. 1994; Gebremedhin, Lange et al. 2000). Interestingly, transmural pressure elevation increases 20-HETE levels in rat middle cerebral arteries, thus augmenting myogenic constriction of these vessels (Gebremedhin, Lange et al. 2000).

Nevertheless, 20-HETE has also some beneficial effects as it has anti-platelet effects (Hill, Fitzpatrick et al. 1992) and it inhibits sodium reabsorption in the renal tubules (Fleming 2005). Also 20-HETE inhibits renal Na^+-K^+-ATPase activity as well as sodium transport in the proximal tubule (Schwartzman, Ferreri et al. 1985; Quigley, Baum et al. 2000). Similar to EETs, 20-HETE mediates pressure natriuresis and long-term control of blood pressure (Dos Santos, Dahly-Vernon et al. 2004). On the other hand, 19-HETE stimulates sodium transport in the proximal tubule, most probably by competitively antagonizing 20-HETE (Alonso-Galicia, Falck et al. 1999).

1.6 Soluble epoxide hydrolase (sEH)

sEH enzyme is a phase I DME which has a C-terminal epoxide hydrolase activity which acts on epoxy fatty acids and an N-terminal phosphatase activity which acts on lipid phosphates (Newman, Morisseau et al. 2003; Enayetallah, French et al. 2006). Although the epoxide hydrolase activity is well defined, the biological role of the phosphatase activity is still unknown (Tran, Aronov et al. 2005). Similar to CYP enzymes, sEH plays an important role in arachidonic acid metabolism as it is responsible for metabolizing the EETs to their corresponding DHETs, thus decreasing their biological activity (Imig and Hammock 2009). sEH is widely distributed in numerous tissues in humans as well as in experimental animals; however, it is highly abundant in the liver and kidney (Newman, Morisseau et al. 2005). With regard to its subcellular localization, it is mainly in the cytosolic fraction, but it can also be localized in the peroxisomes (Enayetallah, French et al. 2006). The *EPHX2* gene encodes sEH enzyme which primarily exists as an anti-parallel homodimer of two 62.5 kDa proteins (Morisseau and Hammock 2008).

1.6.1 sEH regulation

Several studies have demonstrated that some endogenous chemical mediators as well as xenobiotics can regulate sEH. sEH has been shown to be induced by the administration of PPARα agonists in rodents (Pinot, Grant et al. 1995). Nevertheless, PPARα-responsive elements have not been identified upstream of the human *EPHX2* gene (Tanaka, Kamita et al. 2008). Of interest, male mice show higher sEH activity in the kidney and liver in comparison to

female mice (Pinot, Grant et al. 1995). However, androgen-responsive elements were not found in the 5'-flanking region of the human *EPHX2* gene (Tanaka, Kamita et al. 2008). In addition, ovarectomy increased sEH activity in both the kidney and liver of female mice, indicating a suppressive effect of female sex hormones on sEH (Pinot, Grant et al. 1995). Angiotensin II has also been shown to directly upregulate *EPHX2* expression in the vascular endothelium and to increase sEH protein and activity in renal cortical tissues (Imig, Zhao et al. 2002; Ai, Fu et al. 2007). This effect can be mediated through the binding of c-Jun to the AP-1 binding site of the *EPHX2* promoter (Tanaka, Kamita et al. 2008). Of interest, *EPHX2* expression was induced in lung, heart, and aortic endothelial cells by exposure to cigarette smoke (Maresh, Xu et al. 2005). Similarly, exposure to gamma radiation has been shown to induce *EPHX2* expression in human cell lines which appears to result from NF-κB induction (Park, Hwang et al. 2002). Recently, it has been found that the redox-sensitive transcriptional factor Sp1 binds to several regulatory elements upstream of the *EPHX2* gene transcriptional start site, and this binding is essential for *EPHX2* gene expression (Tanaka, Kamita et al. 2008).

1.6.2 sEH in CVDs

Inhibition of sEH has been shown to result in a hypotensive effect in a variety of animal models of hypertension (Imig and Hammock 2009). The mechanism by which sEH inhibition causes this hypotensive effect is thought to depend on decreased vascular resistance and increased kidney sodium excretion which are consistent with the known biological actions of EETs (Yu, Xu et al.

2000; Spector, Fang et al. 2004; Imig 2005). In addition, sEH inhibition offered some protection against end-organ damage in these hypertensive models (Zhao, Yamamoto et al. 2004). In addition to its hypotensive effects, inhibition of sEH has been shown to have cardioprotective effects in animal models of ischemia-reperfusion injury (Gross, Gauthier et al. 2008). Interestingly, *Ephx2*-deficient mice demonstrated improved functional recovery with reduced infarct size after ischemia-reperfusion injury (Seubert, Sinal et al. 2006).

With regard to its role in cardiac hypertrophy, sEH inhibition has been shown to prevent cardiac hypertrophy in stroke-prone spontaneous hypertensive and angiotensin-infused rats (Li, Carroll et al. 2008; Ai, Pang et al. 2009). Similarly, sEH inhibition prevented and reversed left ventricular hypertrophy in mice with pressure overload-induced cardiac hypertrophy (Xu, Li et al. 2006). In addition, *Ephx2*-deficient mice are protected from pressure overload-induced HF and cardiac arrhythmias (Monti, Fischer et al. 2008). Recently, it has been shown that sEH inhibition protects against BaP-induced cardiac hypertrophy in male SD rats (Aboutabl, Zordoky et al. 2011).

1.7 The role of the AhR in cardiac hypertrophy

CVDs are considered the main cause of death in the Western world and cigarette smoking is responsible for about one third of those CVD deaths (Korashy and El-Kadi 2006). Cigarette smoke contains thousands of PAHs which are known to activate the AhR (Ding, Trommel et al. 2005). Therefore, several studies suggested the role of AhR ligands in the pathogenesis of CVDs including ischemic heart diseases, myocardial infarction, hypertension, atherosclerosis, HF, and cardiac hypertrophy (Korashy and El-Kadi 2006).

2,3,7,8-Tetrachlorodibenzo-p-dioxin (TCDD), the most potent AhR ligand, has been shown to cause significant cardiotoxic effects in several avian and fish models (Walker, Pollenz et al. 1997; Kanzawa, Kondo et al. 2004; Aragon, Goens et al. 2008). Injection of TCDD, 0.24 to 0.4 pmol/g in chicken eggs, resulted in cardiac hypertrophy which was manifested by a 77% increase in heart size (Kanzawa, Kondo et al. 2004). In another chick embryo model, TCDD injection caused dilated cardiomyopathy and congestive HF (Walker and Catron 2000). In utero TCDD administration caused cardiac hypertrophy in the adult offspring with a significant induction of genes associated with extra-cellular matrix remodeling (Aragon, Kopf et al. 2008). Of interest, it has been shown that sub-chronic administration of TCDD causes hypertension and cardiac hypertrophy in adult male C57BL/6 mice (Kopf, Huwe et al. 2008). Similarly, chronic administration of TCDD for 2 years to female SD rats was associated with significant cardiomyopathy (Walker and Catron 2000). More recently, it has been shown that a one week treatment with two other AhR ligands, BaP and 3-methyl

cholanthrene (3-MC), cause cardiac hypertrophy in adult male SD rats (Aboutabl, Zordoky et al. 2009).

AhR activation has been shown to mediate the cardiotoxic effect of TCDD and other halogenated aromatic hydrocarbons (Heid, Walker et al. 2001). Interestingly, it has been shown that AhR mRNA and protein are highly expressed in the heart and the AhR protein is two-fold higher in dilated and ischemic cardiomyopathy than in healthy subjects (Dolwick, Swanson et al. 1993; Mehrabi, Steiner et al. 2002) which implies an important role of the AhR in the pathogenesis of heart diseases. In addition, it has been shown that both AhR and its common dimer partner, ARNT, are constitutively expressed in the atria and ventricles of embryonic chicken hearts during the cardiogenesis process (Kanzawa, Kondo et al. 2004). Similarly, ARNT is markedly expressed in chicken embryo as well as rat heart (Carver, Hogenesch et al. 1994; Walker, Pollenz et al. 1997; Catron, Mendiola et al. 2001).

The mechanisms by which AhR ligands can cause cardiac hypertrophy are not fully elucidated. However, three mechanisms have been proposed: oxidative stress and DNA adduct formation, induction of inflammatory and hypertrophic genes, and disrupted metabolism of endogenous compounds such as arachidonic acid (Korashy and El-Kadi 2006; Rifkind 2006). AhR regulates the expression of many CYP enzymes including members of CYP1 family (CYP1A1, CYP1A2, and CYP1B1) which play an important role in arachidonic acid metabolism (Korashy and El-Kadi 2006; Rifkind 2006). CYP1A1 and CYP1B1 mRNAs have been detected in the rat heart (Thum and Borlak 2002). In human, the expression

of CYP1A1 mRNA has been reported in the right ventricle and the left atrium of patients with dilated cardiomyopathy and in the left ventricle of healthy subjects (Thum and Borlak 2000). It has been shown that treatments with AhR ligands such as BaP and 3-MC significantly induce cardiac CYP1A1 and CYP1B1 in male SD rats, which result in derailed arachidonic acid metabolism with an increase in the 20-HETE to EETs ratio (Aboutabl, Zordoky et al. 2009). Interestingly, AhR ligand-induced cardiac hypertrophy was partially prevented by inhibiting the 20-HETE formation with an ω-hydroxylase inhibitor or increasing the level of EETs by an sEH inhibitor (Aboutabl, Zordoky et al. 2009; Aboutabl, Zordoky et al. 2011).

1.8 RATIONALE, HYPOTHESES, AND OBJECTIVES

1.8.1 Rationale

HF affects more than 5 million people in North America with about half a million of new cases every year (Kim and Hunt 2003). In Canada, HF affects more than 400,000 patients and costs more than one billion dollars annually for inpatient care alone (O'Connell 2000). Cardiac hypertrophy is an independent risk factor for developing HF (Ritter and Neyses 2003). The expression of several *CYP* genes was identified in the heart and their levels have been reported to be altered during cardiac hypertrophy and HF; however, there is a great discrepancy among various reports on CYP alterations during cardiac hypertrophy and HF, likely due to differences in the aetiology of hypertrophy, disease severity, species in question and other underlying conditions.

CYP enzymes are considered one of the major metabolic enzymes for the metabolism of arachidonic acid in addition to COXs and LOXs. In the presence of NADPH and oxygen, CYP enzymes metabolize arachidonic acid to metabolites of EETs and HETEs, which have significant biological roles in the regulation of the cardiovascular system (Imig, Zhao et al. 2002). However, the effect of experimentally induced cardiac hypertrophy on CYP expression or the effect of cardiac hypertrophy on CYP-mediated arachidonic acid metabolism has never been investigated.

Smoking is responsible for about one third of deaths related to CVDs (Korashy and El-Kadi 2006). Cigarette smoke contains thousands of PAHs which are known to activate the AhR (Ding, Trommel et al. 2005). Therefore, several

studies suggested the role of AhR ligands in the pathogenesis of CVDs including ischemic heart diseases, myocardial infarction, hypertension, atherosclerosis, HF, and cardiac hypertrophy (Korashy and El-Kadi 2006). Nevertheless, the mechanisms by which AhR activation causes cardiac hypertrophy are not fully elucidated. AhR regulates the expression of many CYP enzymes including members of CYP1 family, *CYP1A1*, *CYP1A2*, and *CYP1B1* (Korashy and El-Kadi 2006). However, the role of CYP induction and the subsequent alteration of CYP-mediated arachidonic acid metabolism as a possible mechanism of AhR-induced cardiac hypertrophy have not been investigated before.

In addition to cardiac hypertrophy as a predisposing factor to HF, drug-induced cardiotoxicity is another common cause of HF (Maxwell and Jenkins 2011). A well characterized example of drug-induced HF is DOX-induced cardiotoxicity. DOX is a potent anthracycline chemotherapeutic agent used to treat a wide variety of human malignancies. However, the clinical use of this highly effective drug is limited by a significant DOX-induced cardiotoxicity which can progress to end-stage HF (Christiansen and Autschbach 2006; Outomuro, Grana et al. 2007). The exact mechanism of DOX-induced cardiotoxicity and its progression to HF has not been fully elucidated yet; however, several mechanisms have been suggested. Nevertheless, the effect of DOX-induced cardiotoxicity on CYP expression and CYP-mediated arachidonic acid metabolism has never been reported.

1.8.2 Hypotheses

Our studies were done to test the following hypotheses:

(1) Isoproterenol-induced cardiac hypertrophy alters cardiac CYP and sEH expression with a subsequent decrease of the cardioprotective EETs and an increase of the formation of the cardiotoxic 20-HETE.

(2) The cardiac-derived H9c2 cells express CYP enzymes at comparable levels to those expressed in the rat heart.

(3) AhR ligands induce hypertrophy of the cardiac-derived H9c2 cells.

(4) Acute DOX cardiotoxicity induces cardiac CYP and sEH enzymes both *in vitro* and *in vivo*.

(5) Acute DOX toxicity causes selective and organ-specific alteration of CYP-mediated arachidonic acid metabolism.

1.8.3 Objectives

The specific objectives of the studies described here were:

(1) To investigate the effect of isoproterenol-induced cardiac hypertrophy on the expression of CYP and *EPHX2* genes in the heart, lung, kidney, and liver of male SD rats.

(2) To examine the effect of isoproterenol-induced cardiac hypertrophy on the CYP-mediated arachidonic acid metabolism in the hearts of male SD rats.

(3) To investigate *CYP* gene expression in cardiac-derived H9c2 cells as compared to the rat heart and liver.

(4) To determine whether two AhR ligands, TCDD and BNF, induce hypertrophy in cardiac-derived H9c2 cells.

(5) To investigate the effect of DOX on the expression of *CYP* genes in cardiac-derived H9c2 cells.

(6) To examine the effect of acute DOX toxicity on the expression of CYP and sEH enzymes as well as CYP-mediated arachidonic acid metabolism in the heart of male SD rats.

(7) To examine the effect of acute DOX toxicity on the expression of CYP and sEH enzymes as well as CYP-mediated arachidonic acid metabolism in the kidney and liver of male SD rats.

The significance of this work derives from its great impact on understanding the role of CYP enzymes and their associated arachidonic acid metabolites in the pathogenesis of cardiac hypertrophy and DOX-induced cardiotoxicity. Better understanding of the pathogenesis of cardiac hypertrophy and DOX-induced cardiotoxicity may allow us to develop rational therapies to prevent and/or treat them. As cardiac hypertrophy and DOX-induced cardiotoxicity are predisposing factors to HF, these rational therapies will diminish morbidity and mortality of HF.

CHAPTER 2

MATERIALS AND METHODS

2.1. CHEMICALS

Dulbecco's modified Eagle's medium base (DMEM), BNF, and ethidium bromide were purchased from Sigma-Aldrich (St. Louis, MO). Amphotericin B and 100x vitamin supplements were purchased from ICN Biomedicals Canada (Montreal, QC). Gentamicin sulfate, penicillin-streptomycin, L-glutamine, minimal essential medium nonessential amino acids solution, fetal bovine serum, agarose, and TRIzol reagent were purchased from Invitrogen (Carlsbad, CA). Bromphenol blue was purchased from Bio-Rad (Hercules, CA). High-Capacity cDNA Reverse Transcription Kit, SYBR Green SuperMix, and 96-well optical reaction plates with optical adhesive films were purchased from Applied Biosystems (Foster City, CA). Primers for conventional as well as real-time polymerase chain reaction (PCR) were synthesized by Integrated DNA Technologies Inc. (San Diego, CA) according to previously published sequences. Arachidonic acid metabolites standards 5,6-EET, 8,9-EET, 11,12-EET, 14,15-EET, 5,6-DHET, 8,9-DHET, 11,12-DHET, 14,15-DHET and 20-HETE were obtained from Cayman Chemical (Ann Arbor, MI). Reagents used for liquid chromatographic-electrospray ionization-mass spectrometry (LC-ESI-MS) were at HPLC-grade. Acetonitrile and water (HPLC grade) were purchased from EM Scientific (Gibbstawn, NJ). CytoTox-ONE kit was purchased from Promega (Madison, WI). Trans-4-[4-(3-Adamantan-1-yl-ureido)-cyclohexyloxy]-benzoic acid (tAUCB) was a generous gift from Dr Bruce Hammock (University of California, Davis, CA). Acrylamide, *N*',*N*'-bis-methylene-acrylamide, ammonium persulphate, ß-mercaptoethanol, glycine, nitrocellulose membrane (0.45 μm), and

TEMED were purchased from Bio-Rad Laboratories (Hercules, CA). Chemiluminescence Western blotting detection reagents were purchased from GE Healthcare Life Sciences (Piscataway, NJ). CYP1B1 rabbit polyclonal primary antibody was purchased from BD Gentest (Bedford, MA). CYP2J and sEH primary antibodies were obtained as generous gifts from Dr Darryl Zeldin (National Institute of Environmental Health Sciences, National Institutes of Health, Research Triangle Park, NC) and Dr Bruce Hammock (Department of Entomology, University of California, Davis, CA), respectively. Other primary and secondary antibodies were purchased from Santa Cruz Biotechnology, Inc. (Santa Cruz, CA). All other chemicals were purchased from Fisher Scientific Co. (Toronto, ON).

2.2. Cell culture and treatments

To test the hypotheses raised in this work, cardiac-derived H9c2 cells were utilized. H9c2 cells (American Type Culture Collection, Manassas, VA) were maintained in DMEM, without phenol red, supplemented with 0.45% glucose, 0.15% sodium bicarbonate, 0.11% sodium pyruvate, 10% fetal bovine serum, 20 μM L-glutamine, 50 μg/ml gentamicin sulfate, 100 IU/ml penicillin, 10 μg/ml streptomycin, and 25 ng/ml amphotericin B. Cells were grown in 75-cm^2 tissue culture flasks at 37°C in a 5% CO_2 humidified incubator.

To investigate the inducible expression of CYP1A1, CYP1A2, and CYP1B1 in H9c2 cells, the cells were treated with BNF. BNF was dissolved in dimethyl sulfoxide (DMSO). The control cells were treated with the same solvent

concentration. For analysis of mRNA, ~1 x 10^6 cells were added to a petri-dish tissue culture plate in 6 ml of serum-free culture media. On 60 to 80% confluence (2–3 days), appropriate stock solutions of BNF were directly added to the culture media for 6 hours. To investigate the hypertrophic effect of AhR ligands on H9c2 cells, cells were grown at a density of 1–1.5 × 10^6 cells per well in a 6-well tissue culture plate. On 60 to 80% confluence (2–3 days), appropriate stock solutions of TCDD and BNF were directly added to the culture media for 24 h or 48 h. To investigate the effect of DOX on *CYP* and *EPHX2* gene expression, cells were grown at a density of 1-1.5 x 10^6 cells per well in a 6-well tissue culture plate. On 60 to 80% confluence (2–3 days), appropriate stock solutions of DOX were directly added to the culture media for two hours then replaced by normal medium for 24 hours.

2.3. Measurement of cell viability

The effect of TCDD, BNF, and DOX on cell viability was determined by measuring the capacity of reducing enzymes present in viable cells to convert 3-[4,5-dimethylthiazol-2-yl]-2,5-diphenyltetrazolium bromide (MTT) to formazan crystals as described previously (Korashy and El-Kadi 2004). Briefly, after incubating the cells with the test compounds for the specified time period in a 96-well cell culture plate at 37 °C under a 5% CO_2 humidified incubator, the media were removed and a 100 µl of serum-free medium containing 1.2 mM MTT was added to each cell culture well. The plate was then re-incubated at 37 °C for 2 h. The media were then decanted off and 100 µl of isopropyl alcohol were added to

each well with shaking for 1 h to dissolve the formed formazan crystals. The color intensity in each well was measured at a wavelength of 550 nm using EL 312e 96-well microplate readers, Bio-Tek Instruments Inc (Winooski, VT). The percentage of cell viability was calculated relative to control wells designated as 100% viable cells. To investigate the effect of TCDD and BNF on cell viability, H9c2 cells were treated for 48 h with increasing concentrations of TCDD and BNF, whereas to test the effect of DOX on cell viability, H9c2 cells were treated for 2 h with increasing concentrations of DOX. Thereafter, the media were replaced by DOX-free media for 24 h before assessment of the cell viability as described above.

2.4. Measurement of cell surface area

The hypertrophic effect of TCDD and BNF was determined by measuring H9c2 cell surface area after 48 h incubation with 1 nM TCDD or 10 μM BNF as compared to control untreated cells. Phase contrast images have been taken with Zeiss Axio Observer Z1 inverted microscope using a 20x objective lens. Surface area was then quantified by imaging to the complete boundary of individual cells with Zeisss Axion Vision Software (Carl Zeiss Imaging Solutions). Ten different images have been taken and twenty five cells were counted for each treatment group.

2.5 Determination of ROS production

Intracellular ROS was analyzed fluorometrically by measuring the oxidation of a non-fluorescent probe, dichlorofluorescin diacetate (DCF-DA), to a fluorescent metabolite, dichlorofluorescein (DCF), by the ROS as described

previously (Korashy and El-Kadi 2006). Cells grown to 90% confluence in 96-well cell culture plates were treated for 24 h with the AhR ligands, TCDD and BNF and 10 μM DCF-DA. DOX was used as a positive control. Thereafter, the fluorescence was directly measured using excitation and emission wavelengths of 485 and 535 nm, respectively using a Baxter 96-well reader.

2.6 RNA extraction from cell cultures

After incubation with the test compounds for the specified time periods, total RNA from H9c2 cells was isolated using TRIzol reagent (Invitrogen, Grand Island, NY) according to the manufacturer's instructions. Briefly, 600 μl of TRIzol reagent were added to each well in the six-well cell culture plates to lyse the cells. Cell lysates were then collected into 1.5 ml Eppendorf tubes and mixed with 120 μl chloroform followed by centrifugation at 12,000x g for 15 min at 4 °C. The aqueous upper phase which contains the RNA was then transferred to a fresh tube and 300 μl isopropyl alcohol were then added to each tube to precipitate the RNA by cooling the samples at – 20 °C for at least 4 h. Following centrifugation at 12,000x g for 10 min at 4 °C, the RNA pellet was washed once with 75% ethanol in diethyl pyrocarbonate (DEPC)-treated water, and then dissolved in DEPC-treated water. RNA was then quantified by measuring the absorbance at 260 nm.

2.7 Animals

All experimental procedures involving animals were approved by the University of Alberta Health Sciences Animal Policy and Welfare Committee. Male SD rats weighing 250-350 g were obtained from Charles River Canada (St. Constant, QC). To compare the inducible expression of CYP1A1, CYP1A2, and CYP1B1 in H9c2 cells to those in the rat heart, animals were treated intraperitoneally (IP) with 80 mg/kg BNF (dissolved in warm corn oil) or corn oil alone for 3 days and euthanized 24 hours following the last injection under halothane anesthesia (n = 3 in each group). All animals were allowed free access to food and water throughout the treatment period. Liver and heart tissues were excised, immediately frozen in liquid nitrogen, and stored at -80°C until analysis.

To investigate the effect of isoproterenol-induced cardiac hypertrophy on *CYP* and *EPHX2* gene expression, animals were treated with 5 mg/kg isoproterenol (dissolved in normal saline) by IP injections daily for 7 days (n = 6). Weight-matched controls received the same volume of normal saline daily for 7 days (n = 6). Animals were euthanized 24 h following the last injection under isoflurane anesthesia. All animals were allowed free access to food and water throughout the treatment period. Heart, lung, kidney, and liver tissues were excised, immediately frozen in liquid nitrogen, and stored at -80°C until analysis. The heart and body weights were recorded for each animal and the heart weight to body weight ratio was calculated.

For the acute DOX toxicity study, animals were treated IP with a single 15 mg/kg DOX (n = 18). Weight-matched controls received the same volume of normal saline (n = 18). Animals were euthanized at 6, 18, and 24 h following the treatment under isoflurane anesthesia. All animals were allowed free access to food and water throughout the treatment period. The amount of food consumed by each animal was recorded and the animals were weighed before and 24 h after DOX administration. The hearts, kidneys, and livers were excised, immediately frozen in liquid nitrogen, and stored at -80°C until analysis.

2.8 RNA extraction from tissues

Total RNA from frozen tissues was isolated using TRIzol reagent (Invitrogen, Grand Island, NY) according to the manufacturer's instructions. Briefly, 800 µl of TRIzol reagent were used to homogenize approximately 0.25 g of the tissue. The tissue homogenates were then collected into 1.5 ml Eppendorf tubes and mixed with 160 µl chloroform followed by centrifugation at 12,000 x g for 15 min at 4 °C. The aqueous upper phase which contains the RNA was then transferred to a fresh tube and 400 µl of isopropyl alcohol were then added to each tube to precipitate the RNA by cooling the samples at – 20 °C for at least 4 h. Following centrifugation at 12,000 x g for 10 min at 4 °C, the RNA pellet was washed once with 75% ethanol in DEPC-treated water, and then dissolved in DEPC-treated water. RNA was then quantified by measuring the absorbance at 260 nm.

2.9 Reverse Transcription (RT) and conventional PCR

Purified total RNA (2.5 μg) was used in each reaction. PCR was performed using Taq DNA polymerase (Invitrogen, Grand Island, NY) according to the manufacturer's instructions. RT reaction mixture (5 μl) was used for each PCR reaction. The primers used in the current study were chosen from previously published studies (Thum and Borlak 2002; Caron, Rioux et al. 2005; Imaoka, Hashizume et al. 2005) and are listed in Table 2.1. PCR reactions were carried out in a thermal cycler (Perkin Elmer, Norwalk, CT) using the following melting, annealing, and extension cycling conditions: initial denaturation for 5 min at 95°C, denaturation for 90 sec at 95°C, annealing for 60 sec at 55°C, and extension for 90 sec at 72°C for 40 cycles and final extension for 7 min at 72°C. Agarose gel electrophoresis was used to separate PCR-amplified products. Ethidium bromide was added to the gel before solidification. PCR products were visualized under a UV transluminator and digitally recorded using Gel DOC-It imaging system, UVP Bioimaging system (Upland, CA).

2.10 RT and Real-time PCR

After isolation and quanification of the total RNA, first-strand cDNA synthesis was performed by using the High-Capacity cDNA RT kit (Applied Biosystems) according to the manufacturer's instructions. Briefly, 1.5 μg of total RNA from each sample was added to a mix of 2.0 μl 10X RT buffer, 0.8 μl 25X dNTP mix (100 mM), 2.0 μl 10X RT random primers, 1.0 μl MultiScribe™ reverse transcriptase, and 3.2 μl nuclease-free water. The final reaction mix was kept at 25 °C for 10 min, heated to 37 °C for 120 min, heated for 85 °C for 5 sec,

and finally cooled to 4 °C. Quantitative analysis of specific mRNA expression was performed by real time-PCR by subjecting the resulting cDNA to PCR amplification using 96-well optical reaction plates in the ABI Prism 7500 System (Applied Biosystems). Each 25-µl reaction mix contained 0.1 µl of 10 µM forward primer and 0.1 µl of 10 µM reverse primer (40 nM final concentration of each primer), 12.5 µl of SYBR Green Universal Mastermix, 11.05 µl of nuclease-free water, and 1.25 µl of cDNA sample. The primers used in the current study were chosen from previously published studies (Bleicher, Pippert et al. 2001; Kalsotra, Anakk et al. 2002; Wang, Hartley et al. 2003; Hirasawa, Kawagoe et al. 2005; Rollin, Mediero et al. 2005; Baldwin, Bramhall et al. 2006) and are listed in Table 2.2. Assay controls were incorporated onto the same plate, namely, no-template controls to test for the contamination of any assay reagents. After sealing the plate with an optical adhesive cover, the thermocycling conditions were initiated at 95°C for 10 min, followed by 40 PCR cycles of denaturation at 95°C for 15 sec, and annealing/extension at 60°C for 1 min. Melting curve (dissociation stage) was performed by the end of each cycle to ascertain the specificity of the primers and the purity of the final PCR product. The real-time PCR data were analyzed using the relative gene expression i.e. ($2^{-\Delta\Delta CT}$) method as described in Applied Biosystems User Bulletin No.2 and explained further by Livak et al (Livak and Schmittgen 2001). Briefly, the data are presented as the fold change in gene expression normalized to the endogenous reference gene and relative to a calibrator. The untreated control was used as the calibrator when the change of gene expression by a specific treatment is being studied, the *CYP* of lowest

expression was used as a calibrator to compare the expression of different *CYP* genes, and the expression in the heart was used as a calibrator to compare the expression of a specific gene among different organs.

Table 2.1. Primer sequences used for conventional PCR reactions

Gene	Forward Primer	Reverse Primer
CYP1A1	CTGGTTCTGGATACCCAGCTG	CCTAGGGTTGGTTACCAGG
CYP1A2	GTCACCTCAGGGAATGCTGTG	GTTGACAATCTTCTCCTGAGG
CYP1B1	CTCTCCCCCATCCACATCTA	AGACGAACATGACCCCTACG
CYP2A1	CACAGGGCAGCTCTATGACA	CAGACCCAGCAAAGAAGAGG
CYP2B1	GCTCAAGTACCCCCATGTCG	ATCAGTGTATGGCATTTTACTGCGG
CYP2B2	CTTTGCTGGCACTGAGACCG	ATCAGTGTATGGCATTTTGGTACGA
CYP2C11	CTGCTGCTGCTGAAACACGTG	GGATGACAGCGATACTATCAC
CYP2C13	CTGGCAATCATGGTGACTGA	GAAACTCCTTGCTGTCATGC
CYP2C23	GATGCTGTCTTCCGTCATGC	GTAATAGGCTTGATGTCAAG
CYP2E1	CTCCTCGTCATATCCATCTG	GCAGCCAATCAGAAATGTGG
CYP2J3	GGCATGCCCTTAATCAAAGA	AGCCTCAGCATCTCCTGAAA
CYP3A1	GGAAATTCGATGTGGAGTGC	AGGTTTGCCTTTCTCTTGCC
CYP3A2	TACTACAAGGGCTTAGGGAG	CTTGCCTGTCTCCGCCTCTT
GAPDH	GGCCAAGGTCATCCATGA	TCAGTGTAGCCCAGGATG

Table 2.2. Primer sequences used for real-time PCR reactions

Gene	Forward Primer	Reverse Primer
CYP1A1	CCAAACGAGTTCCGGCCT	TGCCCAAACCAAAGAGAATGA
CYP1B1	GCTTTACTGTGCAAGGGAGACA	GGAAGGAGGATTCAAGTCAGGA
CYP2B1	AACCCTTGATGACCGCAGTAAA	TGTGGTACTCCAATAGGGACAAGATC
CYP2B2	CCATCCCTTGATGATCGTACCA	AATTGGGGCAAGATCTGCAAA
CYP2C11	CACCAGCTATCAGTGGATTTGG	GTCTGCCCTTTGCACAGGAA
CYP2E1	AAAGCGTGTGTGTGTTGGAGAA	AGAGACTTCAGGTTAAAATGCTGCA
CYP2J3	CATTGAGCTCACAAGTGGCTTT	CAATTCCTAGGCTGTGATGTCG
CYP4A1	TTGAGCTACTGCCAGATCCCAC	CCCATTTTTGGACTTCAGCACA
CYP4A2	CTCGCCATAGCCATGCTTATC	CCTTCAGCTCATTCATGGCAATT
CYP4A3	CTCGCCATAGCCATGCTTATC	CCTTCAGCTCATTCATGGCAATC
CYP4F1	CCCCCAAGGCTTTTTGATG	GAGCGCAACGGCAGCT
CYP4F4	CAGGTCTGAAGCAGGTAACTAAGC	CCGTCAGGGTGGCACAGAGT
CYP4F5	AGGATGCCGTGGCTAACTG	GGCTCCAAGCAGCAGAAGA
CYP4F6	TCACTTGACCTTGATGAAGAACAAC	AAGAGAGGTGGATATCACGGAAG
EPHX2	CACATCCAAGCCACCAAGCC	CAGGCCTCCATCCTCCAG
ANP	GGAGCCTGCGAAGGTCAA	TATCTTCGGTACCGGAAGCTGT
BNP	CAGAAGCTGCTGGAGCTGATAAG	TGTAGGGCCTTGGTCCTTTG
IL-6	ATATGTTCTCAGGGAGATCTTGGAA	GTGCATCATCGCTGTTCATACA
iNOS	GTGCTAATGCGGAAGGTCATG	GCTTCCGACTTTCCTGTCTCAGTA
TNFα	CAAGGTCATCCATGACAACTTTG	GGGCCATCCACAGTCTTCTG
B actin	CCAGATCATGTTTGAGACCTTCAA	GTGGTACGACCAGAGGCATACA
GAPDH	CAAGGTCATCCATGACAACTTTG	GGGCCATCCACAGTCTTCTG

2.11 Microsomal preparation and incubation

Microsomal protein was prepared from heart, lung, kidney, and liver tissues as described previously (Barakat, El-Kadi et al. 2001). Briefly, approximately 1 g of the tissues was washed in ice-cold potassium chloride (1.15% w/v), cut into pieces, and homogenized separately in cold sucrose solution (1 g of tissue in 5 mL of 0.25 M sucrose). Microsomal protein from homogenized tissues was separated by differential ultracentrifugation. The final pellet was reconstituted in cold sucrose and stored at -80°C. Microsomal protein concentration was determined by the Lowry method using bovine serum albumin as a standard (Lowry, Rosebrough et al. 1951). Microsomes (1 mg protein/ml) were incubated in the incubation buffer (5 mM magnesium chloride hexahydrate dissolved in 0.5 M potassium phosphate buffer pH=7.4) at 37°C in a shaking water bath (50 rpm). A pre-equilibration period of 5 min was performed. The reaction was initiated by the addition of 1 mM NADPH. Arachidonic acid was added to a final concentration of 50 μM and incubated for 30 min. The reaction was terminated by the addition of 600 μl ice cold acetonitrile followed by the internal standard, 4-hydroxybenzophenone. Arachidonic acid metabolites were extracted twice by 1 ml ethyl acetate and dried using speed vacuum (Savant, Farmingdale, NY). The concentrations of the eicosanoids in the samples were calculated by comparing the ratios of peak heights to their corresponding standards.

2.12 Extraction of endogenous arachidonic acid metabolites

Kidney and liver tissue concentrations of arachidonic acid metabolites were determined according to a previously published method (Poloyac, Tortorici et al. 2004) with some modifications. Briefly, kidney or liver tissues (1 g) were homogenzied in the incubation buffer and centrifuged at 10,000x g for 30 min. After the addition of acetonitrile and the internal standard (4-hydroxybenzophenone), the supernatant was extracted twice with 1 ml ethyl acetate and dried using speed vacuum (Savant, Farmingdale, NY).

2.13 Analysis of different arachidonic acid metabolites

Extracted arachidonic acid metabolites were analyzed using an LC-ESI-MS (Waters Micromass ZQ 4000 spectrometer) method as described previously (Nithipatikom, Grall et al. 2001). The mass spectrometer was operated in negative ionization mode with single ion recorder acquisition. The nebulizer gas was obtained from an in house high purity nitrogen source. The temperature of the source was set at 150 ^{o}C, and the voltages of the capillary and the cone were 3.51 KV and 25 V, respectively. The samples (10 μL) were separated on reverse phase C18 column (Kromasil, 250 x 3.2 mm) using linear gradient mobile phase system water/acetonitrile with 0.005% acetic acid as mobile phase at flow rate of 0.2 mL/min. The mobile phase system started at 60% acetonitrile, linearly increased to 80% acetonitrile in 30 min, increased to 100% acetonitrile in 5 min, and was held there for 5 min. 4-Hydroxybenzophenone was used as internal standard.

2.14 Western Blot Analysis

Western blot analysis was performed according to a previously described method (Gharavi and El-Kadi 2005). Briefly, 2.5 - 40 μg of heart, kidney, or liver microsomal protein from each treatment group was separated by 10% sodium dodecyl sulfate-polyacrylamide gel (SDS-PAGE), and then electrophoretically transferred to nitrocellulose membrane. Protein blots were then blocked overnight at 4 °C in blocking solution containing 0.15 M sodium chloride, 3 mM potassium chloride, 25 mM Tris-base (TBS), 5% skim milk, 2% bovine serum albumin, and 0.5% Tween-20. After blocking, the blots were incubated with a primary polyclonal mouse anti-rat CYP1A1, rabbit anti-rat CYP1B1, mouse anti-rat CYP2B1, rabbit anti-rat CYP2C11, rabbit anti-rat CYP2E1, rabbit anti-mouse CYP2J, mouse anti-rat CYP4A, rabbit anti-mouse sEH and rabbit anti-rat actin for 2 h. Incubation with a peroxidase-conjugated goat anti-rabbit IgG secondary antibody for CYP1B1, CYP2C11, CYP2E1, CYP2J, sEH, and actin, or goat anti-mouse IgG secondary antibody for CYP1A1, CYP2B1, and CYP4A was carried out for 1 h at room temperature. The bands were visualized using the enhanced chemiluminescence method according to the manufacturer's instructions (GE Healthcare Life Sciences, Piscataway, NJ). The intensity of the protein bands were quantified, relative to the signals obtained for actin, using ImageJ software [National Institutes of Health, Bethesda, MD, http://rsb.info.nih.gov/ij.].

2.15 Determination of Lactate Dehydrogenase (LDH)

LDH was estimated in rat serum by commercially available kit (CytoTox-One kit, Promega). LDH is measured with a 15-min coupled enzymatic assay that results in the conversion of resazurin into florescent resurofin. The fluorescence produced was then recorded with an excitation wavelength of 560 nm and an emission wavelength of 590 nm according to manufacturer's instructions (Promega) using a Baxter 96-well reader. The amount of fluorescence produced is proportional to the amount of LDH which was calculated relative to the control.

2.16 Nitrite assay

Nitrites were measured in serum samples of control and 24 h DOX treated rats as described previously (Nussler, Glanemann et al. 2006). Briefly, a 200 μM working nitrite standard was prepared from a 2.0 mM sodium nitrite stock solution in endotoxin-free deionized water, and stored at 4°C until use. A working 2,3-diaminonaphthalene (DAN) solution of 50 μg/mL was prepared by diluting a 20 mg/mL stock solution with 0.62N HCl. All assays were conducted in 96-well plates, with each condition performed in quadruplet. In each well, 20 μL of standard or sample was added to 80 μL of deionized water. Then, 10 μL of working DAN solution was added to each well. The plate was allowed to sit in the dark at room temperature for 10 min. Using the same timing and sequence as for the additions of DAN, 20 μL of 2.8 N NaOH was added to each well, and the plate was gently shaken. The plate then was incubated in the dark for 1 min,

following which it was read in a fluorescence plate reader with an excitation of 360 nm and an emission of 430 nm.

2.17 Statistical Analysis

Data are presented as mean ± standard error of the mean (SEM). Control and treatment measurements were compared using the student t-test. Comparisons among more than two groups were performed by a one way analysis of variance (ANOVA) followed by a Student-Newman-Keul's post hoc comparison. Statistical analysis was performed using SigmaStat for windows, Systat Software Inc. (San Jose, CA). A result was considered statistically significant where $P < 0.05$.

CHAPTER 3 - RESULTS

3.1 Modulation of Cytochrome P450 gene expression and arachidonic acid metabolism during isoproterenol-induced cardiac hypertrophy in rats

3.1.1 Expression of *CYP* and *EPHX2* genes in the heart, lung, kidney, and liver

To examine the constitutive expression of various *CYP* and *EPHX2* genes in the heart, lung, liver, and kidney tissues of male SD rats, total RNA was isolated from different tissues and different genes were determined by real time-PCR. The gene expression profiles of different *CYP* and *EPHX2* genes were found to be tissue-specific. All the examined genes except *CYP4A2* were found to be constitutively expressed in the heart at different levels (Fig. 3.1A). *CYP4A1* was the lowest expressed gene and was used as calibrator. *CYP4F5*, *CYP2E1*, *CYP1B1*, and *EPHX2* were the most highly expressed genes, at about 10000 fold higher than the calibrator (Fig. 3.1A). *CYP1A1* and *CYP2J3* were also highly expressed, at about 1000 fold higher than the calibrator (Fig. 3.1A). *CYP2B1*, *CYP2B2*, *CYP2C11*, and *CYP4F4* were moderately expressed genes, at about 100 fold higher than the calibrator. *CYP4A3* was constitutively expressed at a low level, at about two fold higher than the calibrator (Fig. 3.1A).

Similar to the heart, not all the examined genes were expressed in the lung; CYP4A1, CYP4A2, and CYP4A3 mRNAs were not detected in the lung tissue. *CYP2B2* was the lowest expressed gene and was considered as calibrator. *CYP2B1* was the most highly expressed gene, at about 120000 fold higher than the calibrator (Fig. 3.1B). *CYP1A1*, *CYP2E1*, *CYP4F5*, and *EPHX2* were highly

expressed, at about 5000, 4600, 2200, and 1400 fold higher than the calibrator, respectively (Fig. 3.1B). *CYP2J3*, *CYP1B1*, *CYP4F4*, and *CYP2C11* were moderate to low expressed genes, at about 290, 65, 17, and 11 fold higher than the calibrator, respectively (Fig. 3.1B).

In contrast to the heart and lung, all the examined genes were found to be constitutively expressed in the liver but at different levels. *CYP1B1* was the lowest expressed gene and was considered as calibrator. *CYP2E1* and *CYP2C11* were the most highly expressed genes, at about 13000 and 11000 fold higher than the calibrator, respectively (Fig. 3.1C). *EPHX2*, *CYP4A2*, and *CYP4A3* were also highly expressed, at about 5000, 4600, and 2000 fold higher than the calibrator, respectively (Fig. 3.1C). *CYP4F4*, *CYP2J3*, *CYP2B2*, and *CYP4A1* were moderately expressed genes, at about 840, 800, 750, and 350 fold higher than the calibrator, respectively (Fig. 3.1C). The constitutive expression of *CYP2B1*, *CYP1A1*, and *CYP4F5* was low, at about 35, 10, and 10 fold higher than the calibrator, respectively (Fig. 3.1C).

Similar to the liver, all the examined genes were found to be constitutively expressed at different levels in the kidney. *CYP2B2* was the lowest expressed gene and was considered as calibrator (Fig. 3.1D). *CYP4A2* and *CYP4A3* were the most highly expressed genes, at about 50000 and 24000 fold higher than the calibrator, respectively. *EPHX2* and *CYP2E1* were highly expressed genes, at about 6000 fold higher than the calibrator (Fig. 3.1D). *CYP2C11*, *CYP4A1*, *CYP4F5*, *CYP2J3*, *CYP1A1*, and *CYP1B1* were high to moderate expressed genes, at about 750, 360, 210, 200, 150, and 60 fold higher than the calibrator,

respectively (Fig. 3.1D). The constitutive expression of *CYP4F4* and *CYP2B1* was very low, at about 2 and 1.5 fold higher than the calibrator, respectively (Fig. 3.1D).

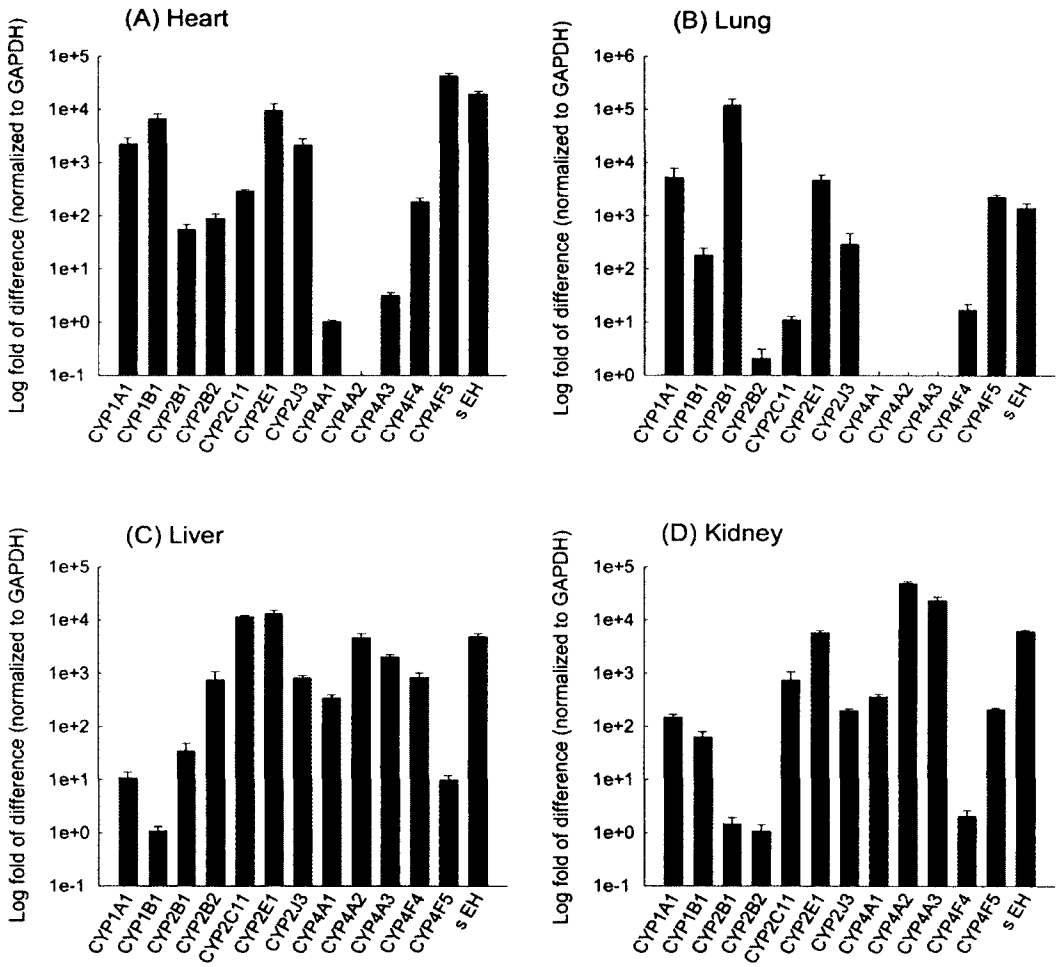

Fig. 3.1. Constitutive expression of *CYP* and *EPHX2* genes in different tissues. Total RNA was isolated from different tissues and the relative expression of *CYP* and *EPHX2* genes in the heart (A), lung (B), liver (C), and kidney (D) was determined by reverse transcription followed by real time-PCR. The data were analyzed using the relative gene expression method. The data were normalized to the endogenous reference gene (GAPDH) and relative to a calibrator. The gene of lowest expression in each tissue was used as a calibrator as described under materials and methods. Results are presented as mean ± SEM (n = 6).

3.1.2 Effect of isoproterenol treatment on hypertrophic markers and the heart to body weight ratio

In order to investigate whether isoproterenol treatment caused cardiac hypertrophy in the treated SD rats, we measured the cardiac gene expression of the hypertrophic markers, ANP and BNP, relative to control rats. Our results showed that isoproterenol treatment caused statistically significant induction of both hypertrophic markers, ANP and BNP, by 10 and 3 fold, respectively (Fig. 3.2A). In addition, isoproterenol treatment caused a statistically significant increase in the heart to body weight ratio by about 30% (Fig. 3.2B).

3.1.3 Effect of isoproterenol treatment on *CYP* gene expression

To examine the effect of isoproterenol-induced cardiac hypertrophy on the expression of several *CYP* and *EPHX2* genes in different tissues, total RNA was extracted from the heart, lung, liver, and kidney tissues of both control and isoproterenol-treated rats. Thereafter, the expression of different genes was measured using RT followed by real time-PCR as described under materials and methods.

Figure 3.3 shows the effect of isoproterenol-induced cardiac hypertrophy on *CYP1* family gene expression. At the constitutive level, our results demonstrate that *CYP1A1* is highly expressed in the lung, moderately expressed in the liver and kidney, and expressed at low level in the heart (Fig. 3.3A). However, *CYP1B1* was expressed in the lung, heart, and kidney more than the liver (Fig. 3.3B). Isoproterenol treatment caused a significant induction of *CYP1A1* and

CYP1B1 gene expression in the heart by about 2.8 and 4.2 fold, respectively (Fig. 3.3C and D). In addition, isoproterenol treatment caused a significant induction of *CYP1A1*, but not *CYP1B1*, in the kidney by 2.8 fold (Fig. 3.3C and D). However, there was no change in *CYP1A1* and *CYP1B1* gene expression in the other tissues (Fig. 3.3C and D).

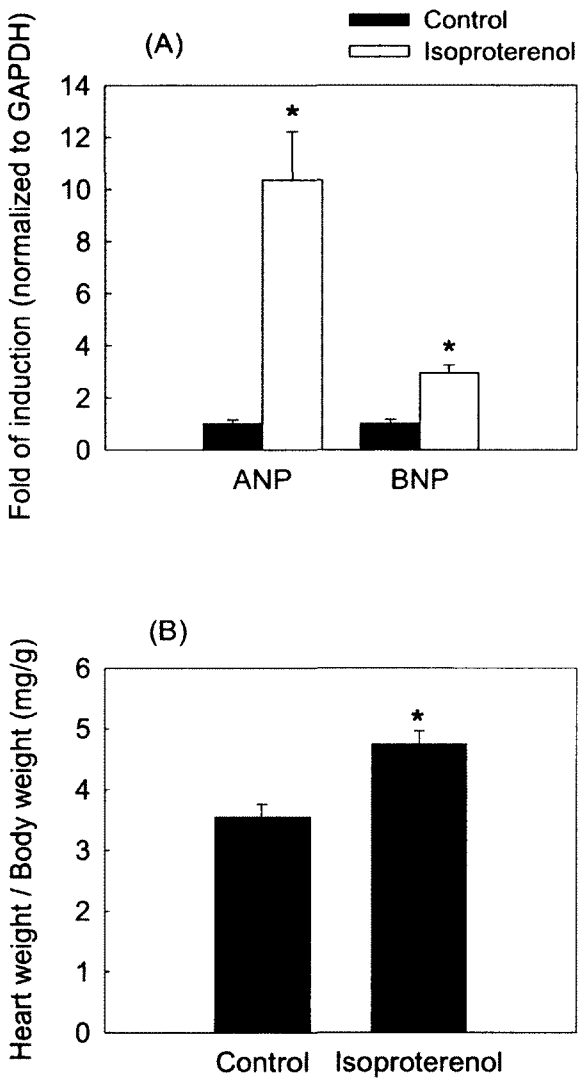

Fig. 3.2 Effect of isoproterenol treatment on the hypertrophic markers in the rat. A: Gene expression of hypertrophic markers was determined in the heart. Total RNA was isolated from control and isoproterenol-treated animals. ANP and BNP gene expression were determined by real time-PCR. B: Heart to body weight ratio (mg/g) was determined for each animal after 7 daily IP injections of isoproterenol or saline. Results are presented as mean ± SEM (n = 6). * $P < 0.05$ compared with control.

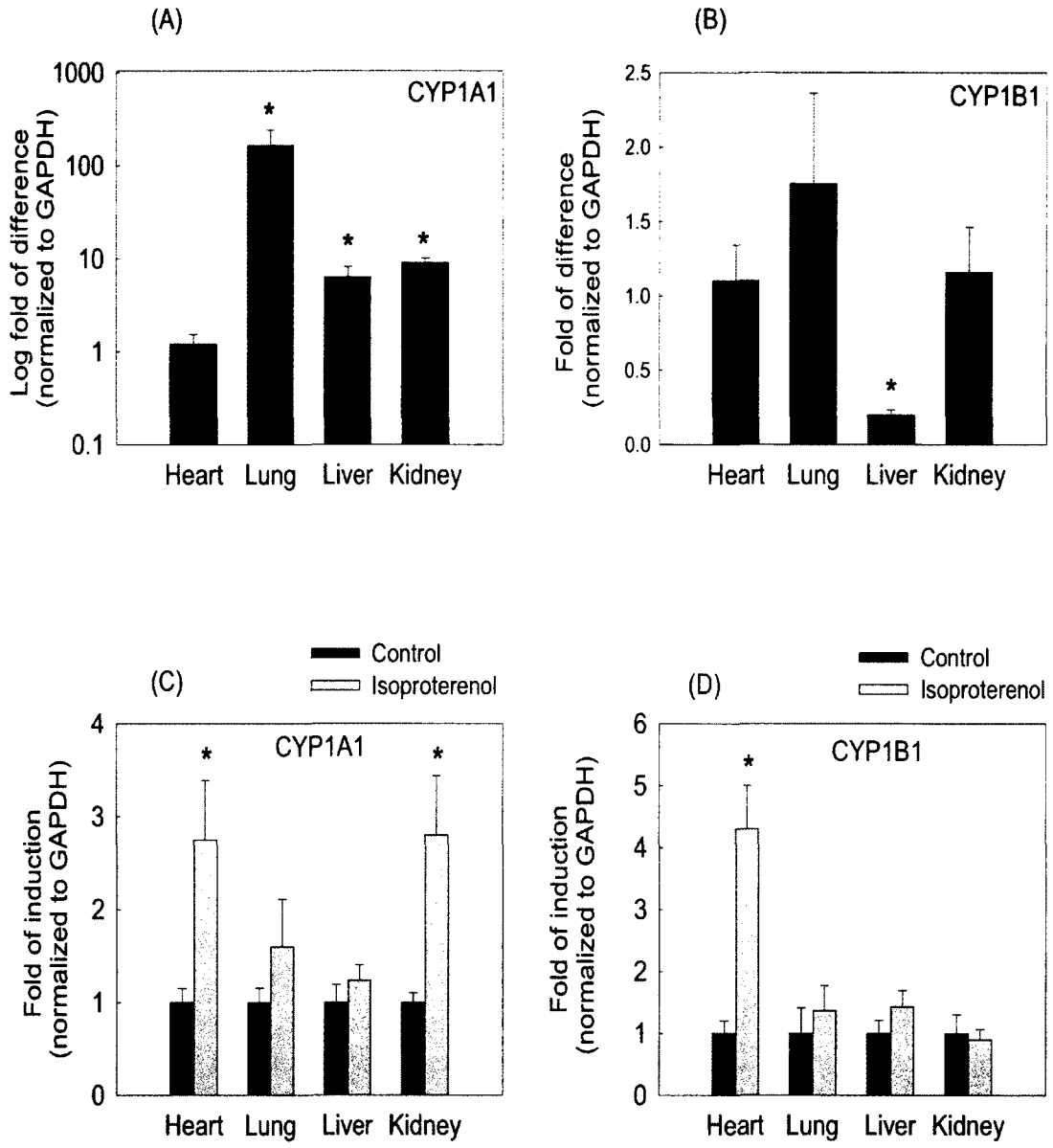

Fig. 3.3 Expression of *CYP1A1* and *CYP1B1* in different tissues and their modulation during isoproterenol-induced cardiac hypertrophy. Gene expression of *CYP1A1* (A) and *CYP1B1* (B) in the lung, liver, and kidney relative to the heart. Total RNA was isolated from different tissues and the relative constitutive expression of *CYP1A1* and *CYP1B1* were determined by real time-PCR. * $P < 0.05$ compared with the heart. Gene expression of *CYP1A1* (C) and *CYP1B1* (D) during isoproterenol-induced cardiac hypertrophy. Cardiac hypertrophy was induced by seven daily IP injections of isoproterenol. At 24 h after the last injection, the heart, lung, liver, and kidney were collected. Total RNA was isolated and gene expression of *CYP1A1* and *CYP1B1* were determined by real time-PCR in control and isoproterenol-treated rats. Results are presented as mean ± SEM (n = 6). * $P < 0.05$ compared with control.

With regard to the CYP2B subfamily, *CYP2B1* was highly expressed in the lung, at about 100000 fold higher than the heart (Fig. 3.4A). The liver expresses *CYP2B1* to a moderate degree, while the constitutive expression of *CYP2B1* in the heart and kidney was low (Fig 3.4A). Unlike *CYP2B1*, *CYP2B2* was highly expressed in the liver, at about 10000 fold higher than its expression in the other organs (Fig 3.4B). Isoproterenol treatment did not cause any statistically significant change of *CYP2B1* or *CYP2B2* gene expression in any of the examined tissues (Fig 3.4C and D).

Figure 3.5 shows the relative expression of *CYP2C11* and *CYP2E1* in the different tissues as well as the changes in their expression during isoproterenol-induced cardiac hypertrophy. *CYP2C11* is highly expressed in the liver, moderately expressed in the kidney, and expressed at low level in the lung and heart (Fig. 3.5A). Similarly, *CYP2E1* is highly expressed in the liver, moderately expressed in the kidney and lung, and low expressed in the heart (Fig. 3.5B). Isoproterenol-induced cardiac hypertrophy caused a significant inhibition of *CYP2C11* gene expression in the heart by 50% (Fig. 3.5C). Nevertheless, *CYP2C11* gene expression did not change significantly in the other tissues (Fig. 3.5C). Similar to *CYP2C11*, isoproterenol treatment caused a significant inhibition of *CYP2E1* gene expression in the heart by 80% (Fig. 3.5D). However, unlike *CYP2C11*, isoproterenol treatment caused a paradoxical induction of *CYP2E1* in the kidney (Fig. 3.5D). There was no change in *CYP2E1* gene expression in the liver or lung during isoproterenol-induced cardiac hypertrophy (Fig. 3.5D).

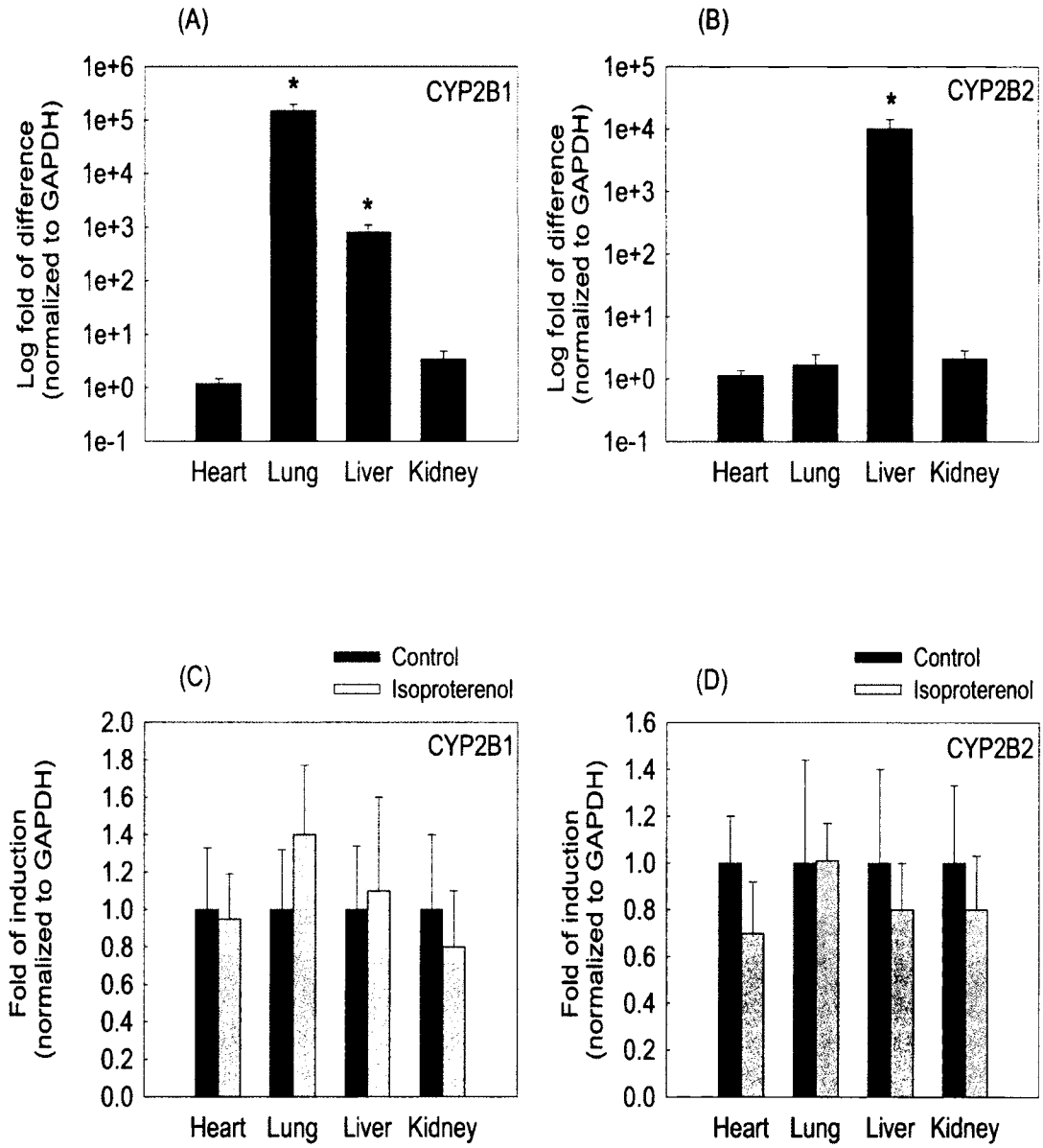

Fig. 3.4 Expression of *CYP2B1* and *CYP2B2* in different tissues and their modulation during isoproterenol-induced cardiac hypertrophy. Gene expression of *CYP2B1* (A) and *CYP2B2* (B) in the lung, liver, and kidney relative to the heart. Total RNA was isolated from different tissues and the relative expression of *CYP2B1* and *CYP2B2* were determined by real time-PCR. * $P < 0.05$ compared with the heart. Gene expression of *CYP2B1* (C) and *CYP2B2* (D) during isoproterenol-induced cardiac hypertrophy. Cardiac hypertrophy was induced by seven daily IP injections of isoproterenol. At 24 h after the last injection, the heart, lung, liver, and kidney were collected. Total RNA was isolated and gene expression of *CYP2B1* and *CYP2B2* were determined by real time-PCR in control and isoproterenol-treated rats. Results are presented as mean ± SEM ($n = 6$).

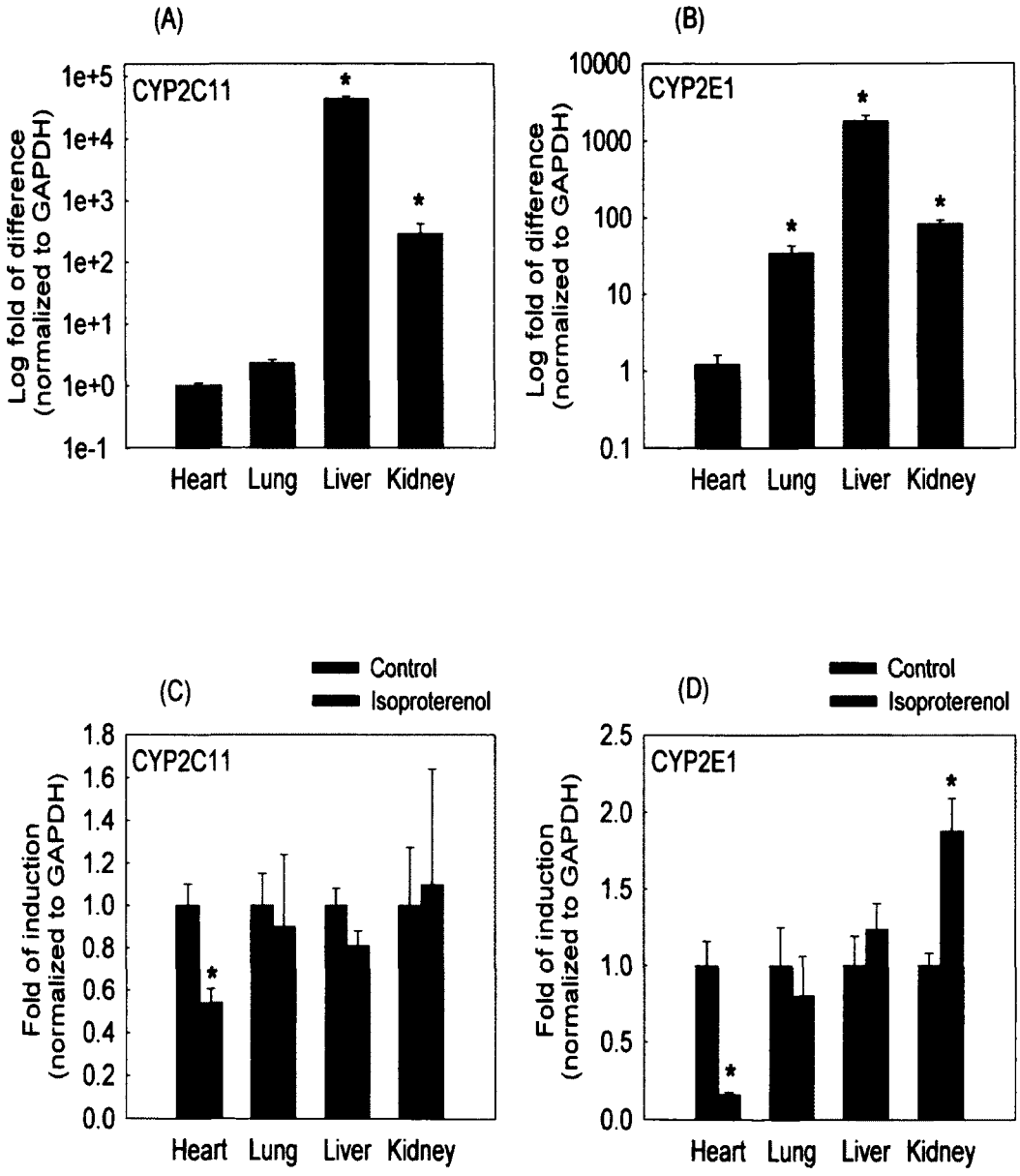

Fig. 3.5 Expression of *CYP2C11* and *CYP2E1* in different tissues and their modulation during isoproterenol-induced cardiac hypertrophy. Gene expression of *CYP2C11* (A) and *CYP2E1* (B) in the lung, liver, and kidney relative to the heart. Total RNA was isolated from different tissues and the relative expression of *CYP2C11* and *CYP2E1* were determined by real time-PCR. * $P < 0.05$ compared with the heart. Gene expression of *CYP2C11* (C) and *CYP2E1* (D) during isoproterenol-induced cardiac hypertrophy. Cardiac hypertrophy was induced by seven daily IP injections of isoproterenol. At 24 h after the last injection, the heart, lung, liver, and kidney ($n = 6$) were collected. Total RNA was isolated and gene expression of *CYP2C11* and *CYP2E1* were determined by real time-PCR in control and isoproterenol-treated rats. Results are presented as mean ± SEM ($n = 6$). * $P < 0.05$ compared with control.

With regard to *CYP2J3*, it was found to be highly expressed in the liver, moderately expressed in the kidney and lung, and expressed at low level in the heart (Fig. 3.6A). *CYP4A1* is also highly expressed in the liver and kidney, low expressed in heart, but not constitutively expressed in the lung (Fig. 3.6B). Isoproterenol-induced cardiac hypertrophy did not cause any changes in the gene expression of either *CYP2J3* or *CYP4A1* in any of the examined tissues (Fig. 3.6C and D).

Figure 3.7 shows the relative gene expression of *CYP4A2* and *CYP4A3* enzymes. *CYP4A2* was constitutively expressed in the liver and kidney but not in the heart or lung (Fig. 3.7A); however, *CYP4A3* was constitutively expressed in the heart, liver, and kidney but not in the lung (Fig. 3.7B). Isoproterenol-induced cardiac hypertrophy did not cause any changes in the gene expression of *CYP4A2* in the liver and kidney (Fig. 3.7C); nevertheless, it caused a significant induction of *CYP4A3* in the heart, liver, and kidney by 2.4, 1.6, and 1.7 fold, respectively (Fig. 3.7D).

With regard to CYP4F subfamily, *CYP4F4* and *CYP4F5* were found to be expressed in all the examined tissues. *CYP4F4* was highly expressed in the liver compared to the other examined tissues (Fig. 3.8A). On the other hand, *CYP4F5* was found to be highly expressed in the lung, moderately expressed in the heart and kidney, and of low expression in the liver (Fig. 3.8B). The gene expression of *CYP4F4* and *CYP4F5* was not altered during isoproterenol-induced cardiac hypertrophy in any of the examined tissues (Fig. 3.8C and D).

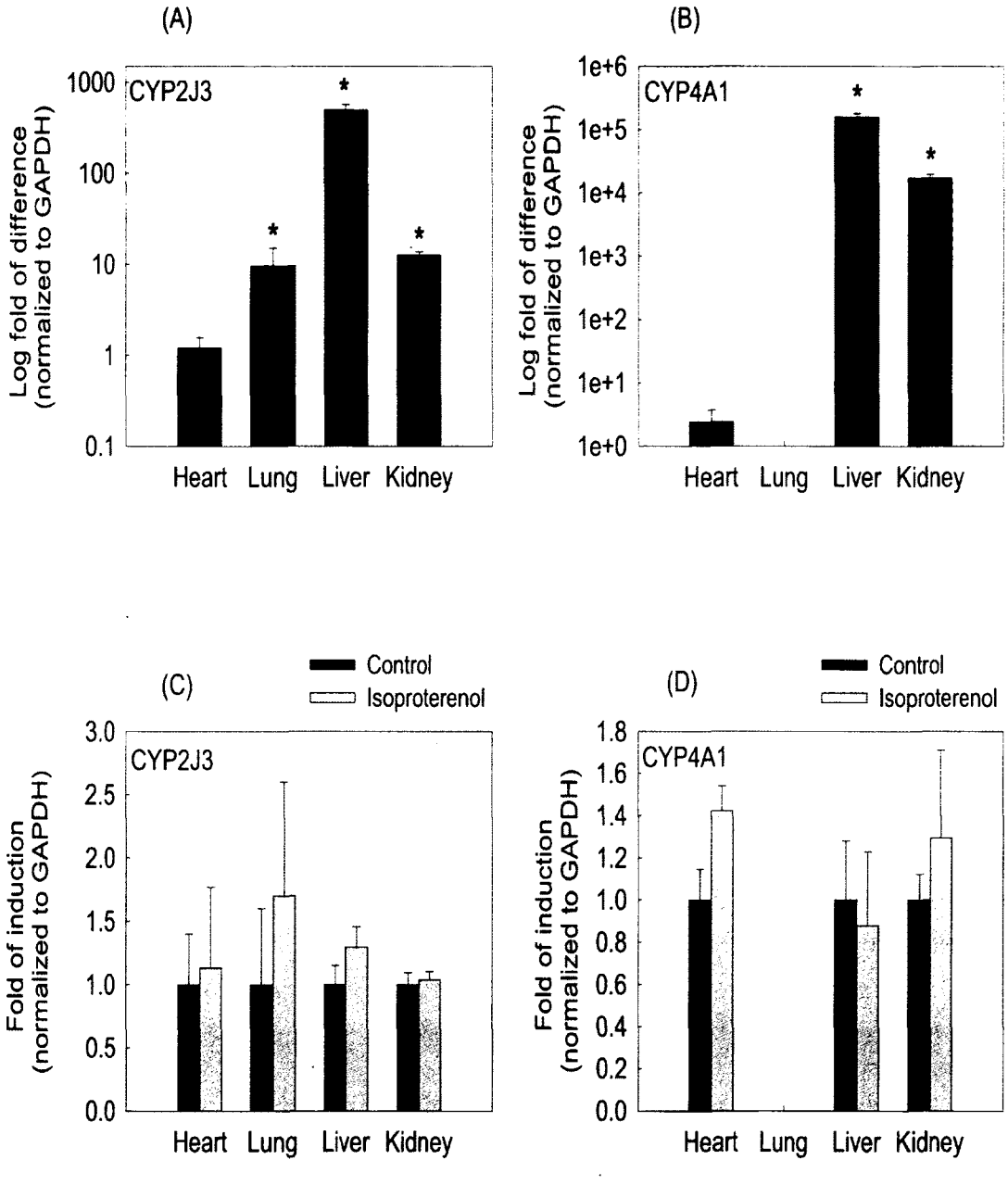

Fig. 3.6 Expression of *CYP2J3* and *CYP4A1* in different tissues and their modulation during isoproterenol-induced cardiac hypertrophy. Gene expression of *CYP2J3* (A) and *CYP4A1* (B) in the lung, liver, and kidney relative to the heart. Total RNA was isolated from different tissues and the relative expression of *CYP2J3* and *CYP4A1* were determined by real time-PCR. * $P < 0.05$ compared with the heart. Gene expression of *CYP2J3* (C) and *CYP4A1* (D) during isoproterenol-induced cardiac hypertrophy. Cardiac hypertrophy was induced by seven daily IP injections of isoproterenol. At 24 h after the last injection, the heart, lung, liver, and kidney (n = 6) were collected. Total RNA was isolated and gene expression of *CYP2J3* and *CYP4A1* were determined by real time-PCR in control and isoproterenol-treated rats. Results are presented as mean ± SEM (n = 6).

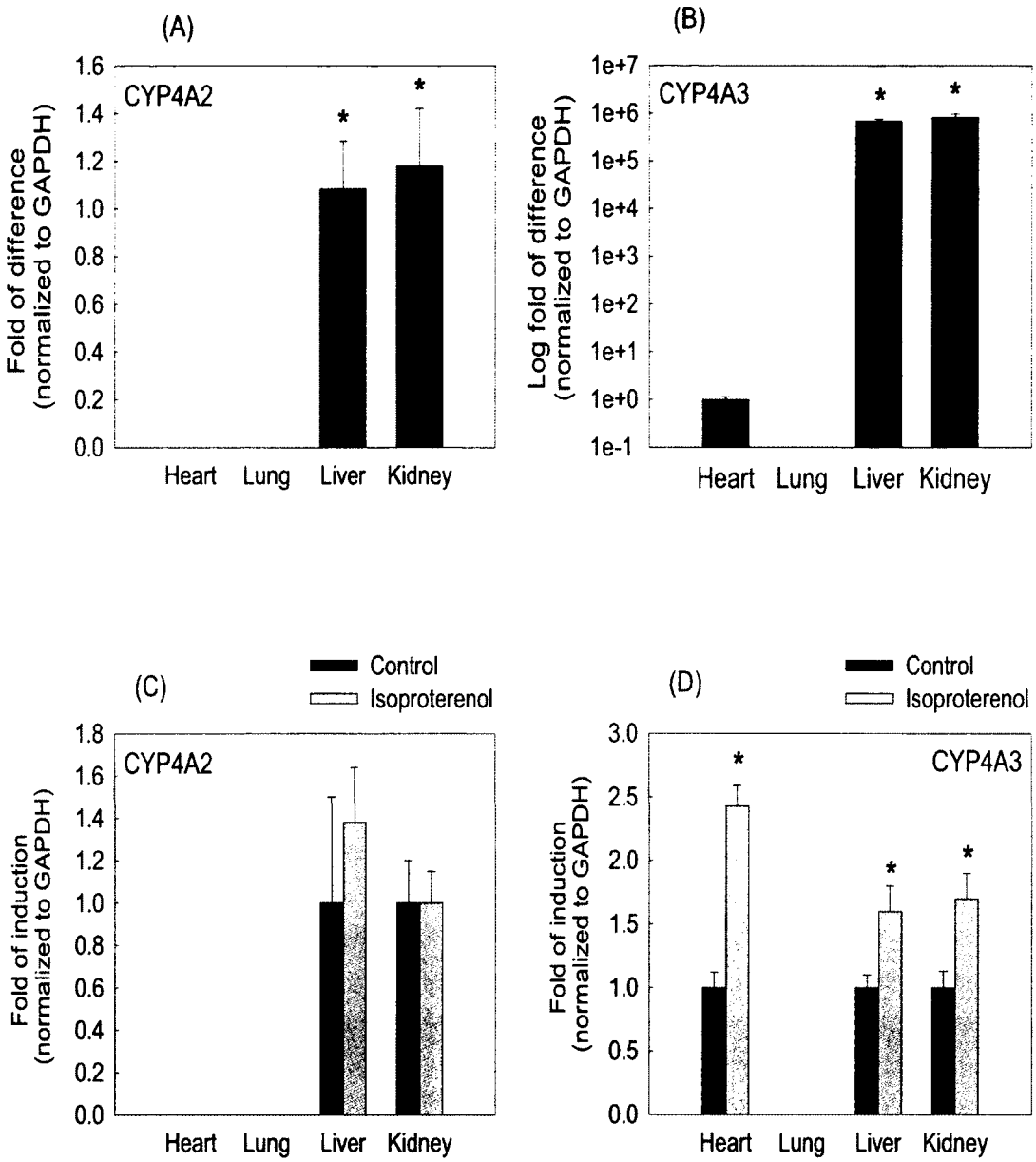

Fig. 3.7 Expression of *CYP4A2* and *CYP4A3* in different tissues and their modulation during isoproterenol-induced cardiac hypertrophy. Gene expression of *CYP4A2* (A) and *CYP4A3* (B) in the lung, liver, and kidney relative to the heart. Total RNA was isolated from different tissues and the relative expression of *CYP4A2* and *CYP4A3* were determined by real time-PCR. * $P < 0.05$ compared with the heart. Gene expression of *CYP4A2* (C) and *CYP4A3* (D) during isoproterenol-induced cardiac hypertrophy. Cardiac hypertrophy was induced by seven daily IP injections of isoproterenol. At 24 h after the last injection, the heart, lung, liver, and kidney (n = 6) were collected. Total RNA was isolated and gene expression of *CYP4A2* and *CYP4A3* were determined by real time-PCR in control and isoproterenol-treated rats. Results are presented as mean ± SEM (n = 6). * $P < 0.05$ compared with control.

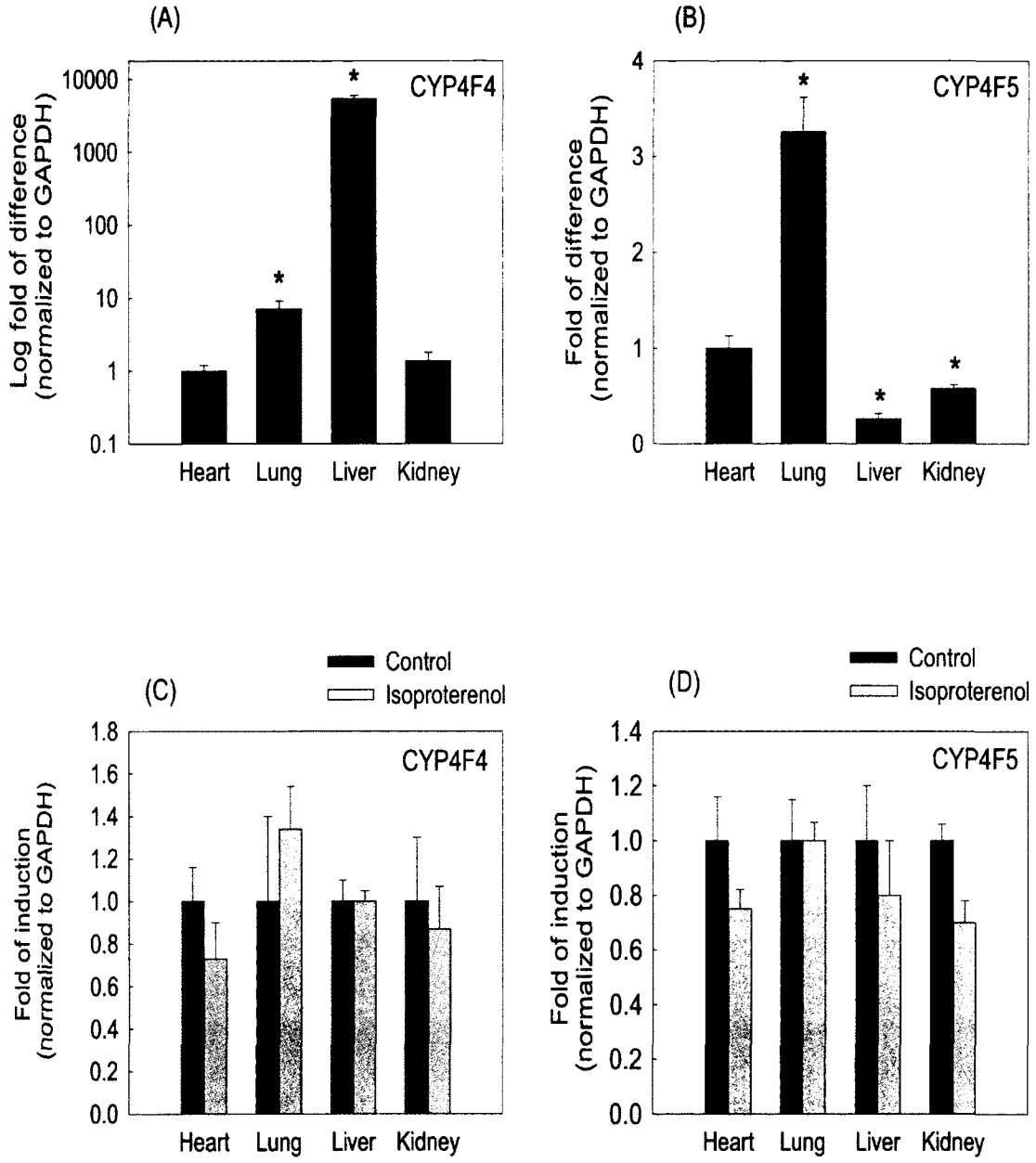

Fig. 3.8 Expression of *CYP4F4* and *CYP4F5* in different tissues and their modulation during isoproterenol-induced cardiac hypertrophy. Gene expression of *CYP4F4* (A) and *CYP4F5* (B) in the lung, liver, and kidney relative to the heart. Total RNA was isolated from different tissues and the relative expression of *CYP4F4* and *CYP4F5* were determined by real time-PCR. * $P < 0.05$ compared with the heart. Gene expression of *CYP4F4* (C) and *CYP4F5* (D) during isoproterenol-induced cardiac hypertrophy. Cardiac hypertrophy was induced by seven daily IP injections of isoproterenol. At 24 h after the last injection, the heart, lung, liver, and kidney ($n = 6$) were collected. Total RNA was isolated and gene expression of *CYP4F4* and *CYP4F5* were determined by real time-PCR in control and isoproterenol-treated rats. Results are presented as mean ± SEM ($n = 6$).

3.1.4 Effect of isoproterenol treatment on *EPHX2* gene expression

EPHX2 was found to be highly expressed in the liver, moderately expressed in the kidney, and expressed at low level in the lung and heart (Fig. 3.9A). Isoproterenol treatment caused a significant induction of *EPHX2* gene expression in the heart by 1.8 fold (Fig. 3.9B). However, the gene expression of *EPHX2* was not significantly altered in the other tissues (Fig. 3.9B).

3.1.5 Separation of arachidonic acid metabolites using LC-ESI-MS

LC-ESI-MS has been used in this study for the separation and quantification of CYP-derived metabolites of arachidonic acid. The mass spectrometer was operated in negative ionization mode with single ion recorder acquisition where the most abundant ion is corresponding to the m/z = $[M-1]^-$. All four regioisomeric EETs (5,6-, 8,9-, 11,12-, and 14,15-EET) exhibited the most abundant ions corressponding m/z = 319 ion, while their corresponding DHETs has m/z = 337 ion and 20-HETE has m/z = 319 ion. The fact of having functional groups at different positions in the eicosanoid structure allowed successful separation which was achieved through the use of a reverse phase C_{18} HPLC column and linear gradient mobile phase. Using authentic standards, 14,15-, 11,12-, 8,9-, 5,6 -EET were found to be eluted at 26.3, 28.6, 29.4, and 30.1 min respectively, while 20-HETE eluted at 15.1 min. The elution times of 14,15-, 11,12-, 8,9-, and 5,6-DHET were 11.4, 12.6, 13.6, and 14.7 min, respectively.

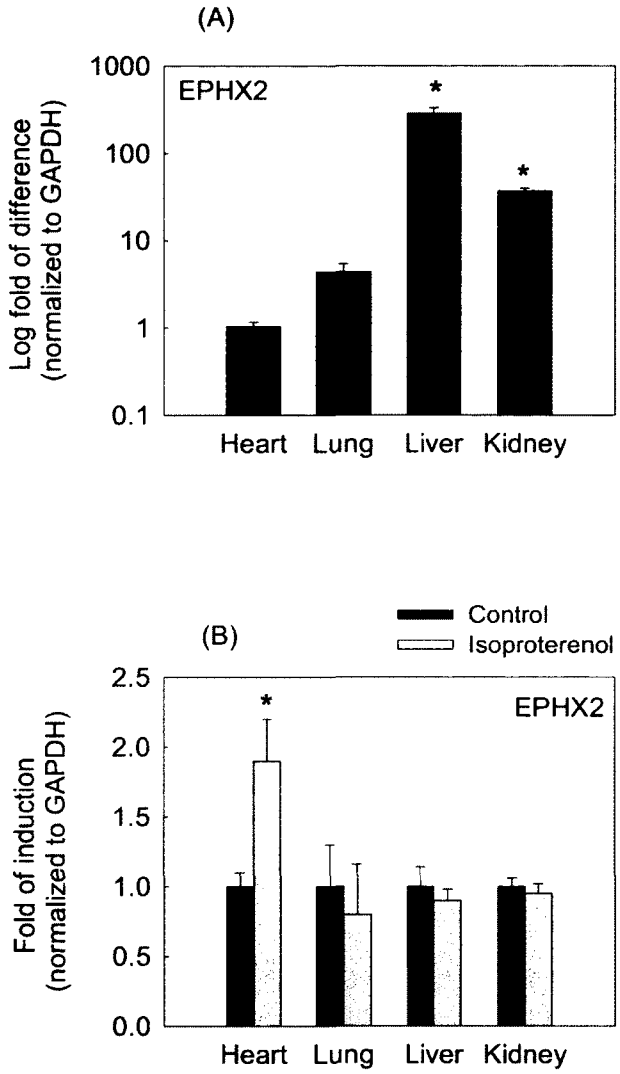

Fig. 3.9 Expression of *EPHX2* in different tissues and its modulation during isoproterenol-induced cardiac hypertrophy. Gene expression of *EPHX2* in the lung, liver, and kidney relative to the heart (A). Total RNA was isolated from different tissues and the relative expression of *EPHX2* was determined by real time-PCR. * $P < 0.05$ compared with the heart. Gene expression of *EPHX2* during isoproterenol-induced cardiac hypertrophy (B). Cardiac hypertrophy was induced by seven daily IP injections of isoproterenol. At 24 h after the last injection, the heart, lung, liver, and kidney (n = 6) were collected. Total RNA was isolated and gene expression of *EPHX2* was determined by real time-PCR in control and isoproterenol-treated rats. Results are presented as mean ± SEM (n = 6). * $P < 0.05$ compared with control.

3.1.6 Effect of isoproterenol treatment on CYP-mediated arachidonic metabolism

To investigate the effect of isoproterenol treatment on the formation of arachidonic acid metabolites, heart microsomes of either control or isoproterenol-treated rats were incubated with 50 μM arachidonic acid for 30 min. Thereafter, arachidonic acid metabolites were determined using LC-ESI-MS. Our results clearly show that, 5,6-EET was the major metabolite produced in both control and isoproterenol treated rats followed by 8,9-, 14,15- and 11,12-EET, respectively. In comparison to control animals, in microsomes of hypertrophied hearts, the formation of 5,6-, 8,9-, 11,12- and 14,15-EET was significantly lower by 34%, 44%, 51% and 44%, respectively (Fig. 3.10A). We also measured levels of enzymatic hydroxylation of EET products, i.e. DHETs. As shown in Figure 3.10B, the formation of 8,9- and 14,15-DHET were significantly higher by 123 % and 84 %, respectively, compared to control. On the other hand, the formation rates of 5,6- and 11,12-DHET were not significantly altered. To determine the effect of isoproterenol treatment on CYP ω-hydroxylases activitiy, we determined the formation of 20-HETE in microsomes from control and hypertrophied rats. Isoproterenol treatment significantly increased the 20-HETE formation rate by 192% in comparison to the control group (Fig. 3.10C).

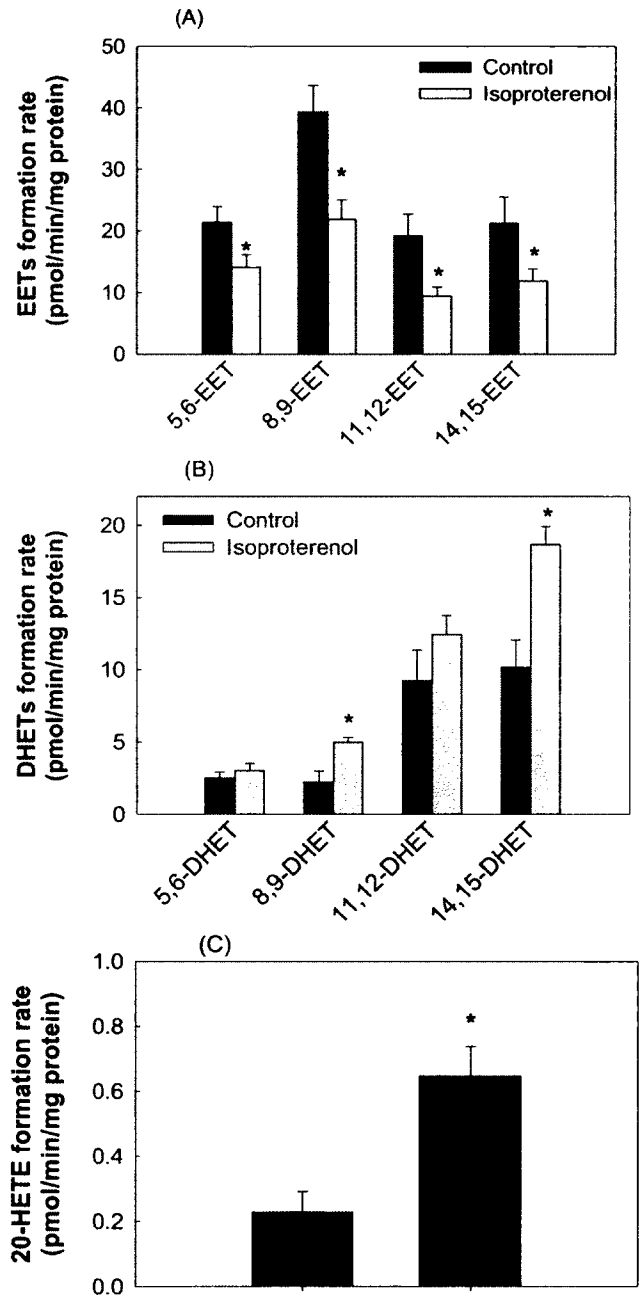

Fig. 3.10 Effect of isoproterenol treatment on formation of (A) EETs, (B) DHETs, and (C) 20-HETE. Heart microsomes of control or isoproterenol-treated rats were incubated with 50 μM arachidonic acid. The reaction was started by the addition of 1 mM NADPH and lasted for 30 min. The reaction was terminated by the addition of ice cold acetonitrile. EETs, DHETs, and 20-HETE were extracted twice by 1 ml ethyl acetate and dried using speed vacuum. Reconstituted metabolites were injected into LC-ESI-MS for metabolite determination. Results are presented as mean ± SEM (n=5). * $P < 0.05$ compared with control.

3.2 H9c2 cell line is a valuable *in vitro* model to study the drug metabolizing enzymes in the heart

In the present study, we showed that *CYP1A1* and *1B1* genes are constitutively expressed in both H9c2 cells and the rat heart (Fig. 3.11). Treatment with a CYP1 inducer, BNF, significantly increased *CYP1A1* expression in H9c2 cells and the rat heart, whereas *CYP1B1* was induced only in the heart but not in H9c2 cells under the current experimental conditions (Fig. 3.11). On the other hand, CYP1A2 mRNA was not detected either constitutively or after induction with BNF in either H9c2 cells or the rat heart (Fig. 3.11).

The expression of *CYP2B1*, *CYP2B2*, *CYP2E1* and *CYP2J3* in H9c2 cells in comparison to those expressed in the heart and the liver are shown in Figure 3.12. Our results showed that all *CYP* genes are highly expressed in the liver, while they are expressed to a varying degree in H9c2 cells and the heart. *CYP2B1* was found to be highly expressed in H9c2 cells and its expression level is comparable to that of the liver but significantly higher than that of the heart (Fig. 3.12). CYP2B2 mRNA was detected in H9c2 cells and the liver but not in the heart (Fig. 3.12). On the other hand, CYP2E1 mRNA was detected at lower level in H9c2 cells in comparison to the heart and liver (Fig 3.12). Interestingly, CYP2J3 mRNA was detected at almost equal amounts in H9c2 cells and the heart but lower than those in the liver (Fig. 3.12).

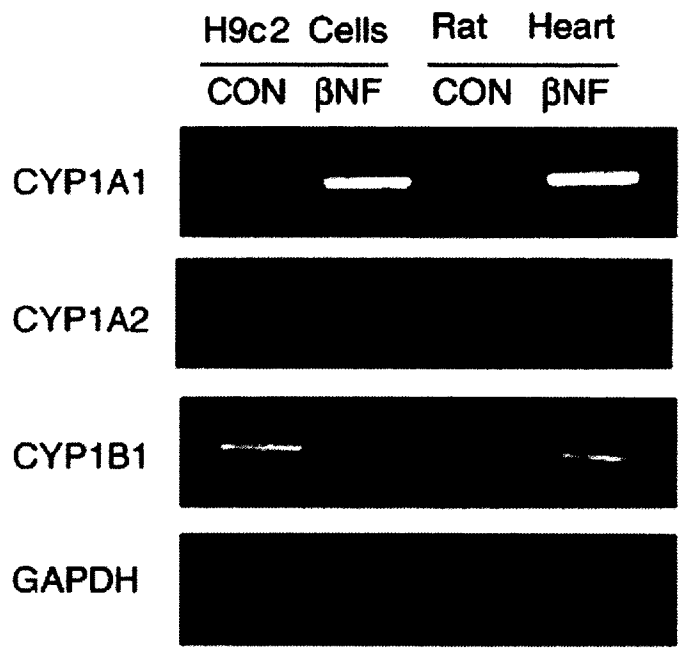

Fig. 3.11 Expression of *CYP1A1*, *CYP1A2*, and *CYP1B1* in H9c2 cells and rat heart. Cells or animals were treated with vehicle or BNF as described under Materials and Methods. CYP1A1, CYP1A2 and CYP1B1 mRNA were determined in H9c2 cells and rat heart using the conventional RT-PCR method and GAPDH was included as the endogenous control. This experiment was repeated on three occasions, but only one representative result is shown.

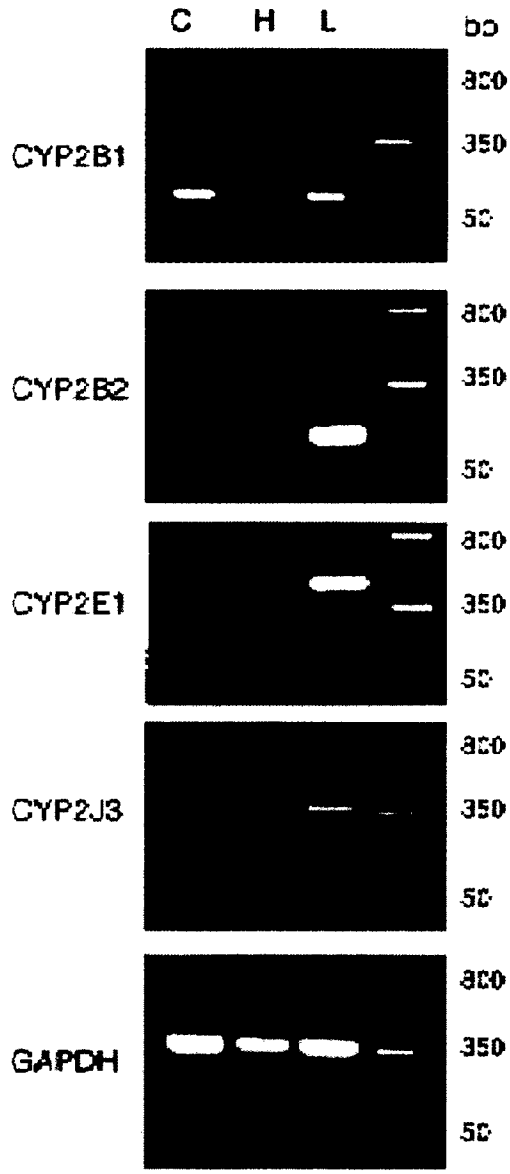

Fig. 3.12 Expression of *CYP2B1*, *CYP2B2*, *CYP2E1*, and *CYP2J3* in H9c2 cells, rat heart, and rat liver. CYP2B1, CYP2B2, CYP2E1, and CYP2J3 mRNAs were determined in H9c2 cells (C), rat heart (H) and rat liver (L) using the conventional RT-PCR method and GAPDH was included as endogenous control. This experiment was repeated on three occasions, but only one representative result is shown.

CYP2C11, *CYP2C13*, and *CYP2C23* genes were expressed abundantly in the liver but to a limited extent if any in the heart and to a varying degree in H9c2 cells (Fig. 3.13). Interestingly, CYP2C11 mRNA was detected in H9c2 cells but not in the heart (Fig. 3.13). CYP2C13 mRNA was detected at very low level in H9c2 cells but not in the heart (Fig. 3.13). On the other hand, CYP2C23 mRNA was detected in H9c2 cells at higher amounts than those in the heart (Fig. 3.13). The gene expressions of *CYP2A1*, *CYP3A1*, and *CYP3A2* are demonstrated in Figure 3.14. The three genes were expressed in the liver but not in H9c2 cells nor in the heart (Fig. 3.14).

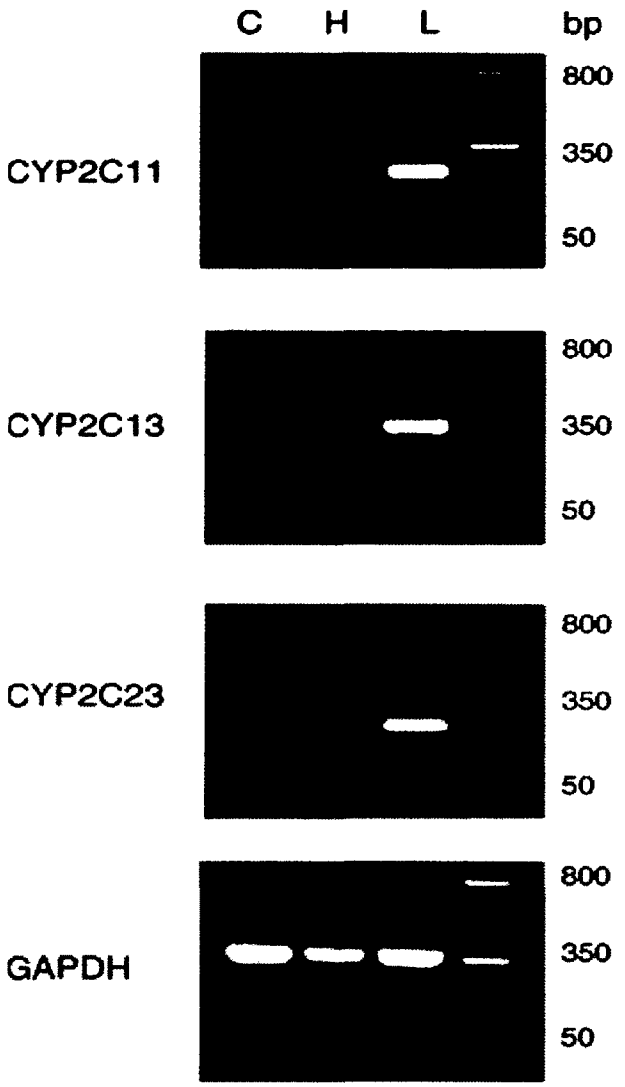

Fig. 3.13 Expression of *CYP2C11*, *CYP2C13*, and *CYP2C23* in H9c2 cells, rat heart, and rat liver. CYP2C11, CYP2C13, and CYP2C23 mRNAs were determined in H9c2 cells (C), rat heart (H) and rat liver (L) using the conventional RT-PCR method and GAPDH was included as endogenous control. This experiment was repeated on three occasions, but only one representative result is shown.

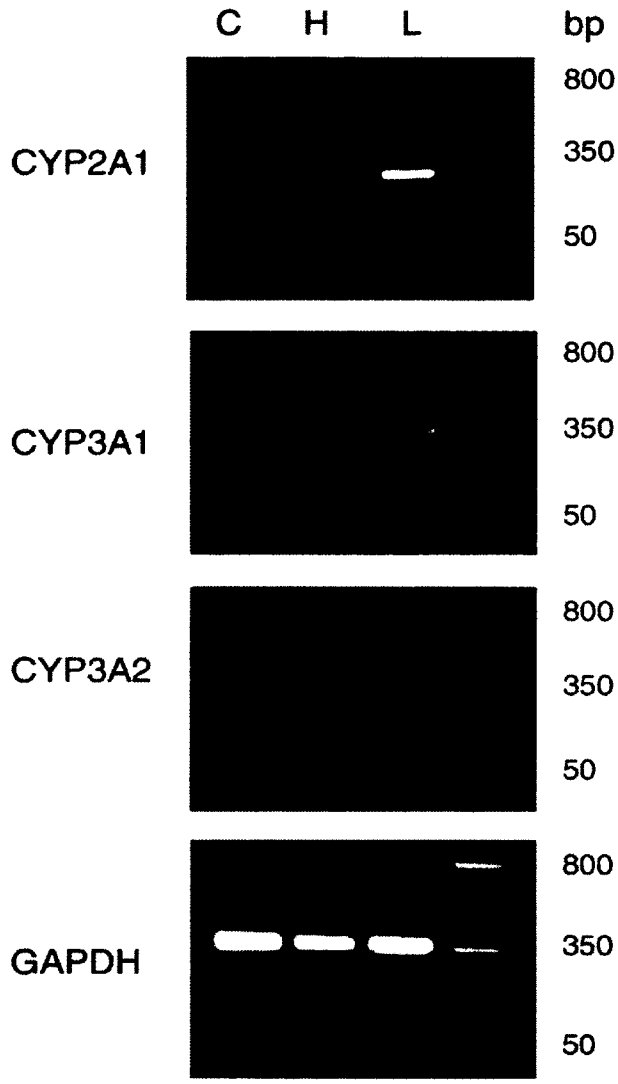

Fig. 3.14 Expression of *CYP2A1*, *CYP3A1*, and *CYP3A2* in H9c2 cells, rat heart, and rat liver. CYP2B1, CYP2A1, CYP3A1, and CYP3A2 mRNAs were determined in H9c2 cells (C), rat heart (H) and rat liver (L) using the conventional RT-PCR method and GAPDH was included as endogenous control. This experiment was repeated on three occasions, but only one representative result is shown.

3.3. 2,3,7,8-Tetrachlorodibenzo-p-dioxin and β-naphthoflavone induce cellular hypertrophy in H9c2 cells

3.3.1. Effect of TCDD and BNF on cell viability

To determine the cytotoxic effect of TCDD and BNF, H9c2 cells were incubated with increasing concentrations of TCDD (1 – 20 nM) or BNF (10 – 50 μM). Thereafter, cell viability was measured by the MTT assay as described under maeterials and methods. Our results clearly demonstrate that cells treated with TCDD (0 - 20 nM) or BNF (0 - 10 μM) maintained more than 98% cell viability with no significant difference as compared to the control (Fig. 3.15). Therefore, the observed changes in gene expression are not due to decreased cell viability or toxicity.

3.3.2. Effect of TCDD and BNF on the hypertrophic markers

In order to investigate whether TCDD or BNF treatment causes hypertrophy in H9c2 cells, we measured the gene expression of the hypertrophic markers, ANP and BNP, relative to the untreated cells following 24 h and 48 h of incubation with the AhR ligands. At the 24 h time-point, neither TCDD nor BNF caused a significant change in the gene expression of the hypertrophic markers ANP and BNP (Fig. 3.16A and B). On the other hand, at the 48 h time point both AhR ligands, TCDD and BNF, caused a significant induction of ANP by 2.5 and 2 fold, respectively (Fig. 3.16A).

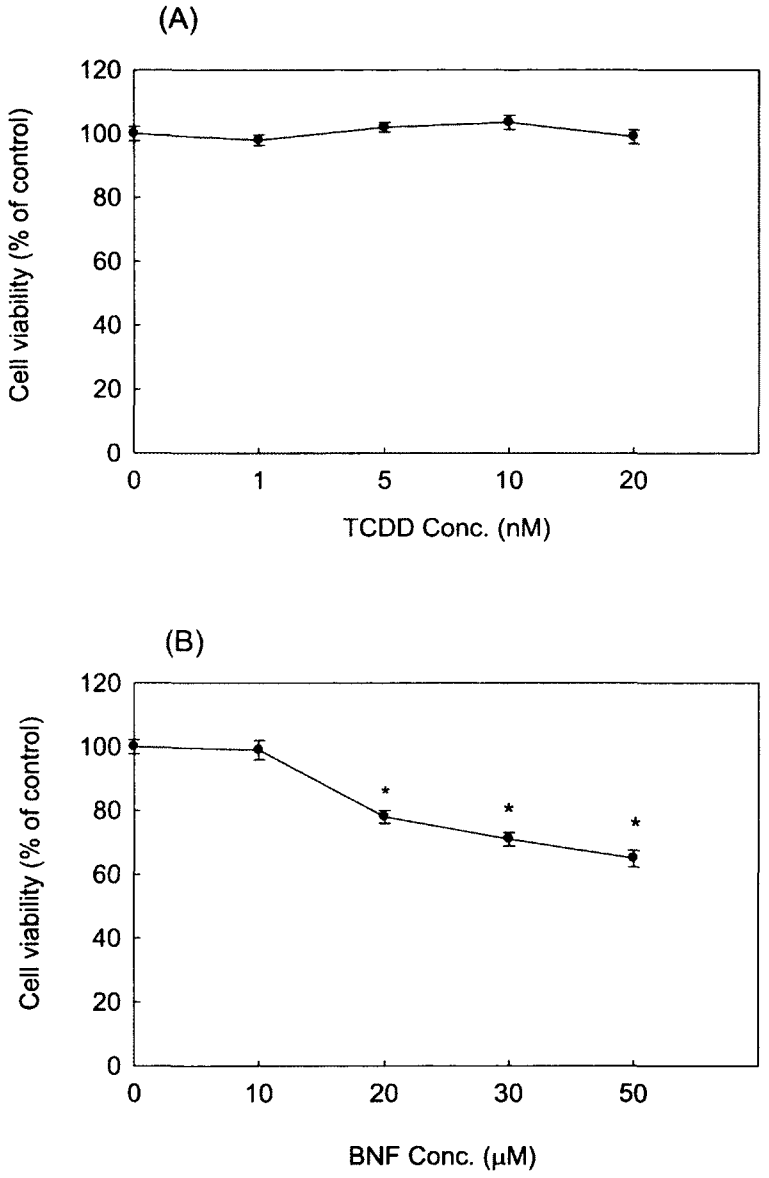

Fig. 3.15 Effect of TCDD (A) and BNF (B) on cell viability. H9c2 cells were incubated with increasing concentrations of TCDD (1-20 nM) or BNF (10-50 μ) for 48 h. Thereafter, cell viability was measured by the MTT assay as described under materials and methods. Values are presented as percentage of the control (mean ± SEM, $n = 8$). * $P < 0.05$ compared to control.

Similarly, TCDD and BNF caused a significant induction of BNP by about 3 and 4 fold, respectively (Fig. 16.B). In agreement with the induction of the hypertrophic markers, 48 h incubation with TCDD or BNF caused a significant increase in the cell surface area by about 20% and 30%, respectively (Fig. 16.C).

3.3.3. Effect of TCDD and BNF on *CYP* gene expression

To examine the effect of TCDD and BNF on the expression of various *CYP* genes, the cells were treated with TCDD or BNF for 24 and 48 h. Thereafter, the expression of different *CYP* genes was measured using real-time PCR.

Figure 3.17 shows the effect of TCDD and BNF on the expression of *CYP1* genes. After 24 h treatment, TCDD and BNF caused 15 and 10 fold induction of *CYP1A1* gene expression, respectively. Similarly, after 48 h treatment, TCDD and BNF caused 16 and 14 fold induction of *CYP1A1* gene expression (Fig. 3.17A). Similar to CYP1A1, TCDD and BNF caused a significant induction of *CYP1B1* by about 4 and 5 fold, respectively at both 24 h and 48 h time-points (Fig. 3.17 B).

With regard to the *CYP2* family, Figures 3.18 and 3.19 show the effect of TCDD and BNF on the *CYP2B1*, *CYP2B2*, *CYP2C11*, *CYP2E1*, and *CYP2J3* gene expression. There was no significant change in the gene expression of *CYP2B1*, *CYP2B2*, or *CYP2C11* after treating H9c2 cells with TCDD or BNF for 24 or 48 h (Fig. 3.18). Similarly, treatment of H9c2 cells with TCDD and BNF for 24 h did not change the expression of *CYP2E1* or *CYP2J3* significantly (Fig. 3.19).

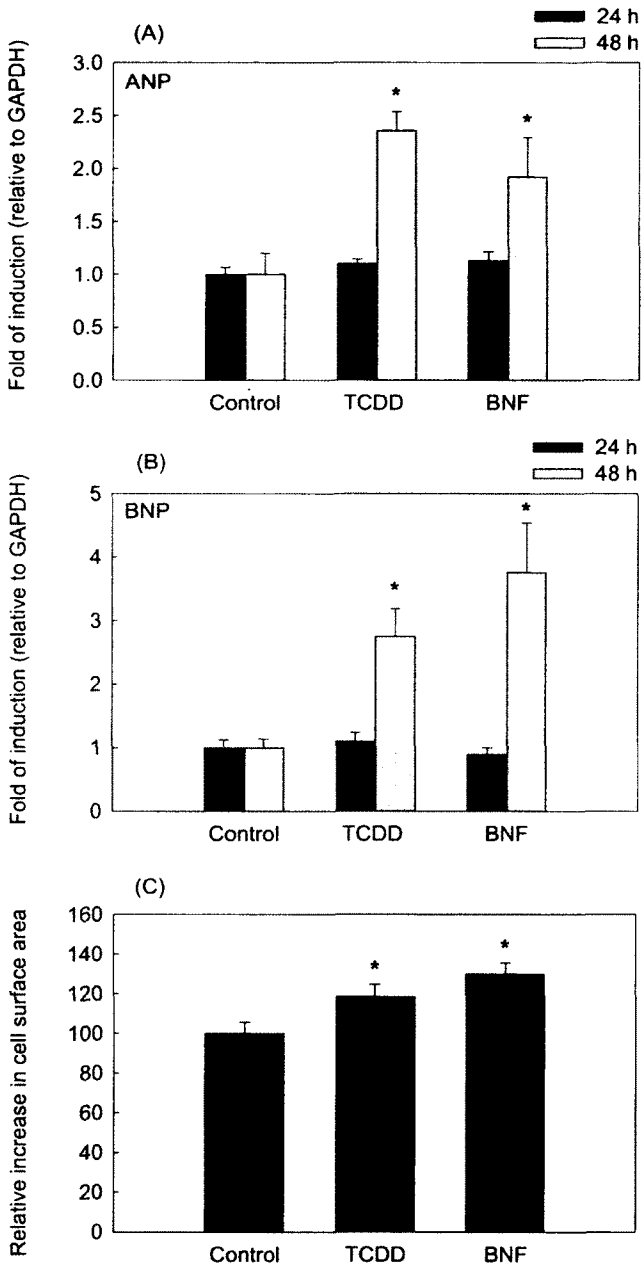

Fig. 3.16 Effect of TCDD and BNF on the hypertrophic markers, ANP (A) and BNP (B), and cell surface area (C). A and B. Cells were treated for 24 h and 48 h with 1 nM TCDD or 10 μM BNF. Thereafter, total RNA was isolated and the expression of the hypertrophic markers (ANP and BNP) were determined by real time-PCR as described under materials and methods. Fold of induction was calculated as target gene expression (normalized to GAPDH) divided by the control value (the control value was set as 1). Values are the mean ± SEM from 4 different treatments. **C.** Cells were treated for 48 h with 1 nM TCDD or 10 μM BNF. Thereafter, phase contrast images were taken and the relative cell surface area was analyzed using Zeiss Axion Visions software. Values are the mean ± SEM of 25 cells from 10 different images per treatment. * $P < 0.05$ compared to control.

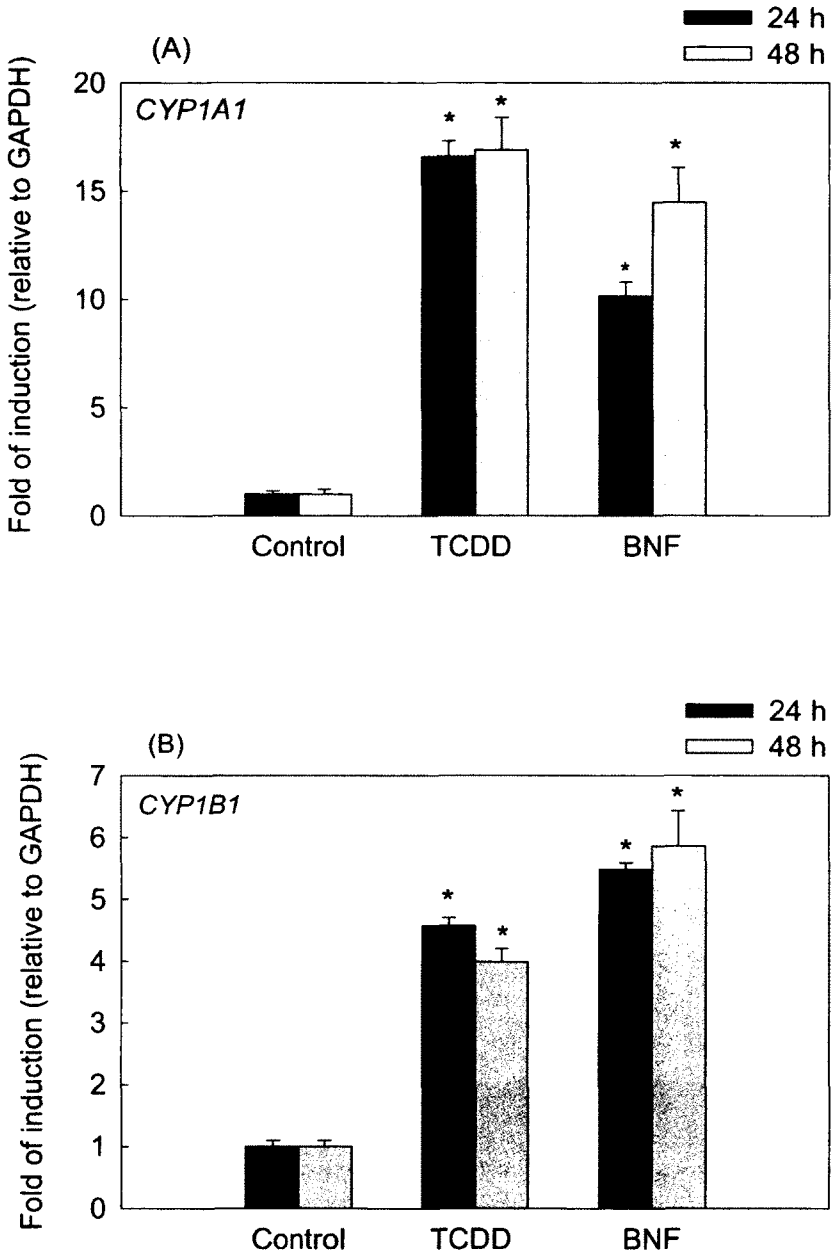

Fig. 3.17 Effect of TCDD and BNF on *CYP1A1* and *CYP1B1* gene expression. Cells were treated for 24 h and 48 h with 1 nM TCDD or 10 μM BNF. Thereafter, total RNA was isolated and the expressions of the *CYP1A1* and *CYP1B1* genes were determined by real time-PCR as described under materials and methods. Fold of induction was calculated as target gene expression (normalized to GAPDH) divided by the control value (control value was set as 1). Values are the mean ± SEM from 4 different treatments. * $P < 0.05$ compared to control.

On the other hand, after 48 h treatment, TCDD and BNF caused a significant induction of *CYP2E1* by 1.8 and 2.8 fold, respectively (Fig. 3.19A). Similarly, TCDD and BNF caused a significant induction of *CYP2J3* by 2.4 and 3.8 fold, respectively (Fig. 3.19B).

Figures 3.20, 3.21, and 3.22 show the effect of TCDD and BNF on the gene expression of the *CYP4* family. There was a significant induction in the gene expression of *CYP4A1* by the treatment with TCDD or BNF for 24 h but not for 48 h (Fig. 3.20A). However, there was no significant change in the gene expression of *CYP4A3* by the treatment with TCDD or BNF for 24 h or 48 h (Fig. 3.20B). With regard to the CYP4F subfamily, neither TCDD nor BNF caused a significant change in CYP4F1 at either of the two time points (Fig. 3.21A). Similarly, TCDD and BNF did not cause any significant change in *CYP4F4* gene expression after 24 h of treatment. However, TCDD and BNF caused a significant induction of *CYP4F4* by 2.4 and 4.4 fold, respectively, after 48 h treatment (Fig 3.21B). Similar to *CYP4F1*, there was no significant change in the gene expression of *CYP4F5* and *CYP4F6* by the treatment with TCDD or BNF for 24 h or 48 h (Fig. 3.22).

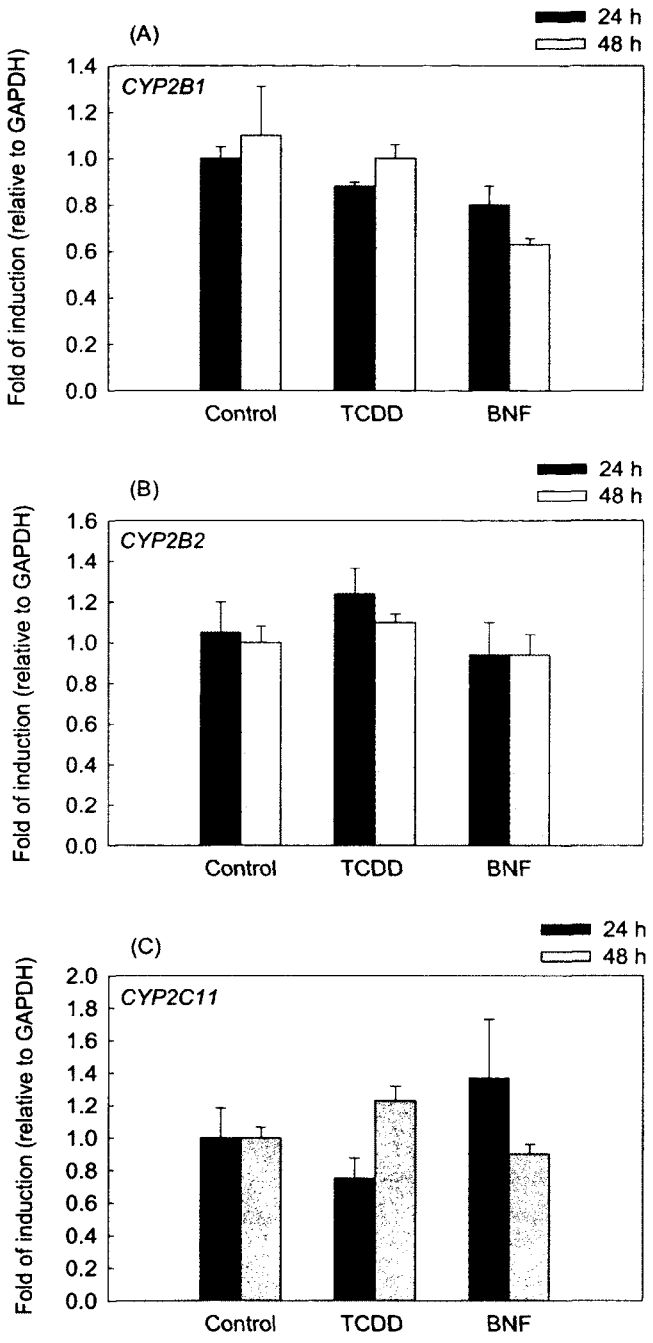

Fig. 3.18 Effect of TCDD and BNF on *CYP2B1, CYP2B2,* and *CYP2C11* gene expression. Cells were treated for 24 h and 48 h with 1 nM TCDD or 10 μM BNF. Thereafter, total RNA was isolated and the expressions of the *CYP2B1, CYP2B2,* and *CYP2C11* genes were determined by real time-PCR as described under materials and methods. Fold of induction was calculated as target gene expression (normalized to GAPDH) divided by the control value (control value was set as 1). Values are the mean ± SEM from 4 different treatments. * $P < 0.05$ compared to control.

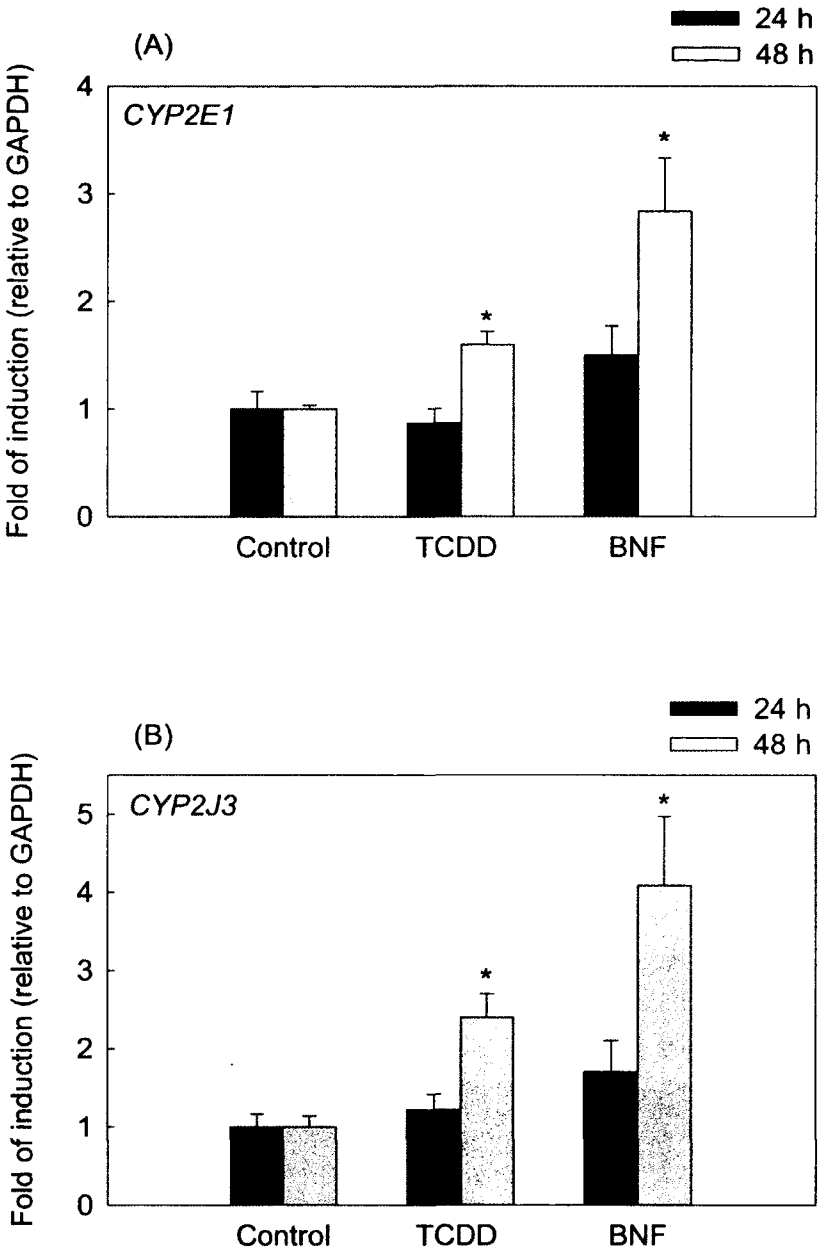

Fig. 3.19 Effect of TCDD and BNF on *CYP2E1* and *CYP2J3* gene expression. Cells were treated for 24 h and 48 h with 1 nM TCDD or 10 μM BNF. Thereafter, total RNA was isolated and the expressions of the *CYP2E1* and *CYP2J3* genes were determined by real time-PCR as described under materials and methods. Fold of induction was calculated as target gene expression (normalized to GAPDH) divided by the control value (control value was set as 1). Values are the mean ± SEM from 4 different treatments. * $P < 0.05$ compared to control.

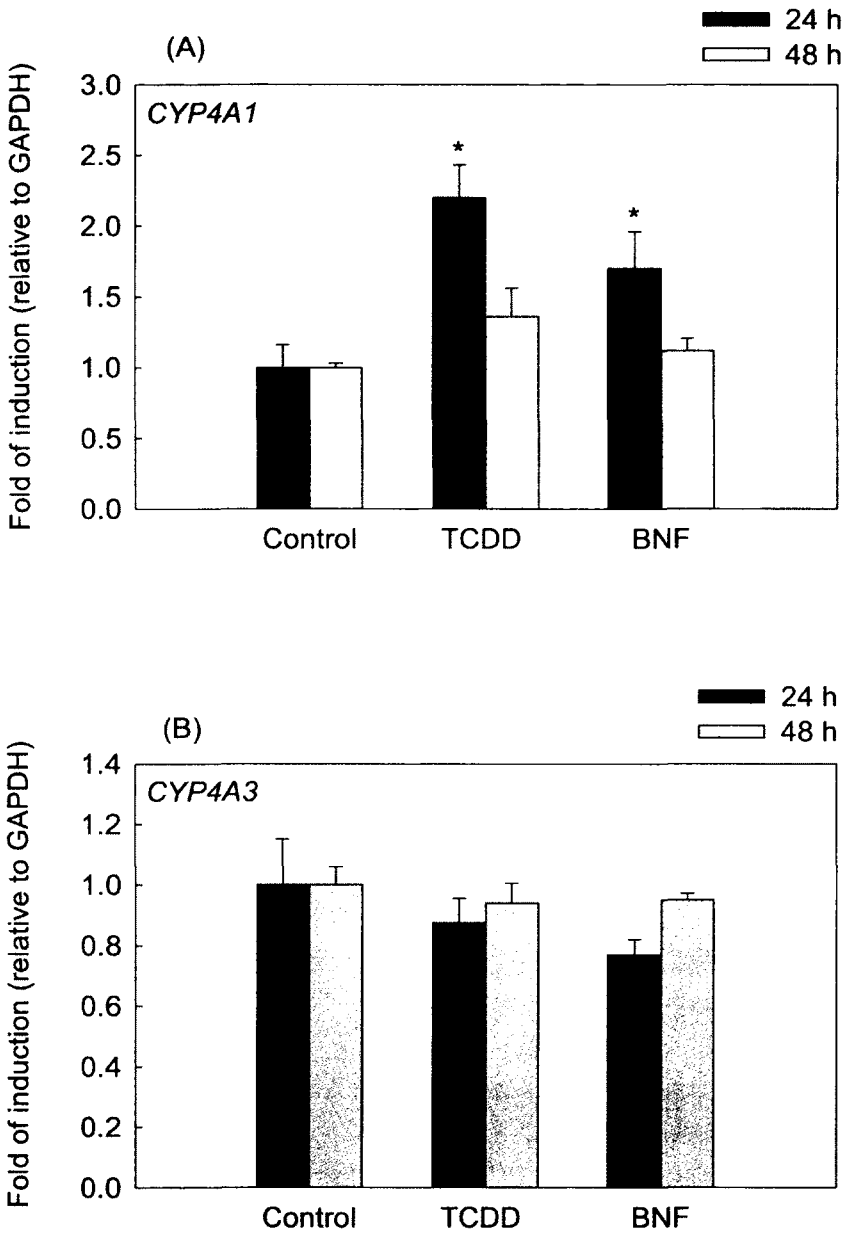

Fig. 3.20 Effect of TCDD and BNF on *CYP4A1* and *CYP4A3* gene expression. Cells were treated for 24 h and 48 h with 1 nM TCDD or 10 μM BNF. Thereafter, total RNA was isolated and the expressions of the *CYP4A1* and *CYP4A3* genes were determined by real time-PCR as described under materials and methods. Fold of induction was calculated as target gene expression (normalized to GAPDH) divided by the control value (control value was set as 1). Values are the mean ± SEM from 4 different treatments. * $P < 0.05$ compared to control.

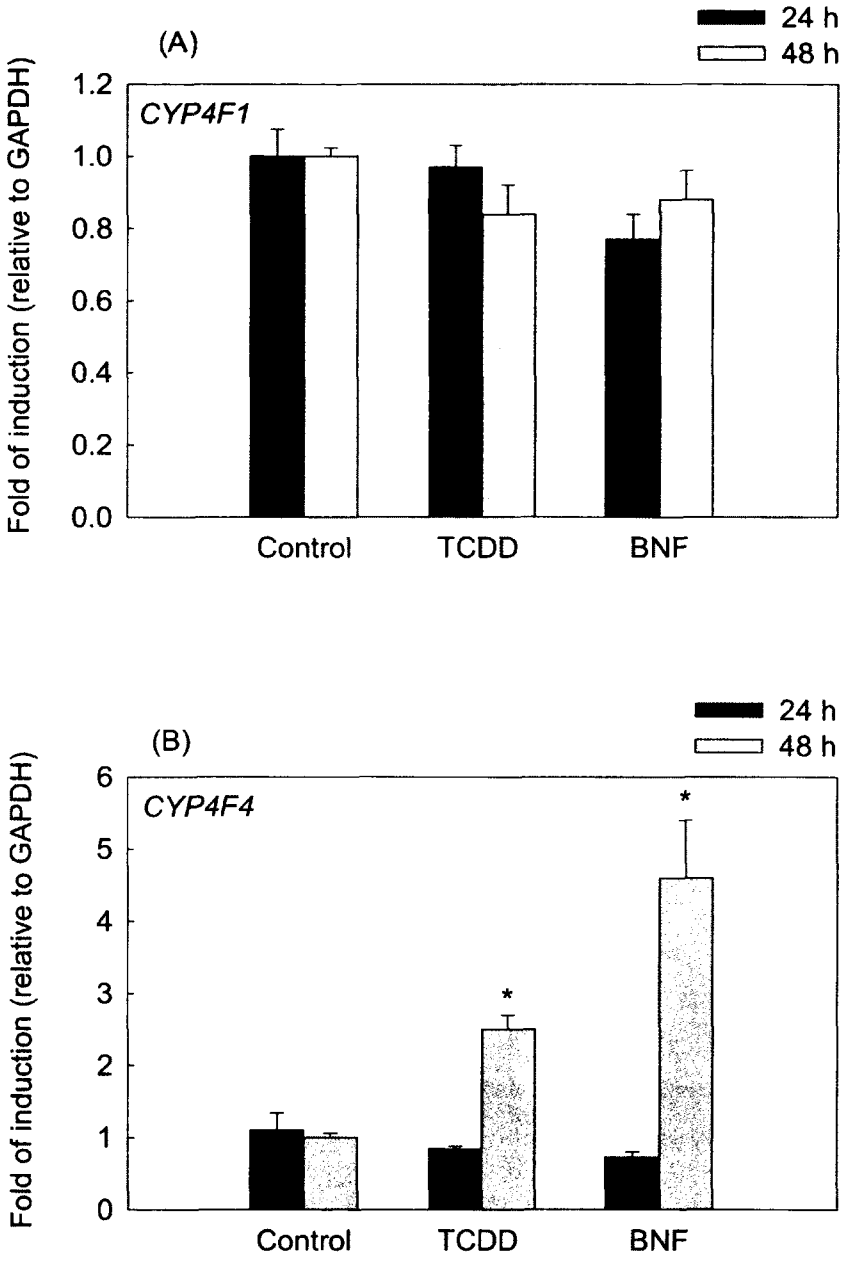

Fig. 3.21 Effect of TCDD and BNF on *CYP4F1* and *CYP4F4* gene expression. Cells were treated for 24 h and 48 h with 1 nM TCDD or 10 μM BNF. Thereafter, total RNA was isolated and the expression of the *CYP4F1* and *CYP4F4* genes were determined by real time-PCR as described under materials and methods. Fold of induction was calculated as target gene expression (normalized to GAPDH) divided by the control value (control value was set as 1). Values are the mean ± SEM from 4 different treatments. * $P < 0.05$ compared to control.

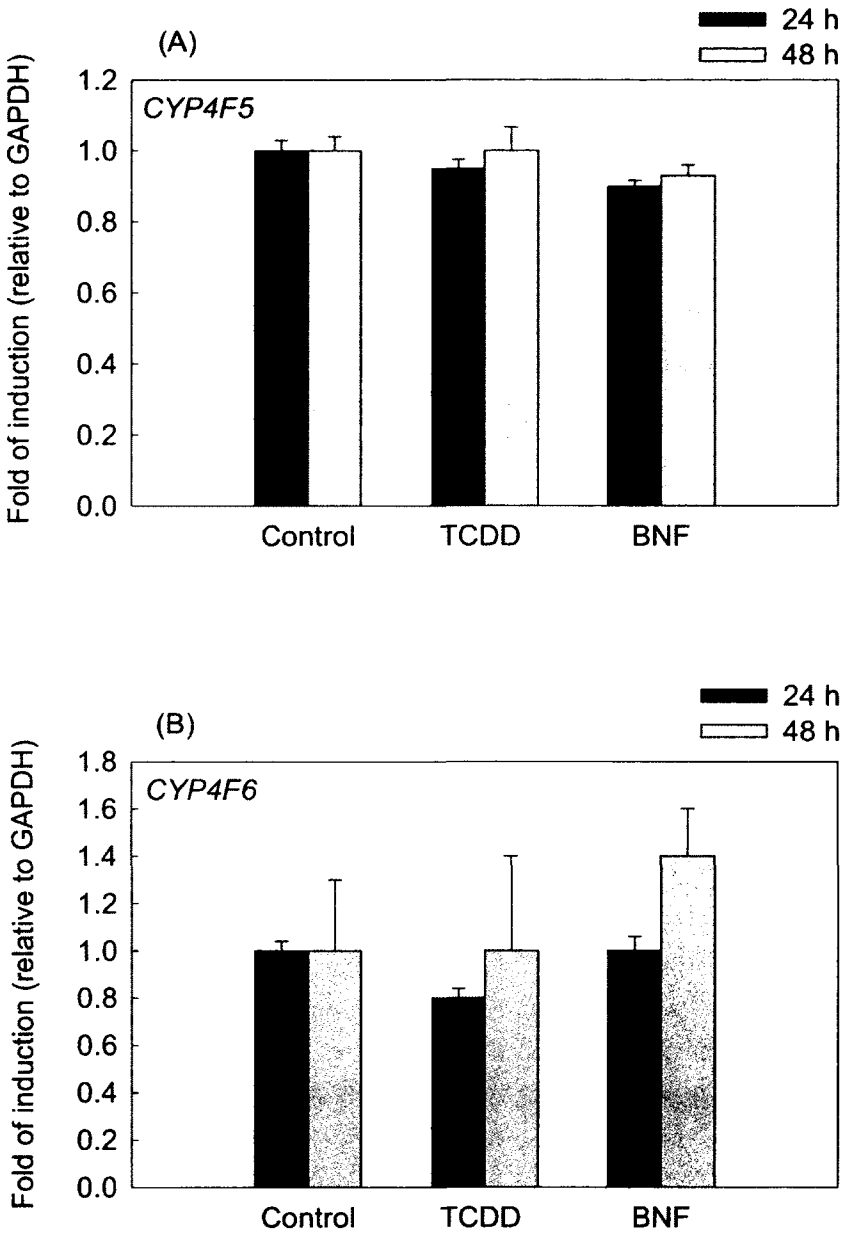

Fig. 3.22 Effect of TCDD and BNF on *CYP4F5* and *CYP4F6* gene expression. Cells were treated for 24 h and 48 h with 1 nM TCDD or 10 μM BNF. Thereafter, total RNA was isolated and the expression of the *CYP4F5* and *CYP4F6* genes were determined by real time-PCR as described under materials and methods. Fold of induction was calculated as target gene expression (normalized to GAPDH) divided by the control value (control value was set as 1). Values are the mean ± SEM from 4 different treatments. * $P < 0.05$ compared to control.

3.3.4. Effect of TCDD and BNF on ROS production

We examined whether the hypertrophic effect of TCDD and BNF was associated with an increase of intracellular ROS production. ROS was analyzed fluorometrically by measuring the oxidation a non-fluorescent probe (DCF-DA) to a fluorescent metabolite (DCF) by the ROS as described under materials and methods. Neither 1 nM TCDD nor 10 μM BNF caused any significant change in the ROS production, whereas DOX, used as a positive control, caused a significant increase in the ROS production (Fig. 3.23).

3.3.5. Effect of resveratrol on TCDD-mediated hypertrophy

To examine the protective effect of the AhR antagonist, resveratrol, against TCDD-induced hypertrophy, H9c2 cells were pretreated with 20 μM resveratrol for 2 h and then 1 nM TCDD or TCDD alone was added for an additional 48 h. Thereafter, the gene expression of the hypertrophic markers, ANP and BNP, was measured as described under materials and methods. TCDD alone caused a significant induction of ANP and BNP. Pretreatment with resveratrol significantly decreased the TCDD-mediated effect by 120% and 70% for ANP and BNP, respectively (Fig. 3.24).

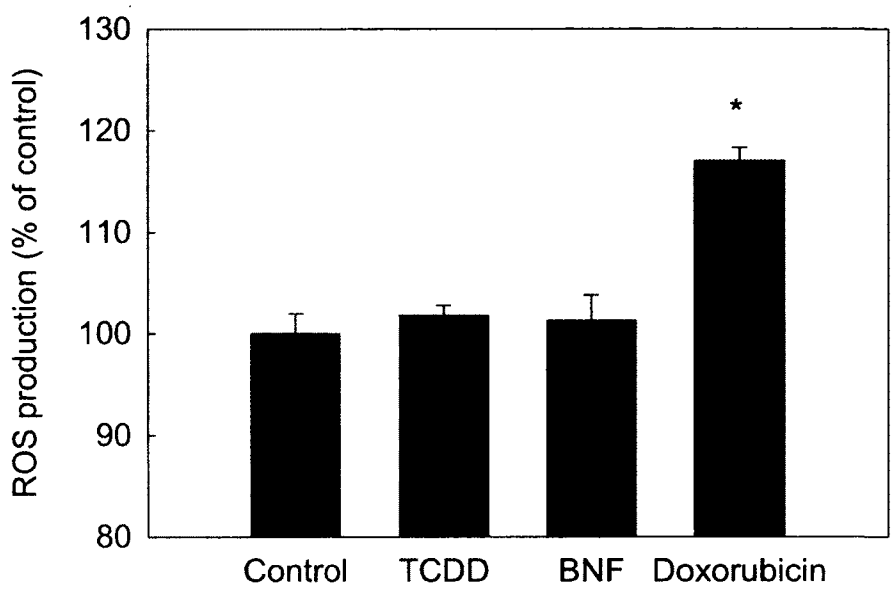

Fig. 3.23 Effect of TCDD and BNF on ROS production. Cells were treated for 48 h with 1 nM TCDD or 10 μM BNF with 10 μM DCF-DA. ROS production was measured flurometrically using excitation/emission wavelengths of 484/535 nm as described under materials and methods. Values are presented as mean ± SEM (n = 6). * $P < 0.05$ compared with control.

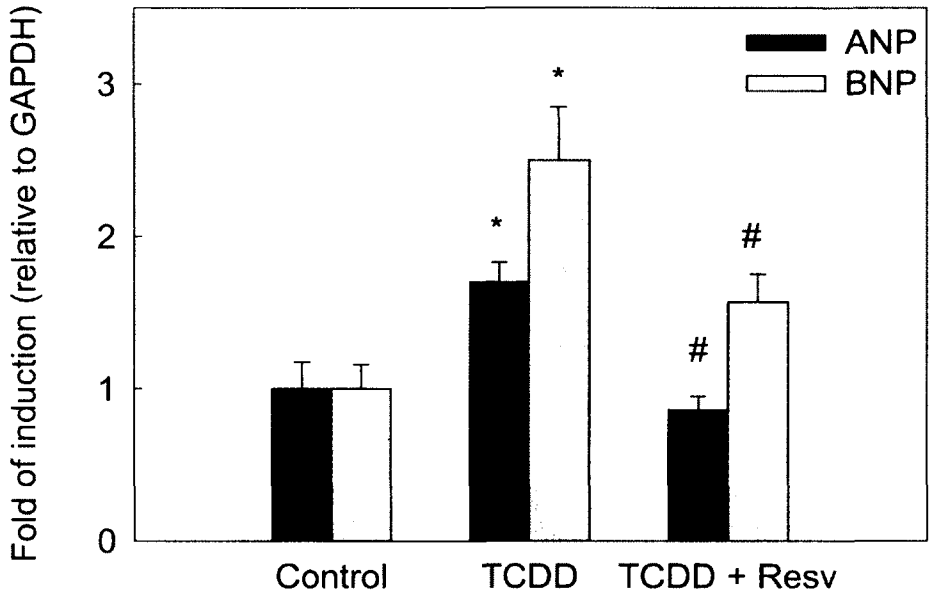

Fig. 3.24 Effect of resveratrol on the TCDD-induced hypertrophy. Cells were pretreated with 20 μM resveratrol for 2 h prior to addition of 1 nM TCDD for 48 h. Thereafter, total RNA was isolated and the expressions of the hypertrophic markers (ANP and BNP) were determined by real time-PCR as described under materials and methods. Fold of induction was calculated as target gene expression (normalized to GAPDH) divided by the control value (the control value was set as 1). Values are the mean ± SEM from 4 different treatments. * $P < 0.05$ compared to control.

3.4. Induction of several Cytochrome P450 genes by doxorubicin in H9c2 cells

3.4.1. Expression of various *CYP* genes in H9c2 cells

To examine the constitutive expression of various *CYP* genes in H9c2 cells, total RNA was isolated from control untreated cells and different *CYP* genes were determined by real-time PCR. All the examined genes were found to be constitutively expressed in H9c2 cells at varying levels (Fig. 3.25). *CYP2B2* was the lowest expressed gene and was considered as calibrator. *CYP1B1* was the most highly expressed gene, at about 10000 fold higher than the calibrator, CYP2B2. *CYP2B1*, *CYP2J3*, *CYP1A1*, *CYP2C11*, *CYP2C23*, *CYP2E1* and *CYP1A2* genes were expressed at moderate to low levels, at about 215, 52, 22, 16, 16, 7 and 2 fold higher than the calibrator, respectively (Fig. 3.25).

3.4.2. Effect of DOX on cell viability

To determine the cytotoxic effect of DOX, H9c2 cells were incubated with increasing concentrations of DOX for 2 h and the medium was replaced by fresh medium for another 24 h. Thereafter, cell viability was measured by the MTT assay. Our results clearly demonstrate that cells treated with DOX (1-10 μM) for 2 h maintained more than 90% cell viability (Fig. 3.26). Therefore, the observed changes in gene expression are not due to decreased cell viability or toxicity.

3.4.3. Effect of DOX on hypertrophic markers

In order to investigate whether DOX treatment causes cellular hypertrophy in H9c2 cells, we measured the gene expression of the hypertrophic markers, ANP and BNP, relative to the untreated cells. DOX at lower concentrations, 1-5 μM, caused a minor but statistically significant induction of the hypertrophic marker ANP; however, it did not significantly alter the gene expression of hypertrophic marker BNP at these low concentrations (Fig. 3.27). Treatment of H9c2 cells with 10 μM DOX, the highest concentration tested, caused significant induction of both hypertrophic markers, ANP and BNP, by 3 and 7 fold, respectively (Fig. 3.27).

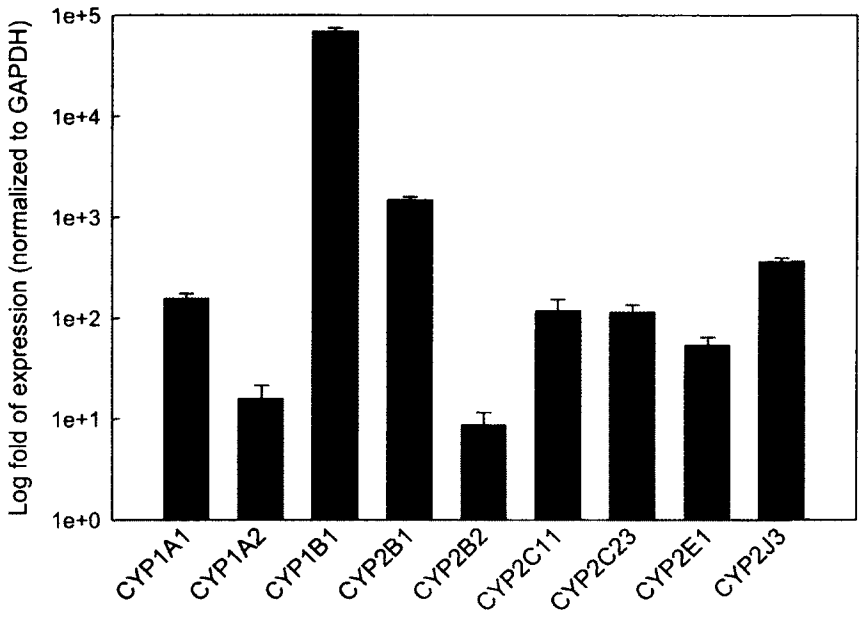

Fig. 3.25 Relative expression of several *CYP* genes in the H9c2 cells. To examine the constitutive expression of different *CYP* genes in the heart, total RNA was isolated from H9c2 cells using TRIzol reagent. First-strand cDNA was synthesized from 1.5 μg total RNA. cDNA fragments were amplified and quantified using ABI 7500 real-time PCR system as described under materials and methods. Relative expression was calculated as target gene expression (normalized to GAPDH) divided by the lowest gene expressed, *CYP2B2* (*CYP2B2* value was set as 1). Values are the mean ± SEM from 4 different biological replicates.

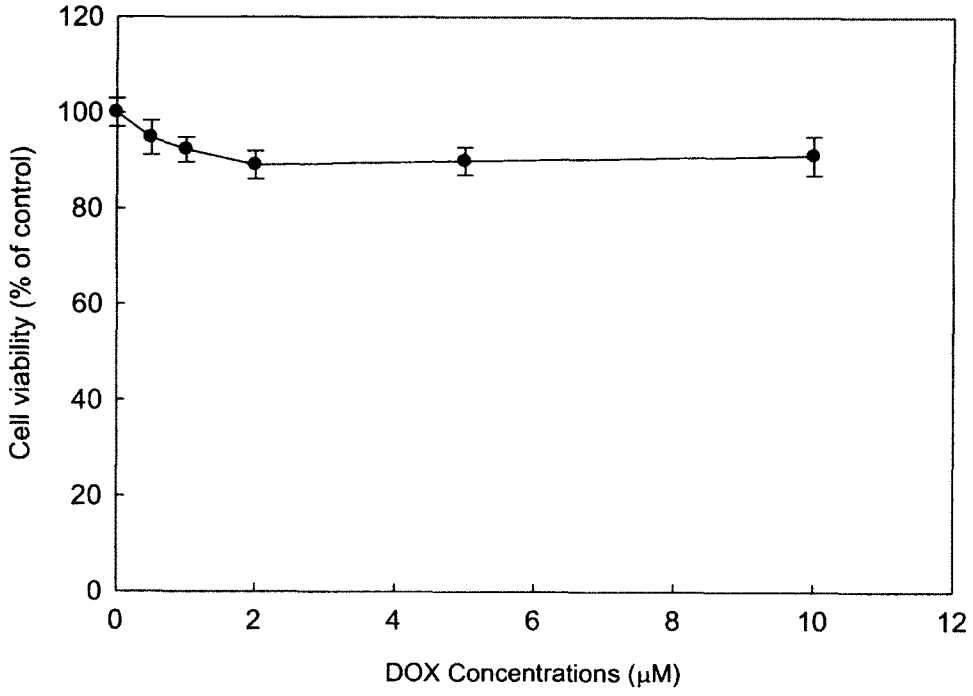

Fig. 3.26 Effect of DOX on cell viability. H9c2 cells were incubated with increasing concentrations of DOX for 2 h and the medium was replaced by fresh medium for another 24 h. Cell viability was measured by the MTT assay as described under materials and methods. Values are presented as percentage of the control (mean ± SEM, n = 8).

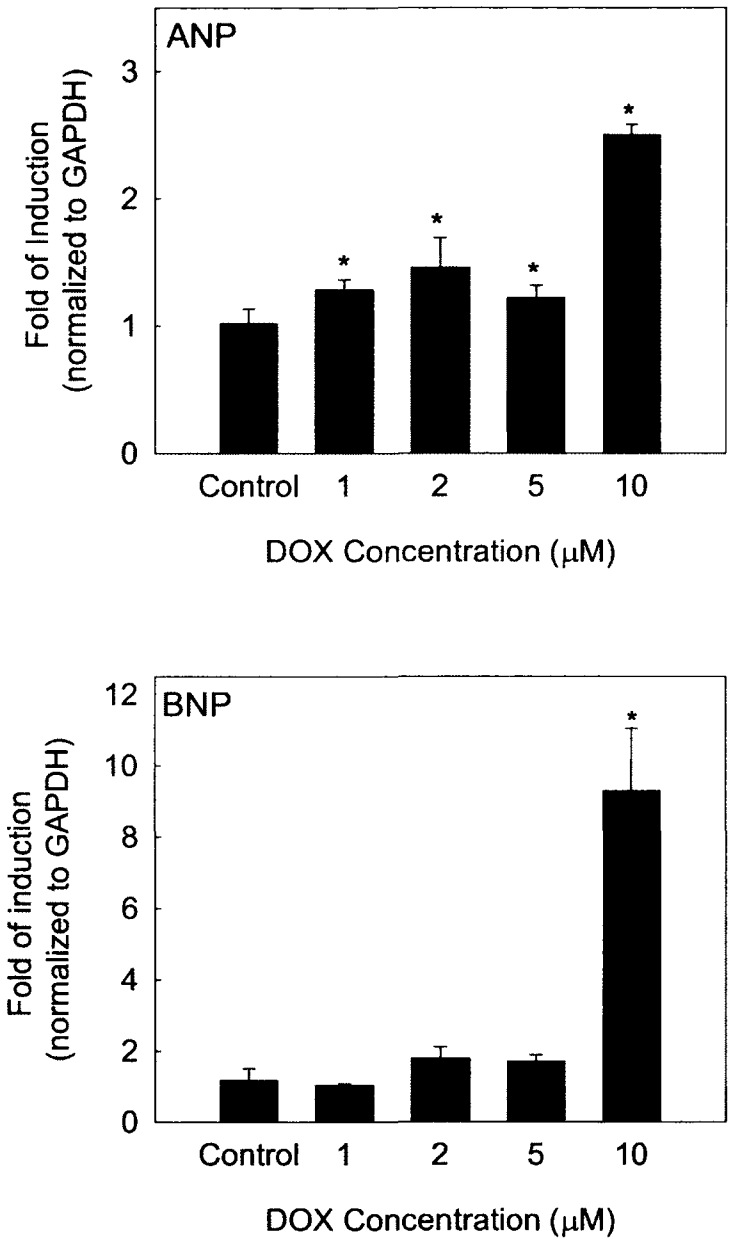

Fig. 3.27 Effect of DOX on the hypertrophic markers, ANP and BNP. Cells were treated for 2 h with increasing concentrations of DOX (1-10 μM) as described under materials and methods. Thereafter, total RNA was isolated and the expressions of the hypertrophic markers (ANP and BNP) were determined by real time-PCR. First-strand cDNA was synthesized from 1.5 μg total RNA. cDNA fragments were amplified and quantified using ABI 7500 real-time PCR system as described under materials and methods. Fold of induction was calculated as target gene expression (normalized to GAPDH) divided by the control value (the control value was set as 1). Values are the mean ± SEM from 4 different treatments. * $P < 0.05$ compared to control.

3.4.4. Effect of DOX on *CYP* gene expression

To examine the effect of DOX on the expression of various *CYP* genes, the cells were treated with increasing concentrations of DOX. Thereafter, the expression of different *CYP* genes was measured using real-time PCR.

Figure 3.28 shows the effect of DOX on *CYP1* family gene expression. Our results demonstrate that treatment of H9c2 cells with increasing concentrations of DOX caused a concentration-dependent induction of *CYP1A1*. The induction was 2, 2.5, and 18 fold higher than the controls with DOX concentrations of 2, 5, and 10 μM, respectively (Fig. 3.28). On the other hand, induction of *CYP1A2* was significantly higher at all concentrations of DOX tested. The fold of *CYP1A2* induction was higher than that of *CYP1A1*. The induction was 5, 15, 18, and 45 fold higher than control with DOX concentrations of 1, 2, 5, and 10 μM, respectively (Fig. 3.28). Similar to *CYP1A1* and *CYP1A2*, DOX caused a concentration-dependent induction of *CYP1B1* starting at 2 μM concentration. The induction was 2, 3, and 5 fold higher than controls with DOX concentrations of 2, 5, and 10 μM, respectively (Fig. 3.28).

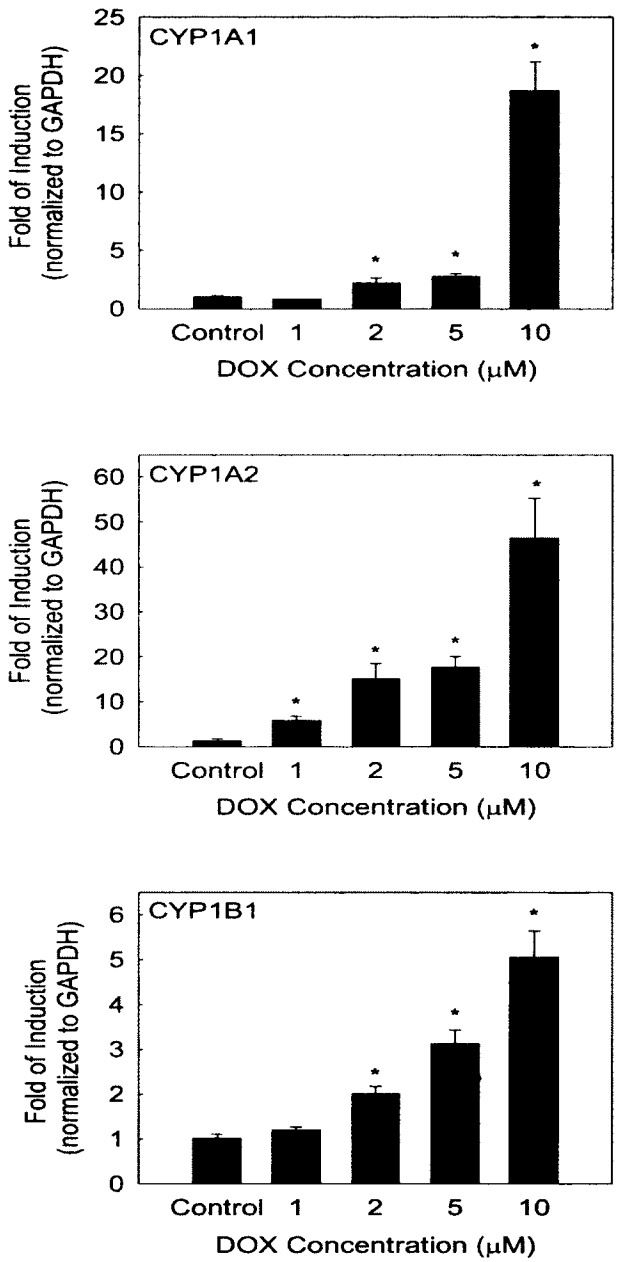

Fig. 3.28 Effect of DOX on *CYP1A1*, *CYP1A2*, and *CYP1B1* gene expression. Cells were treated for 2 h with increasing concentrations of DOX (1-10 μM) as described under materials and methods. Thereafter, total RNA was isolated and the expressions of the *CYP1A1*, *CYP1A2*, and *CYP1B1* genes were determined by real time-PCR. First-strand cDNA was synthesized from 1.5 μg total RNA. cDNA fragments were amplified and quantified using ABI 7500 real-time PCR system as described under materials and methods. Fold of induction was calculated as target gene expression (normalized to GAPDH) divided by the control value (control value was set as 1). Values are the mean ± SEM from 4 different treatments. * $P < 0.05$ compared to control.

With regard to the *CYP2* family, Figures 3.29, 3.30 and 3.31 show the effect of DOX on *CYP2B1*, *CYP2B2*, *CYP2C11*, *CYP2C23*, *CYP2E1*, and *CYP2J3* gene expression. Treatment of H9c2 cells with DOX did not significantly alter the gene expression of *CYP2B1* at all concentrations tested. However, at concentrations of 5 and 10 μM DOX there was a trend of inhibition of *CYP2B1* but it did not reach the statistical significance (Fig. 3.29). On the contrary, DOX caused a concentration-dependent induction of *CYP2B2* at all the tested concentrations. DOX concentrations of 1, 2, 5 and 10 μM caused a significant induction of *CYP2B2* gene expression by 8, 20, 54, and 96 fold, respectively as compared to the controls (Fig. 3.29).

CYP2C11 and *CYP2C23* genes were constitutively expressed almost at the same level in H9c2 cells (Fig. 3.30). Our results show that only the highest concentration of DOX tested, which was 10 μM, significantly induced *CYP2C11* gene expression, whereas the lowest concentrations tested, 1-5 μM did not significantly alter its expression (Fig. 3.30). On the other hand, DOX did not significantly alter the gene expression of *CYP2C23* at all the tested concentrations. With regard to *CYP2E1* gene expression, DOX treatment caused a concentration-dependent induction of *CYP2E1* by 2, 4, 6, and 12-fold with DOX concentrations of 1, 2, 5, and 10 μM, respectively (Fig. 3.31). Similarly, *CYP2J3* was induced in a concentration-dependent manner by DOX treatment; however, the fold of induction was 1.5, 1.6, 2.5, and 2.5 with DOX concentration of 1, 2, 5, and 10 μM, respectively (Fig. 3.31).

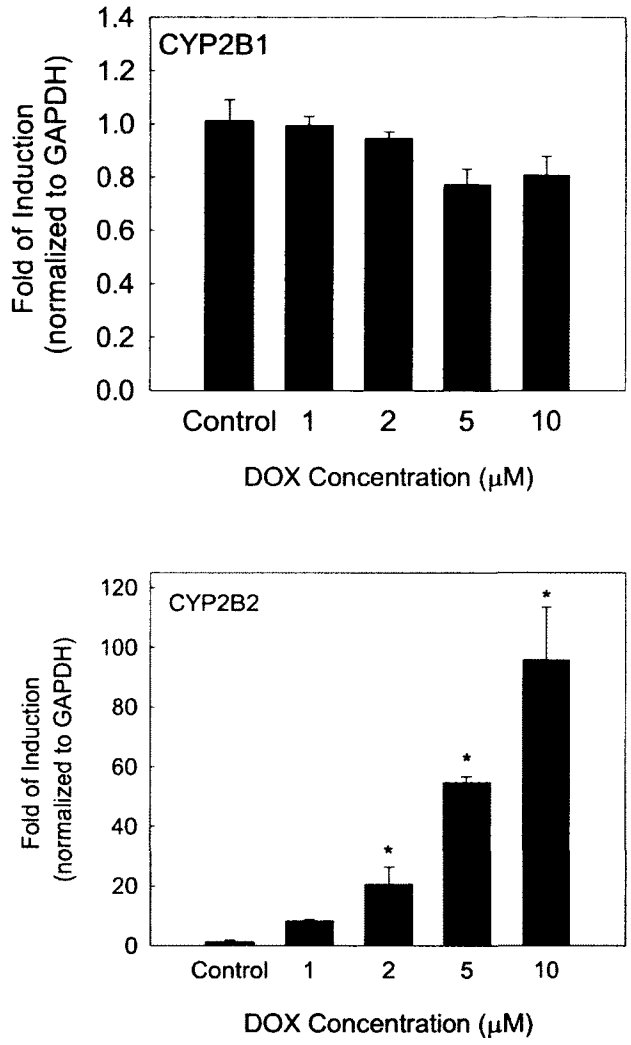

Fig. 3.29 Effect of DOX on *CYP2B1* and *CYP2B2* gene expression. Cells were treated for 2 h with increasing concentrations of DOX (1-10 μM) as described under materials and methods. Thereafter, total RNA was isolated and the expressions of the *CYP2B1* and *CYP2B2* genes were determined by real time-PCR. First-strand cDNA was synthesized from 1.5 μg total RNA. cDNA fragments were amplified and quantitated using ABI 7500 real-time PCR system as described under materials and methods. Fold of induction was calculated as target gene expression (normalized to GAPDH) divided by the control value (the control value was set as 1). Values are the mean ± SEM from 4 different treatments. * $P < 0.05$ compared to control.

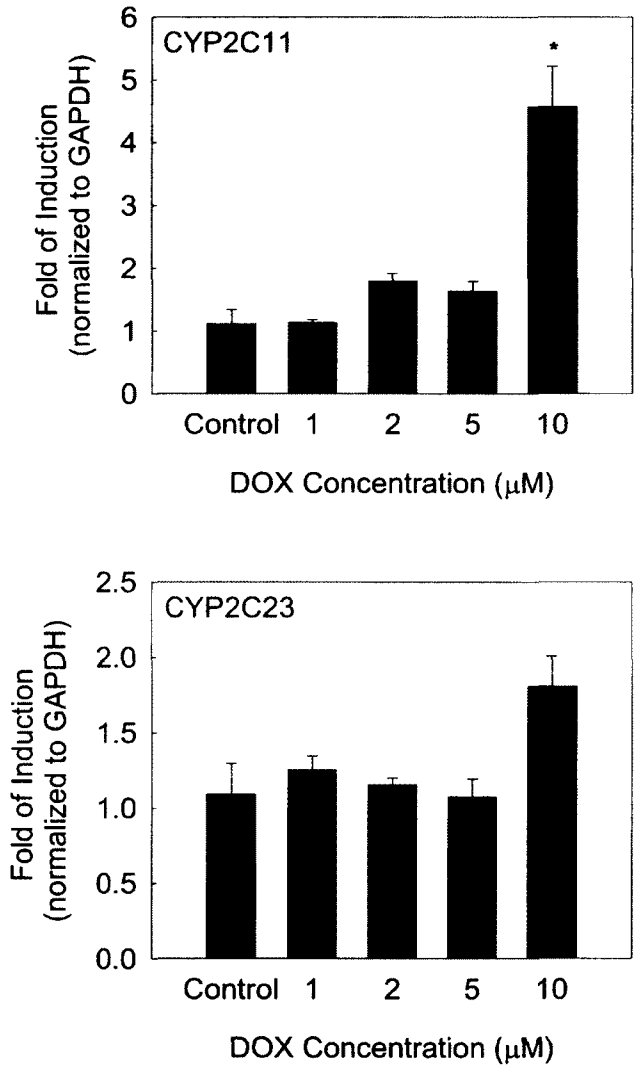

Fig. 3.30 Effect of DOX on *CYP2C11* and *CYP2C23* gene expression. Cells were treated for 2 h with increasing concentrations of DOX (1-10 μM) as described under materials and methods. Thereafter, total RNA was isolated and the expressions of the *CYP2C11* and *CYP2C23* genes were determined by real time-PCR. First-strand cDNA was synthesized from 1.5 μg total RNA. cDNA fragments were amplified and quantitated using ABI 7500 real-time PCR system as described under materials and methods. Fold of induction was calculated as target gene expression (normalized to GAPDH) divided by the control value (the control value was set as 1). Values are the mean ± SEM from 4 different treatments. * $P < 0.05$ compared to control.

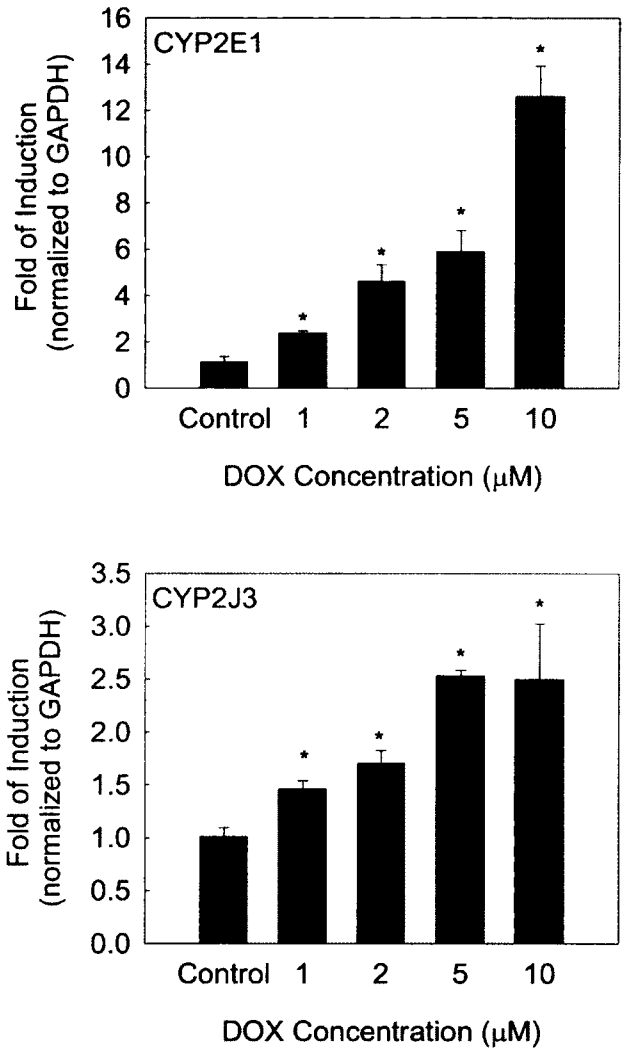

Fig. 3.31 Effect of DOX on *CYP2E1* and *CYP2J3* gene expression. Cells were treated for 2 h with increasing concentrations of DOX (1-10 μM) as described under materials and methods. Thereafter, total RNA was isolated and the expressions of the *CYP2E1* and *CYP2J3* genes were determined by real time-PCR. First-strand cDNA was synthesized from 1.5 μg total RNA. cDNA fragments were amplified and quantitated using ABI 7500 real-time PCR system as described under materials and methods. Fold of induction was calculated as target gene expression (normalized to GAPDH) divided by the control value (the control value was set as 1). Values are the mean ± SEM from 4 different treatments. *P < 0.05 compared to control.

3.5. Acute doxorubicin cardiotoxicity alters cardiac Cytochrome P450 expression and arachidonic acid metabolism in rats

3.5.1. Effect of DOX treatment on LDH and on the hypertrophic markers

In order to confirm the occurrence of acute cardiotoxicity by DOX treatment, serum LDH was determined. LDH was significantly increased in the serum of DOX-treated rats to about 180% of its control value at 24 h after DOX administration; however, LDH level was not changed at 6 and 12 h after DOX administration (Fig. 3.32A). In order to investigate the effect of acute DOX cardiotoxicity on hypertrophic markers, we measured the cardiac gene expression of ANP and BNP relative to control rats. Our results showed that DOX treatment caused statistically significant inhibition of the hypertrophic marker ANP by 40% and 50%, 12 and 24 h after DOX administration, respectively. However, ANP expression was not significantly altered 6 h after DOX administration. On the other hand, there was a time-dependent statistically significant inhibition of BNP by 60%, 70%, and 80% at 6, 12, and 24 h after DOX administration, respectively (Fig. 3.32B).

3.5.2. Effect of DOX treatment on cardiac *CYP* gene expression

To examine the effect of DOX treatment on the cardiac expression of several *CYP* genes, total RNA was extracted from the heart of both control and DOX-treated rats. Thereafter, the expression of different genes was measured using RT followed by real time-PCR as described under materials and methods.

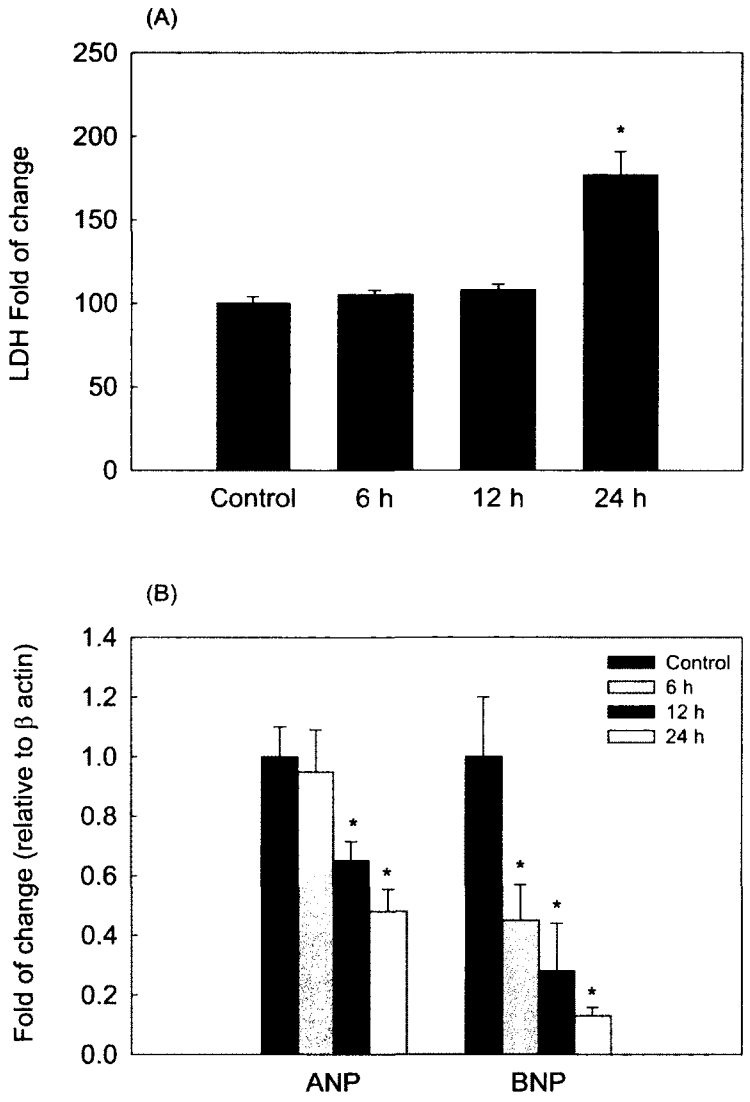

Fig. 3.32 Effect of acute DOX cardiotoxicity on LDH (A) and on the hypertrophic markers (B). (A) LDH was estimated in the serum by commercially available kit as described under materials and methods. The amount of LDH was calculated relative to the control and presented as percentage of control and DOX-treated animals for 6, 12, and 24 h. (B) Total RNA was isolated from the hearts of control and DOX-treated animals for 6 , 12 , and 24 h. ANP and BNP gene expressions were determined by real-time PCR. Results are presented as mean ± SEM (n = 6). * $P < 0.05$ compared with control.

Figure 3.33A shows the effect of DOX-induced cardiotoxicity on *CYP1* family gene expression 24 h after DOX administration. DOX treatment caused a significant induction of *CYP1A1* and *CYP1B1* gene expression in the heart by 100% and 230%, respectively. With regard to *CYP2* family, DOX treatment caused a significant induction of the gene expression of two important epoxygenases, *CYP2C11* and *CYP2J3*, by 380% and 80%, respectively, 24 h after DOX administration. However, the gene expression of *CYP2B1* and *CYP2E1* was not significantly altered (Fig. 3.33B).

With regard to the gene expression of major ω-hydroxylases, figure 3.34 shows the effect of DOX treatment on *CYP4* family gene expression 24 h after DOX administration. Acute DOX cardiotoxicity caused a significant induction of *CYP4A1* and *CYP4A3* by 280% and 200%, respectively (Fig. 3.34A). Similarly, DOX treatment caused a significant induction of *CYP4F1* and *CYP4F4* gene expression by 100% and 150%, respectively. However, the expression of *CYP4F5* and *CYP4F6* was not significantly altered (Fig. 3.34B). Interestingly, all *CYP* gene expression was not significantly altered 6 and 12 h after DOX administration.

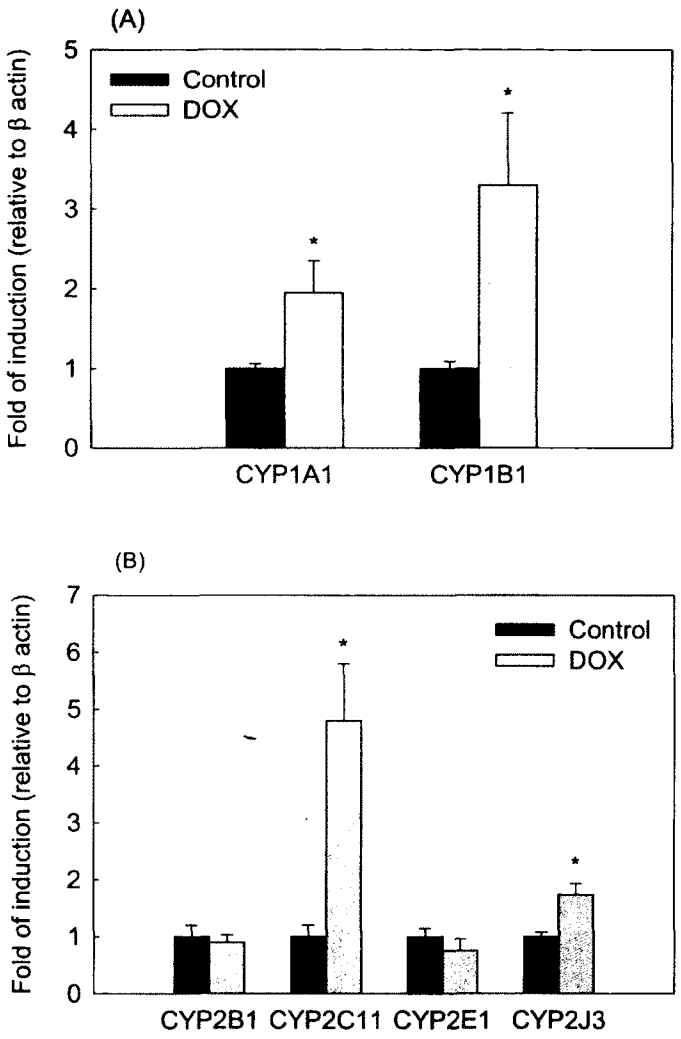

Fig. 3.33 Effect of acute DOX cardiotoxicity on CYP1 (A) and CYP2 family gene expression (B). Total RNA was isolated from the hearts of controls and animals treated with DOX for 24 h. *CYP1A1*, *CYP1B1*, *CYP2B1*, *CYP2C11*, *CYP2E1*, and *CYP2J3* gene expressions were determined by real-time PCR. Results are presented as mean ± SEM (n = 6). * $P < 0.05$ compared with control.

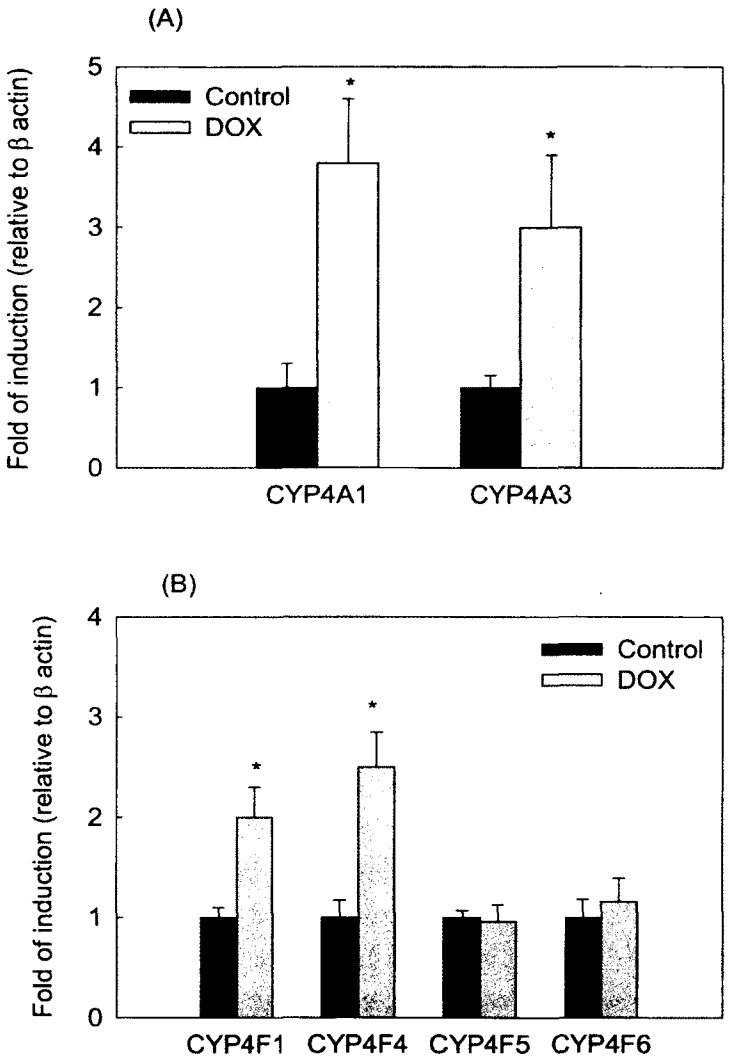

Fig. 3.34 Effect of acute DOX cardiotoxicity on CYP4A (A) and CYP4F (B) sub-family gene expression. Total RNA was isolated from the hearts of controls and animals treated with DOX for 24 h. *CYP4A1*, *CYP4A3*, *CYP4F1*, *CYP4F4*, *CYP4F5* and *CYP4F6* gene expressions were determined by real-time PCR. Results are presented as mean ± SEM (n = 6). * $P < 0.05$ compared with control.

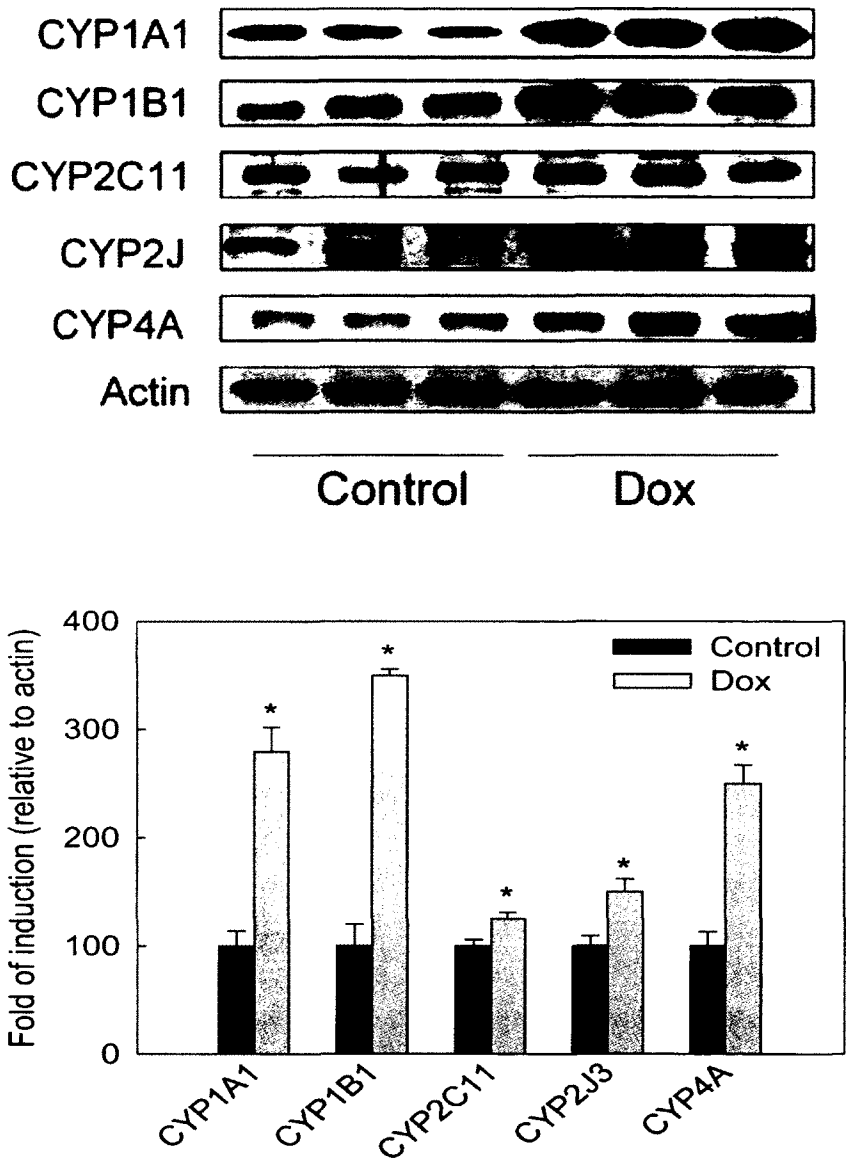

Fig. 3.35 Effect of acute DOX cardiotoxicity on CYP protein expression. Heart microsomal protein was isolated from the hearts of controls and animals treated with DOX for 24 h. Microsomal protein (20 μg) was separated on a 10% SDS-PAGE. CYP1A1, CYP1B1, CYP2C11, CYP2J, and CYP4A proteins were detected using the enhanced chemiluminescence method. The graph represents the relative amount of CYP protein normalized to the endogenous control (mean ± SEM, n = 3), and the results are expressed as percentage of the control values taken as 100%. * $P < 0.05$ compared with control.

3.5.3. Effect of DOX treatment on CYP protein expression

To investigate whether the induction of *CYP* gene expression was further translated to protein, microsomal protein was prepared from hearts of control and rats treated with DOX for 24 h. Thereafter, CYP1A1, CYP1B1, CYP2C11, CYP2J3, and CYP4A protein levels were determined using Western blot analysis relative to actin as an endogenous control. DOX treatment caused a significant induction of CYP1A1, CYP1B1, CYP2C11, CYP2J3, and CYP4A protein levels by 180%, 245%, 25%, 35%, 150%, respectively (Fig. 3.35).

3.5.4. Effect of DOX treatment on CYP-mediated arachidonic acid metabolism

To investigate the effect of DOX treatment on the formation of CYP-derived arachidonic acid metabolites, heart microsomes of either control or 24 h DOX-treated rats were incubated with 50 μM arachidonic acid for 30 min. Thereafter, arachidonic acid metabolites were determined using LC-ESI-MS. In comparison to control animals, in heart microsomes of DOX-treated rats, the formation rates of 5,6-, 8,9-, 11,12- and 14,15-EET were significantly lower by about 60%, 30%, 50% and 40%, respectively (Fig. 3.36A). We also measured levels of enzymatic hydration of EETs products, DHETs. As shown in Figure 3.36B, the formation rates of 5,6-, 8,9-, 11,12, and 14,15-DHET were significantly increased by 60%, 100%, 60%, and 50%, respectively compared to control.

In order to investigate the effect of DOX treatment on total epoxygenase activity, we calculated the sum of all the products of epoxygenase enzymes, namely the total EETs and DHETs, in control and rats treated with DOX for 24 h. The total epoxygenase activity was significantly increased in the heart microsomes of DOX-treated rats by 20% as compared to the control rats (Fig. 3.37A). On the other hand, to determine the effect of DOX treatment on CYP ω-hydroxylases activity, we determined the formation of 20-HETE in microsomes from control and DOX-treated rats. DOX treatment significantly increased 20-HETE formation by 90% in comparison to the control group (Fig. 3.37B).

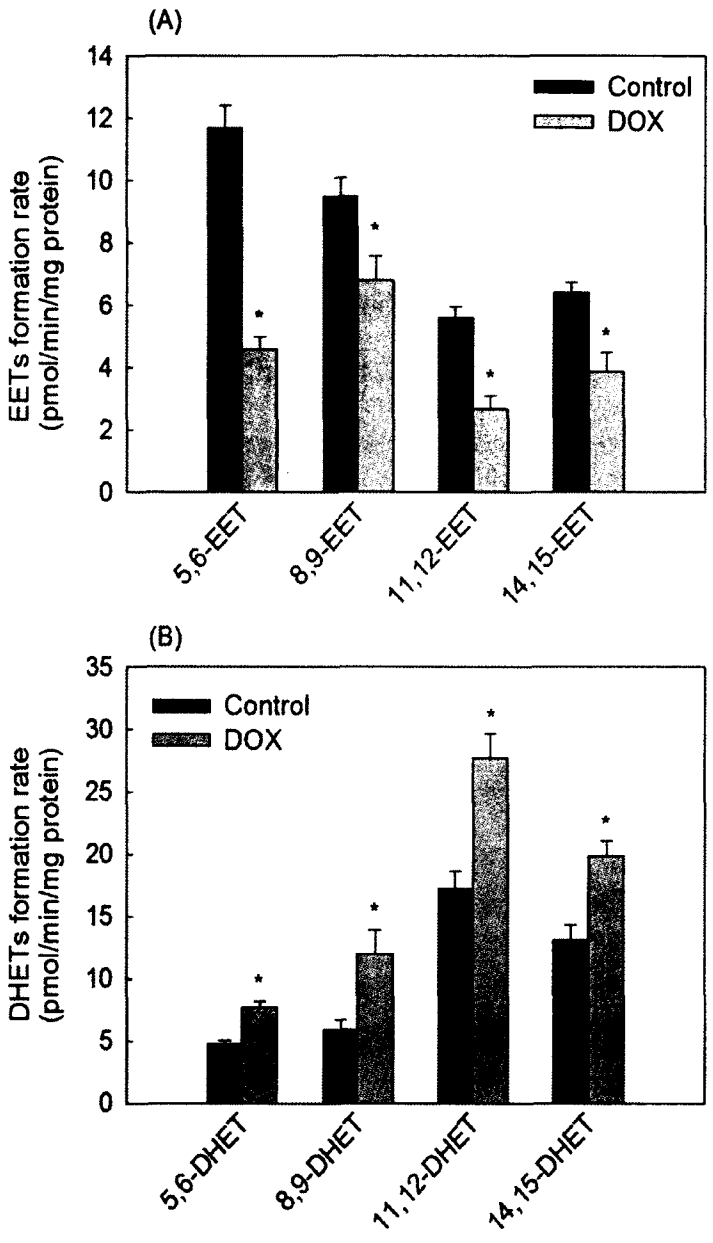

Fig. 3.36 Effect of acute DOX cardiotoxicity on formation of EETs (A) and DHETs (B). Heart microsomes of controls or animals treated with DOX for 24 h were incubated with 50 μM arachidonic acid. The reaction was started by the addition of 1 mM NADPH and lasted for 30 min. The reaction was terminated by the addition of ice-cold acetonitrile. EETs and DHETs were extracted twice by 1 ml of ethyl acetate and dried using speed vacuum. A reconstituted solution of metabolites was injected into LC-ESI-MS for metabolite determination. Results are presented as mean ± SE (n = 6). * $p < 0.05$ compared with control.

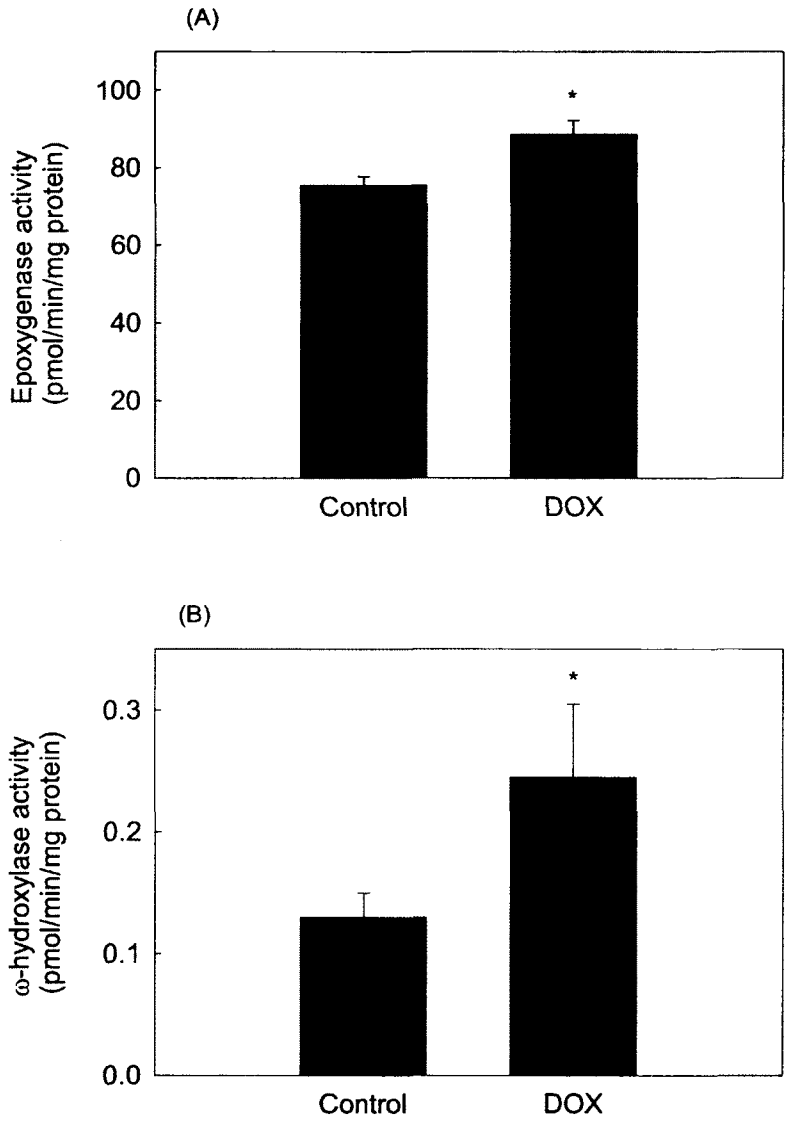

Fig. 3.37 Effect of acute DOX cardiotoxicity on epoxygenase (A) and ω-hydroxylase activity (B). (A) Epoxygenase activity was determined from the sum of formation rates of EETs and DHETs. (B) ω-hydroxylase activity was determined from the 20-HETE formation. Heart microsomes of control or animals treated with DOX for 24 h were incubated with 50 μM arachidonic acid. The reaction was started by the addition of 1 mM NADPH and lasted for 30 min. The reaction was terminated by the addition of ice-cold acetonitrile. 20-HETE was extracted twice by 1 ml of ethyl acetate and dried using speed vacuum. A reconstituted solution of metabolites was injected into LC-ESI-MS for metabolite determination. Results are presented as mean ± SEM (n = 6). * $P < 0.05$ compared with control.

3.5.5 Effect of DOX treatment on sEH expression and activity

To investigate the mechanism responsible for lower levels of EETs in the heart microsomes of DOX-treated rats despite the increase in the epoxygenase activity, the expression of the *EPHX2* gene was determined. Our results show that DOX treatment caused a significant time-dependent induction of *EPHX2* gene expression in the heart by 150%, 200%, and 230% at 6, 12, and 24 h after DOX administration, respectively (Fig. 3.38A). To confirm the induction of *EPHX2* gene, sEH protein expression was assessed by Western blot analysis. Similar to the induction observed at the mRNA level, sEH protein was significantly induced in the heart microsomes of rats treated with DOX for 24 h by 50% (Fig. 3.38B).

In addition, sEH activity has been assessed by calculating the ratio of the total DHETs to the total EETs formed in the heart microsomes of controls and rats treated with DOX for 24 h. In accordance with the induction at the gene and protein expression levels, sEH activity was induced by 220% in the heart microsomes of rats treated with DOX for 24 h (Fig. 3.39). In order to confirm that the increase in total DHETs/total EETs ratio was due to sEH induction, heart microsomes from control and rats treated with DOX for 24 h were incubated with 100 nM of the selective sEH inhibitor, tAUCB, for 5 min followed by incubation with arachidonic acid as described under materials and methods. Our results show that inhibition of sEH markedly decreased the total DHETs/total EETs ratio from 1.2 in the control group to 0.3 after incubation with tAUCB. Similarly, the total DHETs/total EETs ratio was decreased from 3.2 in the DOX-treated group to 0.3 after incubation with tAUCB (Fig. 3.39)

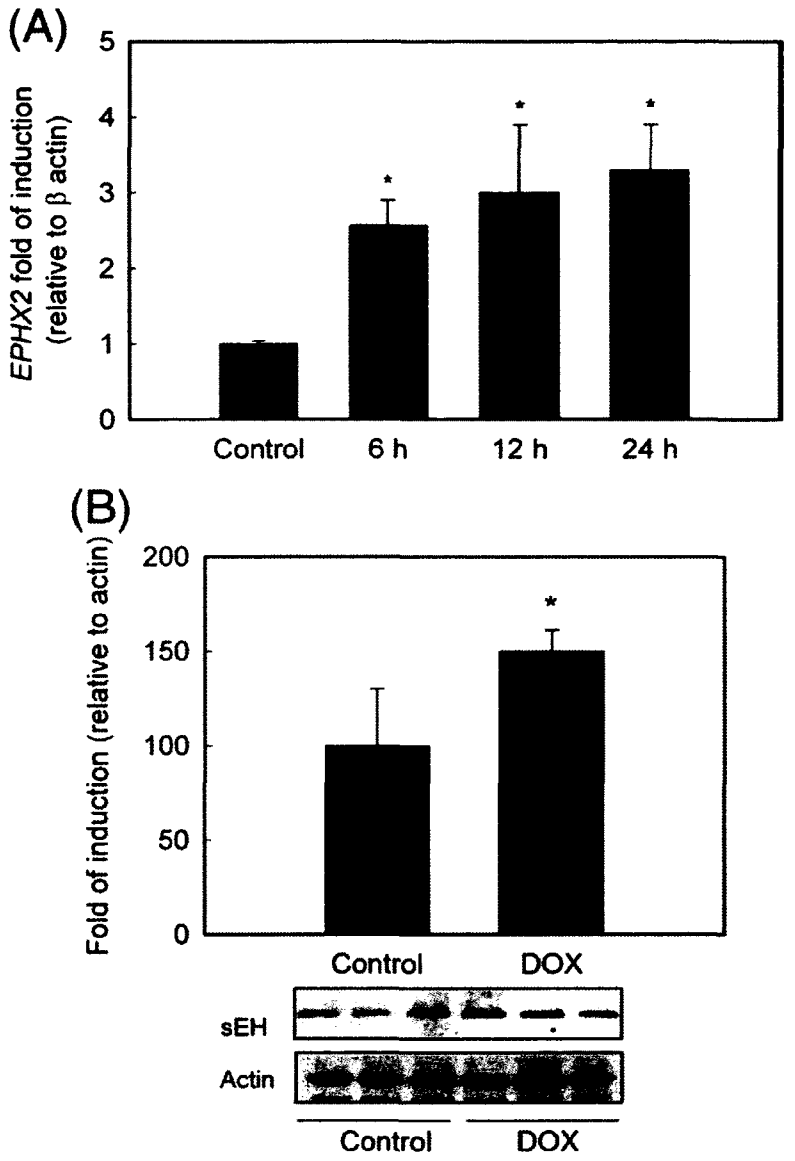

Fig. 3.38 Effect of acute DOX cardiotoxicity on *EPHX2* gene expression (A) and sEH protein expression (B). (A) Total RNA was isolated from the hearts of control and animals treated with DOX for 6 , 12 , and 24 h. *EPHX2* gene expression was determined by real-time PCR (n = 6). (B) Heart microsomal protein was isolated from the hearts of controls and animals treated with DOX for 24 h. Microsomal protein (20 μg) was separated on a 10% SDS-PAGE. sEH protein was detected using the enhanced chemiluminescence method. The graph represents the relative amount of sEH protein normalized to the endogenous control (n = 3). Results are presented as mean ± SEM. * $P < 0.05$ compared with control.

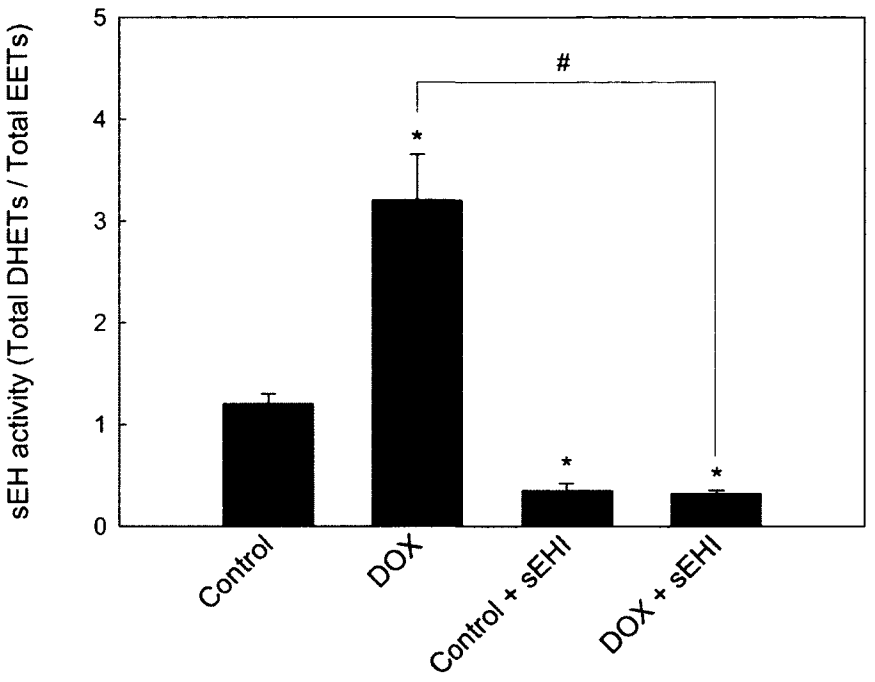

Fig. 3.39 Effect of acute DOX cardiotoxicity on sEH activity. Heart microsomes of controls or animals treated with DOX for 24 h were incubated with 100 nM tAUCB for 5 min followed by incubation with 50 μM arachidonic acid. The reaction was started by the addition of 1 mM NADPH and lasted for 30 min then terminated by the addition of ice-cold acetonitrile. EETs and DHETs were extracted twice by 1 ml of ethyl acetate and dried using speed vacuum. Reconstituted metabolites were injected into LC-ESI-MS for metabolite determination. sEH activity was calculated as the ratio of total DHETs/ total EETs. Results are presented as mean ± SEM (n = 6). * $P < 0.05$ compared with control, # $p < 0.05$ compared with heart microsomes from animals treated with DOX for 24 h in the absence of sEH inhibitor (sEHI).

3.5.6. Effect of DOX on *EPHX2* gene expression in H9c2 cells

To investigate whether the induction of *EPHX2* gene expression is due to the direct effect of DOX on the cardiomyocytes, cardiac-derived H9c2 cells were treated with increasing concentrations of DOX. Thereafter, the expression of *EPHX2* was measured using real-time PCR as described under materials and methods. Our results demonstrated that treatment of H9c2 cells with increasing concentrations of DOX caused a significant concentration-dependent induction of *EPHX2* by 80%, 110%, and 200% with DOX concentrations of 1, 2, and 5 μM, respectively (Fig. 3.40).

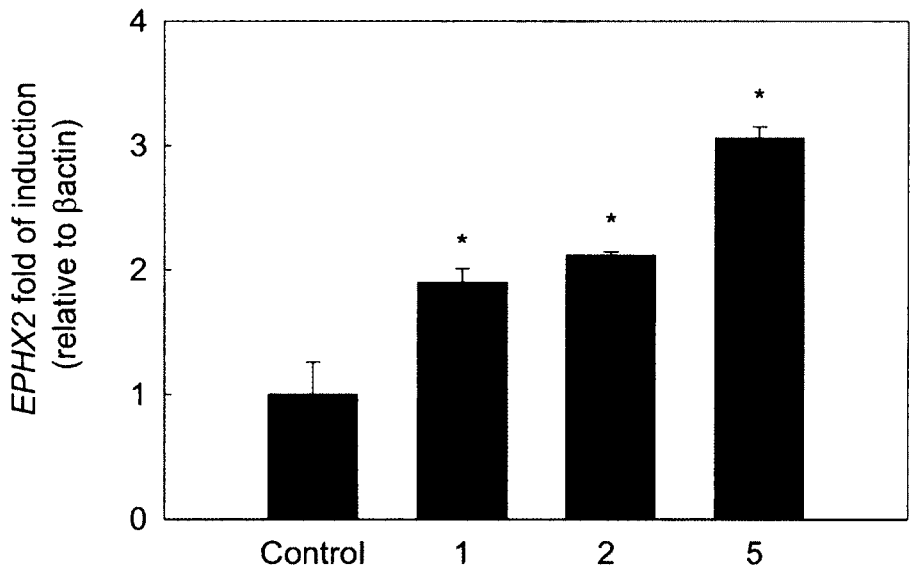

Fig. 3.40 Effect of DOX on *EPHX2* gene expression in H9c2 cells. H9c2 cells were incubated with increasing concentrations of DOX for 2 h and the medium was replaced by fresh medium for another 24 h as described under materials and methods. Thereafter, total RNA was isolated and the expression of *EPHX2* was determined by real-time PCR. Results are presented as mean ± SEM (n = 6). * $P < 0.05$ compared with control.

3.6. Acute doxorubicin toxicity differentially alters Cytochrome P450 expression and arachidonic acid metabolism in rat kidney and liver

3.6.1. Effect of DOX treatment on food intake and animal body weight

Taking into account the possible effect of fasting on CYP expression, we investigated the effect of DOX treatment on the food intake and animal body weight. The food intake in DOX-treated animals was significantly reduced by almost 50% from the control. In addition, DOX-treated animals lost an average of 5% body weight as compared to the control.

3.6.2. Effect of DOX treatment on *CYP* gene expression

To examine the effect of DOX treatment on the renal and hepatic expression of several *CYP* genes, total RNA was extracted from the kidney and liver of both control and DOX-treated rats. Thereafter, the expression of different genes was measured using RT followed by real time-PCR. Fig 3.41 shows the effect of DOX-induced toxicity on *CYP1* family gene expression at 6 and 24 h after DOX administration. DOX treatment did not cause a statistically significant difference in *CYP1A1* gene expression in either the kidney or liver (Fig. 3.41A). On the other hand, DOX treatment caused a significant induction of *CYP1B1* gene expression in the kidney by 100% after 24 h of DOX administration. In addition, DOX caused a significant induction of *CYP1B1* in the liver by 250% and 200% at the 6 and 24 h, respectively (Fig. 3.41B). With regard to the *CYP2* family, DOX treatment caused a significant inhibition of *CYP2C11* gene expression in the kidney and liver by 70% and 50% after 24 h, respectively (Fig. 3.42A). Similarly,

there was a significant inhibition of *CYP2B1* gene expression in the kidney and liver by 45% and 80% after 24 h, respectively (Fig. 3.42B). In contrast to *CYP2B1* and *CYP2C11*, DOX treatment for 24 h caused a significant induction of *CYP2E1* gene expression by 150% in the kidney only (Fig. 3.42C). Finally, DOX treatment for 24 h caused a significant inhibition in the gene expression of *CYP2J3* by 55% in the liver only (Fig. 3.42D).

With regard to the major CYP ω-hydroxylases, the gene expression of *CYP4A* and *CYP4F* was assessed. Figure 3.43 shows the effect of DOX-induced toxicity on the gene expression of *CYP4A* at 6 and 24 h after DOX administration. Interestingly, DOX administration caused a significant induction of *CYP4A1* in the kidney by 500% at the 24 h time point (Fig. 3.43A). In a similar manner, DOX-toxicity caused a significant induction of *CYP4A2* in the kidney at 24 h and in the liver at 6 h by 100% and 230%, respectively (Fig. 3.43B). Finally, there was a significant induction of *CYP4A3* in the kidney at the 24 h time point; whereas, it was significantly induced in the liver by 220% and 70% at the 6 and 24 h, respectively. In a similar pattern to *CYP4A* gene expression, acute DOX toxicity caused a significant induction of *CYP4F1* by 60% only in the kidney at 24 h (Fig. 3.44A). On the contrary, acute DOX toxicity caused a 40% inhibition of *CYP4F4* gene expression only in the liver at both 6 and 24 h (Fig. 3.44B). Also, *CYP4F5* was significantly inhibited in the kidney of DOX-treated rats at the 6 h time point by about 35% (Fig. 3.44C). Finally, there was no significant difference in *CYP4F6* gene expression in either the kidney or liver at the two time points (Fig. 3.44D).

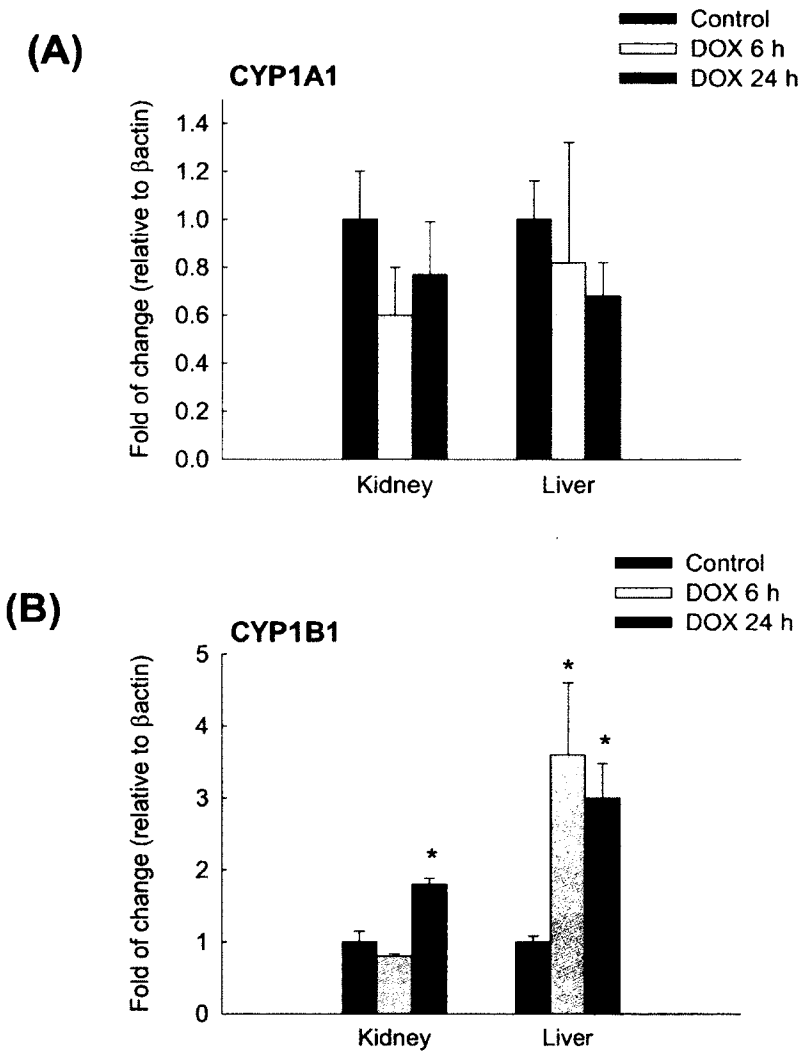

Fig. 3.41 Effect of DOX toxicity on CYP1 family gene expression. Total RNA was isolated from the kidneys and livers of controls and animals treated with DOX after 6 and 24 h. *CYP1A1* (A) and *CYP1B1* (B) gene expressions were determined by real-time PCR. Results are presented as mean ± SEM (n = 6). * $P < 0.05$ compared to control.

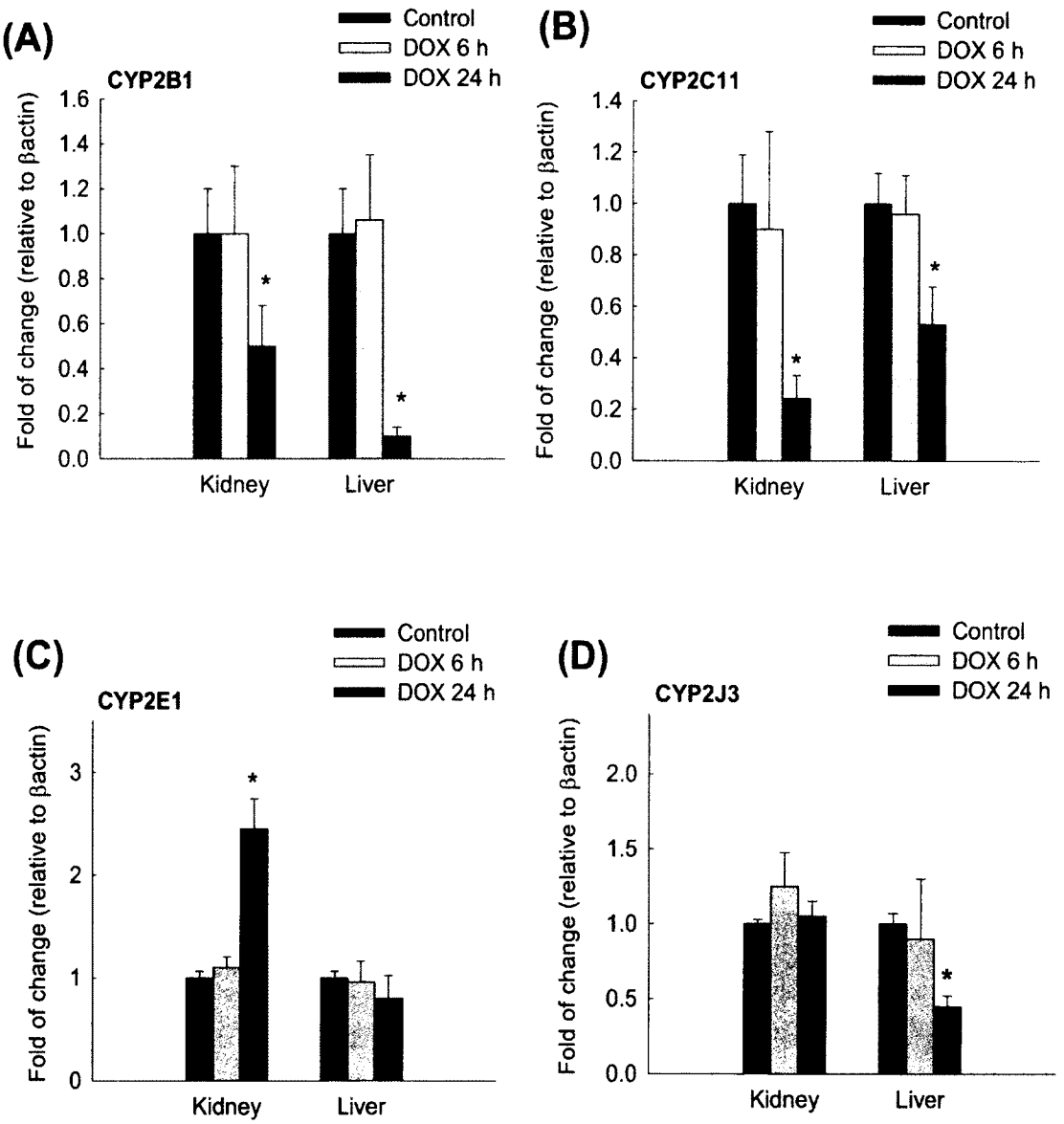

Fig. 3.42 Effect of DOX toxicity on CYP2 family gene expression. Total RNA was isolated from the kidneys and livers of controls and animals treated with DOX after 6 and 24 h. *CYP2B1* (A), *CYP2C11* (B), *CYP2E1* (C), and *CYP2J3* (D) gene expressions were determined by real-time PCR. Results are presented as mean ± SEM (n = 6). * $P < 0.05$ compared to control.

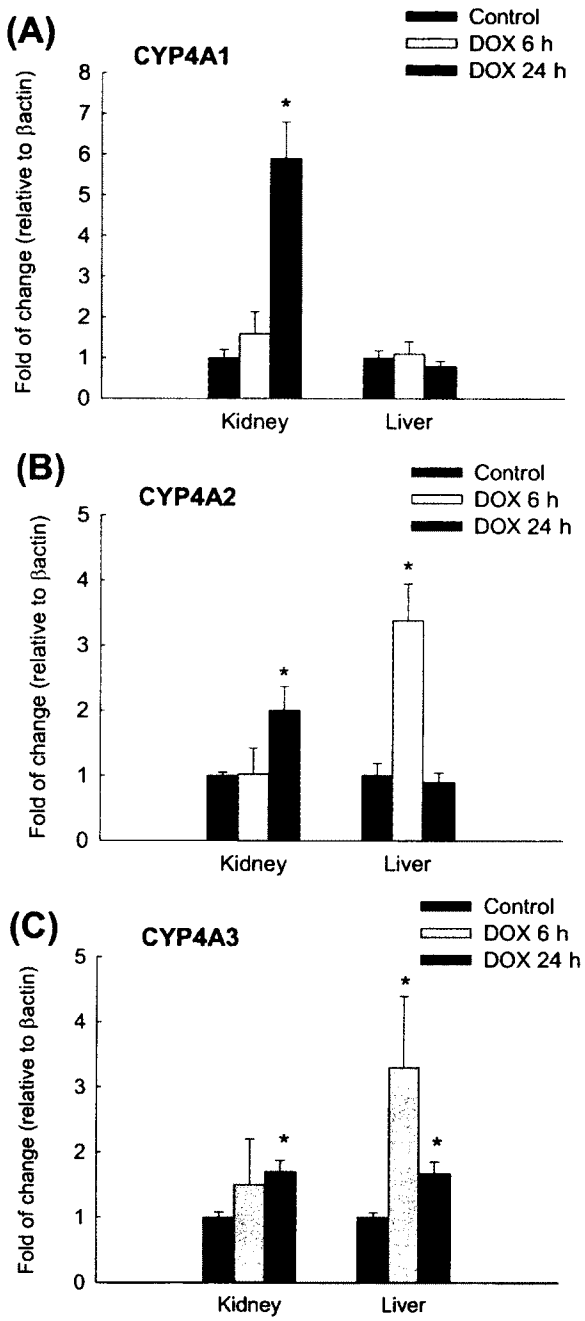

Fig. 3.43 Effect of DOX toxicity on CYP4A subfamily gene expression. Total RNA was isolated from the kidneys and livers of controls and animals treated with DOX after 6 and 24 h. *CYP4A1* (A), *CYP4A2* (B), and *CYP4A3* (C) gene expressions were determined by real-time PCR. Results are presented as mean ± SEM (n = 6). * $P < 0.05$ compared to control.

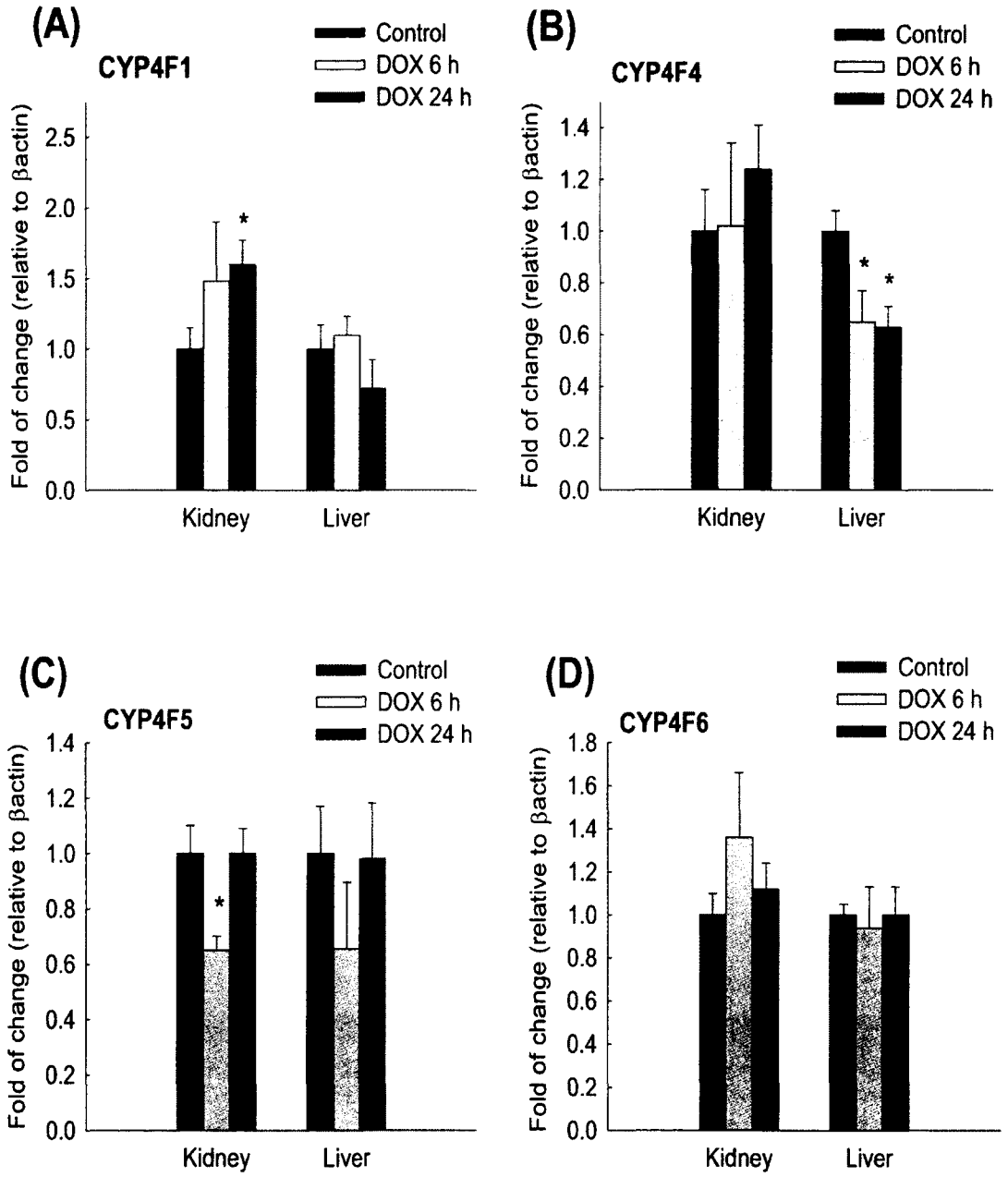

Fig. 3.44 Effect of DOX toxicity on CYP4F subfamily gene expression. Total RNA was isolated from the kidneys and livers of controls and animals treated with DOX after 6 and 24 h. *CYP4F1* (A), *CYP4F4* (B), *CYP4F5* (C), and *CYP4F6* (D) gene expressions were determined by real-time PCR. Results are presented as mean ± SEM (n = 6). * $P < 0.05$ compared to control.

3.6.3. Effect of DOX treatment on *EPHX2* gene expression

Because of its important role in converting EETs to the less biologically active DHETs, we investigated the effect of acute DOX toxicity on the expression of the *EPHX2* gene which encodes for the sEH enzyme. In the current study, acute DOX toxicity did not cause any significant change in *EPHX2* gene expression in the kidney at either the 6 or 24 h time points. However, there was a significant induction of the *EPHX2* gene expression by 160% in the liver only at the 6 h time point but not at the 24 h (Fig. 3.45).

3.6.4. Effect of DOX treatment on CYP and sEH protein expression

To investigate whether the changes of *CYP* and *EPHX2* gene expression were further translated into protein, microsomal protein was prepared from kidneys and livers of controls and rats treated with DOX for 24 h. Thereafter, CYP1B1, CYP2B1, CYP2C11, CYP2E1, CYP2J3, and CYP4A protein levels were determined using Western blot analyses relative to actin as a loading control. In the kidney, DOX treatment caused a significant inhibition of both CYP2B1 and sEH by about 60%, whereas CYP2E1 and CYP4A protein expression was induced by 90% and 110%, respectively. On the other hand, there was no significant change in the protein expression of CYP1B1, CYP2C11, and CYP2J3 (Fig. 3.46). In the liver, DOX treatment caused an inhibition of CYP2B1 and CYP2C11 by 74% and 65%, respectively, while there was a significant induction of CYP4A by 370%. The protein expression of CYP2E1, CYP2J3, and sEH was

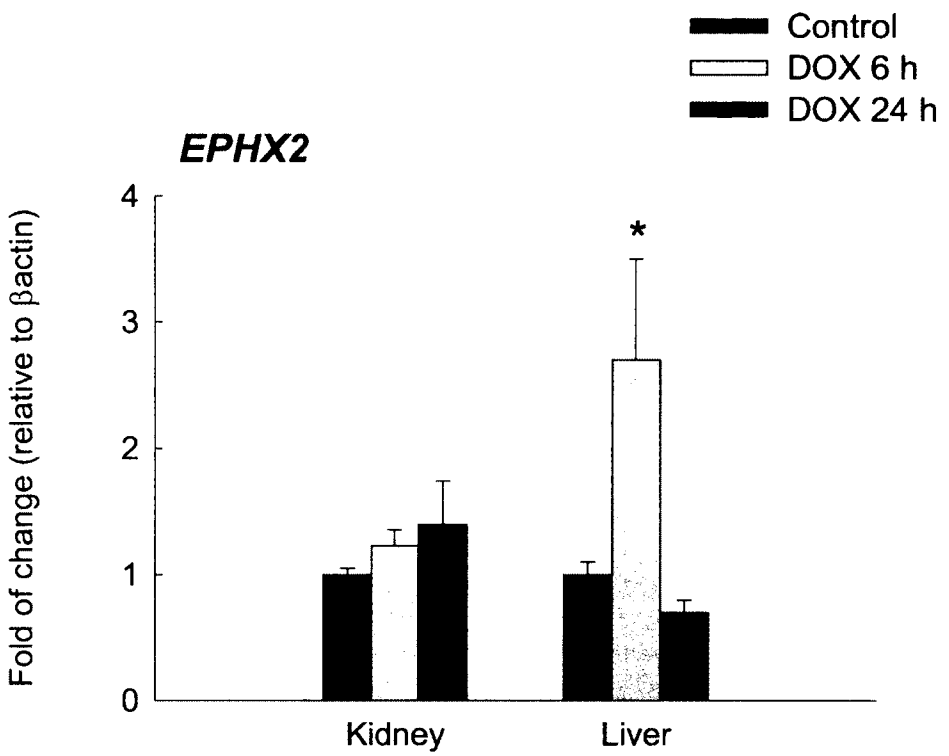

Fig. 3.45 Effect of DOX toxicity on *EPHX2* gene expression. Total RNA was isolated from the kidneys and hearts of control and animals treated with DOX after 6 and 24 h. *EPHX2* gene expression was determined by real-time PCR. Results are presented as mean ± SEM (n = 6). * $P < 0.05$ compared to control.

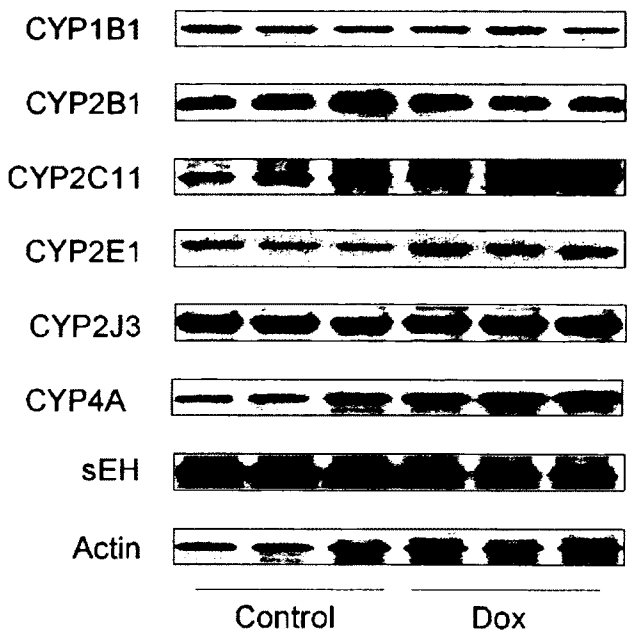

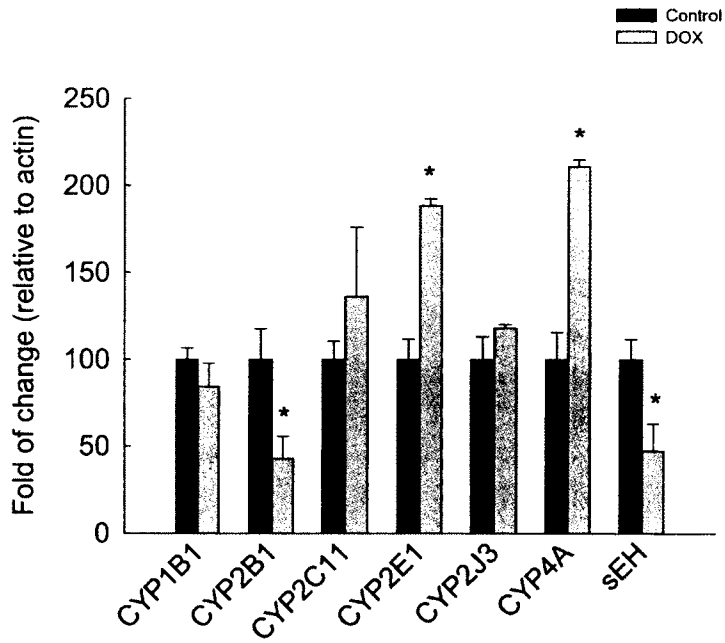

Fig. 3.46 Effect of DOX toxicity on CYP and sEH protein expression in the kidney. Kidney microsomal protein was isolated from the kidney of controls and animals treated with DOX for 24 h. Microsomal protein was separated on a 10% SDS-PAGE. CYP1B1, CYP2B1, CYP2C11, CYP2E1, CYP2J3, CYP4A, sEH, and actin proteins were detected by the enhanced chemiluminescence method. The graph represents the relative amount of protein normalized to the loading control (mean ± SEM, n = 3), and the results are expressed as percentage of the control values taken as 100%. * $P < 0.05$ compared with control.

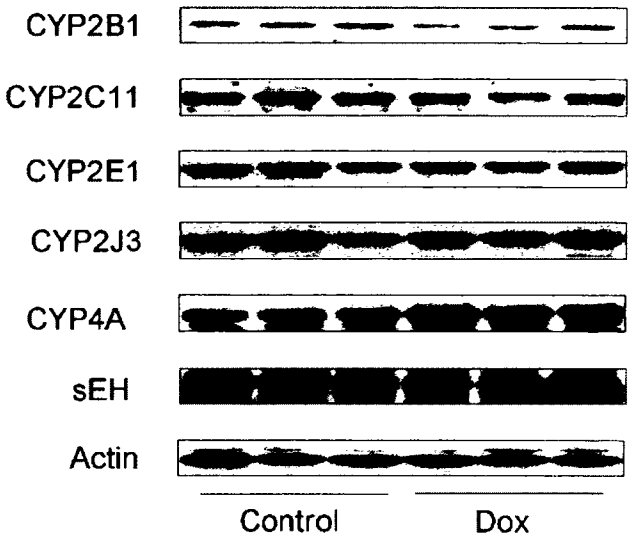

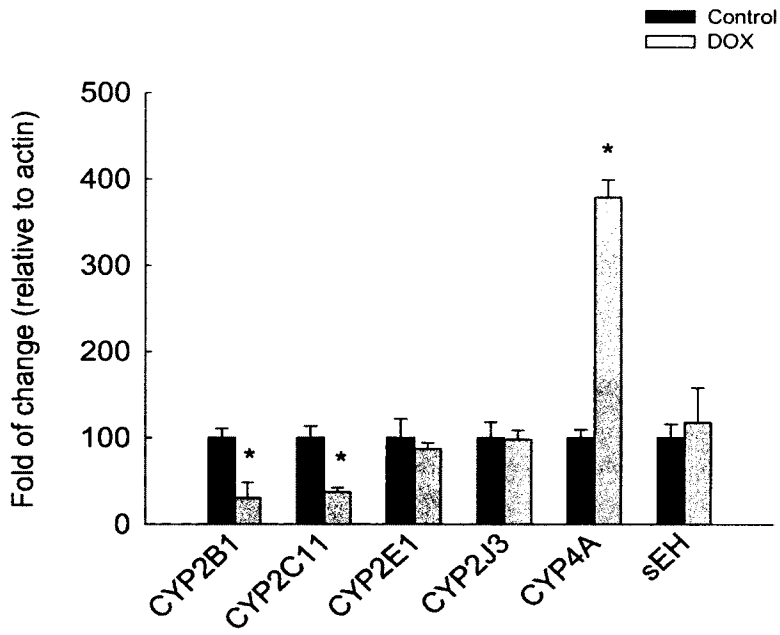

Fig. 3.47 Effect of DOX toxicity on CYP and sEH protein expression in the liver. Liver microsomal protein was isolated from the kidneys of controls and animals treated with DOX for 24 h. Microsomal protein was separated on a 10% SDS-PAGE. CYP2B1, CYP2C11, CYP2E1, CYP2J3, CYP4A, sEH, and actin proteins were detected by the enhanced chemiluminescence method. The graph represents the relative amount of protein normalized to the loading control (mean ± SEM, n = 3), and the results are expressed as percentage of the control values taken as 100%. * $P < 0.05$ compared with control.

not significantly altered (Fig. 3.47). CYP1B1 protein could not be detected in the liver under the current experimental conditions.

3.6.5. Effect of DOX treatment on the inflammatory markers

In an attempt to investigate the mechanism by which DOX causes the aforementioned changes in CYP and sEH expression, the gene expression of three major inflammatory markers, IL-6, iNOS, and TNFα were assessed in the liver of DOX-treated rats as compared to the controls. Interestingly, there was a significant induction of the three inflammatory markers: interleukin-6 (IL-6), inducible nitric oxide synthase (iNOS), and TNFα by 2700%, 225%, 100%, respectively after 6 h of DOX administration. Moreover, there was a higher induction of the IL-6, iNOS, and TNFα by 5700%, 1500%, 260%, respectively after 24 h of DOX administration (Fig. 3.48A). In order to investigate whether DOX caused a systemic inflammation, we measured serum nitrite levels in the control and rats treated with DOX for 24 h. Consistent with the gene expression data, there was a significant increase of nitrite in the sera of DOX treated rats as compared to the controls by about 110% (Fig. 3.48B).

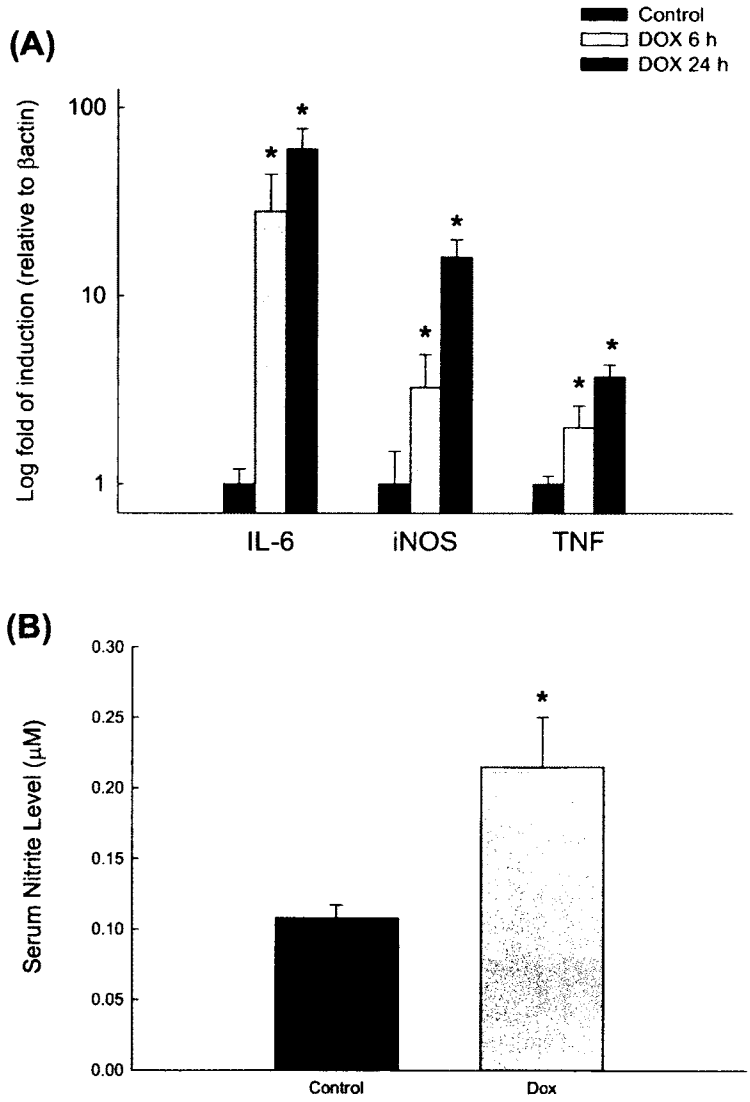

Fig. 3.48 Effect of DOX toxicity on inflammatory markers gene expression (A) and serum nitrite levels (B). (A) Total RNA was isolated from the livers of control and animals treated with DOX after 6 and 24 h. IL-6, iNOS, and TNFα gene expressions were determined by real-time PCR. (B) Nitrite levels were determined in the sera of control and animals treated with DOX for 24 h as described under materials and methods. Results are presented as mean ± SEM (n = 6). * $P < 0.05$ compared to control.

3.6.6. Effect of DOX treatment on CYP-mediated arachidonic acid metabolism

To investigate the effect of DOX treatment on the formation of CYP-derived arachidonic acid metabolites, kidney and liver microsomes of either controls or 24 h DOX-treated rats were incubated with 50 μM arachidonic acid for 30 min. Thereafter, arachidonic acid metabolites were measured using LC-ESI-MS. In kidney microsomes of DOX-treated rats, the formation of 8,9-, 11,12- and 14,15-EET were significantly higher than the control values by about 165%, 240%, and 250%, respectively (Fig. 3.49A). We also measured the levels of enzymatic hydration products of EETs, the DHETs. As shown in Fig. 3.49B, there was no significant change in the rate of formation of DHETs compared to the controls.

In order to investigate the effect of DOX on the total epoxygenase activity, we calculated the sum of all the products of epoxygenase enzymes, the total EETs and DHETs, in controls and rats treated with DOX for 24 h. The total epoxygenase activity was not significantly changed in the kidney microsomes of DOX-treated rats as compared to the controls (Fig. 3.50A). In accordance with the inhibition of sEH protein expression, DOX treatment caused a significant 45% inhibition of the sEH activity (calculated as the total DHETs/total EETs) (Fig. 3.50B). On the other hand, to determine the effect of DOX treatment on CYP ω-hydroxylases activitiy, we determined the rate of 20-HETE formation in the kidney microsomes from controls and DOX-treated rats. DOX treatment

significantly increased the 20-HETE formation by 120% in comparison to the control group (Fig. 3.50C).

In liver microsomes of DOX-treated rats, there was no significant change in the formation rate of all the EET and DHET regioisomers compared to the control (Fig. 3.51). Similarly, both the total epoxygenase activity and sEH activity were not significantly changed in the liver microsomes of DOX-treated rats as compared to the controls (Fig. 3.52A and B). On the contrary, DOX treatment significantly increased the 20-HETE formation by 40% in comparison to the control group (Fig. 3.52C).

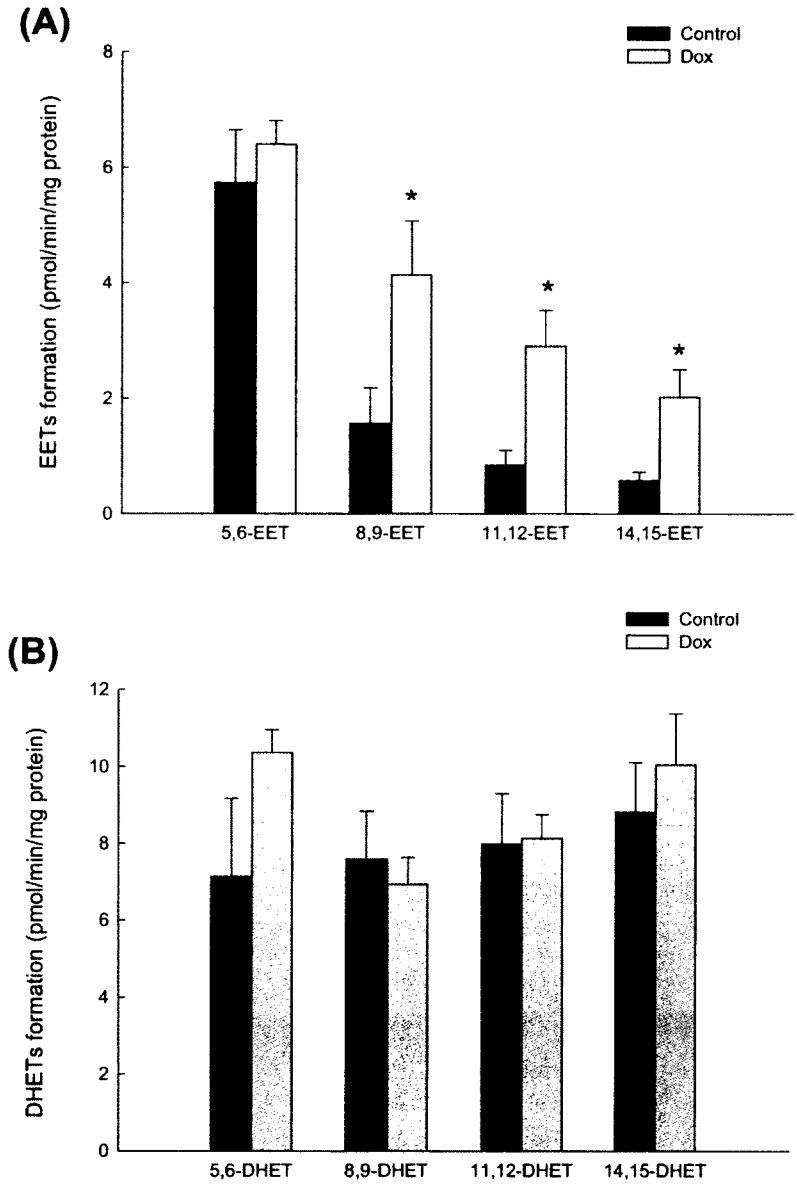

Fig. 3.49 Effect of DOX toxicity on formation of EETs (A) and DHETs (B) in the kidney. Kidney microsomes of controls or animals treated with DOX for 24 h were incubated with 50 μM arachidonic acid. The reaction was started by the addition of 1 mM NADPH and lasted for 30 min. The reaction was terminated by the addition of ice-cold acetonitrile. EETs and DHETs were extracted twice by 1 ml of ethyl acetate and dried using speed vacuum. Reconstituted metabolites were injected into LC-ESI-MS for metabolite determination. Results are presented as mean ± SEM (n = 6). * $P < 0.05$ compared with control.

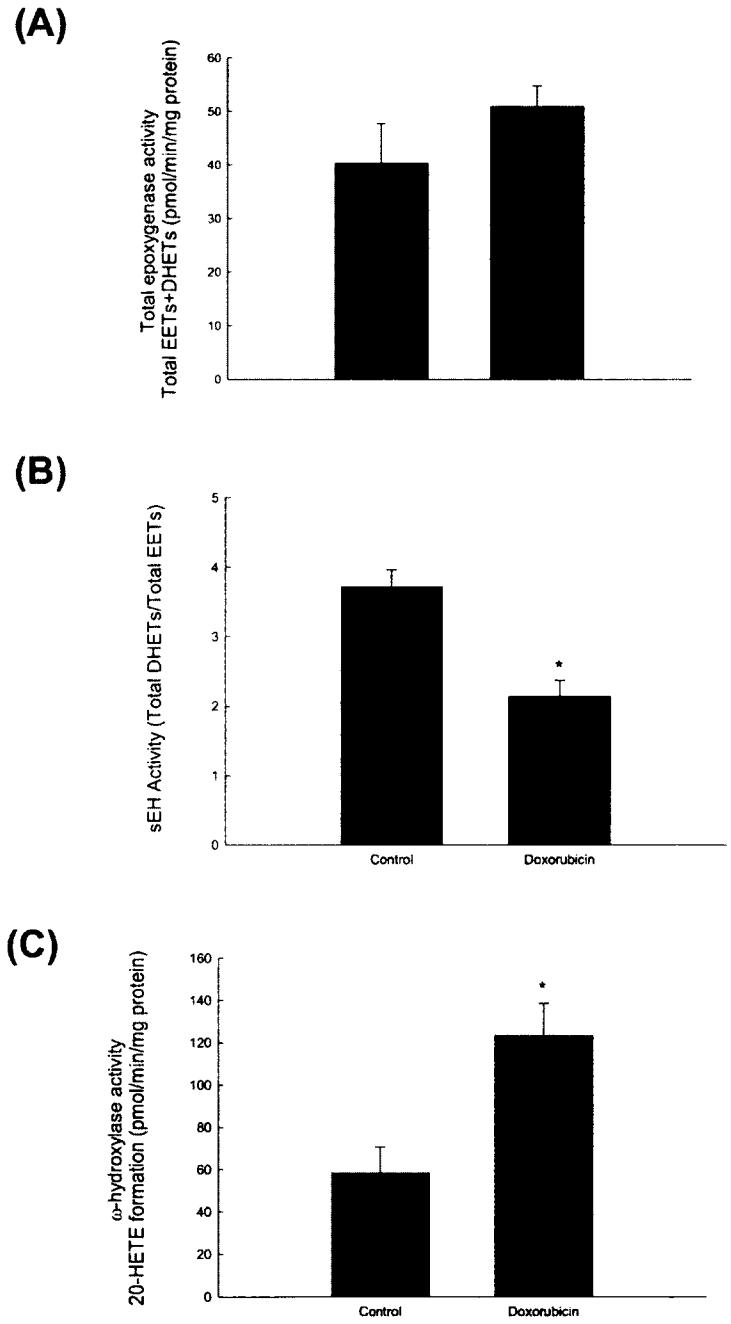

Fig. 3.50 Effect of DOX toxicity on the total epoxygenase (A), sEH (B), and ω-hydroxylase activity (C) in the kidney. (A) The total epoxygenase activity was determined from the sum of formation rates of EETs and DHETs. (B) sEH activity was determined by dividing the total DHETs over the total EETs. (C) ω-hydroxylase activity was determined from the 20-HETE formation. Kidney microsomes of controls or animals treated with DOX for 24 h were incubated with 50 μM arachidonic acid. The reaction was started by the addition of 1 mM NADPH and lasted for 30 min. The reaction was terminated by the addition of ice-cold acetonitrile. 20-HETE was extracted twice by 1 ml of ethyl acetate and dried using speed vacuum. Reconstituted metabolite was injected into LC-ESI-MS for metabolite determination. Results are presented as mean ± SEM (n = 6). * $P < 0.05$ compared with control.

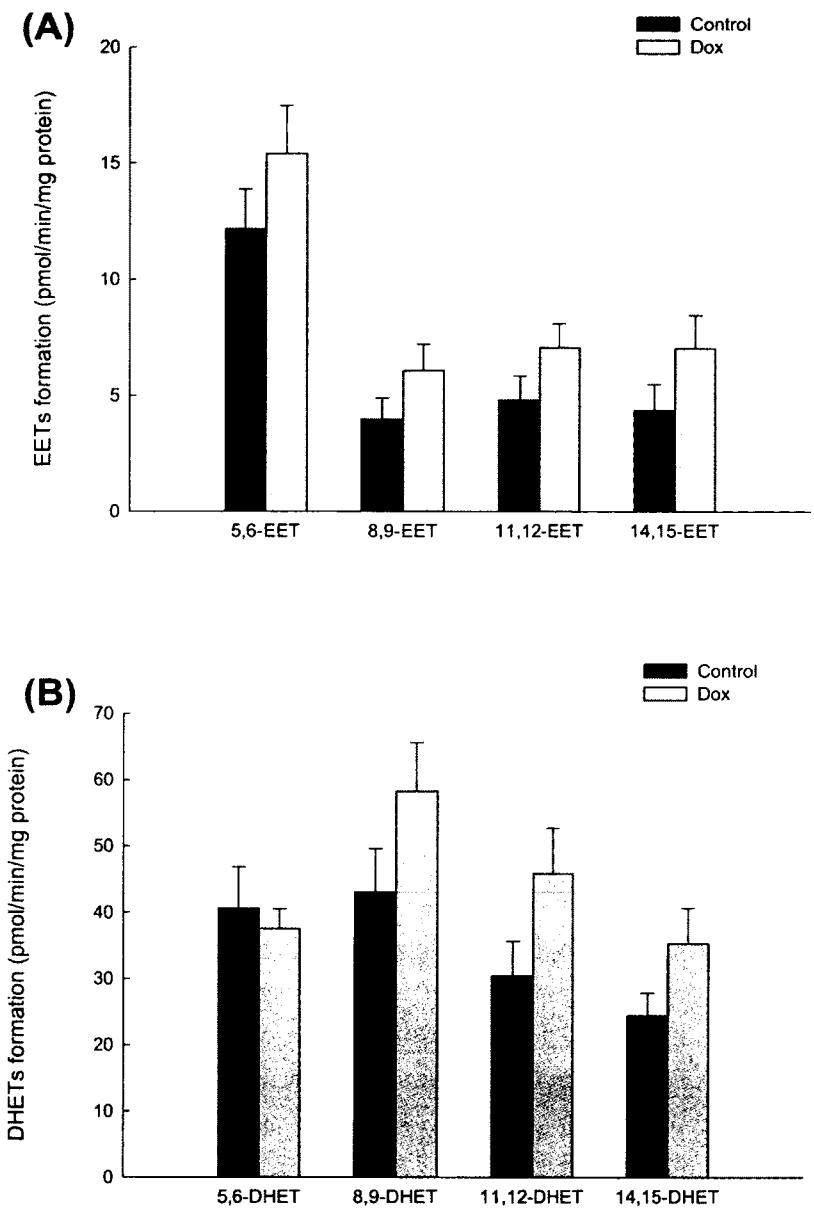

Fig. 3.51 Effect of DOX toxicity on EETs (A) and DHETs formation (B) in the liver. Liver microsomes of controls or animals treated with DOX for 24 h were incubated with 50 μM arachidonic acid. The reaction was started by the addition of 1 mM NADPH and lasted for 30 min. The reaction was terminated by the addition of ice-cold acetonitrile. EETs and DHETs were extracted twice by 1 ml of ethyl acetate and dried using speed vacuum. Reconstituted metabolites were injected into LC-ESI-MS for metabolite determination. Results are presented as mean ± SEM (n = 6). * $P < 0.05$ compared with control.

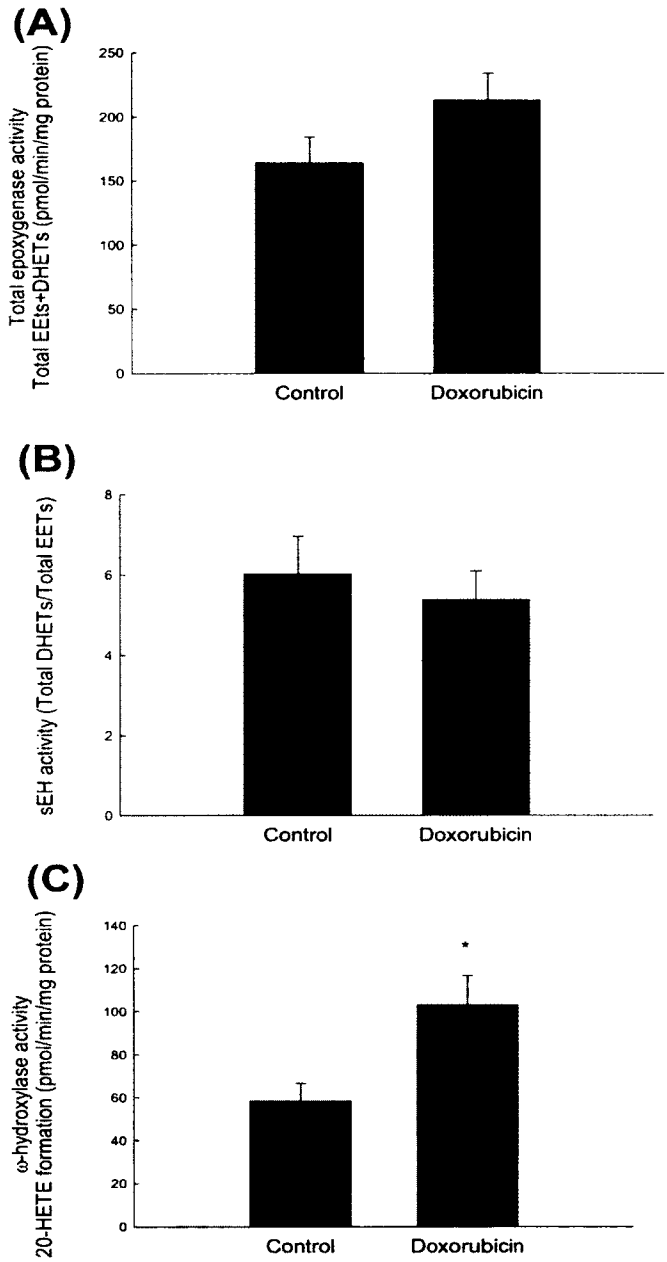

Fig. 3.52 Effect of DOX toxicity on the total epoxygenase (A), sEH (B), and ω-hydroxylase activity (C) in the liver. (A) The total epoxygenase activity was determined from the sum of formation rates of EETs and DHETs. (B) sEH activity was determined by dividing the total DHETs over the total EETs. (C) ω-hydroxylase activity was determined from the 20-HETE formation. Liver microsomes of control or animals treated with DOX for 24 h were incubated with 50 μM arachidonic acid. The reaction was started by the addition of 1 mM NADPH and lasted for 30 min. The reaction was terminated by the addition of ice-cold acetonitrile. 20-HETE was extracted twice by 1 ml of ethyl acetate and dried using speed vacuum. Reconstituted metabolite was injected into LC-ESI-MS for metabolite determination. Results are presented as mean ± SEM (n = 6). * $P < 0.05$ compared with control.

3.6.7. Effect of acute DOX toxicity on endogenous arachidonic acid metabolites concentrations

To investigate the effect of the altered CYP and sEH activity on the endogenous arachidonic acid metabolite concentration, kidney and liver tissues were extracted to measure the endogenous concentrations of these metabolites. Out of the 9 metabolites under investigation, we were able to quantify 8,9-DHET, 11,12-DHET, 14,15-DHET, and 20-HETE. The other metabolites were not detected or below the limit of quantification. In the kidney, there was a significant decrease in the endogenous concentration of the DHETs, whereas there was no significant change in the 20-HETE concentration (Fig. 3.53A). On the other hand, there was no significant change in the concentrations of DHETs in the liver, whereas there was a significant 2-fold increase in the 20-HETE concentration (Fig 3.53B).

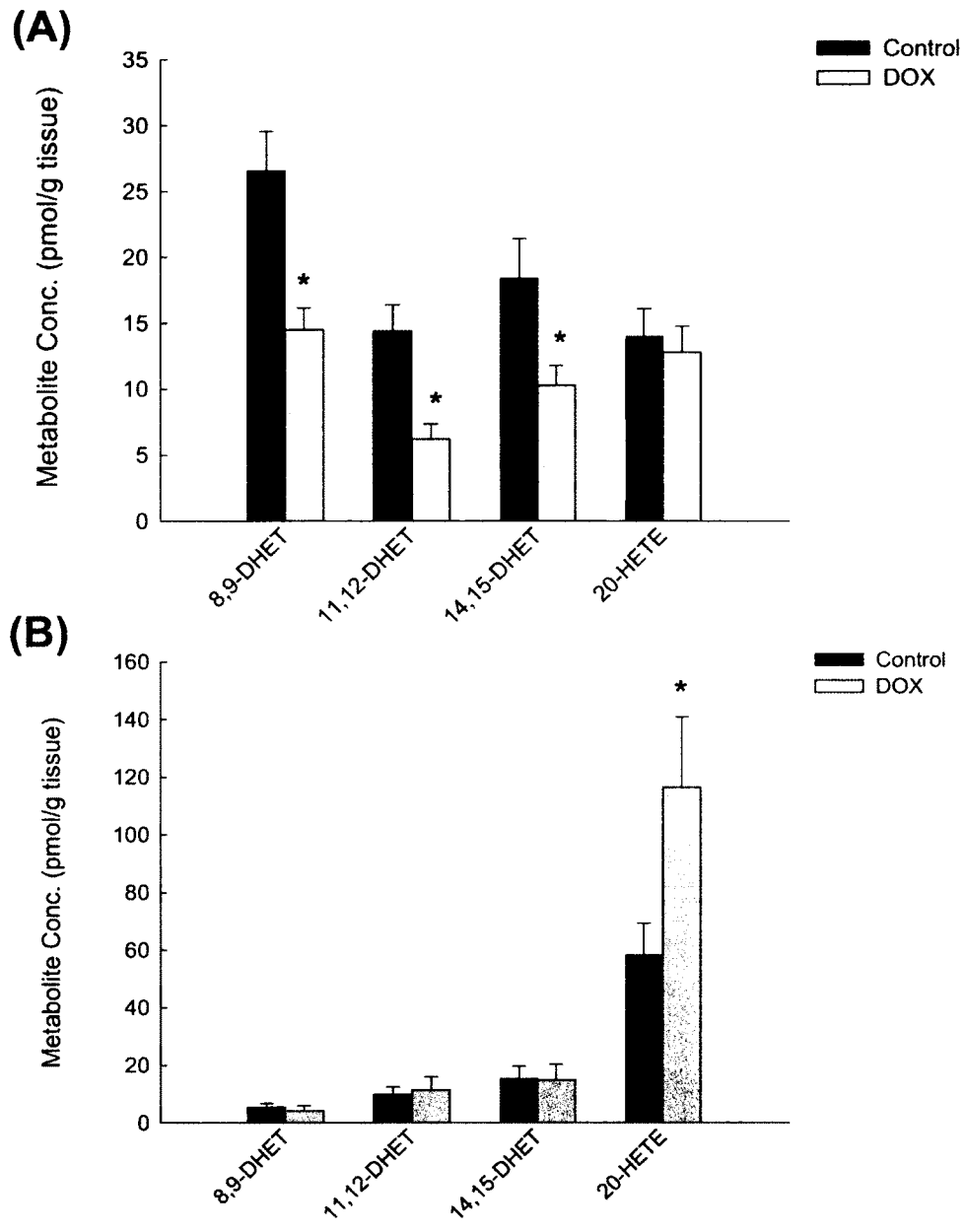

Fig. 3.53 Effect of acute DOX toxicity on endogenous arachidonic acid metabolites concentrations in the kidbey (A) and Liver (B). After homogenization and centrifugation, endogenous arachidonic acid metabolites were extracted twice from kidney and liver tissues by 1 ml of ethyl acetate and dried using speed vacuum. The reconstituted solution of metabolites was injected into LC-ESI-MS for metabolite determination. Results are presented as mean ± SEM (n = 6). * $P < 0.05$ compared with control.

CHAPTER 4 - DISCUSSION

4.1. Modulation of cytochrome P450 gene expression and arachidonic acid metabolism during isoproterenol-induced cardiac hypertrophy in rats

Although cardiac hypertrophy is an important condition that usually precedes HF (Carreno, Apablaza et al. 2006), there are limited reports of altered expression of *CYP* genes during cardiac hypertrophy. The expression of CYP has been studied in SHRs as compared to SD rats (Thum and Borlak 2002) and the expression of sEH has been studied in Spontaneously Hypertensive HF (SHHF) rats as compared to normal strains (Monti, Fischer et al. 2008). Nevertheless, there are no data about the effect of experimentally induced cardiac hypertrophy on the expression of *CYP* and *EPHX2* genes and their associated CYP-derived metabolites of arachidonic acid. To the best of our knowledge, this work demonstrates for the first time the effect of experimentally induced cardiac hypertrophy on the expression of several *CYP* genes as well as CYP-dependent arachidonic acid metabolism in rats. In addition, the current study demonstrates the tissue specific expression of many *CYP* and *EPHX2* genes in male SD rats.

There are several discrepancies in the literature on tissue-specific expression of *CYP* genes in the rat (Imaoka, Hashizume et al. 2005). Several factors may have led to these discrepancies. The first factor is the use of conventional PCR technique in most of these studies which may be insensitive due to the low level of CYP expression, especially in extra-hepatic tissues. Secondly, most of the previous studies focused on only one tissue without giving comparative information regarding the other tissues. Therefore, it was necessary to examine the expression of multiple *CYP* genes simultaneously in different

organs by a sensitive technique such as real time-PCR. In the current study, we showed that *CYP1A1*, *CYP1B1*, *CYP2B1*, *CYP2B2*, *CYP2C11*, *CYP2E1*, *CYP2J3*, *CYP4F4*, *CYP4F5*, and *EPHX2* genes are constitutively expressed in all the examined tissues, whereas *CYP4A1* and *CYP4A3* genes are expressed in the heart, kidney, and liver but not in the lung and *CYP4A2* gene was expressed in the liver and kidney only. The lung has the highest constitutive expression of *CYP1A1*, *CYP1B1*, *CYP2B1* and *CYP4F5* genes; the liver and kidney have the highest expression of CYP4A2 and CYP4A3, whereas the liver has the highest expression level of all other *CYP* genes as well as *EPHX2*. Generally, the heart has the lowest level of constitutive *CYP* expression except for *CYP1B1*and *CYP4F5* which are expressed in the heart at higher levels than those in the liver.

To induce cardiac hypertrophy experimentally, we used a regimen of 7 daily IP injections of isoproterenol (5 mg/kg) which is known to induce cardiac hypertrophy without HF or blood pressure elevation (Meszaros and Pasztor 1995; Kralova, Mokran et al. 2008). In the current study, isoproterenol treatment caused cardiac hypertrophy in SD rats as manifested by significant induction of the hypertrophic markers, ANP and BNP, as well as the increase of the heart to body weight ratio. In agreement with our results, isoproterenol infusion of 4 mg/kg/day for seven days caused a significant increase of the heart to body weight and a significant induction of ANP (Masson, Arosio et al. 1998). Similarly, BNP is known to be increased in various models of cardiac hypertrophy (Shimoike, Iwai et al. 1997; Magga, Vuolteenaho et al. 1998); however, there is limited

information about the effect of isoproterenol-induced cardiac hypertrophy on BNP gene expression.

CYP1A1 and CYP1B1 are highly expressed in the heart at the constitutive level; therefore, their role in arachidonic acid metabolism in the heart cannot be ignored. CYP1A1 has been shown to be involved in the synthesis of ω-terminal HETEs, whereas CYP1B1 can metabolize arachidonic acid to both mid chain HETEs and EETs (Choudhary, Jansson et al. 2004). Accordingly, it was very important to investigate the effect of isoproterenol-induced cardiac hypertrophy on the gene expression of *CYP1A1* and *CYP1B1* in the heart as well as in other tissues. In the current study, we found that *CYP1A1* gene expression is induced in the heart and kidney in isoproterenol-treated rats but not in the lung or liver, whereas CYP1B1 gene expression was induced only in the hypertrophied hearts. In agreement with our results, expression of *CYP1A1* and *CYP1B1* were significantly increased in left ventricular tissues of SHRs as compared to normotensive SD rats (Thum and Borlak 2002). Furthermore, a selective inhibitor of CYP1B1 has been shown to prevent deoxycorticosterone-salt-induced hypertension and cardiac hypertrophy in uninephrectomized rats (Sahan-Firat, Jennings et al. 2010). Both CYP1A1 and CYP1B1 are mainly regulated through the AhR pathway; therefore, CYP1A1 and CYP1B1 induction may be attributed to AhR activation during isoproterenol-induced cardiac hypertrophy. Of interest, AhR activation has been associated with the development of cardiac hypertrophy in several studies (Kǒrashy and El-Kadi 2006).

In contrast to *CYP1A1* and *CYP1B1*, *CYP2C11* gene expression was significantly lower in the hypertrophied hearts than the control hearts; however, its gene expression was not altered in the other tissues. CYP2C11 is an important epoxygenase enzyme which is involved in arachidonic acid metabolism and synthesis of EETs (Ng, Huang et al. 2007). *CYP2C11* gene expression is inhibited in several models of inflammation (Iber, Li-Masters et al. 2001; Anwar-mohamed, Zordoky et al. 2010). Taking into account the fact that several inflammatory mediators are activated during cardiac hypertrophy and HF (Yndestad, Damas et al. 2007), CYP2C11 inhibition might be attributed to the inflammation that happens during isoproterenol-induced cardiac hypertrophy. Unlike CYP2C11, CYP2E1 metabolizes arachidonic acid to 18- and 19-HETEs (Laethem, Balazy et al. 1993). Isoproterenol-induced cardiac hypertrophy caused a significant inhibition of *CYP2E1* gene expression in the heart and a significant induction of its expression in kidney. Contrary to this finding, CYP2E1 has been reported to be higher in SHR than in normotensive SD rats (Thum and Borlak 2002).

In spite of previous reports that showed increased gene expression of *CYP2B1/2* and *CYP2J3* in SHR as compared to normotensive SD rats (Thum and Borlak 2002), our results showed that *CYP2B1*, *CYP2B2*, and *CYP2J3* gene expressions were not altered during isoproterenol-induced cardiac hypertrophy. The discrepancy between our results and those of Thum and Borlak is likely due to strain and model differences. CYP4A3 was significantly induced in the heart, liver, and kidney in isoproterenol-treated rats as compared to controls. The premise of this observation emerges from the fact that CYP4A3 is a major ω-

hydroxylase enzyme involved in arachidonic acid metabolism to 20-HETE (Wang, Stec et al. 1996; Wang, Guan et al. 1999; Roman 2002). Isoproterenol-treatment did not significantly alter the gene expression of *CYP4A1*, *CYP4F4*, and *CYP4F5* in any of the examined tissues (table 4.1).

sEH enzyme is a crucial determinant of EETs level because it catalyzes the conversion of EETs to DHETs thus abolishing their biological activity (Imig, Zhao et al. 2002). Therefore, any change in arachidonic acid metabolism due to alteration of CYP expression can be augmented or opposed by an altered level of sEH. Moreover, *EPHX2*, the gene encoding sEH, was found to be a susceptibility factor for HF in SHHF rats (Monti, Fischer et al. 2008). Therefore, it was necessary to investigate the effect of cardiac hypertrophy on *EPHX2* expression. In the current study, *EPHX2* gene expression in the heart was found to be increased during isoproterenol-induced cardiac hypertrophy. In agreement with our results, it has been shown that sEH activity is higher in SHHF rats than in normal controls (Monti, Fischer et al. 2008); however, ours is the first report to show an induction of *EPHX2* gene expression in experimentally-induced cardiac hypertrophy. More recently, it has been shown that sEH protein level was elevated in the hypertrophied hearts of angiotensin II-infused rats (Ai, Pang et al. 2009). In addition, angiotensin II induced sEH expression in isolated neonatal rat cardiomyocytes and inhibition of sEH significantly attenuated the hypertrophic effect of angiotensin II (Ai, Pang et al. 2009). Similarly, induction of cardiac hypertrophy by AhR ligands has been associated with an increase in sEH expression and activity (Aboutabl, Zordoky et al. 2009).

Table 4.1. Effect of isoproterenol-induced cardiac hypertrophy on *CYP* and *EPHX2* gene expression

	Heart	Liver	Lung	Kidney
CYP1A1	↑	↔	↔	↑
CYP1B1	↑	↔	↔	↔
CYP2C11	↓	↔	↔	↔
CYP2E1	↓	↔	↔	↑
CYP4A3	↑	↑	ND	↑
EPHX2	↑	↔	↔	↔

In order to investigate the effect of altered *CYP* gene expression on arachidonic acid metabolism, we performed *in vitro* incubation of heart microsomes with arachidonic acid. We found a significant decrease in 5,6-, 8,9-, 11,12-, and 14,15-EET formation in microsomes of hypertrophied hearts in comparison to controls. The decrease in formation of EETs was accompanied by a significant increase in 8,9- and 14,15-DHET formation, whereas formation of 5,6- and 11,12-DHET was not significantly altered. The decreased formation of EETs during isoproterenol-induced cardiac hypertrophy may be attributed to lower expression of CYP2C11 and higher expression of sEH. The significantly higher formation of 8,9- and 14,15-DHET is consistent with the higher expression of sEH because 14,15-EET is the best substrate for sEH followed by 8,9-EET (Karara, Dishman et al. 1991). The decrease in EETs formation during isoproterenol-induced cardiac hypertrophy can be considered a maladaptive response, because EETs are known to possess cardioprotective properties (Larsen, Campbell et al. 2007). There are several proposed mechanisms to explain the protective effect of EETs against cardiac hypertrophy. It has been shown that EETs inhibit the activation of NF-κB which is involved in the development of cardiac hypertrophy (Node, Huo et al. 1999). Interestingly, sEH inhibitors significantly attenuated angiotensin II- and phenylephrine-induced hypertrophy in mice neonatal cardiomyocytes through inhibition of NF-κB activation (Xu, Li et al. 2006). Similarly, EETs have been shown to inhibit matrix metalloproteinase-9 which is also implicated in the development of cardiac hypertrophy (Moshal, Zeldin et al. 2008). In addition, EETs have demonstrated a protective role against

apoptosis of cardiomyocytes which is one of the hallmarks of pathological hypertrophy (Dhanasekaran, Gruenloh et al. 2008).

Moreover, our results demonstrate that 20-HETE formation is significantly higher in microsomes of hypertrophied hearts in comparison to untreated rats. 20-HETE formation is mainly catalyzed by CYP ω-hydroxylases (Kroetz and Xu 2005). CYP ω-hydroxylases involved in the formation of HETEs are CYP1A, CYP1B1, CYP4A and CYP4F (Wang, Stec et al. 1996; Wang, Guan et al. 1999; Roman 2002; Choudhary, Jansson et al. 2004; Elbekai and El-Kadi 2006). Therefore, the increase in 20-HETE formation in the present work could be attributed to the increased expression of CYP1A1, CYP1B1 and CYP4A3. The increased formation of 20-HETE is suggestive of its role in cardiac hypertrophy. 20-HETE has been shown to activate several pathways that are known to be involved in the development of cardiac hypertrophy. For instance, 20-HETE has been shown to activate NF-κB and stimulate the production of inflammatory cytokines in human endothelial cells (Ishizuka, Cheng et al. 2008). Likewise, 20-HETE has been demonstrated to translocate the transcription factot NFAT from the cytoplasm into the nucleus in pulmonary VSMCs (Yaghi and Sims 2005). In addition, 20-HETE also activates p38 MAPK in VSMCs (Kalyankrishna and Malik 2003). Similarly, 20-HETE has been shown to activate matrix metalloproteinase-9 in non-small cell lung cancer (Yu, Chen et al. 2010). Unfortunately, none of these studies has been conducted in cardiomyocytes; therefore, further studies are warranted to explore the mechanisms by which 20-HETE can induce cardiac hypertrophy. Of interest, 20-HETE has been recently

shown to induce apoptosis in neonatal rat cardiomyocytes which further confirms its detrimental role in the development of pathological cardiac hypertrophy (Bao, Wang et al. 2011).

In conclusion, isoproterenol-induced cardiac hypertrophy caused significant changes of expression of several *CYP* and *EPHX2* genes which is mostly specific to the heart. The overall balance of these changes has lead to higher production of 20-HETE and lower production of EETs in the hypertrophied hearts. 20-HETE is known to be involved in many CVDs; however, there is indirect evidence about its role in the development of cardiac hypertrophy (Wen, Gu et al. 2003; Lee, Landon et al. 2004; Chabova, Kramer et al. 2007). On the other hand, EETs are reported to have cardioprotective effects mainly by inhibiting the activation of NF-κB (Campbell 2000; Hirotani, Otsu et al. 2002; Xu, Li et al. 2006). Interestingly, the combined inhibition of 20-HETE formation and EETs degradation attenuated hypertension and cardiac hypertrophy in Ren-2 transgenic rats (Certikova Chabova, Walkowska et al. 2010). Increased gene expression of *CYP1A1*, *CYP2E1*, and *CYP4A3* in the kidney during isoproterenol-induced cardiac hypertrophy could also lead to altered CYP-mediated arachidonic acid metabolites which play a critical role in kidney function (Elbekai and El-Kadi 2006). Therefore, cardiac and renal CYP may play an important role in the development and/or progression of cardiac hypertrophy. However, more studies are needed to explore the mechanisms by which cardiac hypertrophy modulates *CYP* and *EPHX2* gene expression.

4.2. H9c2 cell line is a valuable *in vitro* model to study drug metabolizing enzymes in the heart

CYP reaction products, or metabolites, have been detected in cardiovascular tissue (Roman 2002; Gottlieb 2003; Spiecker and Liao 2005) and recently, specific isoforms of the CYP enzymes superfamily have been detected in rat heart (Imaoka, Hashizume et al. 2005) and in different regions of human heart (Delozier, Kissling et al. 2007; Michaud, Frappier et al. 2010). Emerging studies have documented the role of these endogenous CYP metabolites in the maintenance of cardiovascular health (Roman, 2002); therefore, dysregulation of their production may be associated with various CVDs. Several studies demonstrated that cultured primary cardiomyocytes can offer a valuable tool for studying the role of CYP-mediated arachidonic acid metabolism in the pathogenesis of heart diseases (Thum and Borlak 2000; Borlak and Thum 2002). However, a major limitation for isolated cardiomyocytes is that they are difficult to isolate and maintain in cell culture; therefore, we investigated the expression of different *CYP* genes in the H9c2 cell line as an alternative to isolated cardiomyocytes.

The H9c2 cell line is a commercially available myogenic cell line derived from embryonic rat heart ventricle (Kimes and Brandt 1976). Although H9c2 cells show morphological characteristics similar to embryonic rat cardiomyocytes, they preserve several biochemical and electrophysiological properties of the adult cardiomyocytes (Hescheler, Meyer et al. 1991). However, the expression of CYP enzymes has never been studied in this valuable cell line. In the present study, we

showed for the first time that *CYP1A1* and *CYP1B1* are constitutively expressed in both H9c2 cells and the heart. *CYP1A1* was induced by BNF in H9c2 cells and the heart, whereas *CYP1B1* was only induced in the heart under the current experimental conditions. In agreement with our results, Thum and Borlak detected CYP1A1 and CYP1B1 mRNAs in the left ventricle of SD and SHR. The same authors did not detect CYP1A2 mRNA in the rat heart (Thum and Borlak 2002). Of interest, Aboutabl *et al* reported the constitutive and inducible expression of CYP1A1 in H9c2 cells at the mRNA, protein, and activity levels (Aboutabl and El-Kadi 2007).

CYP2B1, *CYP2B2*, *CYP2E1*, and *CYP2J3* genes were expressed in H9c2 cells and the heart at a comparable level but significantly lower than that detected in the liver. In agreement with our results, Thum and Borlak detected CYP2B1 and CYP2J3 at the mRNA level in the left ventricle of SD and SHR rats (Thum and Borlak 2002) and in isolated cultured cardiomyocytes (Thum and Borlak 2000). On the other hand, there is insufficient data on the expression of CYP2B2 in the heart; however, one study detected CYP2B2 in fetal rat heart at the protein level (Czekaj, Wiaderkiewicz et al. 2000). It is important to mention here that rat CYP2B1 and CYP2B2 are different in only 14 residues and catalyze almost the same reactions (Guengerich 1997). In addition, CYP2E1 was shown to be expressed in the rat heart and in all regions of the human heart (Thum and Borlak 2000).

Gene expression of *CYP2C11*, *CYP2C13*, and *CYP2C23* appeared to be greater in the cell line than in heart. Although Thum and Borlak detected

CYP2C11 mRNA in freshly isolated cardiomyocytes (Thum and Borlak 2000), they did not detect its expression in the left ventricle of SD and SHR rats (Thum and Borlak 2002). Similar to our results, Imaoka *et al* detected low levels of CYP2C23 mRNA in the rat heart (Imaoka, Hashizume et al. 2005). To the best of our knowledge, there are no previous published data about the expression of CYP2C13 in the heart.

In the present work, *CYP2A1*, *CYP3A1*, and *CYP3A2* were not expressed either in H9c2 cells or in the heart. In contrast to our results, Thum and Borlak detected CYP2A1/2 mRNA in the left ventricle of SD and SHR rats (Thum and Borlak 2002); however, in agreement with our results, Imaoka *et al* did not detect CYP2A1 mRNA in the heart (Imaoka, Hashizume et al. 2005). CYP3A1 mRNA was previously detected in 12 – 24 h old cultured rat cardiomyocytes but not in freshly isolated cardiomyocytes (Thum and Borlak 2000) or in the left ventricle of SD or SHR rats (Thum and Borlak 2002). In addition, CYP3A expression was not detected in any region of the human heart (Thum and Borlak 2000).

We conclude that multiple *CYP* genes are expressed in H9c2 cells at comparable levels to those expressed in the rat heart or cardiomyocytes. Therefore, this cell line offers a unique *in vitro* model to study the CYP-mediated metabolic activity of the heart and to investigate the possible role of CYP enzymes in the pathogenesis of various CVDs.

4.3. 2,3,7,8-Tetrachlorodibenzo-p-dioxin and β-naphthoflavone induce cellular hypertrophy in H9c2 cells

Several studies have demonstrated the cardiotoxic effect of AhR ligands as they cause structural malformation, ventricular hypertrophy, and abnormal myocyte contractility in several *in vivo* models (Canga, Paroli et al. 1993; Walker and Catron 2000; Heid, Walker et al. 2001). However, to the best of our knowledge, no previous study investigated whether AhR ligands exert a hypertrophic effect at the cardiomyocyte level. In the current study, we demonstrated for the first time the hypertrophic effect of two AhR ligands, TCDD and BNF, on H9c2 cells. In addition, we related this hypertrophic response to changes in *CYP* gene expression.

The H9c2 cell line is a commercially available myogenic cell line derived from embryonic rat heart ventricles (Kimes and Brandt 1976). We have previously shown that TCDD and BNF cause a significant induction of CYP1A1 in H9c2 cells at the mRNA, protein, and activity levels (Aboutabl and El-Kadi 2007). In addition, H9c2 cells are commonly used as an *in vitro* model to study the cardiotoxic effect of several agents such as DOX, lipopolysaccharides (LPS), and H_2O_2 (Chen, Tu et al. 2000; Merten, Jiang et al. 2006; Liu, Cheng et al. 2008). Therefore, in the current study we examined the hypertrophic effect of TCDD and BNF on H9c2 cells.

Treatment of H9c2 cells with TCDD and BNF caused a significant induction of gene expression of the hypertrophic markers, ANP and BNP, only

after 48 h. A significant induction of ANP and BNP has been observed in various models of cardiac hypertrophy *in vivo* (Magga, Vuolteenaho et al. 1998; Masson, Arosio et al. 1998). Similarly, several *in vitro* models of cardiomyocyte hypertrophy caused by IGF, DOX, LPS, and H_2O_2 showed an induction of both hypertrophic markers, ANP and BNP, in H9c2 cells (Chu, Tzang et al. 2008; Huang, He et al. 2008; Liu, Cheng et al. 2008). In addition to the induction of these hypertrophic markers, TCDD and BNF caused a significant increase in the cells surface area after 48 h which further confirms the hypertrophic effect of these AhR ligands at the cardiomyocyte level. In agreement with our results, the increased expression of ANP has been reported in hearts of TCDD-exposed chick embryos (Walker and Catron 2000; Kanzawa, Kondo et al. 2004) and in fetal mice hearts after *in utero* exposure to TCDD (Aragon, Kopf et al. 2008). In addition, sub-chronic administration of TCDD to C57BL/C mice caused cardiac hypertrophy which was attributed to the generation of superoxides and to blood pressure elevation (Kopf, Huwe et al. 2008). Recently, the AhR ligands BaP and 3-MC have been shown to induce cardiac hypertrophy in male SD rats which was attributed to derailed arachidonic acid metabolism (Aboutabl, Zordoky et al. 2009). Several other mechanisms have been postulated to explain the cardiotoxic effect of AhR ligands. These mechanisms include oxidative stress, modulation of cardiac and cell cycle genes, DNA adduct formation, and disruption of the metabolism of endogenous substances (Korashy and El-Kadi 2006). In this context, it is important to note that induction of hypertrophic markers by the AhR ligands did not occur after 24 h of treatment. Therefore, it is assumed that AhR

activation causes hypertrophy through several cellular processes that need time to commence.

In the current study, AhR ligands caused a significant induction of *CYP1A1* and *CYP1B1* at both the 24 h and 48 h time-points. In our previous studies, we have shown that induction of CYP1A1 mRNA by BNF in H9c2 cells occurred after 6 h of exposure. Although induction of the CYP1 family is the most prominent effect of AhR activation (Rifkind 2006), the role of CYP1 induction in mediating the cardiotoxic effect of TCDD is usually overlooked. *CYP1A1* and *CYP1B1* are found to be highly expressed in the heart at both constitutive and inducible levels (Sinal, Webb et al. 1999). We have previously shown that *CYP1A1* and *CYP1B1* expression is higher in the hypertrophied rat hearts than in normal hearts. Moreover, *CYP1B1* gene expression is higher in hypertrophied hearts of SHR than normotensive rats (Thum and Borlak 2002). CYP1A1 and CYP1B1 are known to metabolize arachidonic acid to different regioisomers of HETEs (Choudhary, Jansson et al. 2004; Schwarz, Kisselev et al. 2004). Moreover, we have previously shown that induction of CYP1A1 and CYP1B1 in hypertrophied hearts caused a significant increase in the formation of 20-HETE. HETEs are known to be involved in the pathogenesis of cardiac hypertrophy as well as other CVDs (Elbekai and El-Kadi 2006; Chabova, Kramer et al. 2007). Interestingly, inhibition of 20-HETE formation has been shown to partially prevent AhR ligand-induced cardiac hypertrophy in male SD rats (Aboutabl, Zordoky et al. 2009).

With regard to the CYP2 family, there was a significant induction of CYP2E1 and CYP2J3 after 48 h exposure to TCDD and BNF. The physiological importance of these enzymes emerges from their ability to metabolize arachidonic acid to various EETs and HETEs (Kroetz and Zeldin 2002). CYP2E1 is known to catalyze ω-1 hydroxylation of arachidonic acid to form 19-HETE, while CYP2J3 is an important epoxygenase enzyme that metabolizes arachidonic acid to different EETs (Laethem, Balazy et al. 1993; Wu, Moomaw et al. 1996). In agreement with our results, CYP2E1 and CYP2J3 mRNAs were significantly increased by 6 and 4 fold, respectively in the left ventricular tissues of SHRs as compared to control rats (Thum and Borlak 2002). Similarly, myocardial CYP2E1 expression was found to be much higher in dilated cardiomyopathy than that in healthy human hearts (Sidorik, Kyyamova et al. 2005). In addition, BNF treatment increased CYP2E1 mRNA in the heart of male rats which was attributed to the pathological state caused by BNF (Sinal, Webb et al. 1999). Likewise, BaP and 3-MC treatment caused a significant induction of CYP2E1 in the heart of male SD rats (Aboutabl, Zordoky et al. 2009).

Despite previous reports that showed increased expression of CYP2B1/2 in hearts of SHR as compared to normotensive rats (Thum and Borlak 2002), our results showed that *CYP2B1* and *CYP2B2* gene expression was not altered during AhR ligand-induced hypertrophy in H9c2 cells. Similarly, the AhR ligands BaP and 3-MC did not induce *CYP2B1* or *CYP2B2* in male SD rats (Aboutabl, Zordoky et al. 2009). Regarding CYP2C11, there has been some discrepancy regarding its expression in different models of cardiac hypertrophy. On one hand,

we have demonstrated that isoproterenol treatment caused a significant inhibition of *CYP2C11* gene expression in the hypertrophied hearts of male rats as compared to controls. On the other hand, *CYP2C11* gene expression was not significantly altered during AhR ligand-induced cardiac hypertrophy in male SD rats (Aboutabl, Zordoky et al. 2009). Similarly, *CYP2C11* gene expression was not altered in the current study.

CYP4A and CYP4F subfamilies are considered the most important CYP ω-hydroxylases which are involved in the metabolism of arachidonic acid to 20-HETE (Roman 2002; Rifkind 2006). In the current study, treatment with AhR ligands for 24 h caused a significant induction of CYP4A1 and treatment for 48 h caused a significant induction of CYP4F4, whereas there was no significant change in the expression of the other genes. To the best of our knowledge, this was the first report about the effect of AhR ligands on CYP4 family gene expression.

Oxidative stress is known to be a central player in the development and/or progression of cardiac hypertrophy (Takimoto and Kass 2007). In addition, many reports have linked the toxicity of AhR ligands to the induction of oxidative stress (Reichard, Dalton et al. 2005). Therefore, it was necessary to investigate whether the observed hypertrophic effect of TCDD and BNF was mediated though the generation of oxidative stress. In the present work, TCDD and BNF did not cause a significant increase of intracellular ROS in H9c2 cells. In agreement with our results, it has been shown that BNF concentrations less than 50 μM did not increase H_2O_2 production or lipid peroxidation, two markers of oxidative stress, in

Hepa1c1c7 cells (Elbekai, Korashy et al. 2004). Similarly, 10 nM TCDD did not increase lipid peroxidation in neuroblastoma cells (Sul, Kim et al. 2009). Therefore, oxidative stress could not be a possible mechanism by which TCDD and BNF caused the hypertrophic response in the present study.

In order to explore the role of AhR in the development of hypertrophy, we examined whether the AhR antagonist, resveratrol, could prevent the TCDD-induced cellular hypertrophy. Resveratrol, a naturally occurring polyphenolic compound, has been shown to inhibit the expression of several CYP enzymes including CYP1A1, CYP1B1, and CYP2E1 (Upadhyay, Singh et al. 2008; Beedanagari, Bebenek et al. 2009). Interestingly, our results show that resveratrol prevented the TCDD-induced hypertrophy in H9c2 cells. Therefore, induction of CYP enzymes by AhR ligands may be involved, at least in part, in their hypertrophic effect. In agreement with our results, resveratrol has been shown to possess a significant cardioprotective effect against DOX-induced cardiotoxicity, phenylephrine-induced cardiac hypertrophy, and hypoxia-induced cardiomyocyte apoptosis through several mechanisms (Cao and Li 2004; Chan, Dolinsky et al. 2008; Chen, Yu et al. 2009; Dolinsky, Chan et al. 2009). However, the possible role of resveratrol in protection against TCDD-induced cardiac hypertrophy has never been studied.

In conclusion, AhR ligands caused a significant induction of the hypertrophic markers ANP and BNP as well as several *CYP* genes in H9c2 cells. To the best of our knowledge, this is the first time to demonstrate the hypertrophic effect of AhR ligands at the cardiomyocyte level. Induction of CYP enzymes

would result in alteration of arachidonic acid metabolism which has been associated with cardiac hypertrophy and HF. In addition, this hypertrophic effect has been prevented by resveratrol which is known to inhibit several CYP enzymes. Therefore, CYP induction may be one of the mechanisms by which AhR ligands cause cardiotoxicity.

4.4. Induction of several Cytochrome P450 genes by DOX in H9c2 cells

The current study demonstrates for the first time the effect of DOX on *CYP* gene expression in general and on cardiac *CYP* genes in particular. Although there are many proposed hypotheses to explain the mechanism by which DOX induces cardiotoxicity (Nakamura, Ueda et al. 2000; Mordente, Meucci et al. 2001; Chaiswing, Cole et al. 2004; Oliveira, Bjork et al. 2004; Ueno, Kakinuma et al. 2006), there is no study that examined the possible role of CYP in DOX-induced cardiotoxicity. The importance of CYP enzymes in the heart emerges from their ability to produce various metabolites that can confer cardioprotective or cardiotoxic effects (Elbekai and El-Kadi 2006). Therefore, in the current study we examined the effect of DOX on the expression of multiple *CYP* genes as well as hypertrophic markers in H9c2 cells. The DOX concentrations studied are in the same micromolar range as those reported in the plasma of patients treated with DOX for various types of cancers (Bressolle, Jacquet et al. 1992; Wihlm, Limacher et al. 1997; Palle, Frost et al. 2006).

H9c2 cells are commonly used as an *in vitro* model to study the mechanisms involved in DOX-induced cardiotoxicity (Spallarossa, Fabbi et al. 2005; Chiosi, Spina et al. 2007; Turakhia, Venkatakrishnan et al. 2007; Venkatakrishanan, Dunsmore et al. 2008). This cell line has also been used as an experimental model of H_2O_2-induced hypertrophy (Chen, Tu et al. 2000) as well as DOX-induced hypertrophy (Merten, Jiang et al. 2006). Recently, we showed that H9c2 cells express multiple *CYP* genes at comparable levels to those expressed in the heart. The reported relative expression of multiple *CYP* genes in

the current study using real-time PCR was very similar to that reported in our previous work using the conventional RT-PCR. However, by using a more sensitive real-time PCR in the current study, we are able to detect the mRNA of CYP1A2 in these cells.

Treatment of H9c2 cells with DOX for 2 h has been shown to cause hypertrophy which is characterized by increased cellular protein content and cell size (Merten, Jiang et al. 2006). In the present study, we showed that DOX caused a significant induction of gene expression of hypertrophic markers ANP and BNP in H9c2 cells. In the literature, there is a great discrepancy regarding the effect of DOX on the gene expression of these hypertrophic markers. It has been previously reported that there is an increase in plasma ANP level in DOX-treated patients and this increase was correlated with the deterioration of heart function (Nousiainen, Jantunen et al. 1999). Moreover, there was a five-fold increase of ANP mRNA in the hearts of DOX-treated dogs and rats (Rahman, Alam et al. 2001). However, *in vitro* DOX treatment significantly decreased ANP expression in cultured neonatal cardiomyocytes (Rahman, Alam et al. 2001). Nevertheless, an *in vitro* model of H_2O_2-induced cardiomyocyte hypertrophy showed an induction of gene expression of both hypertrophic markers ANP and BNP in H9c2 cells (Huang, He et al. 2007).

The effect of DOX on hepatic CYP activity has been reported previously. DOX has been shown to lower hepatic CYP content and decrease a variety of CYP-catalyzed enzyme activities when given to rodents (Marchand and Renton 1981). This effect has been attributed to a combination of direct inhibition of CYP

enzymes and destruction of CYP heme (Mimnaugh, Trush et al. 1981). Later, it was reported that DOX does not cause direct mechanism-based inactivation of hepatic CYP (Di Re, Lee et al. 1999). Nevertheless, the effect of DOX on the expression of genes encoding specific CYP enzymes was not addressed previously (Riddick, Lee et al. 2005).

In the present study, we showed that treatment of H9c2 cells with DOX for 2 h caused a significant induction of CYP1A1, CYP1A2 and CYP1B1 mRNA levels. In agreement with our results, it has been previously reported that the expression of *CYP1B1* is significantly higher in left ventricular tissues of SHRs as compared to normotensive rats (Thum and Borlak 2002). Of special interest, it has been recently reported that DOX activates the AhR which regulates the expression of *CYP1A1*, *CYP1A2*, and *CYP1B1* genes (Volkova, Palmeri et al. 2011). CYP1A1, CYP1A2, and CYP1B1 enzymes are involved in the metabolism of 17β-estradiol to the more potent hydroxyestradiols in cardiac fibroblasts (Dubey, Gillespie et al. 2003). It has been reported that 17β-estradiol is cardioprotective by inhibiting cardiomyocyte loss in HF (Pelzer, Schumann et al. 2000). In addition, the CYP1 family is important in arachidonic acid metabolism either to HETEs or to EETs (Kroetz and Zeldin 2002; Elbekai and El-Kadi 2006). These metabolites play a crucial role in maintaining the cardiac homeostasis as alterations of their levels have been associated with the pathogenesis of cardiac hypertrophy and HF (Pelzer, Schumann et al. 2000; Wen, Gu et al. 2003; Levick, Loch et al. 2007). Nevertheless, it has been shown that AhR activation by DOX plays a

cardioprotective role as DOX-induced cardiotoxicity was aggravated in AhR null mice (Volkova, Palmeri et al. 2011).

In the current study, DOX treatment significantly induced the gene expression of *CYP2B2*, *CYP2C11*, *CYP2E1*, and *CYP2J3* to varying degrees, whereas *CYP2B1* and *CYP2C23* genes were not significantly altered. The differential effect of DOX on various *CYP* genes can be explained by different regulatory mechanisms involved in their transcription (Rushmore and Kong 2002; Xu, Li et al. 2005). In agreement with these results, we have previously reported that cardiac hypertrophy is associated with induction of several *CYP* genes. In rats, the expression of *CYP2B1/2*, *CYP2E1*, and *CYP2J3* was significantly higher by 6-, 6-, and 4-fold respectively in left ventricular tissues of SHRs as compared to normotensive rats (Thum and Borlak 2002). In addition, CYP2E1 expression in the microsomal fraction of the myocardium was found to be much higher in dilated cardiomyopathy than that in healthy human hearts (Sidorik, Kyyamova et al. 2005). The physiological importance of these enzymes emerge from their ability to metabolize arachidonic acid to various HETEs and EETs (Kroetz and Zeldin 2002; Spallarossa, Fabbi et al. 2005; Elbekai and El-Kadi 2006).

We conclude that DOX caused a significant induction of the hypertrophic markers, ANP and BNP, as well as several *CYP* genes at the mRNA level. To the best of our knowledge, this is the first study to investigate the effect of DOX on *CYP* gene expression. CYP induction would result in alteration of arachidonic acid metabolism which has been associated with cardiac hypertrophy and HF; therefore, this may be one of the mechanisms by which DOX induces

cardiotoxicity. Furthermore, this study confirms the validity of the H9c2 cell line as a valuable *in vitro* model to study the possible role of *CYP* genes in the pathogenesis of various heart diseases.

4.5. Acute doxorubicin cardiotoxicity alters cardiac cytochrome P450 expression and arachidonic acid metabolism in rats

We have previously demonstrated that DOX causes a concentration-dependent induction of several *CYP* genes in cardiac-derived H9c2 cells. The physiological importance of CYP enzymes depends on their ability to produce various metabolites that confer cardioprotective or cardiotoxic effects (Elbekai and El-Kadi 2006). With regard to their role in arachidonic acid metabolism, CYP enzymes are considered one of the major metabolic enzymes for arachidonic acid in addition to the COX and LOX. CYP epoxygenases metabolize arachidonic acid to several regioisomers of EETs, while CYP ω-hydroxylases metabolize arachidonic acid to 20-HETE (Roman 2002). Therefore, the current study demonstrates for the first time the effect of acute DOX cardiotoxicity on cardiac CYP expression and CYP-mediated arachidonic acid metabolism in male SD rats.

In the present study, acute DOX cardiotoxicity has been induced by a single IP injection of 15 mg/kg of DOX. The development of cardiotoxicity has been confirmed by increased serum LDH levels in DOX-treated rats at 24 h after DOX administration. LDH has been used in several studies as a biomarker of cardiotoxicity (Iqbal, Dubey et al. 2008). In addition, DOX doses between 10-20 mg/kg have been widely used to cause acute cardiotoxicity in rats, with rapid deterioration of cardiac function, elevation of biomarkers of cardiotoxicity, increased lipid peroxidation, and histopathologic changes (Cigremis, Parlakpinar et al. 2006; Hydock, Lien et al. 2007; Mitra, Donthamsetty et al. 2007). In addition, our results show that acute DOX cardiotoxicity caused a significant

inhibition of the hypertrophic markers, ANP and BNP, with more and earlier inhibition of BNP than ANP. In the literature, there is a great discrepancy regarding the effect of DOX on the expression of these markers. In agreement with our results, DOX selectively inhibited BNP versus ANP in cultured neonatal cardiomyocytes (Chen, Garami et al. 1999). On the other hand, there was an increase in ANP mRNA in the hearts of DOX-treated dogs and rats; however, *in vitro* DOX treatment significantly decreased ANP gene expression in neonatal cardiomyocytes (Rahman, Alam et al. 2001). In H9c2 cells, we have shown that DOX treatment caused a significant induction of both ANP and BNP. These discrepancies could be attributed to differences in the dose, timing, and the model used.

In the current study, acute DOX cardiotoxicity caused a significant induction of *CYP1A1*, *CYP1B1*, *CYP2C11*, and *CYP2J3* gene expression in the heart of male SD rats 24 h after DOX administration. In addition, there was a significant induction of the protein expression of these enzymes. In agreement with our results, we have recently shown that DOX treatment causes induction of these *CYP* genes in cardiac-derived H9c2 cells after 24 h of exposure to varying DOX concentrations. More recently, it has been shown that DOX activates the AhR with a subsequent induction of AhR-regulated genes such as *CYP1A1* in H9c2 cells as well as in the rat heart (Volkova, Palmeri et al. 2011). On the other hand, there was no significant change in the expression of *CYP2B1* and *CYP2E1* genes. In accordance with these results, we have demonstrated that *CYP2B1* gene expression was not significantly altered by DOX treatment in H9c2 cells;

however, *CYP2E1* was significantly induced. Regarding the role of these CYP enzymes in arachidonic acid metabolism, CYP1A1 has been shown to be involved in ω-terminal HETE synthesis, whereas CYP1B1 can metabolize arachidonic acid to both mid-chain HETEs and EETs (Choudhary, Jansson et al. 2004). CYP2B1, CYP2C11, and CYP2J3 are major epoxygenase enzymes that are involved in arachidonic acid metabolism to EETs (Laethem, Halpert et al. 1994; Ng, Huang et al. 2007), whereas CYP2E1 has been reported to metabolize arachidonic acid to 18- and 19-HETEs (Laethem, Balazy et al. 1993). In addition, we investigated for the first time the effect of acute DOX cardiotoxicity on the expression of major CYP ω-hydroxylases in the heart of male SD rats. DOX treatment for 24 h caused a significant induction of *CYP4A1*, *CYP4A3*, *CYP4F1*, and *CYP4F4* gene expression, whereas *CYP4F5* and *CYP4F6* expression was not altered. In accordance with the gene expression, there was 200% induction of CYP4A protein in the heart microsomes of rats treated by DOX for 24 h. However, there was no significant change in *CYP* gene expression at 6 and 12 h after DOX administration.

To investigate the effect of CYP induction on arachidonic acid metabolism, we performed *in vitro* incubation of heart microsomes with arachidonic acid. We found a significant decrease in 5,6-, 8,9-, 11,12-, and 14,15-EET formation in the heart microsomes of DOX-treated rats compared to controls. This decrease in formation of EETs was accompanied by a significant increase in the formation of their corresponding DHETs. In order to estimate the total epoxygenase activity, the sum of the total EETs and DHETs was calculated

(Zhao, Quigley et al. 2006). Interestingly, the total epoxygenase activity was significantly higher in the heart microsomes of DOX-treated rats as compared to controls. This increase in the epoxygenase activity can be attributed to the induction of CYP2C11 and CYP2J3, two major CYP epoxygenases, in addition to CYP1B1 which possesses some epoxygenase activity.

Surprisingly, formation of EETs is lower in the heart microsomes of DOX-treated rats despite the increase in the epoxygenase activity. Therefore, it was necessary to investigate the effect of acute DOX cardiotoxicity on the expression and activity of sEH which catalyzes the conversion of EETs to DHETs (Imig, Zhao et al. 2002). In the current study, acute DOX cardiotoxicity caused significant time-dependent induction of cardiac *EPHX2* gene expression at 6, 12, and 24 h after DOX administration. The induction at the mRNA level was translated to higher sEH protein expression and activity in the heart microsomes of DOX-treated rats in comparison to controls. The increase in sEH activity (3.8 fold) was much higher than the increase in the epoxygenase activity (1.2 fold) which explains the lower level of EETs despite the increase in epoxygenase activity. To examine whether DOX directly induces *EPHX2* gene expression at the cardiomyocyte level, we used H9c2 cells, a commercially available myogenic cell line derived from embryonic rat heart ventricles (Kimes and Brandt 1976). In agreement with the *in vivo* results, DOX treatment caused a significant concentration-dependent induction of *EPHX2 in vitro*. Of importance, the DOX concentrations used in the *in vitro* study are in the same micromolar range as those reported in the plasma of patients treated with DOX for various types of

cancers (Bressolle, Jacquet et al. 1992; Wihlm, Limacher et al. 1997; Palle, Frost et al. 2006).

EETs are reported to have cardioprotecive effects through several mechanisms, most notably by inhibiting the activation of NF-κB (Hirotani, Otsu et al. 2002; Xu, Li et al. 2006). Interestingly, DOX has been shown to induce myocardial apoptosis through activation of NF-κB (Li, E et al. 2008). Taken together, lower cardiac formation of EETs due to sEH induction may be involved in DOX-induced NF-κB activation and the subsequent myocardial apoptosis and cardiotoxicity. In addition, increased oxidative stress has been suggested as one of the main mechanisms of DOX-induced cardiotoxicity (Takemura and Fujiwara 2007). Taking into account the indirect antioxidant properties of EETs, we can postulate that lower cardiac formation of EETs augments DOX-generated oxidative stress and further contributes to its cardiotoxicity. In this context, it has been recently reported that EETs are able to minimize the adverse effects of DOX in cardiac-derived H9c2 cells (Zhang, El-Sikhry et al. 2009). In addition, sEH inhibitors which prevent degradation of EETs thus enhancing their biological activity have been reported to demonstrate a cardioprotective effect in several CVD models (Xu, Li et al. 2006; Loch, Hoey et al. 2007). In the present study, a selective sEH inhibitor, tAUCB, inhibited more than 70% of the conversion of EETs to DHETs in heart microsomes of both controls and DOX-treated rats. These results demonstrate that sEH is the major enzyme catalyzing the conversion of EETs to DHETs in rat heart microsomes. In addition, it confirms that the increase in the total DHETs/total EETs ratio in heart microsomes of DOX-treated

rats is due to sEH induction. Therefore, sEH inhibitors may provide a new approach to prevent DOX-induced cardiotoxicity. However, the limitation of this approach is the cancer-promoting effect of EETs (Jiang, Ning et al. 2007).

With regard to the ω-hydroxylase activity, our results demonstrated that 20-HETE formation is significantly higher in the heart microsomes of rats treated with DOX for 24 h in comparison to vehicle-treated animals. The increase in 20-HETE formation in the present work could be attributed to the increased expression of CYP1A1, CYP1B1, CYP4A1, CYP4A3, CYP4F1, and CYP4F4. 20-HETE is known to be involved in many CVDs, and its formation has been reported to be higher in the hearts of rats with streptozocin-induced diabetes (Yousif, Benter et al. 2009) and isoproterenol-induced cardiac hypertrophy. The increase in 20-HETE formation in the microsomes of hypertrophied hearts has been attributed to the induction of *CYP1A1*, *CYP1B1*, and *CYP4A3* gene expression. Interestingly, inhibition of 20-HETE formation caused improvement of the cardiac function following ischemia-reperfusion injury in diabetic rats (Yousif, Benter et al. 2009) and reduced cardiomyocyte apoptosis in another model of ischemia-reperfusion injury (Lv, Wan et al. 2008). Recently, it has been reported that 20-HETE induces apoptosis in neonatal rat cardiomyocytes (Bao, Wang et al. 2011), which further confirms its role in aggravating DOX cardiotoxicity. It is important to mention that, the induction of CYP enzymes at 24 h following DOX treatment paralleled the initial cardiotoxic effect of DOX which also occurred at 24 h after DOX administration. Therefore, CYP induction can be considered as a result of acute DOX cardiotoxicity. However, induction of ω-

hydroxylases and increased 20-HETE formation cannot be ignored as a contributing factor in the progression of acute DOX cardiotoxicity to end-stage HF. Taken together, CYP ω-hydroxylase inhibitors may provide another approach to protect against the progression of DOX-induced cardiotoxicity.

In conclusion, DOX-induced cardiotoxicity caused a significant induction of several cardiac CYP and sEH enzymes in male SD rats as well as in cardiac-derived H9c2 cells. The overall effect on arachidonic acid metabolism was a decrease in formation of cardioprotective EETs and an increase in the cardiotoxic 20-HETE. Induction of sEH may be involved, at least in part, in the development of acute DOX cardiotoxicity. However, CYP induction was a result of acute DOX cardiotoxicity that may be involved in its progression to end-stage HF. Therefore, reversal of these changes by inhibiting degradation of EETs or formation of 20-HETE may provide new strategies to protect against the development and/or progression of acute DOX cardiotoxicity.

4.6. Acute doxorubicin toxicity differentially alters cytochrome P450 expression and arachidonic acid metabolism in rat kidney and liver

DOX is a potent anthracycline anti-neoplastic drug used to treat a wide variety of malignancies. However, the clinical use of this agent is limited by a significant dose-dependent cardiotoxicity which may progress to end-stage HF (Outomuro, Grana et al. 2007). In addition to DOX-induced cardiotoxicity, it also causes nephrotoxicity and hepatotoxicity (Injac, Boskovic et al. 2008; Bulucu, Ocal et al. 2009). DOX-induced nephrotoxicity causes increased capillary permeability and glomerular atrophy (Injac, Boskovic et al. 2008). Although the exact mechanism of DOX-induced nephrotoxicity is not fully elucidated, it is thought to be mediated through DOX-induced oxidative damage (Liu, Li et al. 2007). Similarly, DOX-induced hepatotoxicity is generally mediated through the generation of free radicals (Bulucu, Ocal et al. 2009). In addition to oxidative damage, DOX toxicity has been shown to induce inflammatory changes in the heart, kidney, and liver tissues of DOX-administered rats (Deepa and Varalakshmi 2005).

We have previously shown that DOX-induced cardiotoxicity induces sEH and several CYP enzymes in the heart of male SD rats as well as in the heart-derived H9c2 cells with subsequent alteration of CYP-mediated arachidonic acid metabolism. In addition, it has been recently reported that DOX activates the AhR with a subsequent induction of CYP1A1 (Volkova, Palmeri et al. 2011). On the other hand, administration of DOX to rats and mice has been shown to decrease the catalytic activity of several hepatic CYP enzymes, although it does not cause

mechanism-based inactivation of these enzymes (Di Re, Lee et al. 1999). Therefore, the effect of DOX on CYP enzymes seems to be tissue and enzyme specific.

CYP enzymes play an important role in arachidonic acid metabolism in addition to the COX- and the LOX-mediated pathways (Roman 2002). Although the role of CYP-derived arachidonic acid metabolites in the cardiovascular physiology and pathophysiology have received major scientific attention (Elbekai and El-Kadi 2006), their roles in the kidney and liver cannot be ignored. Renal and hepatic CYP epoxygenases metabolize arachidonic acid to different EET regioisomers, while CYP hydroxylases metabolize it to HETEs (Roman 2002; Sacerdoti, Gatta et al. 2003). Furthermore, the sEH enzyme which catalyzes the conversion of EETs to the less biologically active DHETs is also abundantly expressed in the kidney and liver in both humans and experimental animals (Enayetallah, French et al. 2004).

Several investigators have addressed the role of CYP-derived arachidonic acid metabolites in renal and hepatic function (Maier and Roman 2001; Sacerdoti, Gatta et al. 2003). Generally, it has been shown that EETs dilate the preglomerular arterioles, whereas 20-HETE elicits a vasoconstricting effect on these blood vessels (Zhao and Imig 2003). However, both EETs and 20-HETE have a diuretic effect through inhibiting sodium reabsorption in the proximal tubule (Moreno, Maier et al. 2001). Nevertheless, little information is known about the role of these eicosanoids in the liver (Sacerdoti, Gatta et al. 2003). In contrast to the kidney, 11,12-EET has been shown to have a vasoconstrictive

effect on the porto-sinusoidal circulation in rat, while 20-HETE showed a weaker vasocontricting effect which was COX-dependent (Sacerdoti, Gatta et al. 2003). In addition, EETs were shown to be involved in vasopressin-induced glycogenolysis in rat hepatocytes (Yoshida, Hirai et al. 1990).

The current study demonstrates for the first time the effect of DOX toxicity on the expression of renal and hepatic CYP enzymes and CYP-mediated arachidonic acid metabolism. In the present study, acute DOX toxicity has been induced by a single IP injection of 15 mg/kg of the drug in male SD rats. This dose has been shown previously to induce cardiotoxicity, nephrotoxicity, and hepatotoxicity (Injac, Boskovic et al. 2008). In the current study, acute DOX toxicity caused a significant induction of the inflammatory markers IL-6, iNOS, and TNFα in the liver as early as 6 h after DOX administration preceding most of the changes in CYP enzyme expression. Although DOX toxicity has been shown previously to increase the biochemical markers of inflammation such as C-reactive protein and fibrinogen (Deepa and Varalakshmi 2005), this is the first study to demonstrate the effect of DOX toxicity on the gene expression of inflammatory markers.

In the current study, acute DOX toxicity significantly increased *CYP1B1* gene expression in both the kidney and liver. Interestingly, DOX has been shown to activate the AhR in cardiac-derived H9c2 cells and in the heart of male SD rats (Volkova, Palmeri et al. 2011). Similarly, we have previously shown that DOX induces the AhR-regulated genes *CYP1A1* and *CYP1B1* in H9c2 cells as well as the rat heart. However, the induction of *CYP1B1* gene expression in the kidney

and liver by DOX cannot be simply attributed to AhR activation because *CYP1A1,* which is also regulated through the AhR, was not induced. DOX-induced inflammation may be a more relevant explanation for *CYP1B1* induction, as it has been previously reported that LPS-induced inflammation causes a significant induction of *CYP1B1* in the liver of male SD rats (Anwar-mohamed, Zordoky et al. 2010). Mechanistically, it was postulated that inflammation induces *CYP1B1* gene expression through the hormonal pathway that also regulates CYP1B1 (Malaplate-Armand, Ferrari et al. 2003). Finally, it is still to be determined whether the effect of DOX on activating the AhR is heart-specific or if it is ubiquitous.

In contrast to *CYP1B1*, DOX toxicity caused a significant inhibition of both *CYP2B1* and *CYP2C11* in the kidney and liver, whereas there was a significant inhibition of *CYP2J3* gene expression only in the liver. CYP2B1, CYP2C11, and CYP2J3 are important epoxygenase enzymes that metabolize arachidonic acid to several EET regioisomers (Kroetz and Zeldin 2002). Several investigators have also reported the down-regulation of these enzymes in different models of inflammation (Iber, Li-Masters et al. 2001; Li-Masters and Morgan 2001; Anwar-mohamed, Zordoky et al. 2010). Therefore, we can attribute the inhibition of CYP2B1 and CYP2C11 to DOX-induced inflammation. Interestingly, CYP2C9 activity was decreased by 315% in breast cancer patients receiving DOX/cyclophosphamide chemotherapy (Elkiran, Harputluoglu et al. 2007). On the other hand, DOX-induced toxicity caused a significant induction of CYP2E1 in the kidney at both the mRNA and the protein level, whereas there was

no significant change in the liver. Similar results have been reported previously in models of irritant-induced inflammation (Iber, Sewer et al. 1999) . It is important to mention that ω-1 hydroxylation and 19-HETE formation were not changed in the kidney by CYP2E1 induction, most probably due to the low basal expression of CYP2E1 as compared to the total CYP content in the kidney (Poloyac, Tortorici et al. 2004).

With regard to CYP ω-hydroxylase enzymes, DOX-induced toxicity caused a significant induction of CYP4A enzymes in both the kidney and the liver of male SD rats. In agreement with these results, we have previously shown that DOX-induced cardiotoxicity causes significant induction of CYP4A enzymes in the heart of male SD rats. In addition, we and other investigators have also demonstrated that CYP4A enzymes are induced in the kidney and liver in several models of inflammation (Mitchell, Sewer et al. 2001; Anwar-mohamed, Zordoky et al. 2010; Theken, Deng et al. 2011). Moreover, it is well established that fasting can induce CYP4A enzymes (Kroetz, Yook et al. 1998). Therefore, we can attribute CYP4A induction to be mediated, at least in part, by DOX-induced inflammation and/or reduction in food consumption. Nevertheless, the increased 20-HETE formation may worsen the inflammatory condition by activating NF-κB and increasing the generation of inflammatory cytokines in a positive feedback circuit (Ishizuka, Cheng et al. 2008). In contrast to CYP4A enzymes, the effect of DOX on CYP4F enzymes was isoform-specific. DOX caused a significant induction of CYP4F1 in the kidney and an inhibition of CYP4F4 and CYP4F5 in the liver and kidney, respectively, while there was no change in CYP4F6

expression in the kidney and liver. Both CYP4F1 and CYP4F4 have been shown to be inhibited in a rat model of LPS-induced inflammation (Anwar-mohamed, Zordoky et al. 2010). Therefore, the observed effect of DOX toxicity on *CYP4F* gene expression is less likely to be attributed to DOX-induced inflammation.

We have previously reported that DOX induces sEH in H9c2 cells and the rat heart. Therefore, it was important to investigate the effect of DOX on the expression of sEH in organs other than the heart to examine whether sEH induction is heart-specific or not. In the present study, DOX caused a significant induction of the *EPHX2* gene only in the liver after 6 h of DOX administration; however, there was no change of sEH protein expression in the liver. In the kidney, there was a significant inhibition in sEH protein expression through a post-transcriptional mechanism because DOX did not change the *EPHX2* gene expression. These results demonstrate that the DOX effect on sEH is tissue-specific and DOX-induced sEH protein expression and activity is specific to the heart which further confirms its role in DOX-specific cardiotoxicity.

In the current study, our results show that DOX administration caused a significant increase in the formation of 8,9-, 11,12 and 14,15-EETs in the kidney, although it did not change the total epoxygenase activity. Therefore, the increase in the formation of EETs can be attributed to the inhibition of sEH activity which in turn is explained by the inhibition of sEH protein expression in the kidney of DOX-treated rats. Although there was no significant change in the formation rate of DHETs in the *in vitro* microsomal incubation experiment, there was a significant decrease in the endogenous concentration of DHETs in the kidney

tissue which may be attributed to the inhibition of sEH expression. Unfortunately, we could not detect endogenous EETs in the kidney tissues to estimate sEH activity. Generally, EETs are considered beneficial endogenous compounds because they have vasodilator, anti-inflammatory, anti-apoptotic, and natriuretic effects (Elbekai and El-Kadi 2006). Therefore, we can assume that the inhibition of sEH protein expression and activity in the kidney with the subsequent increase in formation of EETs is an adaptive response to protect the kidney against DOX toxicity. Despite the inhibition of some epoxygenase enzymes in both the kidney and liver, there was no significant change in the total epoxygenase activity. This could be explained by the fact that the induced CYP4A enzymes have also some epoxygenase activity (Nguyen, Wang et al. 1999) which may compensate for the decrease in the activity of the other enzymes.

Similar to the heart, DOX causes a significant increase in renal and hepatic ω-hydroxylase activity which is attributed to CYP4A induction. CYP4A enzymes are the major ω-hydroxylase enzymes which metabolize arachidonic acid to 20-HETE (Roman 2002). Parallel to the observed increase in the 20-HETE formation rate in the liver microsomes, there was a significant increase in the endogenous 20-HETE concentrations in the liver tissue. However, there was no change in the endogenous 20-HETE concentrations in the kidney tissue despite the increased 20-HETE formation rate in the kidney microsomes. This discrepancy could be attributed to an altered availability of the free arachidonic acid substrate in the kidney tissue, competition from other enzymatic pathways, and/or altered secondary metabolism of the formed 20-HETE. Interestingly, 20-HETE has been

shown to mediate cytotoxicity and apoptosis in ischemic kidney epithelial cells, and its inhibition protects the kidney from ischemia/reperfusion injury (Nilakantan, Maenpaa et al. 2008; Hoff, Lukitsch et al. 2011). Therefore, we can conclude that the induction of CYP4A enzymes and the subsequent increase in 20-HETE formation is a maladaptive response to DOX toxicity that will participate, at least in part, in the deterioration of the renal and hepatic function.

In conclusion, acute DOX toxicity alters the expression of several CYP and sEH enzymes in an organ-specific manner (Table 4.2). Although the exact mechanism is not fully elucidated yet, DOX-induced inflammation contributes, at least in part, to the alteration of CYP enzymes by DOX. The changes in CYP and sEH expression resulted in altered arachidonic acid metabolism as the 20-HETE formation was increased in both the kidney and the liver, whereas formation of EETs was increased only in the kidney. Taking into account the physiological functions of these metabolites, the increase in the formation of EETs and 20-HETE can be considered an adaptive and a maladaptive response, respectively.

Table 4.2 Effect of acute DOX toxicity on *CYP* and *EPHX2* gene expression 6 h after DOX administration

	Heart	Kidney	Liver
CYP1A1	↔	↔	↔
CYP1B1	↔	↔	↑
CYP2B1	↔	↔	↔
CYP2C11	↔	↔	↔
CYP2E1	↔	↔	↔
CYP2J3	↔	↔	↔
CYP4A1	↔	↔	↔
CYP4A3	↔	↔	↑
EPHX2	↑	↔	↑

Table 4.3 Effect of acute DOX toxicity on *CYP* and *EPHX2* gene expression 24 h after DOX administration

	Heart	Kidney	Liver
CYP1A1	↑	↔	↔
CYP1B1	↑	↑	↑
CYP2B1	↔	↓	↓
CYP2C11	↑	↓	↓
CYP2E1	↔	↑	↔
CYP2J3	↑	↔	↓
CYP4A1	↑	↑	↔
CYP4A3	↑	↑	↑
EPHX2	↑	↔	↔

4.7 General Conclusion

The prognosis of HF is still poor despite the advent of several new medications (Roger 2010). Therefore, research is still needed to increase our understanding of the pathogenesis of HF and its predisposing factors. Cardiac hypertrophy is an independent risk factor for HF; therefore, research into the molecular basis of hypertrophy can be considered as research into the initial steps of HF (Ritter and Neyses 2003). Drug-induced cardiotoxicity is another common cause of HF and DOX-induced cardiotoxicity is a well characterized example (Maxwell and Jenkins 2011). Therefore, this work has been focused on investigating the role of CYP enzymes and CYP-mediated arachidonic acid metabolism in cardiac hypertrophy and DOX-induced cardiotoxicity.

In the present work, we have demonstrated that isoproterenol-induced cardiac hypertrophy caused a significant induction of the *CYP1A1*, *CYP1B1*, and *CYP4A3* gene expression in the hypertrophied hearts. As these enzymes are considered CYP ω-hydroxylases, the formation of the cardiotoxic 20-HETE increased significantly in the microsomes of these hypertrophied hearts. On the other hand, there was a significant inhibition of *CYP2C11* and *CYP2E1* gene expression as well as a significant induction of *EPHX2*. These changes resulted in a significant decrease in the formation of the cardioprotective EETs. The increase in cardiotoxic 20-HETE and the decrease in the cardioprotective EETs represent maladaptive response to isoproterenol which may be involved, at least in part, in the development and/or progression of cardiac hypertrophy and subsequent HF.

In an attempt to dissect the cause-effect relationship between cardiac hypertrophy and induction of CYP ω-hydroxylases, we investigated whether the induction of CYP1A1 and CYP1B1 by AhR ligands can induce hypertrophy in the cardiac derived H9c2 cells. Interestingly, the two AhR ligands, TCDD and BNF, induced significant hypertrophy in H9c2 cells as manifested by the induction of the hypertrophic markers, ANP and BNP, as well as the significant increase of the cell surface area. The used concentrations of these AhR ligands were not enough to cause a significant increase in oxidative stress, but were able to induce the CYP enzymes. In addition, inhibition of CYP1A1 and CYP1B1 by the AhR antagonist, resveratrol, protected the cells from this hypertrophic response. Therefore, induction of CYP enzymes and subsequent alteration of arachidonic acid metabolism may be one of the mechanisms by which AhR ligands induce cardiac hypertrophy.

In order to address another model of HF, we investigated the effect of acute DOX toxicity on CYP expression and arachidonic acid metabolism in the heart of male SD rats. Interestingly, acute DOX toxicity caused a significant induction of CYP1A1, CYP1B1, CYP2C11, CYP2J3, CYP4A1, CYP4A3, CYP4F1, and CYP4F4 in the hearts of DOX-treated rats after 24 h of the drug administration. Of special interest, DOX treatment caused a significant induction of sEH as early as 6 h of the drug administration. Therefore, induction of sEH may be involved, at least in part, in the development of acute DOX cardiotoxicity. However, CYP induction was a result of acute DOX cardiotoxicity that may be involved in its progression to end-stage HF. The overall alteration of CYP and

sEH expression resulted in derailed CYP-mediated arachidonic acid metabolism with a significant increase in the cardiotoxic 20-HETE and a significant decrease in the cardioprotective EETs formation. In order to investigate whether therapeutic concentrations of DOX induce cardiac CYP and sEH, we treated H9c2 cells with increasing DOX concentrations at the micro-molar range. Similar to the *in vivo* data, lower DOX concentrations caused a significant induction of several CYP and sEH enzymes in the cardiac derived H9c2 cells.

In order to know whether the effect of DOX on CYP and sEH was specific to the heart, we investigated the effect of acute DOX toxicity on CYP and sEH expression as well as CYP-mediated arachidonic acid metabolism in the kidney and liver of male SD rats. Our results showed that acute DOX toxicity caused an induction of CYP1B1 and CYP4A enzymes and an inhibition of CYP2B1 and CYP2C11 in both the kidney and liver. CYP2E1 was induced and sEH was inhibited in the kidney only. In addition, DOX toxicity caused a significant increase in the EETs formation in the kidney and a significant increase in 20-HETE formation in both the kidney and the liver. In conclusion, acute DOX toxicity alters the expression of several CYP and sEH enzymes in an organ-specific manner.

4.8 Future Research Directions

The results of the present work have highlighted the role of CYP and sEH enzymes as well as CYP-mediated arachidonic acid metabolism in the pathogenesis of cardiac hypertrophy and DOX-induced cardiotoxicity as two predisposing conditions to HF. However, further studies need to be conducted in order to advance the results of this work into clinical practice.

(1) To investigate whether an sEH inhibitor and/or ω-hydroxylase inhibitor could prevent and/or treat isoproterenol-induced cardiac hypertrophy.

(2) To identify the mechanisms by which isoproterenol-induced cardiac hypertrophy causes these alterations in CYP and sEH expression.

(3) To investigate whether 20-HETE directly induces cardiac hypertrophy *in vivo* and *in vitro.*

(4) To investigate whether EETs directly protect against cardiac hypertrophy *in vivo* and *in vitro.*

(5) To identify which CYP isoform is more responsible for AhR ligands-induced cardiac hypertrophy.

(6) To investigate the effect of chronic DOX treatment on CYP and sEH expression and their associated arachidonic acid metabolites.

(7) To investigate whether an sEH inhibitor and/or ω-hydroxylase inhibitor could prevent and/or treat acute and chronic DOX-induced cardiotoxicity.

(8) To identify the mechanisms by which DOX-induced toxicity causes these alterations in CYP and sEH expression.

5. REFERENCES

Aaronaes, M., D. Atar, et al. (2007). "[Congestive heart failure--etiology and diagnostic procedures]." Tidsskr Nor Laegeforen **127**(2): 171-173.

Aboutabl, M. E. and A. O. El-Kadi (2007). "Constitutive expression and inducibility of CYP1A1 in the H9c2 rat cardiomyoblast cells." Toxicol In Vitro **21**(8): 1686-1691.

Aboutabl, M. E., B. N. Zordoky, et al. (2009). "3-methylcholanthrene and benzo(a)pyrene modulate cardiac cytochrome P450 gene expression and arachidonic acid metabolism in male Sprague Dawley rats." Br J Pharmacol **158**(7): 1808-1819.

Aboutabl, M. E., B. N. Zordoky, et al. (2011). "Inhibition of soluble epoxide hydrolase confers cardioprotection and prevents cardiac cytochrome P450 induction by benzo(a)pyrene." J Cardiovasc Pharmacol **57**(3): 273-281.

Ahmed, N. K., R. L. Felsted, et al. (1981). "Daunorubicin reduction mediated by aldehyde and ketone reductases." Xenobiotica **11**(2): 131-136.

Ai, D., Y. Fu, et al. (2007). "Angiotensin II up-regulates soluble epoxide hydrolase in vascular endothelium in vitro and in vivo." Proc Natl Acad Sci U S A **104**(21): 9018-9023.

Ai, D., W. Pang, et al. (2009). "Soluble epoxide hydrolase plays an essential role in angiotensin II-induced cardiac hypertrophy." Proc Natl Acad Sci U S A **106**(2): 564-569.

Alkayed, N. J., E. K. Birks, et al. (1996). "Inhibition of brain P-450 arachidonic acid epoxygenase decreases baseline cerebral blood flow." Am J Physiol **271**(4 Pt 2): H1541-1546.

Alkayed, N. J., E. K. Birks, et al. (1997). "Role of P-450 arachidonic acid epoxygenase in the response of cerebral blood flow to glutamate in rats." Stroke **28**(5): 1066-1072.

Alonso-Galicia, M., J. R. Falck, et al. (1999). "20-HETE agonists and antagonists in the renal circulation." Am J Physiol **277**(5 Pt 2): F790-796.

Anakk, S., A. Kalsotra, et al. (2004). "CAR/PXR provide directives for Cyp3a41 gene regulation differently from Cyp3a11." Pharmacogenomics J **4**(2): 91-101.

Anker, S. D., T. P. Chua, et al. (1997). "Hormonal changes and catabolic/anabolic imbalance in chronic heart failure and their importance for cardiac cachexia." Circulation **96**(2): 526-534.

Anwar-mohamed, A., B. N. Zordoky, et al. (2010). "Alteration of cardiac cytochrome P450-mediated arachidonic acid metabolism in response to lipopolysaccharide-induced acute systemic inflammation." Pharmacol Res **61**(5): 410-418.

Anzenbacher, P. and E. Anzenbacherova (2001). "Cytochromes P450 and metabolism of xenobiotics." Cell Mol Life Sci **58**(5-6): 737-747.

Aragon, A. C., M. B. Goens, et al. (2008). "Perinatal 2,3,7,8-tetrachlorodibenzo-p-dioxin exposure sensitizes offspring to angiotensin II-induced hypertension." Cardiovasc Toxicol **8**(3): 145-154.

Aragon, A. C., P. G. Kopf, et al. (2008). "In utero and lactational 2,3,7,8-tetrachlorodibenzo-p-dioxin exposure: effects on fetal and adult cardiac gene expression and adult cardiac and renal morphology." Toxicol Sci **101**(2): 321-330.

Aries, A., P. Paradis, et al. (2004). "Essential role of GATA-4 in cell survival and drug-induced cardiotoxicity." Proc Natl Acad Sci U S A **101**(18): 6975-6980.

Baes, M., T. Gulick, et al. (1994). "A new orphan member of the nuclear hormone receptor superfamily that interacts with a subset of retinoic acid response elements." Mol Cell Biol **14**(3): 1544-1552.

Baldwin, S. J., J. L. Bramhall, et al. (2006). "Cytochrome P450 gene induction in rats ex vivo assessed by quantitative real-time reverse transcriptase-polymerase chain reaction (TaqMan)." Drug Metab Dispos **34**(6): 1063-1069.

Bao, Y., X. Wang, et al. (2011). "20-Hydroxyeicosatetraenoic acid induces apoptosis in neonatal rat cardiomyocytes through mitochondrial-dependent pathways." J Cardiovasc Pharmacol **57**(3): 294-301.

Barakat, M. M., A. O. El-Kadi, et al. (2001). "L-NAME prevents in vivo the inactivation but not the down-regulation of hepatic cytochrome P450 caused by an acute inflammatory reaction." Life Sci **69**(13): 1559-1571.

Batchu, S. N., E. Law, et al. (2009). "Epoxyeicosatrienoic acid prevents postischemic electrocardiogram abnormalities in an isolated heart model." J Mol Cell Cardiol **46**(1): 67-74.

Beedanagari, S. R., I. Bebenek, et al. (2009). "Resveratrol inhibits dioxin-induced expression of human CYP1A1 and CYP1B1 by inhibiting recruitment of the aryl hydrocarbon receptor complex and RNA polymerase II to the regulatory regions of the corresponding genes." Toxicol Sci **110**(1): 61-67.

Beigneux, A. P., A. H. Moser, et al. (2002). "Reduction in cytochrome P-450 enzyme expression is associated with repression of CAR (constitutive androstane receptor) and PXR (pregnane X receptor) in mouse liver during the acute phase response." Biochem Biophys Res Commun **293**(1): 145-149.

Bernardo, B. C., K. L. Weeks, et al. (2010). "Molecular distinction between physiological and pathological cardiac hypertrophy: experimental findings and therapeutic strategies." Pharmacol Ther **128**(1): 191-227.

Berthiaume, J. M. and K. B. Wallace (2007). "Adriamycin-induced oxidative mitochondrial cardiotoxicity." Cell Biol Toxicol **23**(1): 15-25.

Bieche, I., C. Narjoz, et al. (2007). "Reverse transcriptase-PCR quantification of mRNA levels from cytochrome (CYP)1, CYP2 and CYP3 families in 22 different human tissues." Pharmacogenet Genomics **17**(9): 731-742.

Bisognano, J. D., H. D. Weinberger, et al. (2000). "Myocardial-directed overexpression of the human beta(1)-adrenergic receptor in transgenic mice." J Mol Cell Cardiol **32**(5): 817-830.

Bleicher, K. B., T. R. Pippert, et al. (2001). "Use of real-time gene-specific polymerase chain reaction to measure RNA expression of three family

members of rat cytochrome P450 4A." J Biochem Mol Toxicol **15**(3): 133-142.

Bogoyevitch, M. A., M. B. Andersson, et al. (1996). "Adrenergic receptor stimulation of the mitogen-activated protein kinase cascade and cardiac hypertrophy." Biochem J **314 (Pt 1)**: 115-121.

Borlak, J. and T. Thum (2002). "PCBs alter gene expression of nuclear transcription factors and other heart-specific genes in cultures of primary cardiomyocytes: possible implications for cardiotoxicity." Xenobiotica **32**(12): 1173-1183.

Braunwald, E. (1997). "Shattuck lecture--cardiovascular medicine at the turn of the millennium: triumphs, concerns, and opportunities." N Engl J Med **337**(19): 1360-1369.

Braunwald, E. and M. R. Bristow (2000). "Congestive heart failure: fifty years of progress." Circulation **102**(20 Suppl 4): IV14-23.

Brauze, D., M. Widerak, et al. (2006). "The effect of aryl hydrocarbon receptor ligands on the expression of AhR, AhRR, ARNT, Hif1alpha, CYP1A1 and NQO1 genes in rat liver." Toxicol Lett **167**(3): 212-220.

Bressolle, F., J. M. Jacquet, et al. (1992). "Doxorubicin and doxorubicinol plasma concentrations and excretion in parotid saliva." Cancer Chemother Pharmacol **30**(3): 215-218.

Bronchud, M. H., J. M. Margison, et al. (1990). "Comparative pharmacokinetics of escalating doses of doxorubicin in patients with metastatic breast cancer." Cancer Chemother Pharmacol **25**(6): 435-439.

Bueno, O. F., L. J. De Windt, et al. (2001). "The dual-specificity phosphatase MKP-1 limits the cardiac hypertrophic response in vitro and in vivo." Circ Res **88**(1): 88-96.

Bueno, O. F., L. J. De Windt, et al. (2000). "The MEK1-ERK1/2 signaling pathway promotes compensated cardiac hypertrophy in transgenic mice." EMBO J **19**(23): 6341-6350.

Bueno, O. F., B. J. Wilkins, et al. (2002). "Impaired cardiac hypertrophic response in Calcineurin Abeta -deficient mice." Proc Natl Acad Sci U S A **99**(7): 4586-4591.

Buja, L. M., V. J. Ferrans, et al. (1973). "Cardiac ultrastructural changes induced by daunorubicin therapy." Cancer **32**(4): 771-788.

Bulucu, F., R. Ocal, et al. (2009). "Effects of N-Acetylcysteine, Deferoxamine and Selenium on Doxorubicin-Induced Hepatotoxicity." Biol Trace Elem Res.

Bylund, J., M. Bylund, et al. (2001). "cDna cloning and expression of CYP4F12, a novel human cytochrome P450." Biochem Biophys Res Commun **280**(3): 892-897.

Campbell, W. B. (2000). "New role for epoxyeicosatrienoic acids as anti-inflammatory mediators." Trends Pharmacol Sci **21**(4): 125-127.

Campbell, W. B., C. Deeter, et al. (2002). "14,15-Dihydroxyeicosatrienoic acid relaxes bovine coronary arteries by activation of K(Ca) channels." Am J Physiol Heart Circ Physiol **282**(5): H1656-1664.

Canga, L., L. Paroli, et al. (1993). "2,3,7,8-tetrachlorodibenzo-p-dioxin increases cardiac myocyte intracellular calcium and progressively impairs ventricular contractile responses to isoproterenol and to calcium in chick embryo hearts." Mol Pharmacol **44**(6): 1142-1151.

Cao, Z. and Y. Li (2004). "Potent induction of cellular antioxidants and phase 2 enzymes by resveratrol in cardiomyocytes: protection against oxidative and electrophilic injury." Eur J Pharmacol **489**(1-2): 39-48.

Caron, E., N. Rioux, et al. (2005). "Quantification of the expression and inducibility of 12 rat cytochrome P450 isoforms by quantitative RT-PCR." J Biochem Mol Toxicol **19**(6): 368-378.

Carreno, J. E., F. Apablaza, et al. (2006). "[Cardiac hypertrophy: molecular and cellular events]." Rev Esp Cardiol **59**(5): 473-486.

Carroll, M. A., M. Schwartzman, et al. (1987). "Vasoactivity of arachidonic acid epoxides." Eur J Pharmacol **138**(2): 281-283.

Carver, L. A., J. B. Hogenesch, et al. (1994). "Tissue specific expression of the rat Ah-receptor and ARNT mRNAs." Nucleic Acids Res **22**(15): 3038-3044.

Catron, T., M. A. Mendiola, et al. (2001). "Hypoxia regulates avian cardiac Arnt and HIF-1alpha mRNA expression." Biochem Biophys Res Commun **282**(2): 602-607.

Celander, M. C., M. J. Moore, et al. (2000). "Cellular localization of CYP3A proteins in various tissues from pilot whale (Globicephala melas)." Environ Toxicol Pharmacol **8**(4): 245-253.

Certikova Chabova, V., A. Walkowska, et al. (2010). "Combined inhibition of 20-hydroxyeicosatetraenoic acid formation and of epoxyeicosatrienoic acids degradation attenuates hypertension and hypertension-induced end-organ damage in Ren-2 transgenic rats." Clin Sci (Lond) **118**(10): 617-632.

Chabova, V. C., H. J. Kramer, et al. (2007). "Effects of chronic cytochrome P-450 inhibition on the course of hypertension and end-organ damage in Ren-2 transgenic rats." Vascul Pharmacol **47**(2-3): 145-159.

Chaiswing, L., M. P. Cole, et al. (2004). "Oxidative damage precedes nitrative damage in adriamycin-induced cardiac mitochondrial injury." Toxicol Pathol **32**(5): 536-547.

Chan, A. Y., V. W. Dolinsky, et al. (2008). "Resveratrol inhibits cardiac hypertrophy via AMP-activated protein kinase and Akt." J Biol Chem **283**(35): 24194-24201.

Chen, C. J., W. Yu, et al. (2009). "Resveratrol protects cardiomyocytes from hypoxia-induced apoptosis through the SIRT1-FoxO1 pathway." Biochem Biophys Res Commun **378**(3): 389-393.

Chen, J. K., J. Capdevila, et al. (2001). "Cytochrome p450 epoxygenase metabolism of arachidonic acid inhibits apoptosis." Mol Cell Biol **21**(18): 6322-6331.

Chen, Q. M., V. C. Tu, et al. (2000). "Hydrogen peroxide dose dependent induction of cell death or hypertrophy in cardiomyocytes." Arch Biochem Biophys **373**(1): 242-248.

Chen, S., M. Garami, et al. (1999). "Doxorubicin selectively inhibits brain versus atrial natriuretic peptide gene expression in cultured neonatal rat myocytes." Hypertension **34**(6): 1223-1231.

Chesley, A., M. S. Lundberg, et al. (2000). "The beta(2)-adrenergic receptor delivers an antiapoptotic signal to cardiac myocytes through G(i)-dependent coupling to phosphatidylinositol 3'-kinase." Circ Res **87**(12): 1172-1179.

Childs, A. C., S. L. Phaneuf, et al. (2002). "Doxorubicin treatment in vivo causes cytochrome C release and cardiomyocyte apoptosis, as well as increased mitochondrial efficiency, superoxide dismutase activity, and Bcl-2:Bax ratio." Cancer Res **62**(16): 4592-4598.

Chiosi, E., A. Spina, et al. (2007). "Change in TNF-alpha receptor expression is a relevant event in doxorubicin-induced H9c2 cardiomyocyte cell death." J Interferon Cytokine Res **27**(7): 589-597.

Choudhary, D., I. Jansson, et al. (2003). "Comparative expression profiling of 40 mouse cytochrome P450 genes in embryonic and adult tissues." Arch Biochem Biophys **414**(1): 91-100.

Choudhary, D., I. Jansson, et al. (2004). "Metabolism of retinoids and arachidonic acid by human and mouse cytochrome P450 1b1." Drug Metab Dispos **32**(8): 840-847.

Choudhary, D., I. Jansson, et al. (2005). "Expression patterns of mouse and human CYP orthologs (families 1-4) during development and in different adult tissues." Arch Biochem Biophys **436**(1): 50-61.

Christiansen, S. and R. Autschbach (2006). "Doxorubicin in experimental and clinical heart failure." Eur J Cardiothorac Surg **30**(4): 611-616.

Chu, C. H., B. S. Tzang, et al. (2008). "IGF-II/mannose-6-phosphate receptor signaling induced cell hypertrophy and atrial natriuretic peptide/BNP expression via Galphaq interaction and protein kinase C-alpha/CaMKII activation in H9c2 cardiomyoblast cells." J Endocrinol **197**(2): 381-390.

Cigremis, Y., H. Parlakpinar, et al. (2006). "Beneficial role of aminoguanidine on acute cardiomyopathy related to doxorubicin-treatment." Mol Cell Biochem **285**(1-2): 149-154.

Clerk, A. and P. H. Sugden (2000). "Small guanine nucleotide-binding proteins and myocardial hypertrophy." Circ Res **86**(10): 1019-1023.

Cooper, B. W., T. M. Cho, et al. (2008). "Phthalate induction of CYP3A4 is dependent on glucocorticoid regulation of PXR expression." Toxicol Sci **103**(2): 268-277.

Coumoul, X., M. Diry, et al. (2002). "PXR-dependent induction of human CYP3A4 gene expression by organochlorine pesticides." Biochem Pharmacol **64**(10): 1513-1519.

Cowie, M. R., D. A. Wood, et al. (1999). "Incidence and aetiology of heart failure; a population-based study." Eur Heart J **20**(6): 421-428.

Cui, X., D. R. Nelson, et al. (2000). "A novel human cytochrome P450 4F isoform (CYP4F11): cDNA cloning, expression, and genomic structural characterization." Genomics **68**(2): 161-166.

Czekaj, P., A. Wiaderkiewicz, et al. (2000). "Expression of cytochrome CYP2B1/2 in nonpregnant, pregnant and fetal rats exposed to tobacco smoke." Acta Biochim Pol **47**(4): 1115-1127.

Danielson, P. B. (2002). "The cytochrome P450 superfamily: biochemistry, evolution and drug metabolism in humans." Curr Drug Metab **3**(6): 561-597.

Davis, B. B., D. A. Thompson, et al. (2002). "Inhibitors of soluble epoxide hydrolase attenuate vascular smooth muscle cell proliferation." Proc Natl Acad Sci U S A **99**(4): 2222-2227.

Deepa, P. R. and P. Varalakshmi (2005). "Biochemical evaluation of the inflammatory changes in cardiac, hepatic and renal tissues of adriamycin-administered rats and the modulatory role of exogenous heparin-derivative treatment." Chem Biol Interact **156**(2-3): 93-100.

Delozier, T. C., G. E. Kissling, et al. (2007). "Detection of Human CYP2C8, CYP2C9 and CYP2J2 in Cardiovascular Tissues." Drug Metab Dispos.

Deniaud, A., O. Sharaf el dein, et al. (2008). "Endoplasmic reticulum stress induces calcium-dependent permeability transition, mitochondrial outer membrane permeabilization and apoptosis." Oncogene **27**(3): 285-299.

Dhanasekaran, A., S. K. Gruenloh, et al. (2008). "Multiple antiapoptotic targets of the PI3K/Akt survival pathway are activated by epoxyeicosatrienoic acids to protect cardiomyocytes from hypoxia/anoxia." Am J Physiol Heart Circ Physiol **294**(2): H724-735.

Di Re, J., C. Lee, et al. (1999). "Lack of mechanism-based inactivation of rat hepatic microsomal cytochromes P450 by doxorubicin." Can J Physiol Pharmacol **77**(8): 589-597.

Diedrichs, H., J. Hagemeister, et al. (2007). "Activation of the calcineurin/NFAT signalling cascade starts early in human hypertrophic myocardium." J Int Med Res **35**(6): 803-818.

Ding, Y. S., J. S. Trommel, et al. (2005). "Determination of 14 polycyclic aromatic hydrocarbons in mainstream smoke from domestic cigarettes." Environ Sci Technol **39**(2): 471-478.

Dolinsky, V. W., A. Y. Chan, et al. (2009). "Resveratrol prevents the prohypertrophic effects of oxidative stress on LKB1." Circulation **119**(12): 1643-1652.

Dolwick, K. M., H. I. Swanson, et al. (1993). "In vitro analysis of Ah receptor domains involved in ligand-activated DNA recognition." Proc Natl Acad Sci U S A **90**(18): 8566-8570.

Doroshow, J. H. (1983). "Effect of anthracycline antibiotics on oxygen radical formation in rat heart." Cancer Res **43**(2): 460-472.

Doroshow, J. H., G. Y. Locker, et al. (1979). "The effect of doxorubicin on hepatic and cardiac glutathione." Res Commun Chem Pathol Pharmacol **26**(2): 285-295.

Dos Santos, E. A., A. J. Dahly-Vernon, et al. (2004). "Inhibition of the formation of EETs and 20-HETE with 1-aminobenzotriazole attenuates pressure natriuresis." Am J Physiol Regul Integr Comp Physiol **287**(1): R58-68.

Dube, P. and K. T. Weber (2011). "Congestive heart failure: pathophysiologic consequences of neurohormonal activation and the potential for recovery: part I." Am J Med Sci **342**(5): 348-351.

Dubey, R. K., D. G. Gillespie, et al. (2003). "CYP450- and COMT-derived estradiol metabolites inhibit activity of human coronary artery SMCs." Hypertension **41**(3 Pt 2): 807-813.

Dubey, R. K., E. K. Jackson, et al. (2005). "Cytochromes 1A1/1B1- and catechol-O-methyltransferase-derived metabolites mediate estradiol-induced antimitogenesis in human cardiac fibroblast." J Clin Endocrinol Metab **90**(1): 247-255.

Dyck, J. R. and G. D. Lopaschuk (2006). "AMPK alterations in cardiac physiology and pathology: enemy or ally?" J Physiol **574**(Pt 1): 95-112.

El-Sankary, W., V. Bombail, et al. (2002). "Glucocorticoid-mediated induction of CYP3A4 is decreased by disruption of a protein: DNA interaction distinct from the pregnane X receptor response element." Drug Metab Dispos **30**(9): 1029-1034.

Elbekai, R. H. and A. O. El-Kadi (2006). "Cytochrome P450 enzymes: central players in cardiovascular health and disease." Pharmacol Ther **112**(2): 564-587.

Elbekai, R. H., H. M. Korashy, et al. (2004). "Benzo[a]pyrene, 3-methylcholanthrene and beta-naphthoflavone induce oxidative stress in hepatoma hepa 1c1c7 Cells by an AHR-dependent pathway." Free Radic Res **38**(11): 1191-1200.

Elkiran, T., H. Harputluoglu, et al. (2007). "Differential alteration of drug-metabolizing enzyme activities after cyclophosphamide/adriamycin administration in breast cancer patients." Methods Find Exp Clin Pharmacol **29**(1): 27-32.

Enayetallah, A. E., R. A. French, et al. (2006). "Cell-specific subcellular localization of soluble epoxide hydrolase in human tissues." J Histochem Cytochem **54**(3): 329-335.

Enayetallah, A. E., R. A. French, et al. (2004). "Distribution of soluble epoxide hydrolase and of cytochrome P450 2C8, 2C9, and 2J2 in human tissues." J Histochem Cytochem **52**(4): 447-454.

Fagard, R. H. (1997). "Impact of different sports and training on cardiac structure and function." Cardiol Clin **15**(3): 397-412.

Ferguson, S. S., E. L. LeCluyse, et al. (2002). "Regulation of human CYP2C9 by the constitutive androstane receptor: discovery of a new distal binding site." Mol Pharmacol **62**(3): 737-746.

Fiebeler, A. and H. Haller (2003). "Participation of the mineralocorticoid receptor in cardiac and vascular remodeling." Nephron Physiol **94**(3): p47-50.

Fingar, D. C., S. Salama, et al. (2002). "Mammalian cell size is controlled by mTOR and its downstream targets S6K1 and 4EBP1/eIF4E." Genes Dev **16**(12): 1472-1487.

Fleming, I. (2005). "Cytochrome P-450 under pressure: more evidence for a link between 20-hydroxyeicosatetraenoic acid and hypertension." Circulation **111**(1): 5-7.

Fox, K. F., M. R. Cowie, et al. (2001). "Coronary artery disease as the cause of incident heart failure in the population." Eur Heart J **22**(3): 228-236.

Frantz, S., D. Fraccarollo, et al. (2003). "Sustained activation of nuclear factor kappa B and activator protein 1 in chronic heart failure." Cardiovasc Res **57**(3): 749-756.

Frey, N. and E. N. Olson (2003). "Cardiac hypertrophy: the good, the bad, and the ugly." Annu Rev Physiol **65**: 45-79.

Fulton, D., K. Mahboubi, et al. (1995). "Cytochrome P450-dependent effects of bradykinin in the rat heart." Br J Pharmacol **114**(1): 99-102.

Funder, J. W. (2006). "Mineralocorticoid receptors and cardiovascular damage: it's not just aldosterone." Hypertension **47**(4): 634-635.

Gebremedhin, D., D. R. Harder, et al. (1998). "Bioassay of an endothelium-derived hyperpolarizing factor from bovine coronary arteries: role of a cytochrome P450 metabolite." J Vasc Res **35**(4): 274-284.

Gebremedhin, D., A. R. Lange, et al. (2000). "Production of 20-HETE and its role in autoregulation of cerebral blood flow." Circ Res **87**(1): 60-65.

Gebremedhin, D., Y. H. Ma, et al. (1992). "Mechanism of action of cerebral epoxyeicosatrienoic acids on cerebral arterial smooth muscle." Am J Physiol **263**(2 Pt 2): H519-525.

Geetha, A., T. Marar, et al. (1991). "Effect of alpha-tocopherol on doxorubicin-induced changes in rat liver and heart microsomes." Indian J Exp Biol **29**(8): 782-785.

Gellner, K., R. Eiselt, et al. (2001). "Genomic organization of the human CYP3A locus: identification of a new, inducible CYP3A gene." Pharmacogenetics **11**(2): 111-121.

Gerbal-Chaloin, S., M. Daujat, et al. (2002). "Transcriptional regulation of CYP2C9 gene. Role of glucocorticoid receptor and constitutive androstane receptor." J Biol Chem **277**(1): 209-217.

Gerdes, A. M. (2002). "Cardiac myocyte remodeling in hypertrophy and progression to failure." J Card Fail **8**(6 Suppl): S264-268.

Gharavi, N. and A. O. El-Kadi (2005). "tert-Butylhydroquinone is a novel aryl hydrocarbon receptor ligand." Drug Metab Dispos **33**(3): 365-372.

Ghosh, S., M. J. May, et al. (1998). "NF-kappa B and Rel proteins: evolutionarily conserved mediators of immune responses." Annu Rev Immunol **16**: 225-260.

Gonzalez, F. J. and D. W. Nebert (1990). "Evolution of the P450 gene superfamily: animal-plant 'warfare', molecular drive and human genetic differences in drug oxidation." Trends Genet **6**(6): 182-186.

Goodwin, B., E. Hodgson, et al. (2002). "Transcriptional regulation of the human CYP3A4 gene by the constitutive androstane receptor." Mol Pharmacol **62**(2): 359-365.

Gottlieb, R. A. (2003). "Cytochrome P450: major player in reperfusion injury." Arch Biochem Biophys **420**(2): 262-267.

Gradman, A. H. and F. Alfayoumi (2006). "From left ventricular hypertrophy to congestive heart failure: management of hypertensive heart disease." Prog Cardiovasc Dis **48**(5): 326-341.

Granberg, A. L., B. Brunstrom, et al. (2000). "Cytochrome P450-dependent binding of 7,12-dimethylbenz[a]anthracene (DMBA) and benzo[a]pyrene (B[a]P) in murine heart, lung, and liver endothelial cells." Arch Toxicol **74**(10): 593-601.

Gross, G. J., K. M. Gauthier, et al. (2008). "Effects of the selective EET antagonist, 14,15-EEZE, on cardioprotection produced by exogenous or endogenous EETs in the canine heart." Am J Physiol Heart Circ Physiol **294**(6): H2838-2844.

Guengerich, F. P. (1997). "Comparisons of catalytic selectivity of cytochrome P450 subfamily enzymes from different species." Chem Biol Interact **106**(3): 161-182.

Guengerich, F. P. (2003). "Cytochromes P450, drugs, and diseases." Mol Interv **3**(4): 194-204.

Guengerich, F. P. (2006). "Cytochrome P450s and other enzymes in drug metabolism and toxicity." Aaps J **8**(1): E101-111.

Guijarro, C. and J. Egido (2001). "Transcription factor-kappa B (NF-kappa B) and renal disease." Kidney Int **59**(2): 415-424.

Gupta, S., N. H. Purcell, et al. (2002). "Activation of nuclear factor-kappaB is necessary for myotrophin-induced cardiac hypertrophy." J Cell Biol **159**(6): 1019-1028.

Gustafson, D. L., J. C. Rastatter, et al. (2002). "Doxorubicin pharmacokinetics: Macromolecule binding, metabolism, and excretion in the context of a physiologic model." J Pharm Sci **91**(6): 1488-1501.

Gustafsson, A. B. and R. A. Gottlieb (2008). "Heart mitochondria: gates of life and death." Cardiovasc Res **77**(2): 334-343.

Hahn, M. E. (2002). "Aryl hydrocarbon receptors: diversity and evolution." Chem Biol Interact **141**(1-2): 131-160.

Hakkak, R., S. Korourian, et al. (1996). "Effects of diet and ethanol on the expression and localization of cytochromes P450 2E1 and P450 2C7 in the colon of male rats." Biochem Pharmacol **51**(1): 61-69.

Harder, D. R., N. J. Alkayed, et al. (1998). "Functional hyperemia in the brain: hypothesis for astrocyte-derived vasodilator metabolites." Stroke **29**(1): 229-234.

Harder, D. R., D. Gebremedhin, et al. (1994). "Formation and action of a P-450 4A metabolite of arachidonic acid in cat cerebral microvessels." Am J Physiol **266**(5 Pt 2): H2098-2107.

Harris, R. C., K. A. Munger, et al. (1990). "Mediation of renal vascular effects of epidermal growth factor by arachidonate metabolites." Faseb J **4**(6): 1654-1660.

Hecker, M., A. T. Bara, et al. (1994). "Characterization of endothelium-derived hyperpolarizing factor as a cytochrome P450-derived arachidonic acid metabolite in mammals." J Physiol **481 (Pt 2)**: 407-414.

Heid, S. E., M. K. Walker, et al. (2001). "Correlation of cardiotoxicity mediated by halogenated aromatic hydrocarbons to aryl hydrocarbon receptor activation." Toxicol Sci **61**(1): 187-196.

Hescheler, J., R. Meyer, et al. (1991). "Morphological, biochemical, and electrophysiological characterization of a clonal cell (H9c2) line from rat heart." Circ Res **69**(6): 1476-1486.

Hidestrand, M., M. Oscarson, et al. (2001). "CYP2B6 and CYP2C19 as the major enzymes responsible for the metabolism of selegiline, a drug used in the treatment of Parkinson's disease, as revealed from experiments with recombinant enzymes." Drug Metab Dispos **29**(11): 1480-1484.

Higuchi, Y., K. Otsu, et al. (2002). "Involvement of reactive oxygen species-mediated NF-kappa B activation in TNF-alpha-induced cardiomyocyte hypertrophy." J Mol Cell Cardiol **34**(2): 233-240.

Hill, E., F. Fitzpatrick, et al. (1992). "Biological activity and metabolism of 20-hydroxyeicosatetraenoic acid in the human platelet." Br J Pharmacol **106**(2): 267-274.

Hingtgen, S. D., X. Tian, et al. (2006). "Nox2-containing NADPH oxidase and Akt activation play a key role in angiotensin II-induced cardiomyocyte hypertrophy." Physiol Genomics **26**(3): 180-191.

Hirasawa, F., M. Kawagoe, et al. (2005). "Styrene monomer primarily induces CYP2B1 mRNA in rat liver." Xenobiotica **35**(12): 1089-1099.

Hiroi, T., S. Imaoka, et al. (1998). "Tissue distributions of CYP2D1, 2D2, 2D3 and 2D4 mRNA in rats detected by RT-PCR." Biochim Biophys Acta **1380**(3): 305-312.

Hirota, H., J. Chen, et al. (1999). "Loss of a gp130 cardiac muscle cell survival pathway is a critical event in the onset of heart failure during biomechanical stress." Cell **97**(2): 189-198.

Hirotani, S., K. Otsu, et al. (2002). "Involvement of nuclear factor-kappaB and apoptosis signal-regulating kinase 1 in G-protein-coupled receptor agonist-induced cardiomyocyte hypertrophy." Circulation **105**(4): 509-515.

Ho, Y. L., C. C. Wu, et al. (1998). "Assessment of the coronary artery disease and systolic dysfunction in hypertensive patients with the dobutamine-atropine stress echocardiography: effect of the left ventricular hypertrophy." Cardiology **89**(1): 52-58.

Hoff, U., I. Lukitsch, et al. (2011). "Inhibition of 20-HETE synthesis and action protects the kidney from ischemia/reperfusion injury." Kidney Int **79**(1): 57-65.

Huang, T. H., L. He, et al. (2007). "Salacia oblonga root decreases cardiac hypertrophy in Zucker diabetic fatty rats: inhibition of cardiac expression of angiotensin II type 1 receptor." Diabetes Obes Metab.

Huang, T. H., L. He, et al. (2008). "Salacia oblonga root decreases cardiac hypertrophy in Zucker diabetic fatty rats: inhibition of cardiac expression of angiotensin II type 1 receptor." Diabetes Obes Metab **10**(7): 574-585.

Hunt, S. A., W. T. Abraham, et al. (2005). "ACC/AHA 2005 Guideline Update for the Diagnosis and Management of Chronic Heart Failure in the Adult: a report of the American College of Cardiology/American Heart Association Task Force on Practice Guidelines (Writing Committee to Update the 2001 Guidelines for the Evaluation and Management of Heart Failure): developed in collaboration with the American College of Chest

Physicians and the International Society for Heart and Lung Transplantation: endorsed by the Heart Rhythm Society." Circulation **112**(12): e154-235.

Huss, J. M., S. I. Wang, et al. (1996). "Dexamethasone responsiveness of a major glucocorticoid-inducible CYP3A gene is mediated by elements unrelated to a glucocorticoid receptor binding motif." Proc Natl Acad Sci U S A **93**(10): 4666-4670.

Hydock, D. S., C. Y. Lien, et al. (2007). "Effects of voluntary wheel running on cardiac function and myosin heavy chain in chemically gonadectomized rats." Am J Physiol Heart Circ Physiol **293**(6): H3254-3264.

Iber, H., T. Li-Masters, et al. (2001). "Regulation of hepatic cytochrome P450 2C11 via cAMP: implications for down-regulation in diabetes, fasting, and inflammation." J Pharmacol Exp Ther **297**(1): 174-180.

Iber, H., M. B. Sewer, et al. (1999). "Modulation of drug metabolism in infectious and inflammatory diseases." Drug Metab Rev **31**(1): 29-41.

Imaoka, S., T. Hashizume, et al. (2005). "Localization of rat cytochrome P450 in various tissues and comparison of arachidonic acid metabolism by rat P450 with that by human P450 orthologs." Drug Metab Pharmacokinet **20**(6): 478-484.

Imaoka, S., T. Yamada, et al. (1996). "Multiple forms of human P450 expressed in Saccharomyces cerevisiae. Systematic characterization and comparison with those of the rat." Biochem Pharmacol **51**(8): 1041-1050.

Imig, J. D. (2000). "Epoxygenase metabolites. Epithelial and vascular actions." Mol Biotechnol **16**(3): 233-251.

Imig, J. D. (2005). "Epoxide hydrolase and epoxygenase metabolites as therapeutic targets for renal diseases." Am J Physiol Renal Physiol **289**(3): F496-503.

Imig, J. D. and B. D. Hammock (2009). "Soluble epoxide hydrolase as a therapeutic target for cardiovascular diseases." Nat Rev Drug Discov **8**(10): 794-805.

Imig, J. D., L. G. Navar, et al. (1996). "Actions of epoxygenase metabolites on the preglomerular vasculature." J Am Soc Nephrol **7**(11): 2364-2370.

Imig, J. D., X. Zhao, et al. (2002). "Soluble epoxide hydrolase inhibition lowers arterial blood pressure in angiotensin II hypertension." Hypertension **39**(2 Pt 2): 690-694.

Imig, J. D., A. P. Zou, et al. (1996). "Formation and actions of 20-hydroxyeicosatetraenoic acid in rat renal arterioles." Am J Physiol **270**(1 Pt 2): R217-227.

Injac, R., M. Boskovic, et al. (2008). "Acute doxorubicin nephrotoxicity in rats with malignant neoplasm can be successfully treated with fullerenol C60(OH)24 via suppression of oxidative stress." Pharmacol Rep **60**(5): 742-749.

Inouye, K. and T. Sakaki (2001). "Enzymatic studies on the key enzymes of vitamin D metabolism; 1 alpha-hydroxylase (CYP27B1) and 24-hydroxylase (CYP24)." Biotechnol Annu Rev **7**: 179-194.

Iqbal, M., K. Dubey, et al. (2008). "Protective effects of telmisartan against acute doxorubicin-induced cardiotoxicity in rats." Pharmacol Rep **60**(3): 382-390.

Ishida, H., Y. Kuruta, et al. (1999). "Structure, evolution, and liver-specific expression of sterol 12alpha-hydroxylase P450 (CYP8B)." J Biochem **126**(1): 19-25.

Ishizuka, T., J. Cheng, et al. (2008). "20-Hydroxyeicosatetraenoic acid stimulates nuclear factor-kappaB activation and the production of inflammatory cytokines in human endothelial cells." J Pharmacol Exp Ther **324**(1): 103-110.

Ito, H., S. C. Miller, et al. (1990). "Doxorubicin selectively inhibits muscle gene expression in cardiac muscle cells in vivo and in vitro." Proc Natl Acad Sci U S A **87**(11): 4275-4279.

Ito, T., T. Suzuki, et al. (2008). "Examination of mRNA expression in rat hearts and lungs for analysis of effects of exposure to concentrated ambient particles on cardiovascular function." Toxicology **243**(3): 271-283.

Jenkins, C. M., A. Cedars, et al. (2009). "Eicosanoid signalling pathways in the heart." Cardiovasc Res **82**(2): 240-249.

Jiang, H., J. C. McGiff, et al. (2004). "Identification of 5,6-trans-epoxyeicosatrienoic acid in the phospholipids of red blood cells." J Biol Chem **279**(35): 36412-36418.

Jiang, J. G., Y. G. Ning, et al. (2007). "Cytochrome p450 epoxygenase promotes human cancer metastasis." Cancer Res **67**(14): 6665-6674.

Kalsotra, A., S. Anakk, et al. (2002). "Sexual dimorphism and tissue specificity in the expression of CYP4F forms in Sprague Dawley rats." Drug Metab Dispos **30**(9): 1022-1028.

Kalyankrishna, S. and K. U. Malik (2003). "Norepinephrine-induced stimulation of p38 mitogen-activated protein kinase is mediated by arachidonic acid metabolites generated by activation of cytosolic phospholipase A(2) in vascular smooth muscle cells." J Pharmacol Exp Ther **304**(2): 761-772.

Kanzawa, N., M. Kondo, et al. (2004). "Biochemical and molecular biological analysis of different responses to 2,3,7,8-tetrachlorodibenzo-p-dioxin in chick embryo heart and liver." Arch Biochem Biophys **427**(1): 58-67.

Karara, A., E. Dishman, et al. (1991). "Endogenous epoxyeicosatrienoyl-phospholipids. A novel class of cellular glycerolipids containing epoxidized arachidonate moieties." J Biol Chem **266**(12): 7561-7569.

Ke, Q., Y. F. Xiao, et al. (2007). "Electrophysiological properties of cardiomyocytes isolated from CYP2J2 transgenic mice." Mol Pharmacol **72**(4): 1063-1073.

Keseru, B., E. Barbosa-Sicard, et al. (2008). "Epoxyeicosatrienoic acids and the soluble epoxide hydrolase are determinants of pulmonary artery pressure and the acute hypoxic pulmonary vasoconstrictor response." Faseb J **22**(12): 4306-4315.

Khan, S. A. and J. P. Vanden Heuvel (2003). "Role of nuclear receptors in the regulation of gene expression by dietary fatty acids (review)." J Nutr Biochem **14**(10): 554-567.

Kim, D. H. and S. A. Hunt (2003). "Heart failure management: caregiver versus care plan." Circulation **108**(2): 129-131.

Kim, S. Y., S. J. Kim, et al. (2006). "Doxorubicin-induced reactive oxygen species generation and intracellular Ca2+ increase are reciprocally modulated in rat cardiomyocytes." Exp Mol Med **38**(5): 535-545.

Kim, Y., A. G. Ma, et al. (2003). "Anthracycline-induced suppression of GATA-4 transcription factor: implication in the regulation of cardiac myocyte apoptosis." Mol Pharmacol **63**(2): 368-377.

Kimes, B. W. and B. L. Brandt (1976). "Properties of a clonal muscle cell line from rat heart." Exp Cell Res **98**(2): 367-381.

Kiriazis, H., K. Wang, et al. (2008). "Knockout of beta(1)- and beta(2)-adrenoceptors attenuates pressure overload-induced cardiac hypertrophy and fibrosis." Br J Pharmacol **153**(4): 684-692.

Kobayashi, S., P. Volden, et al. (2010). "Transcription factor GATA4 inhibits doxorubicin-induced autophagy and cardiomyocyte death." J Biol Chem **285**(1): 793-804.

Kopf, P. G., J. K. Huwe, et al. (2008). "Hypertension, cardiac hypertrophy, and impaired vascular relaxation induced by 2,3,7,8-tetrachlorodibenzo-p-dioxin are associated with increased superoxide." Cardiovasc Toxicol **8**(4): 181-193.

Korashy, H. M. and A. O. El-Kadi (2004). "Differential effects of mercury, lead and copper on the constitutive and inducible expression of aryl hydrocarbon receptor (AHR)-regulated genes in cultured hepatoma Hepa 1c1c7 cells." Toxicology **201**(1-3): 153-172.

Korashy, H. M. and A. O. El-Kadi (2006). "The role of aryl hydrocarbon receptor and the reactive oxygen species in the modulation of glutathione transferase by heavy metals in murine hepatoma cell lines." Chem Biol Interact **162**(3): 237-248.

Korashy, H. M. and A. O. El-Kadi (2006). "The role of aryl hydrocarbon receptor in the pathogenesis of cardiovascular diseases." Drug Metab Rev **38**(3): 411-450.

Koskela, S., J. Hakkola, et al. (1999). "Expression of CYP2A genes in human liver and extrahepatic tissues." Biochem Pharmacol **57**(12): 1407-1413.

Kralova, E., T. Mokran, et al. (2008). "Electrocardiography in two models of isoproterenol-induced left ventricular remodelling." Physiol Res.

Kroetz, D. L. and F. Xu (2005). "Regulation and inhibition of arachidonic acid omega-hydroxylases and 20-HETE formation." Annu Rev Pharmacol Toxicol **45**: 413-438.

Kroetz, D. L., P. Yook, et al. (1998). "Peroxisome proliferator-activated receptor alpha controls the hepatic CYP4A induction adaptive response to starvation and diabetes." J Biol Chem **273**(47): 31581-31589.

Kroetz, D. L. and D. C. Zeldin (2002). "Cytochrome P450 pathways of arachidonic acid metabolism." Curr Opin Lipidol **13**(3): 273-283.

Krotz, F., T. Riexinger, et al. (2004). "Membrane-potential-dependent inhibition of platelet adhesion to endothelial cells by epoxyeicosatrienoic acids." Arterioscler Thromb Vasc Biol **24**(3): 595-600.

Kumar, A., Y. Takada, et al. (2004). "Nuclear factor-kappaB: its role in health and disease." J Mol Med **82**(7): 434-448.

Kunert, M. P., R. J. Roman, et al. (2001). "Cytochrome P-450 omega-hydroxylase: a potential O(2) sensor in rat arterioles and skeletal muscle cells." Am J Physiol Heart Circ Physiol **280**(4): H1840-1845.

Kunisada, K., S. Negoro, et al. (2000). "Signal transducer and activator of transcription 3 in the heart transduces not only a hypertrophic signal but a protective signal against doxorubicin-induced cardiomyopathy." Proc Natl Acad Sci U S A **97**(1): 315-319.

Kunisada, K., E. Tone, et al. (1998). "Activation of gp130 transduces hypertrophic signals via STAT3 in cardiac myocytes." Circulation **98**(4): 346-352.

Ladas, E. J., J. S. Jacobson, et al. (2004). "Antioxidants and cancer therapy: a systematic review." J Clin Oncol **22**(3): 517-528.

Laethem, R. M., M. Balazy, et al. (1993). "Formation of 19(S)-, 19(R)-, and 18(R)-hydroxyeicosatetraenoic acids by alcohol-inducible cytochrome P450 2E1." J Biol Chem **268**(17): 12912-12918.

Laethem, R. M., J. R. Halpert, et al. (1994). "Epoxidation of arachidonic acid as an active-site probe of cytochrome P-450 2B isoforms." Biochim Biophys Acta **1206**(1): 42-48.

Lamba, J. K., V. Lamba, et al. (2004). "Expression of constitutive androstane receptor splice variants in human tissues and their functional consequences." J Pharmacol Exp Ther **311**(2): 811-821.

Lambe, K. G. and J. D. Tugwood (1996). "A human peroxisome-proliferator-activated receptor-gamma is activated by inducers of adipogenesis, including thiazolidinedione drugs." Eur J Biochem **239**(1): 1-7.

Larsen, B. T., W. B. Campbell, et al. (2007). "Beyond vasodilatation: non-vasomotor roles of epoxyeicosatrienoic acids in the cardiovascular system." Trends Pharmacol Sci **28**(1): 32-38.

Lebrecht, D. and U. A. Walker (2007). "Role of mtDNA lesions in anthracycline cardiotoxicity." Cardiovasc Toxicol **7**(2): 108-113.

Lee, H. C., T. Lu, et al. (1999). "Effects of epoxyeicosatrienoic acids on the cardiac sodium channels in isolated rat ventricular myocytes." J Physiol **519 Pt 1**: 153-168.

Lee, S. J., C. S. Landon, et al. (2004). "Cytochrome P-450 metabolites in endothelin-stimulated cardiac hormone secretion." Am J Physiol Regul Integr Comp Physiol **286**(5): R888-893.

Lehmann, J. M., S. A. Kliewer, et al. (1997). "Activation of the nuclear receptor LXR by oxysterols defines a new hormone response pathway." J Biol Chem **272**(6): 3137-3140.

Levick, S. P., D. C. Loch, et al. (2007). "Arachidonic acid metabolism as a potential mediator of cardiac fibrosis associated with inflammation." J Immunol **178**(2): 641-646.

Levy, D., S. B. Labib, et al. (1990). "Determinants of sensitivity and specificity of electrocardiographic criteria for left ventricular hypertrophy." Circulation **81**(3): 815-820.

Lewis, D. F. (2003). "Human cytochromes P450 associated with the phase 1 metabolism of drugs and other xenobiotics: a compilation of substrates and inhibitors of the CYP1, CYP2 and CYP3 families." Curr Med Chem **10**(19): 1955-1972.

Lewis, D. F. (2004). "57 varieties: the human cytochromes P450." Pharmacogenomics **5**(3): 305-318.

Li-Masters, T. and E. T. Morgan (2001). "Effects of bacterial lipopolysaccharide on phenobarbital-induced CYP2B expression in mice." Drug Metab Dispos **29**(3): 252-257.

Li, H., A. Rao, et al. (2011). "Interaction of calcineurin with substrates and targeting proteins." Trends Cell Biol **21**(2): 91-103.

Li, J., M. A. Carroll, et al. (2008). "Soluble epoxide hydrolase inhibitor, AUDA, prevents early salt-sensitive hypertension." Front Biosci **13**: 3480-3487.

Li, S., M. E, et al. (2008). "Adriamycin induces myocardium apoptosis through activation of nuclear factor kappaB in rat." Mol Biol Rep **35**(4): 489-494.

Li, T., I. Danelisen, et al. (2002). "Early changes in myocardial antioxidant enzymes in rats treated with adriamycin." Mol Cell Biochem **232**(1-2): 19-26.

Li, Y., T. Ha, et al. (2004). "NF-kappaB activation is required for the development of cardiac hypertrophy in vivo." Am J Physiol Heart Circ Physiol **287**(4): H1712-1720.

Liang, F. and D. G. Gardner (1999). "Mechanical strain activates BNP gene transcription through a p38/NF-kappaB-dependent mechanism." J Clin Invest **104**(11): 1603-1612.

Lieber, C. S. (1997). "Cytochrome P-4502E1: its physiological and pathological role." Physiol Rev **77**(2): 517-544.

Liu, C. J., Y. C. Cheng, et al. (2008). "Lipopolysaccharide induces cellular hypertrophy through calcineurin/NFAT-3 signaling pathway in H9c2 myocardiac cells." Mol Cell Biochem **313**(1-2): 167-178.

Liu, J., W. Mao, et al. (2008). "ERKs/p53 signal transduction pathway is involved in doxorubicin-induced apoptosis in H9c2 cells and cardiomyocytes." Am J Physiol Heart Circ Physiol **295**(5): H1956-1965.

Liu, L. L., Q. X. Li, et al. (2007). "Differential effects of dihydropyridine calcium antagonists on doxorubicin-induced nephrotoxicity in rats." Toxicology **231**(1): 81-90.

Livak, K. J. and T. D. Schmittgen (2001). "Analysis of relative gene expression data using real-time quantitative PCR and the 2(-Delta Delta C(T)) Method." Methods **25**(4): 402-408.

Loch, D., A. Hoey, et al. (2007). "Prevention of hypertension in DOCA-salt rats by an inhibitor of soluble epoxide hydrolase." Cell Biochem Biophys **47**(1): 87-98.

Lou, H., I. Danelisen, et al. (2005). "Involvement of mitogen-activated protein kinases in adriamycin-induced cardiomyopathy." Am J Physiol Heart Circ Physiol **288**(4): H1925-1930.

Lowry, O. H., N. J. Rosebrough, et al. (1951). "Protein measurement with the Folin phenol reagent." J Biol Chem **193**(1): 265-275.

Lu, T., H. C. Lee, et al. (1999). "Modulation of rat cardiac sodium channel by the stimulatory G protein alpha subunit." J Physiol **518 (Pt 2)**: 371-384.

Lu, T., D. Ye, et al. (2006). "Cardiac and vascular KATP channels in rats are activated by endogenous epoxyeicosatrienoic acids through different mechanisms." J Physiol **575**(Pt 2): 627-644.

Luedde, M., H. A. Katus, et al. (2006). "Novel molecular targets in the treatment of cardiac hypertrophy." Recent Pat Cardiovasc Drug Discov **1**(1): 1-20.

Lv, X., J. Wan, et al. (2008). "Cytochrome P450 omega-hydroxylase inhibition reduces cardiomyocyte apoptosis via activation of ERK1/2 signaling in rat myocardial ischemia-reperfusion." Eur J Pharmacol **596**(1-3): 118-126.

Maejima, Y., S. Adachi, et al. (2008). "Induction of premature senescence in cardiomyocytes by doxorubicin as a novel mechanism of myocardial damage." Aging Cell **7**(2): 125-136.

Magga, J., O. Vuolteenaho, et al. (1998). "B-type natriuretic peptide: a myocyte-specific marker for characterizing load-induced alterations in cardiac gene expression." Ann Med **30 Suppl 1**: 39-45.

Maier, K. G. and R. J. Roman (2001). "Cytochrome P450 metabolites of arachidonic acid in the control of renal function." Curr Opin Nephrol Hypertens **10**(1): 81-87.

Malaplate-Armand, C., L. Ferrari, et al. (2003). "Astroglial CYP1B1 up-regulation in inflammatory/oxidative toxic conditions: IL-1beta effect and protection by N-acetylcysteine." Toxicol Lett **138**(3): 243-251.

Mangelsdorf, D. J. and R. M. Evans (1995). "The RXR heterodimers and orphan receptors." Cell **83**(6): 841-850.

Mansur, S. J., F. G. Hage, et al. (2010). "Have the renin-angiotensin-aldosterone system perturbations in cardiovascular disease been exhausted?" Curr Cardiol Rep **12**(6): 450-463.

Marchand, D. J. and K. W. Renton (1981). "Depression of cytochrome P-450-dependent drug biotransformation by adriamycin." Toxicol Appl Pharmacol **58**(1): 83-88.

Maresh, J. G., H. Xu, et al. (2005). "Tobacco smoke dysregulates endothelial vasoregulatory transcripts in vivo." Physiol Genomics **21**(3): 308-313.

Martinez-Jimenez, C. P., R. Jover, et al. (2007). "Transcriptional regulation and expression of CYP3A4 in hepatocytes." Curr Drug Metab **8**(2): 185-194.

Maslov, M. Y., V. P. Chacko, et al. (2010). "Reduced in vivo high-energy phosphates precede adriamycin-induced cardiac dysfunction." Am J Physiol Heart Circ Physiol **299**(2): H332-337.

Masson, S., B. Arosio, et al. (1998). "Remodelling of cardiac extracellular matrix during beta-adrenergic stimulation: upregulation of SPARC in the myocardium of adult rats." J Mol Cell Cardiol **30**(8): 1505-1514.

Maxwell, C. B. and A. T. Jenkins (2011). "Drug-induced heart failure." Am J Health Syst Pharm **68**(19): 1791-1804.

McCallum, G. P., J. E. Horton, et al. (1993). "Microsomal cytochrome P450 1A1 dependent monooxygenase activity in guinea pig heart: induction, inhibition, and increased activity by addition of exogenous NADPH-cytochrome P450 reductase." Can J Physiol Pharmacol **71**(2): 151-156.

Medhora, M., J. Narayanan, et al. (2001). "Identifying endothelium-derived hyperpolarizing factor: recent approaches to assay the role of epoxyeicosatrienoic acids." Jpn J Pharmacol **86**(4): 369-375.

Meguro, T., C. Hong, et al. (1999). "Cyclosporine attenuates pressure-overload hypertrophy in mice while enhancing susceptibility to decompensation and heart failure." Circ Res **84**(6): 735-740.

Mehrabi, M. R., G. E. Steiner, et al. (2002). "The arylhydrocarbon receptor (AhR), but not the AhR-nuclear translocator (ARNT), is increased in hearts of patients with cardiomyopathy." Virchows Arch **441**(5): 481-489.

Menke, J. G., K. L. Macnaul, et al. (2002). "A novel liver X receptor agonist establishes species differences in the regulation of cholesterol 7alpha-hydroxylase (CYP7a)." Endocrinology **143**(7): 2548-2558.

Merten, K. E., Y. Jiang, et al. (2006). "Calcineurin activation is not necessary for Doxorubicin-induced hypertrophy in H9c2 embryonic rat cardiac cells: involvement of the phosphoinositide 3-kinase-Akt pathway." J Pharmacol Exp Ther **319**(2): 934-940.

Messina, A., V. Chirulli, et al. (2008). "Purification, molecular cloning, heterologous expression and characterization of pig CYP1A2." Xenobiotica **38**(12): 1453-1470.

Meszaros, J. and B. Pasztor (1995). "Effect of ouabain in catecholamine-induced cardiac hypertrophy." Acta Physiol Hung **83**(1): 55-62.

Meyer, U. A. (1996). "Overview of enzymes of drug metabolism." J Pharmacokinet Biopharm **24**(5): 449-459.

Michaelis, U. R. and I. Fleming (2006). "From endothelium-derived hyperpolarizing factor (EDHF) to angiogenesis: Epoxyeicosatrienoic acids (EETs) and cell signaling." Pharmacol Ther **111**(3): 584-595.

Michaud, V., M. Frappier, et al. (2010). "Metabolic activity and mRNA levels of human cardiac CYP450s involved in drug metabolism." PLoS One **5**(12): e15666.

Mimnaugh, E. G., M. A. Trush, et al. (1981). "The effects of adriamycin in vitro and in vivo on hepatic microsomal drug-metabolizing enzymes: role of microsomal lipid peroxidation." Toxicol Appl Pharmacol **61**(3): 313-325.

Mitchell, S. R., M. B. Sewer, et al. (2001). "Characterization of CYP4A induction in rat liver by inflammatory stimuli: dependence on sex, strain, and inflammation-evoked hypophagia." Drug Metab Dispos **29**(1): 17-22.

Mitra, M. S., S. Donthamsetty, et al. (2007). "Mechanism of protection of moderately diet restricted rats against doxorubicin-induced acute cardiotoxicity." Toxicol Appl Pharmacol **225**(1): 90-101.

Molkentin, J. D., J. R. Lu, et al. (1998). "A calcineurin-dependent transcriptional pathway for cardiac hypertrophy." Cell **93**(2): 215-228.

Montecucco, F., A. Pende, et al. (2009). "The renin-angiotensin system modulates inflammatory processes in atherosclerosis: evidence from basic research and clinical studies." Mediators Inflamm **2009**: 752406.

Monti, J., J. Fischer, et al. (2008). "Soluble epoxide hydrolase is a susceptibility factor for heart failure in a rat model of human disease." Nat Genet **40**(5): 529-537.

Mordente, A., E. Meucci, et al. (2001). "Human heart cytosolic reductases and anthracycline cardiotoxicity." IUBMB Life **52**(1-2): 83-88.

Moreno, C., K. G. Maier, et al. (2001). "Abnormal pressure-natriuresis in hypertension: role of cytochrome P450 metabolites of arachidonic acid." Am J Hypertens **14**(6 Pt 2): 90S-97S.

Morisseau, C. and B. D. Hammock (2008). "Gerry Brooks and epoxide hydrolases: four decades to a pharmaceutical." Pest Manag Sci **64**(6): 594-609.

Moshal, K. S., D. C. Zeldin, et al. (2008). "Cytochrome P450 (CYP) 2J2 gene transfection attenuates MMP-9 via inhibition of NF-kappabeta in hyperhomocysteinemia." J Cell Physiol **215**(3): 771-781.

Mross, K., U. Mayer, et al. (1990). "Pharmacokinetics and metabolism of iodo-doxorubicin and doxorubicin in humans." Eur J Clin Pharmacol **39**(5): 507-513.

Munzenmaier, D. H. and D. R. Harder (2000). "Cerebral microvascular endothelial cell tube formation: role of astrocytic epoxyeicosatrienoic acid release." Am J Physiol Heart Circ Physiol **278**(4): H1163-1167.

Muthalif, M. M., I. F. Benter, et al. (1998). "20-Hydroxyeicosatetraenoic acid mediates calcium/calmodulin-dependent protein kinase II-induced mitogen-activated protein kinase activation in vascular smooth muscle cells." Proc Natl Acad Sci U S A **95**(21): 12701-12706.

Muthalif, M. M., J. H. Parmentier, et al. (2000). "Ras/mitogen-activated protein kinase mediates norepinephrine-induced phospholipase D activation in rabbit aortic smooth muscle cells by a phosphorylation-dependent mechanism." J Pharmacol Exp Ther **293**(1): 268-274.

Nadal-Ginard, B., J. Kajstura, et al. (2003). "Myocyte death, growth, and regeneration in cardiac hypertrophy and failure." Circ Res **92**(2): 139-150.

Naga Prasad, S. V., G. Esposito, et al. (2000). "Gbetagamma-dependent phosphoinositide 3-kinase activation in hearts with in vivo pressure overload hypertrophy." J Biol Chem **275**(7): 4693-4698.

Nakamura, T., Y. Ueda, et al. (2000). "Fas-mediated apoptosis in adriamycin-induced cardiomyopathy in rats: In vivo study." Circulation **102**(5): 572-578.

Nannelli, A., V. Chirulli, et al. (2008). "Expression and induction by rifampicin of CAR- and PXR-regulated CYP2B and CYP3A in liver, kidney and airways of pig." Toxicology **252**(1-3): 105-112.

Neilan, T. G., S. L. Blake, et al. (2007). "Disruption of nitric oxide synthase 3 protects against the cardiac injury, dysfunction, and mortality induced by doxorubicin." Circulation **116**(5): 506-514.

Newman, J. W., C. Morisseau, et al. (2005). "Epoxide hydrolases: their roles and interactions with lipid metabolism." Prog Lipid Res **44**(1): 1-51.

Newman, J. W., C. Morisseau, et al. (2003). "The soluble epoxide hydrolase encoded by EPXH2 is a bifunctional enzyme with novel lipid phosphate phosphatase activity." Proc Natl Acad Sci U S A **100**(4): 1558-1563.

Ng, V. Y., Y. Huang, et al. (2007). "Cytochrome P450 eicosanoids are activators of peroxisome proliferator-activated receptor alpha." Drug Metab Dispos **35**(7): 1126-1134.

Nguyen, X., M. H. Wang, et al. (1999). "Kinetic profile of the rat CYP4A isoforms: arachidonic acid metabolism and isoform-specific inhibitors." Am J Physiol **276**(6 Pt 2): R1691-1700.

Nicol, R. L., N. Frey, et al. (2000). "From the sarcomere to the nucleus: role of genetics and signaling in structural heart disease." Annu Rev Genomics Hum Genet **1**: 179-223.

Nicol, R. L., N. Frey, et al. (2001). "Activated MEK5 induces serial assembly of sarcomeres and eccentric cardiac hypertrophy." EMBO J **20**(11): 2757-2767.

Nicolay, K., R. J. Timmers, et al. (1984). "The interaction of adriamycin with cardiolipin in model and rat liver mitochondrial membranes." Biochim Biophys Acta **778**(2): 359-371.

Nilakantan, V., C. Maenpaa, et al. (2008). "20-HETE-mediated cytotoxicity and apoptosis in ischemic kidney epithelial cells." Am J Physiol Renal Physiol **294**(3): F562-570.

Nithipatikom, K., A. J. Grall, et al. (2001). "Liquid chromatographic-electrospray ionization-mass spectrometric analysis of cytochrome P450 metabolites of arachidonic acid." Anal Biochem **298**(2): 327-336.

Nithipatikom, K., E. R. Gross, et al. (2004). "Inhibition of cytochrome P450omega-hydroxylase: a novel endogenous cardioprotective pathway." Circ Res **95**(8): e65-71.

Node, K., Y. Huo, et al. (1999). "Anti-inflammatory properties of cytochrome P450 epoxygenase-derived eicosanoids." Science **285**(5431): 1276-1279.

Node, K., X. L. Ruan, et al. (2001). "Activation of Galpha s mediates induction of tissue-type plasminogen activator gene transcription by epoxyeicosatrienoic acids." J Biol Chem **276**(19): 15983-15989.

Nousiainen, T., E. Jantunen, et al. (1999). "Natriuretic peptides as markers of cardiotoxicity during doxorubicin treatment for non-Hodgkin's lymphoma." Eur J Haematol **62**(2): 135-141.

Nusing, R., R. Lesch, et al. (1990). "Immunohistochemical localization of thromboxane synthase in human tissues." Eicosanoids **3**(1): 53-58.

Nussler, A. K., M. Glanemann, et al. (2006). "Fluorometric measurement of nitrite/nitrate by 2,3-diaminonaphthalene." Nat Protoc **1**(5): 2223-2226.

O'Connell, J. B. (2000). "The economic burden of heart failure." Clin Cardiol **23**(3 Suppl): III6-10.

Okita, R. T. and J. R. Okita (2001). "Cytochrome P450 4A fatty acid omega hydroxylases." Curr Drug Metab **2**(3): 265-281.

Oliveira, P. J., J. A. Bjork, et al. (2004). "Carvedilol-mediated antioxidant protection against doxorubicin-induced cardiac mitochondrial toxicity." Toxicol Appl Pharmacol **200**(2): 159-168.

Oltman, C. L., N. L. Weintraub, et al. (1998). "Epoxyeicosatrienoic acids and dihydroxyeicosatrienoic acids are potent vasodilators in the canine coronary microcirculation." Circ Res **83**(9): 932-939.

Outomuro, D., D. R. Grana, et al. (2007). "Adriamycin-induced myocardial toxicity: new solutions for an old problem?" Int J Cardiol **117**(1): 6-15.

Oyekan, A. O. and J. C. McGiff (1998). "Cytochrome P-450-derived eicosanoids participate in the renal functional effects of ET-1 in the anesthetized rat." Am J Physiol **274**(1 Pt 2): R52-61.

Pahl, H. L. (1999). "Activators and target genes of Rel/NF-kappaB transcription factors." Oncogene **18**(49): 6853-6866.

Palle, J., B. M. Frost, et al. (2006). "Doxorubicin pharmacokinetics is correlated to the effect of induction therapy in children with acute myeloid leukemia." Anticancer Drugs **17**(4): 385-392.

Pan, S. S. and N. R. Bachur (1980). "Xanthine oxidase catalyzed reductive cleavage of anthracycline antibiotics and free radical formation." Mol Pharmacol **17**(1): 95-99.

Park, W. Y., C. I. Hwang, et al. (2002). "Identification of radiation-specific responses from gene expression profile." Oncogene **21**(55): 8521-8528.

Pascussi, J. M., M. Busson-Le Coniat, et al. (2003). "Transcriptional analysis of the orphan nuclear receptor constitutive androstane receptor (NR1I3) gene promoter: identification of a distal glucocorticoid response element." Mol Endocrinol **17**(1): 42-55.

Pascussi, J. M., L. Drocourt, et al. (2001). "Dual effect of dexamethasone on CYP3A4 gene expression in human hepatocytes. Sequential role of glucocorticoid receptor and pregnane X receptor." Eur J Biochem **268**(24): 6346-6358.

Pascussi, J. M., Z. Dvorak, et al. (2003). "Pathophysiological factors affecting CAR gene expression." Drug Metab Rev **35**(4): 255-268.

Pascussi, J. M., S. Gerbal-Chaloin, et al. (2003). "The expression of CYP2B6, CYP2C9 and CYP3A4 genes: a tangle of networks of nuclear and steroid receptors." Biochim Biophys Acta **1619**(3): 243-253.

Pelzer, T., M. Schumann, et al. (2000). "17beta-estradiol prevents programmed cell death in cardiac myocytes." Biochem Biophys Res Commun **268**(1): 192-200.

Pereira, S. G. and F. Oakley (2008). "Nuclear factor-kappaB1: regulation and function." Int J Biochem Cell Biol **40**(8): 1425-1430.

Perrino, C., S. V. Naga Prasad, et al. (2006). "Intermittent pressure overload triggers hypertrophy-independent cardiac dysfunction and vascular rarefaction." J Clin Invest **116**(6): 1547-1560.

Pinot, F., D. F. Grant, et al. (1995). "Differential regulation of soluble epoxide hydrolase by clofibrate and sexual hormones in the liver and kidneys of mice." Biochem Pharmacol **50**(4): 501-508.

Poloyac, S. M., M. A. Tortorici, et al. (2004). "The effect of isoniazid on CYP2E1- and CYP4A-mediated hydroxylation of arachidonic acid in the rat liver and kidney." Drug Metab Dispos **32**(7): 727-733.

Pomposiello, S. I., M. A. Carroll, et al. (2001). "Epoxyeicosatrienoic acid-mediated renal vasodilation to arachidonic acid is enhanced in SHR." Hypertension **37**(3): 887-893.

Potente, M., B. Fisslthaler, et al. (2003). "11,12-Epoxyeicosatrienoic acid-induced inhibition of FOXO factors promotes endothelial proliferation by down-regulating p27Kip1." J Biol Chem **278**(32): 29619-29625.

Powell, P. K., I. Wolf, et al. (1998). "Metabolism of arachidonic acid to 20-hydroxy-5,8,11, 14-eicosatetraenoic acid by P450 enzymes in human liver: involvement of CYP4F2 and CYP4A11." J Pharmacol Exp Ther **285**(3): 1327-1336.

Pracyk, J. B., K. Tanaka, et al. (1998). "A requirement for the rac1 GTPase in the signal transduction pathway leading to cardiac myocyte hypertrophy." J Clin Invest **102**(5): 929-937.

Pratt, P. F., P. Li, et al. (2001). "Endothelium-independent, ouabain-sensitive relaxation of bovine coronary arteries by EETs." Am J Physiol Heart Circ Physiol **280**(3): H1113-1121.

Quigley, R., M. Baum, et al. (2000). "Effects of 20-HETE and 19(S)-HETE on rabbit proximal straight tubule volume transport." Am J Physiol Renal Physiol **278**(6): F949-953.

Rahman, A., M. Alam, et al. (2001). "Differential effects of doxorubicin on atrial natriuretic peptide expression in vivo and in vitro." Biol Res **34**(3-4): 195-206.

Reichard, J. F., T. P. Dalton, et al. (2005). "Induction of Oxidative Stress Responses by Dioxin and other Ligands of the Aryl Hydrocarbon Receptor." Dose Response **3**(3): 306-331.

Revermann, M., E. Barbosa-Sicard, et al. (2009). "Inhibition of the soluble epoxide hydrolase attenuates monocrotaline-induced pulmonary hypertension in rats." J Hypertens **27**(2): 322-331.

Riad, A., S. Bien, et al. (2009). "Pretreatment with statin attenuates the cardiotoxicity of Doxorubicin in mice." Cancer Res **69**(2): 695-699.

Riddick, D. S., C. Lee, et al. (2005). "Cancer chemotherapy and drug metabolism." Drug Metab Dispos **33**(8): 1083-1096.

Rifkind, A. B. (2006). "CYP1A in TCDD toxicity and in physiology-with particular reference to CYP dependent arachidonic acid metabolism and other endogenous substrates." Drug Metab Rev **38**(1-2): 291-335.

Ritter, O. and L. Neyses (2003). "The molecular basis of myocardial hypertrophy and heart failure." Trends Mol Med **9**(7): 313-321.

Rockman, H. A., W. J. Koch, et al. (2002). "Seven-transmembrane-spanning receptors and heart function." Nature **415**(6868): 206-212.

Roger, V. L. (2010). "The heart failure epidemic." Int J Environ Res Public Health **7**(4): 1807-1830.

Rohini, A., N. Agrawal, et al. (2010). "Molecular targets and regulators of cardiac hypertrophy." Pharmacol Res **61**(4): 269-280.

Rollin, R., A. Mediero, et al. (2005). "Downregulation of the atrial natriuretic peptide/natriuretic peptide receptor-C system in the early stages of diabetic retinopathy in the rat." Mol Vis **11**: 216-224.

Roman, R. J. (2002). "P-450 metabolites of arachidonic acid in the control of cardiovascular function." Physiol Rev **82**(1): 131-185.

Roy-Chowdhury, J., J. Locker, et al. (2003). "Nuclear receptors orchestrate detoxification pathways." Dev Cell **4**(5): 607-608.

Rushmore, T. H. and A. N. Kong (2002). "Pharmacogenomics, regulation and signaling pathways of phase I and II drug metabolizing enzymes." Curr Drug Metab **3**(5): 481-490.

Saarikoski, S. T., S. P. Rivera, et al. (2005). "CYP2S1: a short review." Toxicol Appl Pharmacol **207**(2 Suppl): 62-69.

Sacerdoti, D., A. Gatta, et al. (2003). "Role of cytochrome P450-dependent arachidonic acid metabolites in liver physiology and pathophysiology." Prostaglandins Other Lipid Mediat **72**(1-2): 51-71.

Sahan-Firat, S., B. L. Jennings, et al. (2010). "2,3',4,5'-Tetramethoxystilbene prevents deoxycorticosterone-salt-induced hypertension: contribution of cytochrome P-450 1B1." Am J Physiol Heart Circ Physiol **299**(6): H1891-1901.

Saito, T. and A. Giaid (1999). "Cyclooxygenase-2 and nuclear factor-kappaB in myocardium of end stage human heart failure." Congest Heart Fail **5**(5): 222-227.

Schrenk, D. (1998). "Impact of dioxin-type induction of drug-metabolizing enzymes on the metabolism of endo- and xenobiotics." Biochem Pharmacol **55**(8): 1155-1162.

Schuetz, E. G. and P. S. Guzelian (1984). "Induction of cytochrome P-450 by glucocorticoids in rat liver. II. Evidence that glucocorticoids regulate induction of cytochrome P-450 by a nonclassical receptor mechanism." J Biol Chem **259**(3): 2007-2012.

Schuetz, E. G., W. Schmid, et al. (2000). "The glucocorticoid receptor is essential for induction of cytochrome P-4502B by steroids but not for drug or steroid induction of CYP3A or P-450 reductase in mouse liver." Drug Metab Dispos **28**(3): 268-278.

Schuetz, E. G., S. A. Wrighton, et al. (1984). "Induction of cytochrome P-450 by glucocorticoids in rat liver. I. Evidence that glucocorticoids and pregnenolone 16 alpha-carbonitrile regulate de novo synthesis of a common form of cytochrome P-450 in cultures of adult rat hepatocytes and in the liver in vivo." J Biol Chem **259**(3): 1999-2006.

Schwartzman, M., N. R. Ferreri, et al. (1985). "Renal cytochrome P450-related arachidonate metabolite inhibits (Na+ + K+)ATPase." Nature **314**(6012): 620-622.

Schwarz, D., P. Kisselev, et al. (2004). "Arachidonic and eicosapentaenoic acid metabolism by human CYP1A1: highly stereoselective formation of 17(R),18(S)-epoxyeicosatetraenoic acid." Biochem Pharmacol **67**(8): 1445-1457.

Seifert, C. F., M. E. Nesser, et al. (1994). "Dexrazoxane in the prevention of doxorubicin-induced cardiotoxicity." Ann Pharmacother **28**(9): 1063-1072.

Seubert, J., B. Yang, et al. (2004). "Enhanced postischemic functional recovery in CYP2J2 transgenic hearts involves mitochondrial ATP-sensitive K+ channels and p42/p44 MAPK pathway." Circ Res **95**(5): 506-514.

Seubert, J. M., C. J. Sinal, et al. (2006). "Role of soluble epoxide hydrolase in postischemic recovery of heart contractile function." Circ Res **99**(4): 442-450.

Shieh, F. K., E. Kotlyar, et al. (2004). "Aldosterone and cardiovascular remodelling: focus on myocardial failure." J Renin Angiotensin Aldosterone Syst **5**(1): 3-13.

Shimada, T., A. Sugie, et al. (2003). "Tissue-specific induction of cytochromes P450 1A1 and 1B1 by polycyclic aromatic hydrocarbons and polychlorinated biphenyls in engineered C57BL/6J mice of arylhydrocarbon receptor gene." Toxicol Appl Pharmacol **187**(1): 1-10.

Shimoike, H., N. Iwai, et al. (1997). "Differential regulation of natriuretic peptide genes in infarcted rat hearts." Clin Exp Pharmacol Physiol **24**(1): 23-30.

Shioi, T., P. M. Kang, et al. (2000). "The conserved phosphoinositide 3-kinase pathway determines heart size in mice." EMBO J **19**(11): 2537-2548.

Shioi, T., J. R. McMullen, et al. (2002). "Akt/protein kinase B promotes organ growth in transgenic mice." Mol Cell Biol **22**(8): 2799-2809.

Sidorik, L., R. Kyyamova, et al. (2005). "Molecular chaperone, HSP60, and cytochrome P450 2E1 co-expression in dilated cardiomyopathy." Cell Biol Int **29**(1): 51-55.

Silvestre, J. S., V. Robert, et al. (1998). "Myocardial production of aldosterone and corticosterone in the rat. Physiological regulation." J Biol Chem **273**(9): 4883-4891.

Simunek, T., M. Sterba, et al. (2009). "Anthracycline-induced cardiotoxicity: overview of studies examining the roles of oxidative stress and free cellular iron." Pharmacol Rep **61**(1): 154-171.

Sinal, C. J., C. D. Webb, et al. (1999). "Differential in vivo effects of alpha-naphthoflavone and beta-naphthoflavone on CYP1A1 and CYP2E1 in rat liver, lung, heart, and kidney." J Biochem Mol Toxicol **13**(1): 29-40.

Singal, P. K., R. J. Segstro, et al. (1985). "Changes in lysosomal morphology and enzyme activities during the development of adriamycin-induced cardiomyopathy." Can J Cardiol **1**(2): 139-147.

Spallarossa, P., P. Fabbi, et al. (2005). "Doxorubicin-induced expression of LOX-1 in H9c2 cardiac muscle cells and its role in apoptosis." Biochem Biophys Res Commun **335**(1): 188-196.

Spector, A. A., X. Fang, et al. (2004). "Epoxyeicosatrienoic acids (EETs): metabolism and biochemical function." Prog Lipid Res **43**(1): 55-90.

Spiecker, M. and J. K. Liao (2005). "Vascular protective effects of cytochrome p450 epoxygenase-derived eicosanoids." Arch Biochem Biophys **433**(2): 413-420.

Sueyoshi, T., T. Kawamoto, et al. (1999). "The repressed nuclear receptor CAR responds to phenobarbital in activating the human CYP2B6 gene." J Biol Chem **274**(10): 6043-6046.

Sul, D., H. S. Kim, et al. (2009). "2,3,7,8-TCDD neurotoxicity in neuroblastoma cells is caused by increased oxidative stress, intracellular calcium levels, and tau phosphorylation." Toxicology **255**(1-2): 65-71.

Sussman, M. A., H. W. Lim, et al. (1998). "Prevention of cardiac hypertrophy in mice by calcineurin inhibition." Science **281**(5383): 1690-1693.

Sussman, M. A., S. Welch, et al. (2000). "Altered focal adhesion regulation correlates with cardiomyopathy in mice expressing constitutively active rac1." J Clin Invest **105**(7): 875-886.

Takeishi, Y., Q. Huang, et al. (2001). "Src and multiple MAP kinase activation in cardiac hypertrophy and congestive heart failure under chronic pressure-overload: comparison with acute mechanical stretch." J Mol Cell Cardiol **33**(9): 1637-1648.

Takemura, G. and H. Fujiwara (2007). "Doxorubicin-induced cardiomyopathy from the cardiotoxic mechanisms to management." Prog Cardiovasc Dis **49**(5): 330-352.

Takimoto, E. and D. A. Kass (2007). "Role of oxidative stress in cardiac hypertrophy and remodeling." Hypertension **49**(2): 241-248.

Tan, F. L., C. S. Moravec, et al. (2002). "The gene expression fingerprint of human heart failure." Proc Natl Acad Sci U S A **99**(17): 11387-11392.

Tanaka, H., S. G. Kamita, et al. (2008). "Transcriptional regulation of the human soluble epoxide hydrolase gene EPHX2." Biochim Biophys Acta **1779**(1): 17-27.

Terasaki, T., T. Iga, et al. (1982). "Experimental evidence of characteristic tissue distribution of adriamycin. Tissue DNA concentration as a determinant." J Pharm Pharmacol **34**(9): 597-600.

Theken, K. N., Y. Deng, et al. (2011). "Activation of the acute inflammatory response alters cytochrome P450 expression and eicosanoid metabolism." Drug Metab Dispos **39**(1): 22-29.

Thum, T. and J. Borlak (2000). "Cytochrome P450 mono-oxygenase gene expression and protein activity in cultures of adult cardiomyocytes of the rat." Br J Pharmacol **130**(8): 1745-1752.

Thum, T. and J. Borlak (2000). "Gene expression in distinct regions of the heart." Lancet **355**(9208): 979-983.

Thum, T. and J. Borlak (2002). "Testosterone, cytochrome P450, and cardiac hypertrophy." Faseb J **16**(12): 1537-1549.

Tokarska-Schlattner, M., T. Wallimann, et al. (2006). "Alterations in myocardial energy metabolism induced by the anti-cancer drug doxorubicin." C R Biol **329**(9): 657-668.

Tokarska-Schlattner, M., M. Zaugg, et al. (2005). "Acute toxicity of doxorubicin on isolated perfused heart: response of kinases regulating energy supply." Am J Physiol Heart Circ Physiol **289**(1): H37-47.

Tokarska-Schlattner, M., M. Zaugg, et al. (2006). "New insights into doxorubicin-induced cardiotoxicity: the critical role of cellular energetics." J Mol Cell Cardiol **41**(3): 389-405.

Tran, K. L., P. A. Aronov, et al. (2005). "Lipid sulfates and sulfonates are allosteric competitive inhibitors of the N-terminal phosphatase activity of the mammalian soluble epoxide hydrolase." Biochemistry **44**(36): 12179-12187.

Tugwood, J. D., T. C. Aldridge, et al. (1996). "Peroxisome proliferator-activated receptors: structures and function." Ann N Y Acad Sci **804**: 252-265.

Turakhia, S., C. D. Venkatakrishnan, et al. (2007). "Doxorubicin-induced cardiotoxicity: direct correlation of cardiac fibroblast and H9c2 cell survival and aconitase activity with heat shock protein 27." Am J Physiol Heart Circ Physiol **293**(5): H3111-3121.

Uddin, M. R., M. M. Muthalif, et al. (1998). "Cytochrome P-450 metabolites mediate norepinephrine-induced mitogenic signaling." Hypertension **31**(1 Pt 2): 242-247.

Ueda, A., H. K. Hamadeh, et al. (2002). "Diverse roles of the nuclear orphan receptor CAR in regulating hepatic genes in response to phenobarbital." Mol Pharmacol **61**(1): 1-6.

Ueno, M., Y. Kakinuma, et al. (2006). "Doxorubicin induces apoptosis by activation of caspase-3 in cultured cardiomyocytes in vitro and rat cardiac ventricles in vivo." J Pharmacol Sci **101**(2): 151-158.

Ueyama, T., S. Kawashima, et al. (1999). "Endothelin-1 activates p38 mitogen-activated protein kinase via endothelin-A receptor in rat myocardial cells." Mol Cell Biochem **199**(1-2): 119-124.

Ullrich, V. and R. Nusing (1990). "Thromboxane synthase. From isolation to function." Stroke **21**(12 Suppl): IV134-138.

Upadhyay, G., A. K. Singh, et al. (2008). "Resveratrol modulates pyrogallol-induced changes in hepatic toxicity markers, xenobiotic metabolizing enzymes and oxidative stress." Eur J Pharmacol **596**(1-3): 146-152.

Van der Heiden, K., S. Cuhlmann, et al. (2010). "Role of nuclear factor kappaB in cardiovascular health and disease." Clin Sci (Lond) **118**(10): 593-605.

Vasan, R. S., J. C. Evans, et al. (2004). "Relations of serum aldosterone to cardiac structure: gender-related differences in the Framingham Heart Study." Hypertension **43**(5): 957-962.

Venkatakrishanan, C. D., K. Dunsmore, et al. (2008). "Hsp27 Regulates p53 Transcriptional Activity in Doxorubicin Treated Fibroblasts and Cardiac H9c2 Cells: p21 Up regulation and G2/M Phase Cell Cycle Arrest." Am J Physiol Heart Circ Physiol.

Volkova, M., M. Palmeri, et al. (2011). "Activation of the aryl hydrocarbon receptor by doxorubicin mediates cytoprotective effects in the heart." Cardiovasc Res.

Von Hoff, D. D., M. W. Layard, et al. (1979). "Risk factors for doxorubicin-induced congestive heart failure." Ann Intern Med **91**(5): 710-717.

Walker, M. K. and T. F. Catron (2000). "Characterization of cardiotoxicity induced by 2,3,7, 8-tetrachlorodibenzo-p-dioxin and related chemicals during early chick embryo development." Toxicol Appl Pharmacol **167**(3): 210-221.

Walker, M. K., R. S. Pollenz, et al. (1997). "Expression of the aryl hydrocarbon receptor (AhR) and AhR nuclear translocator during chick cardiogenesis is consistent with 2,3,7,8-tetrachlorodibenzo-p-dioxin-induced heart defects." Toxicol Appl Pharmacol **143**(2): 407-419.

Wallace, K. B. (2003). "Doxorubicin-induced cardiac mitochondrionopathy." Pharmacol Toxicol **93**(3): 105-115.

Wang, H., S. Faucette, et al. (2003). "A novel distal enhancer module regulated by pregnane X receptor/constitutive androstane receptor is essential for the maximal induction of CYP2B6 gene expression." J Biol Chem **278**(16): 14146-14152.

Wang, H., S. R. Faucette, et al. (2003). "Glucocorticoid receptor enhancement of pregnane X receptor-mediated CYP2B6 regulation in primary human hepatocytes." Drug Metab Dispos **31**(5): 620-630.

Wang, H. and E. L. LeCluyse (2003). "Role of orphan nuclear receptors in the regulation of drug-metabolising enzymes." Clin Pharmacokinet **42**(15): 1331-1357.

Wang, M. H., H. Guan, et al. (1999). "Contribution of cytochrome P-450 4A1 and 4A2 to vascular 20-hydroxyeicosatetraenoic acid synthesis in rat kidneys." Am J Physiol **276**(2 Pt 2): F246-253.

Wang, M. H., D. E. Stec, et al. (1996). "Cloning, sequencing, and cDNA-directed expression of the rat renal CYP4A2: arachidonic acid omega-hydroxylation and 11,12-epoxidation by CYP4A2 protein." Arch Biochem Biophys **336**(2): 240-250.

Wang, M. H., F. Zhang, et al. (2001). "CYP4A1 antisense oligonucleotide reduces mesenteric vascular reactivity and blood pressure in SHR." Am J Physiol Regul Integr Comp Physiol **280**(1): R255-261.

Wang, S., D. P. Hartley, et al. (2003). "Induction of hepatic phase II drug-metabolizing enzymes by 1,7-phenanthroline in rats is accompanied by induction of MRP3." Drug Metab Dispos **31**(6): 773-775.

Wang, Y., X. Wei, et al. (2005). "Arachidonic acid epoxygenase metabolites stimulate endothelial cell growth and angiogenesis via mitogen-activated protein kinase and phosphatidylinositol 3-kinase/Akt signaling pathways." J Pharmacol Exp Ther **314**(2): 522-532.

Weber, K. T. and C. G. Brilla (1993). "Structural basis for pathologic left ventricular hypertrophy." Clin Cardiol **16**(5 Suppl 2): II10-14.

Wen, Y., J. Gu, et al. (2003). "Overexpression of 12-lipoxygenase and cardiac fibroblast hypertrophy." Trends Cardiovasc Med **13**(4): 129-136.

White, P. C. (2003). "Aldosterone: direct effects on and production by the heart." J Clin Endocrinol Metab **88**(6): 2376-2383.

Wihlm, J., J. M. Limacher, et al. (1997). "[Pharmacokinetic profile of high-dose doxorubicin administered during a 6 h intravenous infusion in breast cancer patients]." Bull Cancer **84**(6): 603-608.

Wilkins, B. J., Y. S. Dai, et al. (2004). "Calcineurin/NFAT coupling participates in pathological, but not physiological, cardiac hypertrophy." Circ Res **94**(1): 110-118.

Wu, G., M. G. Yussman, et al. (2001). "Increased myocardial Rab GTPase expression: a consequence and cause of cardiomyopathy." Circ Res **89**(12): 1130-1137.

Wu, S., C. R. Moomaw, et al. (1996). "Molecular cloning and expression of CYP2J2, a human cytochrome P450 arachidonic acid epoxygenase highly expressed in heart." J Biol Chem **271**(7): 3460-3468.

Xiao, Y. F., Q. Ke, et al. (2004). "Enhancement of cardiac L-type Ca2+ currents in transgenic mice with cardiac-specific overexpression of CYP2J2." Mol Pharmacol **66**(6): 1607-1616.

Xiong, H., K. Yoshinari, et al. (2002). "Role of constitutive androstane receptor in the in vivo induction of Mrp3 and CYP2B1/2 by phenobarbital." Drug Metab Dispos **30**(8): 918-923.

Xu, C., C. Y. Li, et al. (2005). "Induction of phase I, II and III drug metabolism/transport by xenobiotics." Arch Pharm Res **28**(3): 249-268.

Xu, D., N. Li, et al. (2006). "Prevention and reversal of cardiac hypertrophy by soluble epoxide hydrolase inhibitors." Proc Natl Acad Sci U S A **103**(49): 18733-18738.

Yaghi, A. and S. M. Sims (2005). "Constrictor-induced translocation of NFAT3 in human and rat pulmonary artery smooth muscle." Am J Physiol Lung Cell Mol Physiol **289**(6): L1061-1074.

Yamada, H., H. Kaneko, et al. (1992). "Tissue-specific expression, induction, and inhibition through metabolic intermediate-complex formation of guinea pig cytochrome P450 belonging to the CYP2B subfamily." Arch Biochem Biophys **299**(2): 248-254.

Yamauchi-Takihara, K. and T. Kishimoto (2000). "A novel role for STAT3 in cardiac remodeling." Trends Cardiovasc Med **10**(7): 298-303.

Yndestad, A., J. K. Damas, et al. (2007). "Role of inflammation in the progression of heart failure." Curr Cardiol Rep **9**(3): 236-241.

Yoshida, S., A. Hirai, et al. (1990). "Possible involvement of arachidonic acid metabolites of cytochrome P450 monooxygenase pathway in vasopressin-stimulated glycogenolysis in isolated rat hepatocytes." Arch Biochem Biophys **280**(2): 346-351.

Yoshimura, M. (2005). "[Aldosterone in heart failure]." Nippon Yakurigaku Zasshi **126**(6): 377-380.

Young, M. E., F. A. Laws, et al. (2001). "Reactivation of peroxisome proliferator-activated receptor alpha is associated with contractile dysfunction in hypertrophied rat heart." J Biol Chem **276**(48): 44390-44395.

Young, M. J., C. D. Clyne, et al. (2001). "Cardiac steroidogenesis in the normal and failing heart." J Clin Endocrinol Metab **86**(11): 5121-5126.

Young, M. J. and J. W. Funder (2002). "Mineralocorticoid receptors and pathophysiological roles for aldosterone in the cardiovascular system." J Hypertens **20**(8): 1465-1468.

Yousif, M. H., I. F. Benter, et al. (2009). "Cytochrome P450 metabolites of arachidonic acid play a role in the enhanced cardiac dysfunction in diabetic rats following ischaemic reperfusion injury." Auton Autacoid Pharmacol **29**(1-2): 33-41.

Yu, S., S. Rao, et al. (2003). "Peroxisome proliferator-activated receptors, fatty acid oxidation, steatohepatitis and hepatocarcinogenesis." Curr Mol Med **3**(6): 561-572.

Yu, W., L. Chen, et al. (2010). "Cytochrome P450 omega-hydroxylase promotes angiogenesis and metastasis by upregulation of VEGF and MMP-9 in non-small cell lung cancer." Cancer Chemother Pharmacol.

Yu, Z., F. Xu, et al. (2000). "Soluble epoxide hydrolase regulates hydrolysis of vasoactive epoxyeicosatrienoic acids." Circ Res **87**(11): 992-998.

Zelarayan, L., A. Renger, et al. (2009). "NF-kappaB activation is required for adaptive cardiac hypertrophy." Cardiovasc Res **84**(3): 416-424.

Zeldin, D. C. (2001). "Epoxygenase pathways of arachidonic acid metabolism." J Biol Chem **276**(39): 36059-36062.

Zeldin, D. C., J. Foley, et al. (1996). "CYP2J subfamily P450s in the lung: expression, localization, and potential functional significance." Mol Pharmacol **50**(5): 1111-1117.

Zhang, T., E. N. Johnson, et al. (2002). "The cardiac-specific nuclear delta(B) isoform of Ca2+/calmodulin-dependent protein kinase II induces hypertrophy and dilated cardiomyopathy associated with increased protein phosphatase 2A activity." J Biol Chem **277**(2): 1261-1267.

Zhang, Y., H. El-Sikhry, et al. (2009). "Overexpression of CYP2J2 Provides Protection against Doxorubicin Induced Cardiotoxicity." Am J Physiol Heart Circ Physiol.

Zhang, Y., H. El-Sikhry, et al. (2009). "Overexpression of CYP2J2 provides protection against doxorubicin-induced cardiotoxicity." Am J Physiol Heart Circ Physiol **297**(1): H37-46.

Zhang, Y., C. L. Oltman, et al. (2001). "EET homologs potently dilate coronary microvessels and activate BK(Ca) channels." Am J Physiol Heart Circ Physiol **280**(6): H2430-2440.

Zhang, Y. W., J. Shi, et al. (2009). "Cardiomyocyte death in doxorubicin-induced cardiotoxicity." Arch Immunol Ther Exp (Warsz) **57**(6): 435-445.

Zhao, X. and J. D. Imig (2003). "Kidney CYP450 enzymes: biological actions beyond drug metabolism." Curr Drug Metab **4**(1): 73-84.

Zhao, X., J. E. Quigley, et al. (2006). "PPAR-alpha activator fenofibrate increases renal CYP-derived eicosanoid synthesis and improves endothelial dilator function in obese Zucker rats." Am J Physiol Heart Circ Physiol **290**(6): H2187-2195.

Zhao, X., T. Yamamoto, et al. (2004). "Soluble epoxide hydrolase inhibition protects the kidney from hypertension-induced damage." J Am Soc Nephrol **15**(5): 1244-1253.

Zhu, D., M. Bousamra, 2nd, et al. (2000). "Epoxyeicosatrienoic acids constrict isolated pressurized rabbit pulmonary arteries." Am J Physiol Lung Cell Mol Physiol **278**(2): L335-343.

Zou, A. P., J. T. Fleming, et al. (1996). "20-HETE is an endogenous inhibitor of the large-conductance Ca(2+)-activated K+ channel in renal arterioles." Am J Physiol **270**(1 Pt 2): R228-237.